A THEORY OF YIELD DESIGN

Jean Salençon

Lecture notes for the course on Yield Design

The City University of Hong Kong

2013

In memoriam

Olivier COUSSY

1953 - 2010

A THEORY OF YIELD DESIGN

"One of the principal objects of theoretical research in any department of knowledge is to find the point of view from which the subject appears in its greatest simplicity"[i]

This book originates from the lecture notes for a Course on Yield Design taught at Hong Kong City University during the recent years. It comes out in the form of a survey of the theory of Yield Design which brings together and summarises the books and lecture notes I published in French on that topic when teaching at *École nationale des ponts et chausssées* and *École polytechnique* (France).

The terminology "Yield Design" has been chosen as a counterpart and translation of the French "Calcul à la rupture" or "Analyse à la rupture" which have been used for long by civil engineers and others to refer to stability analyses of structures where only the concepts of Equilibrium and Resistance are taken into account.

In an explicit form such analyses have been carried out for nearly four centuries, if one takes Galileo's *Discorsi* as a starting point of the story, but they were overshadowed by the achievements of the theory of Elasticity in the 19th century.

Making the long story short, we may jump to the mid of the 20th century when we observe a renewal of interest for the Yield Design methods with the development of the theory of Plasticity. At that time, within the framework of the perfectly plastic model with associated flow rule for the constituent material, the lower and upper bound theorems of Limit Analysis and the Theory of Limit loads are established, which provide the traditional Yield Design approaches with sound theoretical bases. In particular, the upper bound theorem of Limit Analysis refers to the kinematic approach where the rate of work by the external forces is compared with the plastic dissipation rate. Also, after several not fully convincing attempts based on the concept of a rigid perfectly plastic material, the status of the limit loads is definitely settled in the 1970s through the mathematical theorem of existence and uniqueness of the solution to the elastoplastic evolution problem: under the assumption of elastic and perfectly plastic behaviour with associated flow rule, these loads are the maximum loads that can be actually sustained by the system considered in a given geometry.

This is a happy ending to the story from the theoretical point of view but, since it is dependent on the assumption of a perfectly plastic behaviour with associated flow rule, it may appear as substantiating the idea that the Yield Design approaches lose all interest when this assumption is not valid (which is often the case for practical problems: *e.g.* stability analyses of earth structures in civil engineering).

As a matter of fact, the lower and upper bound theorems are just consequences of the sole assumption that the resistance of the constituent material is defined by a convex domain assigned to the internal forces. In particular, the upper bound theorem is derived from the dual definition of this domain without referring to a flow rule or constitutive equation. Therefore, these theorems hold as the lower and upper bound theorems for the extreme loads in the Yield Design theory, encompassing the many aspects of its implementation to various stability analysis problems. From the theoretical viewpoint, the status of the extreme loads is now restricted to that of upper bounds for the stability or load carrying capacity of the system. This does not make any difference in what concerns the application of the method to practice since practical validation is the general rule whatsoever.

The purpose of this book is therefore to present a Theory of Yield Design within the original "Equilibrium/Resistance" framework not referring to the theories of Plasticity or Limit analysis. The general theory is developed for the three-dimensional continuum model in a versatile form based upon simple arguments from the mathematical theory of convexity. It is then straightforwardly transposed to the one-dimensional curvilinear continuum, for the Yield Design analysis of beams, and the two-dimensional continuum model of Plates and thin slabs subjected to bending. The book is structured as follows.

- Chapter I is devoted to an introduction of the concept of Yield Design, starting from historical landmarks and based upon field and laboratory observations of the collapse of mechanical systems. Compatibility between the equilibrium of the considered system subjected to prescribed loads and the resistance of its constituent material is set as the cornerstone of Yield Design analyses as it is apparent in recent construction codes implementing the Ultimate Limit State Design philosophy.
- Chapter II presents the simple example of a truss structure in order to give an outline of the method introducing the concept of potential stability.
- Since the general theory will be developed within the Continuum mechanics framework, Chapter III recalls the fundamentals of this model in its primal formulation, leading to the classical equilibrium equations, and its dual formulation with the theorem/principle of virtual (rate of) work.

Chapters IV to VI present the core of the theory.

- In Chapter IV, after defining the concept of multi-parameter loading mode, the compatibility between equilibrium and resistance is first expressed in its primal form, on the basis of the equilibrium equations and the strength domain of the material defined by a convex strength condition. The definition of the domain of potentially safe loads follows from the mathematical compatibility between the equilibrium equations and the strength condition. As a consequence of the convexity of the strength condition the domain of potentially safe loads is convex, which makes it possible to obtain convenient interior estimates through the construction of statically admissible stress fields which comply with the strength condition.
- Chapters V and VI are devoted to the dual approach of the domain of potentially safe loads. Through the theorem/principle of virtual (rate of) work, it is possible to derive a necessary condition to be satisfied by the potentially safe loads, which does not refer to any stress field but uses kinematically admissible virtual velocity fields as test functions. This leads to the kinematic exterior approach of the domain of potentially safe loads, where the material strength condition is expressed in its mathematical dual formulation of maximum resisting (rate of) work. It is essential to keep in mind that this formulation does not imply any constitutive law and is just the mathematical dualisation of the primal one.

- Chapter VII is some kind of a return to Chapter I, which highlights the role played implicitly by the theory of Yield Design as the fundamental basis of the Ultimate Limit State Design (ULSD) philosophy. It appears that the fundamental inequality of the kinematic exterior approach makes it possible to give an unambiguous quantified meaning to the symbolic inequality of ULSD.
- With the explicit introduction of resistance parameters, Chapter VIII takes advantage of the symmetric roles played by the loads applied to a system on the one side and the resistance of its constituent materials on the other in the equations to be satisfied for potential stability. It introduces the concept of potentially safe dimensioning of a system under a given set of prescribed loads as the counterpart of potentially safe loads when the dimensioning of the system is given. Potentially safe dimensionings generate a convex domain for which interior and kinematic exterior approaches are derived from the general theory. Optimal dimensioning of the system results in minimising a given objective function. Also it is possible to account for the variability of the prescribed loads and for the physical scattering of the resistance parameters by giving a stochastic character to these data. From the definition of the domains of potentially safe loads and potentially safe dimensionings, there is no ambiguity in defining the concept of Probability of stability of a system. Again, the interior approach and, essentially, the kinematic exterior approach provide lower and upper bound estimates for this probability.
- Chapter IX gets on to the Yield Design of structures. The curvilinear one-dimensional continuum model is first recalled with the concepts of wrench of forces and velocity distributor. The implementation of the Yield Design theory is straightforward provided the strength criteria of the constitutive elements, the joints and supports of the structure are correctly written.
- In order to conclude with a concise presentation of the Yield Design analysis of plates and thin slabs, Chapter X is devoted to the construction of the corresponding two-dimensional model. The kinematics is defined by velocity distributor fields. The external forces are represented by force and moment densities, the internal forces are modelled by tensorial wrench fields.
- Chapter XI presents the implementation of the Yield Design theory to metal plates and reinforced concrete slabs subjected to pure bending with strength criteria depending only on the internal moment tensor. The kinematic exterior approach appears as the most popular method, especially with relevant virtual motions based on the concept of *hinge lines*.

Acknowledgment: The author wishes to express his gratitude to Profs. Habibou MAITOURNAM, Noël CHALLAMEL and Pierre SUQUET for their friendly comments and suggestions which contributed to the improvement of this document.

[i] GIBBS, J. W. (1881) – *Proceedings of the American Academy of Arts and Sciences*, May 1880 – June 1881, **XVI**, VIII, Boston, University Press: John Wilson & Co., pp.420-421.

Table of contents

I	Yield Design: origins and topicality of a concept	7
II	An introductory example to the Yield Design approach	23
III	The continuum mechanics framework	33
IV	Primal approach of the theory of Yield Design	51
V	Dual approach of the theory of Yield Design	69
VI	Kinematic exterior approach	83
VII	Ultimate Limit State Design from the theory of Yield Design	99
VIII	Optimality and probability approaches of Yield Design	107
IX	Yield Design of structures	127
X	Yield Design of plates: the model	153
XI	Yield Design of plates subjected to pure bending	173
Alphabetical index		197

Chapter I

Yield Design
Origins and topicality of a concept

Historical milestones

Topicality of the Yield Design approach

References

YIELD DESIGN
Origins and topicality of a concept

Limit state design is, to some extent, a familiar terminology within the syllabuses of civil engineers education, as it appears explicitly in the stability analyses of various types of structures or is present "anonymously" in the methods used for such analyses. Nevertheless, the variety of the corresponding approaches often makes it difficult to recognize that they proceed from the same fundamental principles, which are now the basis of the Ultimate Limit State Design approach to the safety analysis of structures (ULSD). As an introduction to the theory, this chapter will both present some famous historical milestones and the topicality of the subject referring to the principles of ULSD.

1 Historical milestones

1.1 Galileo's *Discorsi e dimostrazioni mathematiche interno à due nuove scienze* (1638)[1]

The fundamental concept to be acknowledged first is that of **Yield strength** as introduced by Galileo in the *Discorsi* [1] on the simple experiment of a specimen in pure tension (Figure 1).

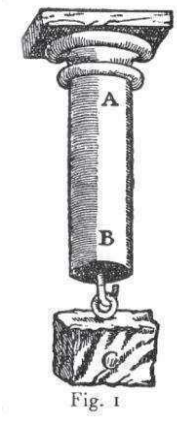

Figure 1. Longitudinal pull test (Galileo, *Discorsi*, 1st day [1])

Galileo uses this first characterization of the tenacity and coherence (*tenacità e coerenza*) of the material to explain the difficulty he finds in breaking a rod or a beam in tension while it is far easier to break it in bending: *"A prism or solid cylinder of glass,*

[1] *"Dialogues concerning two new sciences"* [1].

steel, wood or other breakable material which is capable of sustaining a very heavy weight when applied longitudinally is, as previously remarked, easily broken by the transverse application of a weight which may be much smaller in proportion as the length of the cylinder exceeds its thickness." Considering a cantilever beam (Figure 2) built in a wall (section *AB*) and subjected to a weight applied at the other extremity (section *CD*), he first defines the *"absolute resistance to fracture as that offered to a longitudinal pull"*. Then he assumes that this resistance to tension will be localised in the section of the beam where it is fastened to the wall and that *"this resistance opposes the separation of the part BD lying outside the wall, from that portion lying inside."* The reasoning follows *"it is clear that if the cylinder breaks, fracture will occur at the point B where the edge of the mortise acts as a fulcrum for the lever BC"* [1]. Introducing the second fundamental concept of the Yield Design approach, namely **Equilibrium**, by writing the balance equation for the lever about *B*, Galileo finally relates the *"absolute resistance of the prism BD"* to its *"absolute resistance to fracture"* through the ratio of the short lever arm *BA*/2 to the long one *BC*.

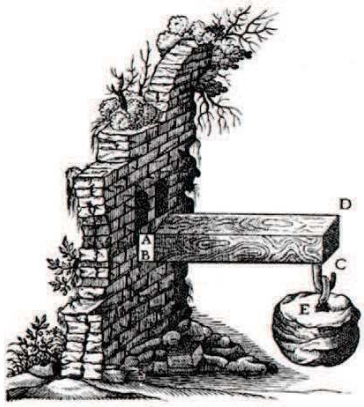

Figure 2. Prism subjected to the transverse application of a weight (Galileo, *Discorsi,* 2nd day)*)*

Galileo's reasoning has been criticized, as shown in Figure 3, on the basis that the equilibrium of the cross section *BA* is not satisfied.

* The one fundamental error which is implicitly introduced into this proposition and which is carried through the entire discussion of the Second Day consists in a failure to see that, in such a beam, there must be equilibrium between the forces of tension and compression over any cross-section. The correct point of view seems first to have been found by E. Mariotte in 1680 and by A. Parent in 1713. Fortunately this error does not vitiate the conclusions of the subsequent propositions which deal only with proportions—not actual strength—of beams. Following K. Pearson (Todhunter's *History of Elasticity*) one might say that Galileo's mistake lay in supposing the fibres of the strained beam to be inextensible. Or, confessing the anachronism, one might say that the error consisted in taking the lowest fibre of the beam as the neutral axis. [*Trans.*]

Figure 3. Translator note, page 115 in [2]

Staying within the framework of the Yield Design approach for the beam, the criticism amounts to pointing out that the global equilibrium equation for the

horizontal resultant force has not been taken into consideration. As a matter of fact, by focusing his attention only on the moment equation for the global equilibrium of the beam, Galileo obtains a necessary condition for the beam to sustain the load in a model where the constituent material is considered at the meso-scale of the section, with its resistance determined through the longitudinal pull test, and not at a more local level such as the longitudinal fibres as the criticism in Figure 3 would require: this is consistent with the fact that resistance to compression is never referred to.

1.2 Coulomb's *Essai sur une application des règles de* Maximis *&* Minimis *à quelques problèmes de Statique relatifs à l'Architecture* (1773)[2]

The appearance of Soil mechanics as an engineering science is often associated with Coulomb's memoir [3] presented to the French Academy of sciences in 1773 after Coulomb returned from his 8-year period in Martinique as a lieutenant in the French military corps of engineers. This *Essay* was devoted to various problems which he had encountered when building the "Fort Bourbon": stability of pillars, arches and vaults, calculation of earth pressure on retaining walls, etc. (Figure 4).

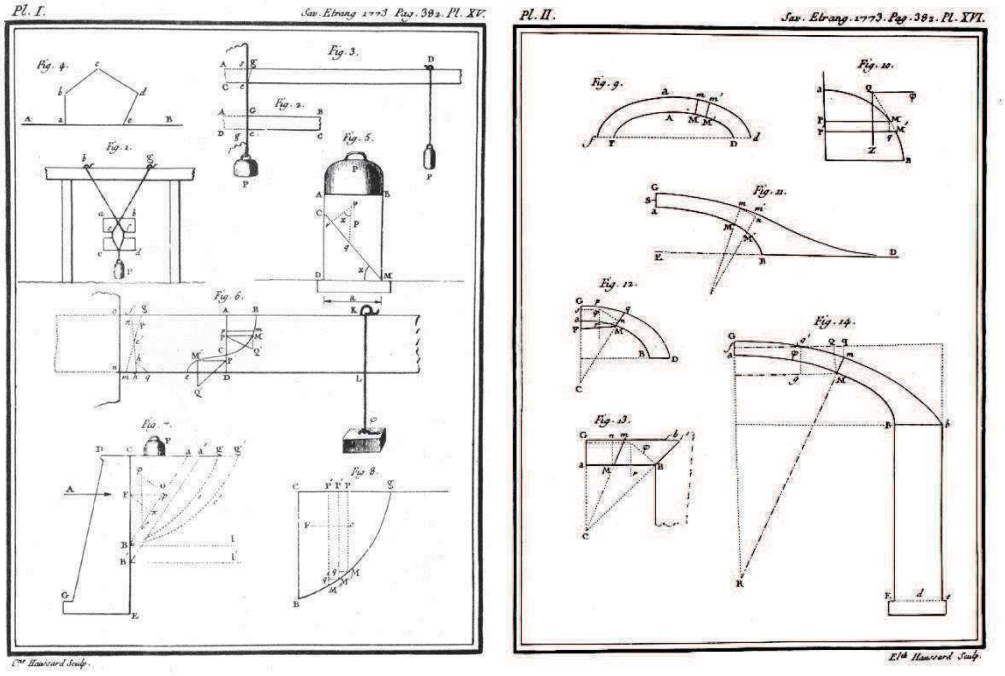

Figure 4. Figure plates in Coulomb's Essay [3]

The first guiding idea of Coulomb's rationale in tackling those problems is making a clear distinction between the **active forces**, that are the prescribed loads acting on the structure under consideration, and the characteristics of **resistance** of the material, which set the bounds to the "**coherence**" forces that can be mobilized (Figure 5).

[2] *"Note on an application of the rules of maximum and minimum to some statical problems, relevant to architecture"* [3].

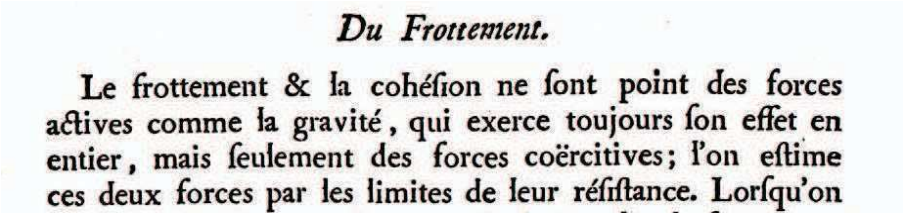

Du Frottement.

Le frottement & la cohéſion ne ſont point des forces actives comme la gravité, qui exerce toujours ſon effet en entier, mais ſeulement des forces coërcitives; l'on eſtime ces deux forces par les limites de leur réſiſtance. Lorſqu'on

Figure 5. Defining friction and cohesion[3] in Coulomb's Essay [3]

The second guiding idea is that the resistance forces are exerted locally along an assumed failure surface, anticipating, to a certain extent, on the concept of stress vector to be introduced some fifty years afterwards. In the simple case of a stone column under a compressive load (Figure 4), Coulomb explains the principles of the analysis: the active force on the assumed fracture surface must be balanced by the "coherence" force; the fracture surface will be determined through a minimisation process.

Based upon the same principle, Coulomb's stability analysis of a retaining wall is a fundamental landmark for the theory of Yield Design. Coulomb starts with the celebrated "Coulomb's wedge" reasoning (Figures 4, 6), where he assumes the failure surface to be plane, and states as a condition for stability that the active forces on the assumed fracture surface *Ba* must be balanced by the "coherence" forces; from which he derives, through minimisation and maximisation processes, two bounds for the horizontal force that can be applied to *CB* so that the wall be stable. Due to its simplicity this reasoning is often presented as *the* Coulomb analysis of the stability of a retaining wall. In fact, Coulomb, after showing how the friction along the wall could be taken into account, states that, to be complete, the analysis should look for the curve that produces the highest pressure on *CB* and sketches the process for this determination.

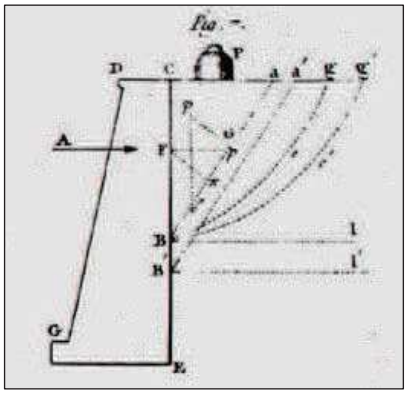

Figure 6. Coulomb's wedge [3]

[3] *"Friction and cohesion are not active forces such as gravity that always act with its full intensity, but only coercive forces; those two forces are characterized by the limits set to their resistance"*

1.3 Compatibility between equilibrium and resistance

It is not difficult to point out the common features of the analyses that have been briefly presented here above.

- First, the concept of **resistance** is introduced as a mechanical characteristic of the constituent material. After having been determined through a given simple experiment, it is used in any other circumstances and sets the **limits** to the resisting forces that can be actually mobilized.
- Then, the idea that the resistance of a given structure – a result at the **global** level – can be derived from the knowledge of the resistance of its constituent material(s), which is a property at the **local** level.
- For this determination, the rationale is based upon the statement that equilibrium equations of the structure must be satisfied while complying with the limits imposed by the resistance of the constituent material(s). In other words, **Equilibrium and Resistance must be mathematically compatible**.
- The practical implementation of this statement is made through the choice or the assumption of some particularly crucial zone in the structure (cross section in the first case, failure surface in the second) where it is anticipated that compatibility between equilibrium and resistance should be checked.

As it appears in Figure 3 in the case of Galileo's analysis, it may be objected that such approaches do not take into account the behaviour of the material, *i.e.* the fact that the material deforms under the forces it is subjected to. But it must be recalled that although the concept of linear elasticity was first introduced by Hooke in the 1660s, it was only in 1807 that Young recognized shear as an elastic deformation; three-dimensional linear elasticity itself was only really formalized in the 1820s (Navier, Cauchy...) at the same time as the concept of stress tensor. As noted before, the Yield Design approach implicitly embodies an anticipation of the concept of internal forces. This is not surprising since the intuition of internal forces is primarily linked to that of rupture being localized on surfaces or lines as observed on full scale, reduced scale or small scale experiments (Figures 7, 8).

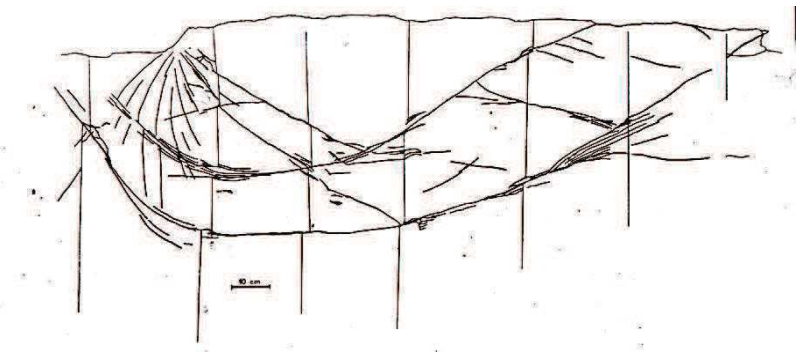

Figure 7. "Slip line" pattern under a foundation in a purely cohesive material (medium scale experiment) [4]

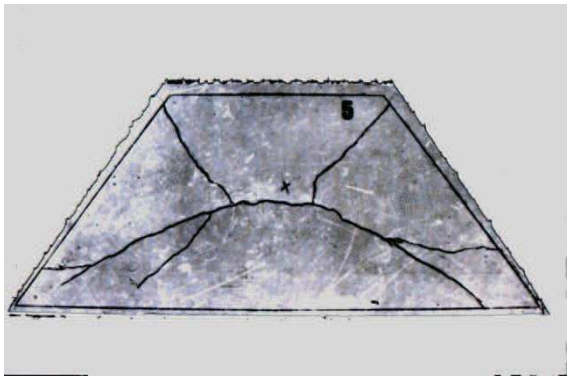

Figure 8. Bending of a reinforced plaster slab: evidence of hinge curves (*M. Milicevic)*

2 Topicality of the Yield Design approach

2.1 – The Coulomb's *Essay* legacy

Coulomb's *Memoir* was at the origin of many methods used by engineers for the stability analyses of various types of structures. In the case of masonry vaults, the works by Méry [5], and Durand-Claye [6, 7] have been extensively studied by Heyman [8-13] and Delbecq [14, 15]: it is interesting to note that they often combined Coulomb's original reasoning with elastic arguments, thus losing its original theoretical meaning without any damage from the practical point of view.

Soil mechanics, which is sometimes considered as having found its very origin in Coulomb's *Memoir*, exhibits numerous methods clearly related to it, for the stability analysis of slopes, retaining walls, fills and earth dams or for the calculation of the bearing capacity of surface foundations [16-63], including the limit equilibrium methods and the slip line methods, which were also applied to solving metal forming problems. Finite element methods have also been developed and used extensively within this framework for applications to Soil mechanics and to some related problems [64-77].

Another field of application is the bearing capacity of metallic plates and reinforced concrete slabs through the yield hinges theory as developed by Johansen, Save, Massonnet… [78-83].

Considerable attention has been devoted by Chen, Drucker and co-workers to applying the theorems of limit analysis to the determination of the bearing capacity of concrete blocks and fibre reinforced concrete [84-87].

More recently, it has been applied to the determination of the resistance of long fibre composites from the knowledge of the resistances of the components, through a homogenization process leading to the definition and determination of a homogenized yield criterion (Suquet, de Buhan, [88-95]).

2.2 – Topicality

Obviously the Yield Design approach did play a highly important role in civil engineering and construction as a scientific approach before the theory of Elasticity was elaborated and could be practically implemented for the design of structures. One may wonder now about its topicality, taking into account both the constant improvement of the formulation and determination of constitutive laws and the development of computational methods and tools which can be applied to determine the behaviour of a structure along a given loading path. It must be understood that there is no inconsistency between the different approaches provided they are used within their proper domain of validity, depending on the available data, and with their results interpreted accordingly. Moreover, the Yield Design approach proves quite efficient for back calculations after the collapse of a structure without knowing the exact circumstances of its occurrence.

Recent construction codes such as the Eurocodes are based on the concept of Limit State Design which includes Ultimate Limit State Design (ULSD) the principle of which may be stated as follows [96]:

"The design criterion is simply to design for equilibrium [under the design loads] *in the design limit state of failure. The design criterion could be expressed in the following way:* $R_d \geq S_d$ *"*
which means that the *design load effect* S_d should be inferior to the *effect of the design resistances* R_d.

Three words are familiar to us in this statement, namely *"equilibrium"*, *"loads"* and *"resistances"*, as a follow up to Coulomb's *Memoir*. The word *"design"* needs being explained and *"effect"* must be defined. As far as *design* is concerned, it means that the values that are considered for the design and the dimensioning of the structures are not the actual values of the loads or of the resistances but conventional values derived from them through properly chosen partial safety coefficients ("partial factors") and thus setting the "rules of the game". Regarding the *effect,* it must be quantified as a scalar in order to make the inequality practically meaningful.

Thanks to the theoretical basis of the ULSD approach to safety provided by the theory of Yield Design [97], it is possible[4] to make the necessary clear distinction between the active forces and the resisting forces, exactly in the same spirit as explained by Coulomb more than 200 years ago. Also, through a quantified definition of the *effects*, it provides at the same time scientifically consistent and efficient methods for its implementation [98, 99].

[4] *Cf.* Chapter VII.

REFERENCES

[1] GALILEI, G. (1638) – *Discorsi e dimostrazioni matematiche intorno à due nuove scienze.* Elsevier, Leyden.

[2] GALILEI, G. (1638) – *Dialogues concerning two new sciences.* CREW, H. & SALVIO, A. transl., Dover Publ., New York, 1954.

[3] COULOMB, C.-A. (1773) – *Essai sur une application des règles de* Maximis *et* Minimis *à quelques problèmes de statique relatifs à l'architecture.* Mémoire présenté à l'Académie Royale des sciences, Paris, **VII**, pp. 343-382.

[4] HABIB, P. (1984) – Les surfaces de glissement en mécanique des sols. *Revue française de géotechnique*, **27**, 7-21.

[5] MÉRY, E. (1840) – Équilibre des voutes en berceau. *Annales des Ponts et Chaussées*, **I**, 50-70.

[6] DURAND-CLAYE, A. (1867) – Stabilité des voûtes en maçonnerie. *Annales des Ponts et Chaussées,* **I**, 63-96.

[7] DURAND-CLAYE, A. (1880) – Stabilité des voûtes et des arcs. *Annales des Ponts et Chaussées,* **I**, 416-440.

[8] HEYMAN, J. (1966) – The stone skeleton. *International Journal of Solids and Structures*, **2**, 2, 249-279.

[9] HEYMAN, J. (1969) – The safety of masonry arches. *International Journal of Mechanical Sciences*, **11**, 363-385.

[10] HEYMAN, J. (1972) – *Coulomb's Memoir on Statics: an Essay in the History of Civil Engineering.* Cambridge University Press (UK)

[11] HEYMAN, J. (1980) – The estimation of the strength of masonry arches. *Proceedings of the American Society of Civil Engineers (A.S.C.E.)*, Part 2, **69**, 921-937.

[12] HEYMAN, J. (1982) – *The Masonry Arch.* Ellis Horwood Ltd, John Wiley, Chichester (UK).

[13] HEYMAN, J. (1998) – *Structural Analysis*. 3rd ed., Prentice Hall, Upper Saddle River, N.J.

[14] DELBECQ, J.-M. (1981) – Analyse de la stabilité des voûtes en maçonnerie de Charles-Augustin Coulomb à nos jours. *Annales des Ponts et Chaussées,* **19**, 36-43.

[15] DELBECQ, J.-M. (1982) – Analyse de la stabilité des voûtes en maçonnerie par le calcul à la rupture. *Journal de Mécanique Appliquée,* **1**, 1, 91-121.

[16] BEREZANCEW, B. G. (1952) – *Axisymmetric Problem of the Theory of Limiting Equilibrium of a Granular Medium.* [in Russian], Gostekhizdat, Moscow (1952).

[17] BISHOP, A. W. (1955) – The use of the Slip Circle in the Stability Analysis of Slopes, *Géotechnique*, **5**, 1, 7-17.

[18] BØNDING, N. (1977) – Kinematical Admissibility of the pure N_γ Rupture Figure. *Proc. 9th Int. Conf. Soil Mech. & Foundation Eng*ineering, **1**, pp. 415-418.

[19] BRINCH-HANSEN (1953) – *Earth Pressure Calculation*. Danish Technical Press, Copenhagen.

[20] de BUHAN, P. & SALENÇON, J. (1993) – A comprehensive stability analysis of soil nailed structures. *European Journal of Mechanics*, A, **12**, n°3, 1993, 325-345.

[21] CHATZIGOGOS, C. T., PECKER, A. & SALENÇON, J. (2007) – Seismic Bearing Capacity of a Circular Footing on a Heterogeneous Soil. *Soils and Foundations*, **47**, 4, 783-797.

[22] CHEN, W. F. (1969) – Soil mechanics and theorems of limit analysis. *Journal of the Soil mechanics and Foundations Division, ASCE,* **95**, (SM2), 493-518.

[23] CHEN, W. F. ,GIGER, M. W. & FANG, H. Y. (1969) – On the limit analysis of stability of slopes. *Soils and Foundations,* **9**, 4, 23-32.

[24] CHEN, W. F. & SCAWTHORN, C. R. (1970) – Limit analysis and limit equilibrium solutions in soil mechanics. *Soils and Foundations*, **10**, 3, 13-49.

[25] CHEN, W. F. (1970) – Discussion on circular and logarithmic spiral slip surfaces. *Journal of the Soil mechanics and Foundations Division, ASCE,* **96**, (SM1), 324-326.

[26] CHEN, W. F. & ROSENFARB, J. L. (1973) – Limit analysis solutions of earth pressure problems. *Soils and Foundations,* **13**, 4, 45-60.

[27] CHEN, W. F. ,SNITBHAN, N. & FANG, H. Y. (1975) – Stability of slope in anisotropic nonhomogeneous soils. *Canadian Geotechnical Journal,* **12**, 1, 146-152.

[28] CHEN, W. F. (1975) – *Limit Analysis and Soil Plasticity*, Elsevier.

[29] COUSSY, O. & SALENÇON, J. (1979) – Analyse de la stabilité des ouvrages en terre par le calcul à la rupture. *Annales des Ponts et Chaussées*, **12**, 1979, 7-35.

[30] DE JOSSELIN DE JONG, G. (1980) – application of the calculus of variations to the vertical cut off in cohesive frictionless soil. *Géotechnique*, **30**, 1, 1-16.

[31] DRUCKER, D. C. & PRAGER, W. (1952) – Soil mechanics and plastic analysis or limit design. *Quarterly of Applied Mathematics,* 157-165.

[32] GREENBERG, H. J. & PRAGER, W. (1952) – On limit design of beams and frames. *Brown University technical report.* A 18, 1, 1, 1949; *Trans. ASCE,* **117**, 447-484.

[33] HILL, R. (1950) – *The mathematical theory of plasticity.* Clarendon Press, Oxford.

[34] HOULSBY, G. T. & WROTH, C. P. (1982) – Direct solution of plasticity problems in soils by the method of characteristics. *Proceedings of the 4th International Conference on Numerical Methods in Geomechanics, Edmonton*, **3**, pp. 1059-1071.

[35] KÖTTER, W. T. (1903) – Die Bestimmung des Druckes an den gekrümmten Gleitflächen, eine Aufgabe aus der Lehre vom Erddruck. *Berliner Akademie Bericht,* 229-233.

[36] KÖTTER, W. T. (1909) – Über den Druck von Sand gegen Öffnungsverschlüsse im horizontalen Boden kastenförmiger Gefäße. *Berliner Akademie Bericht*, 493-510.

[37] LAU, C. K. & BOLTON, M. D. (2011) – The bearing capacity of footings on granular soils. I: numerical analysis. *Géotechnique*, **61**, 8, 627-638.

[38] MANDEL, J. & SALENÇON, J. (1972) – Force portante d'un sol sur une assise rigide (étude théorique). *Géotechnique*, **22**, n°1, 79-93.

[39] MARTIN, C. M. (2005) – Exact bearing capacity calculations using the method of characteristics. *Proceedings of the 11th International Conference. on Computer Methods and Advances in Geomechanics,* **4**, pp. 441-450.

[40] MARTIN, C. M. (2009) – Undrained collapse of a shallow plane-strain trapdoor. *Géotechnique*, **59**, 10, 855-863.

[41] MASSAU, J. (1899) – Mémoire sur l'intégration graphique des équations aux dérivées partielles ; chap. IV: équilibre des terres sans cohésion. *Annales de l'Association des Ingénieurs de l'École de Gand*, 1899; Édition du centenaire, Comité national de mécanique, Brussels, Mons, 1952.

[42] MATAR, M. & SALENÇON, J. (1979) – Capacité portante des semelles filantes. *Revue Française de Géotechnique*, **9**, 51-76.

[43] MEYERHOF, G. G., (1951) – The ultimate bearing capacity of foundations *Géotechnique*, **2**, 4 , 301-332.

[44] MEYERHOF, G. G. (1953) – The bearing capacity of foundations under Eccentric and inclined loads. *Proceedings of the 3rd International Conference on Soil Mechanics and Foundation Engineering,* Zurich, **1**, pp. 440-445.

[45] MEYERHOF, G. G. (1963) – Some recent research on the bearing capacity of foundations. *Canadian Geotechnical Journal*, **1**, 1, 16-21.

[46] MICHALOWSKI, R. L. & YOU L. (1998) – Non-symmetrical limit loads on strip footings. *Soils and Foundations*, **38**, 4, 195-203.

[47] MICHALOWSKI, R. L. & DRESCHER A. (2009) – Three-dimensional stability analysis of slopes and excavations. *Géotechnique*, **59**, 10, 839-850.

[48] PRAGER, W. (1955) – Théorie générale des états d'équilibre limite. *Journal de Mathématiques Pures et Appliquées*, **34**, 395-406.

[49] RENDULIC, L. (1935) – Ein Beitrag zur Bestimmung der Gleitsicherheit. *Der Bauingenieur*, (16) **19-20**, 230-233.

[50] SALENÇON, J. (1974) – Bearing capacity of a footing on a purely cohesive soil with linearly varying shear strength. *Géotechnique*, **24**, n°3, 443-446.

[51] SALENÇON, J., FLORENTIN, P. & GABRIEL, Y. (1976) – Capacité portante globale d'une fondation sur un sol non homogène. *Géotechnique*, **26**, n°2, 351-370.

[52] SALENÇON, J. & MATAR, M. (1982) – Capacité portante des fondations superficielles circulaires. *Journal de Mécanique Théorique et Appliquée*, **1**, n°2, 237-267.

[53] SALENÇON, J. (1984) – Yield-strength of anisotropic soils. *Proceedings of the 16th International Conference of Theoretical and Applied Mechanics*, Lyngby, Denmark, 1984, North-Holland publ., 1985, pp. 369-386.

[54] SALENÇON, J. & PECKER, A. (1995) – Ultimate bearing capacity of shallow foundations under inclined and eccentric loads. Part I: purely cohesive soil. *European Journal of Mechanics*, A, **14**, n°3, 349-375.

[55] SALENÇON, J. & PECKER, A. (1995) – Ultimate bearing capacity of shallow foundations under inclined and eccentric loads. Part II: purely cohesive soil without tensile strength. *European Journal of Mechanics*, A, **14**, n°3, 377-396.

[56] SALENÇON, J., C. CHATZIGOGOS & PECKER, A. (2006) **–** Yield Design Theory applied to the Determination of the Seismic Bearing Capacity of Surface Footings. *Proceedingsof the International Conference on Nonlinear Analysis and Engineering Mechanics Today.* December 11-14, 2006, Institute of Applied Mechanics, Hochiminh City, Vietnam**.**

[57] SOKOLOVSKI, V. V. (1955) – *Theorie der Plastizität*. VEB Verlag Technik, Berlin.

[58] SOKOLOVSKI, V. V. (1960) – *Statics of Soil Media*. Butterworths Scientific Publications, London.

[59] SOKOLOVSKI, V. V. (1965) – *Statics of Granular Media*. Pergamon Press, Oxford.

[60] SARAN, S. & ARGAWAL, R. K. (1991) – Bearing capacity of eccentrically obliquely loaded footing. *Journal of Geotechnical Engineering*, **117**, 11, 1669-1690.

[61] TAYLOR, D. W. (1937) – Stability of earth slopes. *Journal of the Boston Society of. Civil Engineers*, **24**, 3, 337-386.

[62] TAYLOR, D. W. (1937) – *Fundamentals of Soil Mechanics*, John Wiley.

[63] UKRITCHON, B., WHITTLE, A. & SLOAN, W. (1998) – Undrained limit analyses for combined loading of strip footings on clay. *Journal of Geotechnical and Geoenvironmental Engineering*, **124**, 3, 265-276.

[64] ANDERHEGGEN, E. & KNÖPFEL, H. (1972) – Finite element limit analysis using linear programming. *International Journal of Solids and Structures*, **8**, 1413-1431.

[65] DELBECQ, J.M., FRÉMOND, M., PECKER, A, & SALENÇON, J. (1977) – Éléments finis en plasticité et viscoplasticité. *Journal de Mécanique Appliquée*, **1**, n°3, 267-304.

[66] FRÉMOND, M. & SALENÇON, J. (1973) – Limit analysis by finite-element method. *Proceedings of the Symposium on the Role of Plasticity in Soil Mechanics*, September 1973, Cambridge (UK), (PALMER A. C. ed.), pp. 297-308.

[67] KAMMOUN, Z., PASTOR, F., SMAOUI, H. & PASTOR, J. (2010) – Large static problem in numerical analysis: a decomposition approach. *International Journal for Numerical and Analytical Methods in Geomechanics*, **34**, 18, 1960-1980.

[68] KRABBENHOFT, K. & DAMKILDE, L. (2003) – A general optimization algorithm for lower bound limit analysis. *International Journal for Numerical Methods in Engineering*, **56**, 165-184.

[69] KRABBENHOFT, K., LYAMIN, A. V., HIJAJ, M. & SLOAN, M. W. (2005) – A new discontinuous upper bound analysis formulation. *International Journal for Numerical Methods in Engineering*, **63**, 1069-1088.

[70] LYAMIN, A. V. & SLOAN, M. W. (2002) – Lower bound limit analysis using nonlinear programming. *International Journal for Numerical Methods in Engineering*, **55**, 573-611.

[71] LYAMIN, A. V. & SLOAN, M. W. (2002) – Upper bound limit analysis using linear finite elements and non-linear programming. *International Journal for Numerical and Analytical Methods in Geomechanics*, **26**, 181-216.

[72] LYSMER, J. (1970) – Limit analysis of plane problems in soil mechanics. *Journal of the Soil Mechanics and Foundations Division, ASCE*, **96**, 1311-1334.

[73] MAKRODIMOPOULOS, A. & MARTIN, C. M. (2006) – Lower bound limit analysis of cohesive-frictional materials using second-order cone programming. *Int. J. for Numerical Methods in Engineering*, **66**, 4, 604-634.

[74] MAKRODIMOPOULOS, A. & MARTIN, C. M. (2007) – Upper bound limit using simplex strain element and second-order cone programming. *International Journal for Numerical and Analytical Methods in Geomechanics*, **31**, 835-865.

[75] MAKRODIMOPOULOS, A. & MARTIN, C. M. (2008) – Upper bound limit using discontinuous quadratic displacement fields. *Communications in Numerical Methods in Engineering*, **24**, 11, 911-927.

[76] MARTIN, C. M. (2011) – The use of adaptive finite-element limit analysis to reveal slip-line fields. *Géotechnique Letters*, **1**, 2, 23-29.

[77] PASTOR, F., LOUTE, E. & PASTOR, J. (2009) – Limit analysis and convex programming: A decomposition approach of the kinematic mixed method. *International Journal for Numerical Methods in Engineering*, **78**, 254-274.

[78] JOHANSEN, K. W. (1931) – Beregning af krydsarmerede jernbetonpladers brudmoment, *Bygningsstatiske Meddelelser*, **3**, 1, 1931, pp 1-18 (German version: "Bruchmomente der Kreuzweise bewehrten Platten", *Memoirs of the International Association for Bridge and Structure Engineering*, **1**, 1932, pp. 277-296.)

[79] JOHANSEN, K. W. (1962) – *Brudlinieteorier*, Gjellerup, Copenhagen, 1943, 189 pp. (English translation: *Yield-Line Theory*, Cement and Concrete Association, London, 1962).

[80] MASSONNET, C. E. & SAVE, M. (1963) – *Calcul plastique des constructions, II, Structures spatiales*. CBLIA, Brussels.

[81] SAVE, M. & MASSONNET, C. E. (1973) – *Calcul plastique des constructions,* 2nd ed. CBLIA, Brussels.

[82] SAVE, M. (1995) – *Atlas of Limit Loads of Metal Plates, Shells and Disks*. Elsevier, Amsterdam.

[83] BRAESTRUP, M. W. (2007) – Yield line theory and concrete plasticity. *Proceedings of the Morley Symposium on Concrete Plasticity and its Application*, University of Cambridge 23 July, 2007, pp. 43-48.

[84] CHEN, W. F. & DRUCKER, D. C. (1969) – Bearing capacity of concrete blocks or rock. *Journal of the Engineering Mechanics Division, ASCE,* **95**, (EM4), 955-978.

[85] CHEN, W. F. (1970) – Extensibility of concrete and theorems of limit analysis. *Journal of the Engineering Mechanics Division, ASCE,* **96**, (EM3), 341-352.

[86] CHEN, W. F. & COVARRUBIAS, S. (1971) – Bearing capacity of concrete blocks. *Journal of the Engineering Mechanics Division, ASCE,* **96**, (EM5), 1413-1430.

[87] CHEN, W. F. (1973) – Bearing strength of concrete blocks. *Journal of the Engineering Mechanics Division, ASCE,* **99**, (EM6), 1314-1321.

[87] CHEN, W. F. & CARSON, J. L. (1974) – Bearing capacity of fiber reinforced concrete. *International Symposium on Fiber Reinforced Concrete, ACI Spec. Publ.,* SP-44-12, pp. 209-220.

[88] DE BUHAN, P. (1986) – *Approche fondamentale du calcul à la rupture des ouvrages en sols renforcés*. PhD thesis, Université Pierre et Marie Curie, Paris.

[89] DE BUHAN, P., DORMIEUX, L. & SALENÇON, J. (1998) – Modélisation multipolaire de la résistance d'un milieu renforcé par inclusions. *Comptes Rendus de l'Académie des sciences de Paris*, **326**, IIb, 163-170.

[90] DE BUHAN, MANGIAVACCHI, R., NOVA, R., PELLEGRINI, G. & SALENÇON, J. (1989) – Yield design of reinforced earth walls by homogenisation method. *Géotechnique*, **39**, 2, 189-201.

[91] DE BUHAN, P., SALENÇON, J. & SIAD, L. (1986) – Critère de résistance pour le matériau „terre armée". *Comptes Rendus de l'Académie des sciences de Paris*, **302**, II, 377-381.

[92] DE BUHAN, P., SALENÇON, J. & TALIERCIO, A. (1990) – Lower and upper bound estimates for the macroscopic strength criteria of fiber composite materials. *Proceedings of the IUTAM Symposium on on Inelastic Deformation of Composite Materials*, 29 May-1 June 1990, Troy N.Y., Springer Verlag, pp. 563-580.

[93] DE BUHAN, P. & TALIERCIO, A. (1991) – A homogenization approach to the yield strength of composite materials. *European Journal of Mechanics, A/Solids*, **10**, 2, 129-154.

[94] SUQUET, P. (1982) – *Plasticité et homogénéisation*. PhD thesis, Université Pierre et Marie Curie, Paris.

[95] SUQUET, P. (1983) – Analyse limite et homogénéisation. *Comptes Rendus de l'Académie des sciences de Paris*, **296**, II, 1355-1358.

[96] OVESEN, N. K. (1989) – General Report, session 30: Codes and Standards. *Proceedings of the 12th International Conference on Soil Mechanics and Foundation Engineering,* Balkema, Rotterdam, pp. 2751-2764.

[97] SALENÇON, J. (1994) – Approche théorique du calcul aux états limites ultimes. *Les grands systèmes des sciences et des technologies*. HOROWITZ, J. & LIONS, J.-L. eds, Masson, Paris, pp. 701-722.

[98] ANTHOINE, A., DE BUHAN, P., DORMIEUX, L. & SALENÇON, J. (1991) – *STARS 2.00. Computer code for the stability analysis of earth structures.* Presses de l'École Nationale des Ponts et Chaussées, Paris.

[99] SIMON, B. (2009) – Yield design calculation of earth retaining structures. *Ground Engineering*, **49**, 2, 20-25

Chapter II

An introductory example To the Yield Design approach

Setting the problem

Potential stability of the structure

To what extent is potential stability a relevant concept?

References

AN INTRODUCTORY EXAMPLE
To the Yield Design approach

The variety of topics that have been studied through the Yield design approach calls for a unifying presentation that might both enhance the common features of the corresponding analyses and make their joint implementation for the solution of a problem easier. In order to make this general theory as versatile as possible for its application to the different mechanical models commonly used in practice – e.g. *rods, beams, arches, plates, shells, 2-D or 3-D continua, micropolar media – it will be presented within the framework of the classical 3-D continuum mechanics. As a preliminary, a very simple example will now be analysed in order to point out the guidelines of the rationale without being confused by the formalism of the mechanical modelling.*

1 Setting the problem

1.1 The considered structure

The geometry of the structure to be analysed is presented in Figure 1. It consists of three vertical rods $A'A$, $B'B$ and $C'C$ with length ℓ, which are fixed by pinned joints offering no resistance to bending moments in A', B' and C' respectively to a rigid support and in A, B and C to a rigid transverse beam. The points B' and B are in the middle of $A'C'$ and AC respectively.

The structure is thus made of 11 elements, namely the 3 rods, the support, the transverse beam and the 6 pinned joints as encompassed by the broken line in Figure 1.

1.2 Loading mode of the structure

The structure is subjected to two active vertical loads applied in D_1 and D_2, respectively the middle points of AB and BC. The intensities of the loads are Q_1 and Q_2, the loading parameters in the problem, counted positive when the loads are going downwards. We define the two-dimensional loading space of the structure as generated by the vector $\underline{Q} = (Q_1, Q_2)$.

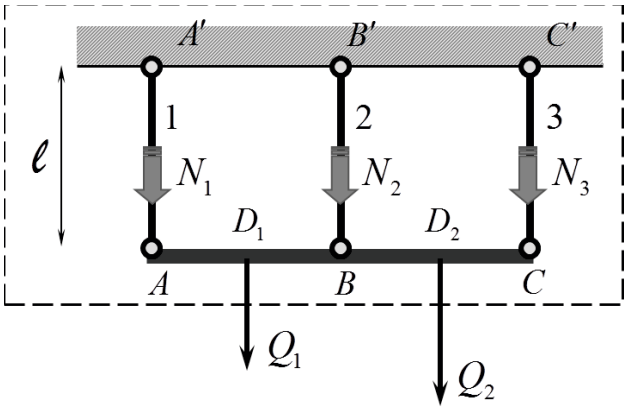

Figure 1. Description of the structure

1.3 Resistance of the elements of the structure

Since no load is applied to the rods except at their extremities by the support and by the rigid transverse beam and due to the fact that these extremities are pin connected with no resistance to bending moment, the internal forces in the vertical rods are constant axial forces. They are denoted N_1, N_2, N_3 and counted positive when tensile.

Regarding the resistance of the constituent elements of the structure, it is assumed that the support and the transverse beam are rigid – which amounts to saying that they can sustain any internal forces whatever their magnitudes – and that the resistances of the joints are infinite in tension or in compression. It follows that the only data to be introduced are the values of the resistances of the vertical rods to axial internal forces. The rods are supposed to be identical and their resistance is defined by Eq. (1)

(1) $$-L^- \le N_i \le L^+, \quad i = 1,2,3 .$$

1.4 The question

It is worth noticing that the data of this problem concern on the one side the structure itself, through the definition of its geometry and the definition of its loading mode which depends on two loading parameters and, on the other side, the elements of the structure which are only characterised by their resistances that are the bounds imposed to the internal forces.

The governing question of the problem is then to investigate whether it is possible to derive some relevant information regarding the resistance of the structure from those crude data. This question will be formulated as follows:

Given the geometry of the structure, given a load $\underline{Q} = (Q_1, Q_2)$*, is it possible to state whether the structure will sustain that load while complying with the resistance of its elements?*

As a short cut the question will also be referred to in terms of *"stability"*:

Is the structure "stable" under the load $\underline{Q} = (Q_1, Q_2)$ *?*

Consistently with the data of the problem, which do not provide any constitutive law for the behaviour of the constituent elements, this question does not refer to any loading process or loading path of the structure nor is there any mention of the initial state of internal forces. As a consequence the answer, if any, will be valid whatever those missing data, but it may be expected that it will suffer some drawbacks which will be commented later on.

2 Potential stability of the structure

2.1 A necessary condition for the stability of the structure

As the meaning of the word "stability" here is explicited in the full version of the question, it follows that a necessary condition to be satisfied for the stability of the structure is the mathematical compatibility between the equations of equilibrium of the structure and Eq. (1) which defines the resistance of its elements.

The two equilibrium equations of the structure are written:

$$\begin{cases} N_1 + N_2 + N_3 = Q_1 + Q_2 \\ 2N_1 - 2N_3 = Q_1 - Q_2 . \end{cases} \tag{2}$$

The structure is statically indeterminate with degree 1. Taking into account Eqs (2) the internal forces in the rods may be written as functions of Q_1, Q_2 and N_2 which is taken as the redundant unknown

$$\begin{cases} N_1 = -N_2 / 2 + 3Q_1 / 4 + Q_2 / 4 \\ N_3 = -N_2 / 2 + 3Q_2 / 4 + Q_1 / 4 . \end{cases} \tag{3}$$

Then Eq. (1) yields:

$$\begin{cases} -2L^+ + 3Q_1 / 2 + Q_2 / 2 \le N_2 \le 2L^- + 3Q_1 / 2 + Q_2 / 2 \\ -L^- \le N_2 \le L^+ \\ -2L^+ + Q_1 / 2 + 3Q_2 / 2 \le N_2 \le 2L^- + Q_1 / 2 + 3Q_2 / 2 . \end{cases} \tag{4}$$

The necessary condition for the existence of at least one set of values N_1, N_2, N_3 satisfying Eqs (1) and (2) is just the existence of N_2 complying with Eqs (4). Writing the mathematical compatibility of the double inequalities in Eqs (4) we obtain:

$$\begin{cases} -6L^- \le 3Q_1 + Q_2 \le 6L^+ \\ -6L^- \le Q_1 + 3Q_2 \le 6L^+ \\ -2(L^+ + L^-) \le Q_1 - Q_2 \le 2(L^+ + L^-) . \end{cases} \tag{5}$$

These conditions must be satisfied by the load $\underline{Q} = (Q_1, Q_2)$ for the existence of at least one set of values N_1, N_2, N_3 satisfying Eqs (1) and (2). They are a necessary condition

for the stability of the structure subjected to $\underline{Q}$. In the two-dimensional loading space, Eqs (5) define a convex domain as shown in Figure 2, which will be denoted by K.

2.2 Instability and potential stability of the structure

It is clear from the rationale which has been developed that any load $\underline{Q}$ **outside** K **will not be sustained** by the structure with the resistance of its elements defined by Eq. (1): the structure is not stable under such a load since it cannot be equilibrated by internal forces complying with Eq. (1). Such loads will be called "**certainly unsafe**".

Regarding the loads **inside** K, the conclusion which can be derived is restricted to **potential stability**. It means that, since we have only been working with a succession of necessary conditions for stability, it is not possible to assert that the structure will be stable under such a load. We can only state, as the logical converse of the above statement about the certainly unsafe loads, that the structure **may be** stable under a load $\underline{Q}$ inside K, depending on the data which have not been specified when setting the problem: initial state of internal forces, loading history, constitutive equation. The loads inside K will thus be called "**potentially safe**" loads.

The loads lying on the boundary of domain K are called the "**extreme**" loads for the problem.

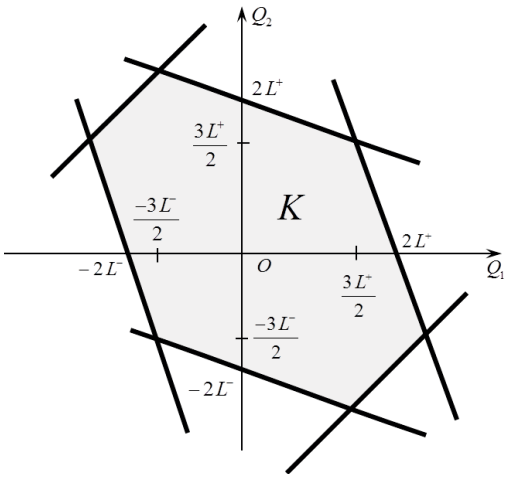

Figure 2. Convex K in the loading space of the structure

3 To what extent is potential stability a relevant concept?

So far, the problem has been treated in its mathematical form without knowing the physical origin of the limits set to the resistance of the rods. This means that the results in terms of "certainly unsafe", "potentially safe" and "extreme" loads are valid in the given geometry, whatever that origin. For instance the limits may come from physical phenomena such as brittle behaviour, plastic behaviour or instability. They may be either the original values determined from the tests performed on the elements to determine their resistance or their constitutive law or they may be

conventional values derived from these tests through the application of various coefficients ("factors") for safety or other reasons, which is the most frequent case. In plain words, the results for what concerns the "certainly unsafe" loads set a limit frame which cannot be exceeded once Eq. (1) has been accepted as the "rule of the game". As an example, Figure 3 presents the results of Figure 2 when $L^- = 0$ and $L^+ = L$, a model for the structure when $A'A$, $B'B$ and $C'C$ are cables with zero resistance to compression due to buckling instability.

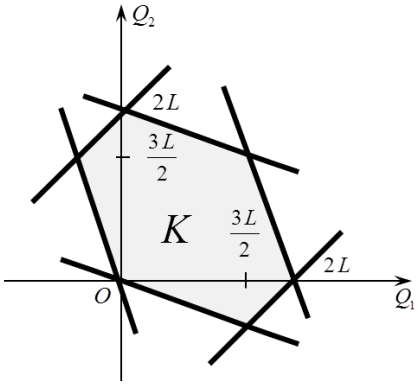

Figure 3. Convex K in the case of no resistance to compression

But it must be observed also that the answer given in section 2.2 to the initial question of section 1.4 is just a partial one through the concept of **potential** stability, which may appear somewhat frustrating for practical applications. It is therefore quite natural to investigate whether a more affirmative conclusion could be derived from the same data.

With this object in view, we will try to investigate the relevance of the extreme loads of the structure in various circumstances depending on the "missing data" which will now be introduced, such as the constitutive laws of the elements, including their behaviour when the limit of resistance is reached, the loading path and loading history of the structure in Figure 1, including the initial state of internal forces.

Linearly elastic and perfectly plastic rods

Let us first assume that the rods in Figure 1 are linearly elastic (with cross section area S and Young modulus E) and exhibit a perfectly plastic behaviour when their limits of resistance either in tension or compression are reached. The loading path starts from $\underline{Q} = (Q_1, Q_2) = 0$ with the initial state of internal forces $N_1 = N_2 = N_3 = 0$. Not taking into account any geometry change, the analysis is classical (*e.g.* [1]). It brings out first the existence of an elastic domain in the loading space where the behaviour of the structure remains linearly elastic. Then it shows that the loading process of the structure can be continued until the boundary of K is reached by the loading path (Figure 4). In other words the loading process of the structure can be pursued until the corresponding extreme load is reached.

If the initial self-equilibrated state of internal forces complying with Eq. (1) is no more zero the same result is obtained as regards the relevance of the extreme loads, while the initial elastic domain changes.

As a conclusion: assuming no geometry change and under the hypothesis of linear elasticity and perfect plasticity for the constitutive law of the elements, the answer to the initial question is independent of the initial state of internal forces and of the loading path: potential stability amounts to stability as defined in the present context.

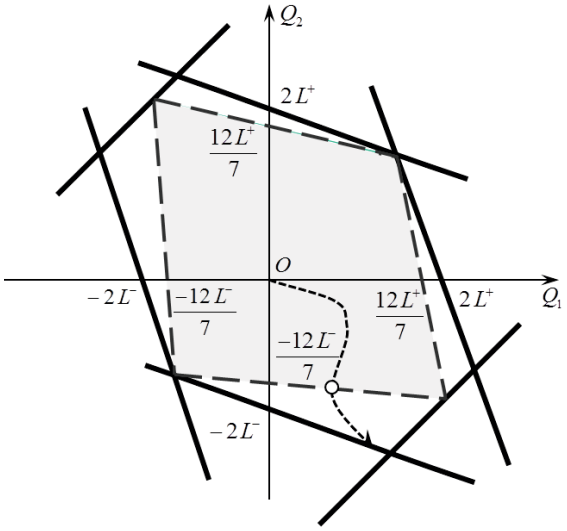

Figure 4. Elastic domain and convex K

Linearly elastic and perfectly plastic/brittle rods

For the same structure we now assume that the rods are linearly elastic (with cross section area S and Young modulus E) in tension and compression, perfectly plastic in compression, and that they exhibit brittle behaviour in tension when the limit value L^+ is reached (Figure 5).

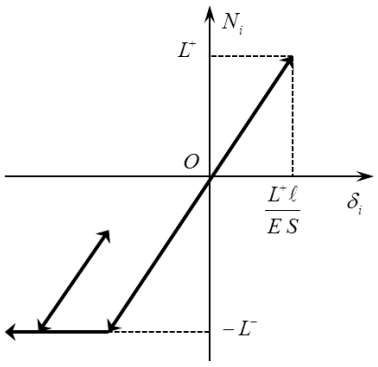

Figure 5. Linearly elastic, perfectly plastic/brittle behaviour

The loading path starts from $\underline{Q}=(Q_1,Q_2)=0$ with the initial state of internal forces $N_1=N_2=N_3=0$ and, just for simplicity, we consider the particular case of a radial loading where Q_1 is kept equal to zero and Q_2 is made to increase.

From the elastic domain in Figure 4, we see that the elastic behaviour of the structure is maintained until $Q_2=\frac{12}{7}L^+$. For this value the tensile force in $C'C$ is $N_3=L^+$. It

results in the brittle fracture of that rod with N_3 dropping to zero. Then, from Eqs (2), equilibrium of the structure would require $N_2 = \frac{18}{7} L^+$, which induces brittle fracture of the rod $B'B$ and, as a consequence, the collapse of the structure.

The conclusion is that, following this loading path and starting from the initial state of zero internal forces, the extreme load $(Q_1 = 0,\ Q_2 = 2L^+)$ cannot be sustained by the structure.

It is clear however that this conclusion is highly dependent on the initial state of internal forces when $\underline{Q} = (Q_1, Q_2) = 0$ and on the chosen loading path as shown by the two following examples.

- If we follow the same loading path with $Q_1 = 0$ and start from the initial self-equilibrated state of internal forces defined by

(6) $$N_1 = -\frac{L^+}{6},\ N_2 = \frac{L^+}{3},\ N_3 = -\frac{L^+}{6},$$

  provided the condition $L^+ < L^-$ is satisfied, then the extreme load $(Q_1 = 0,\ Q_2 = 2L^+)$ will be reached.

- If the radial loading path defined by $Q_1 = Q_2$ is followed, starting from the same initial zero state of internal forces, the extreme loads (either positive or negative) will be sustained.

As a conclusion

As it was already said the "extreme" loads, at the boundary of the domain of the potentially safe loads, set the limits of the resistance of the structure. Thanks to the simplicity of the mechanical model involved, two thorough analyses were easily performed with completed data for the constitutive laws of the constituent elements and on the loading path and loading history of the structure. They have shown that the incomplete relevance of the answer, which is marked by the adjective "potential", is not due to the rationale of the Yield Design approach but is a consequence of the set of available data being restricted.

Physically, full relevance of the Yield design approach is essentially linked to the possibility for the elements to reach and sustain their limit of resistance without breaking. They must exhibit **ductility** as opposed to **brittle** fracture.

When brittle behaviour is encountered, if the loading path is given, **pre-stressing** of the structure by a conveniently determined initial state of internal forces makes it possible to reach the corresponding extreme load when this loading path is followed.

In addition, the assumption that **geometry changes remain negligible** during the whole loading process must be checked systematically. This necessity comes out clearly from second order analyses, taking into account the geometry changes during the loading process, which have been carried out on simple structures made up of linearly elastic and perfectly plastic elements: they brought out what is called the "P-δ " effect, meaning that the actual maximum load that can be supported by the

structure may be either higher or lower than the extreme load determined through the Yield Design approach, depending on the geometric characteristics of the structure [2].

More comments on this topic will appear in Chapter IV (§ 3.4).

REFERENCES

[1] SALENÇON, J. (2000) – *de l'Élasto-plasticité au Calcul à la rupture*. Éditions de l'École polytechnique, Palaiseau, publ.

[2] FONDER, G. A. (1972) – Les effets du second ordre – Le flambement en masse. *Méthodes de calcul aux états limites des structures à barres*. C.T.I.C.M., pp. 507-551.

Chapter III

The continuum mechanics Framework

Modelling the continuum

Dynamics

The theory of virtual work

Statically and Kinematically admissible fields

References

THE CONTINUUM MECHANICS FRAMEWORK

Chapter IV will be devoted to a first step in the presentation of the general theory of Yield Design: the primal approach, which follows the same track as in the example that has just been analysed. The mechanical framework chosen for this presentation is the classical 3D continuum mechanics model which is, at the same time, sufficiently general to be transposed easily later to more or less sophisticated models and quite frequently used for the many applications of the theory to various practical problems. This Chapter recalls the basic fundamental concepts and results of the classical presentation of the continuum mechanics model. We leave it to the reader to refer to comprehensive textbooks and treaties for more precisely detailed and alternative presentations (*e.g.* [1-8]).

1 Modelling the continuum

1.1 Geometrical description

The concept of a continuous medium is a macroscopic physical model arising from common experience. Its mathematical formulation is represented by a volume Ω made up of particles on the differential level. The geometrical state of the system is described by the position of these particles in a reference frame: $\underline{x} = \underline{OM}$ is the position vector of such a particle in a given configuration of the system[1].

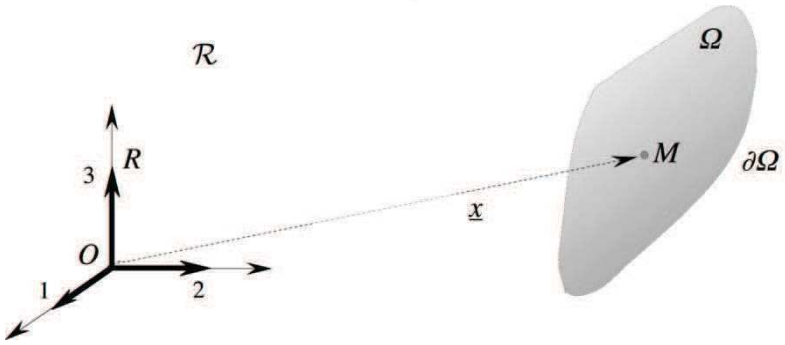

Figure 1. Geometrical description of a system

[1] Notation: one-stroke underlined symbols denote vectors.

1.2 Kinematics

The velocity field

The evolution of the system at a given instant of time t is defined, from the geometrical point of view, by the velocity field of the constituent particles at that instant. For the particle at the point M the velocity is denoted:

$$\underline{U}(\underline{x},t)=\frac{\mathrm{d}}{\mathrm{d}t}(\underline{OM})\,. \tag{1}$$

Since the intuitive perception of *continuity* of the medium appeals to the evolution of the system, during which particles initially close together remain so, the velocity field $\underline{U}(\underline{x},t)$ is subjected to the following mathematical conditions: **piecewise continuity and continuous differentiability** with respect to space and time in Ω.

The strain rate field

The **gradient** of $\underline{U}(\underline{x},t)$ is the second rank tensor noted[2]

$$\underline{\underline{\mathrm{grad}}}\,\underline{U}(\underline{x},t)=\frac{\partial U_i}{\partial x_j}\underline{e}_i\otimes\underline{e}_j \tag{2}$$

with summation on the repeated indices (dummy index convention), where $\underline{e}_i$ $(i=1,\,2,\,3)$ are the unit vectors of an orthonormal basis, and $\otimes$ is the notation for the tensor product.

This tensor is the relevant operator to follow the variation of the metric during the infinitesimal evolution at time t .

Let $\underline{\mathrm{d}M}$ be an infinitesimal material vector at point M

$$\underline{\mathrm{d}M}=\underline{e}_k\mathrm{d}x_k\,; \tag{3}$$

it becomes $\underline{\mathrm{d}M}+(\frac{\mathrm{d}}{\mathrm{d}t}\underline{\mathrm{d}M})\mathrm{d}t$ at time $(t+\mathrm{d}t)$ and we get from Eq. (1)

$$(\frac{\mathrm{d}}{\mathrm{d}t}\underline{\mathrm{d}M})=(\frac{\partial U_i}{\partial x_j}\mathrm{d}x_j)\,\underline{e}_i\,. \tag{4}$$

Denoting by "." the scalar product or dot product, this equation is written:

$$(\frac{\mathrm{d}}{\mathrm{d}t}\underline{\mathrm{d}M})=\frac{\partial U_i}{\partial x_j}\underline{e}_i\,(\underline{e}_j\,.\,\underline{e}_k)\,\mathrm{d}x_k=(\frac{\partial U_i}{\partial x_j}\underline{e}_i\otimes\underline{e}_j).(\underline{e}_k\,\mathrm{d}x_k)=\underline{\underline{\mathrm{grad}}}\,\underline{U}(\underline{x},t).\underline{\mathrm{d}M}\,. \tag{5}$$

Let us now consider the variation of the scalar product of 2 infinitesimal material vectors $\underline{\mathrm{d}M}$ and $\underline{\mathrm{d}M'}$ at point M . From Eq. (5) we derive:

$$\frac{\mathrm{d}}{\mathrm{d}t}(\underline{\mathrm{d}M}.\underline{\mathrm{d}M'})=\underline{\mathrm{d}M}.(\underline{\underline{\mathrm{grad}}}\,\underline{U}(\underline{x},t).\underline{\mathrm{d}M'})+\underline{\mathrm{d}M'}.(\underline{\underline{\mathrm{grad}}}\,\underline{U}(\underline{x},t).\underline{\mathrm{d}M})\,. \tag{6}$$

[2] Notation: two-stroke underlined symbols denote second-rank tensors.

By introducing the symmetric tensor[3]

$$\underline{\underline{d}}(\underline{x},t)=\frac{1}{2}(\underline{\underline{\mathrm{grad}\,U}}(\underline{x},t)+{}^{\mathrm{t}}\,\underline{\underline{\mathrm{grad}\,U}}(\underline{x},t))=\frac{1}{2}(\frac{\partial U_i}{\partial x_j}+\frac{\partial U_j}{\partial x_i})\,\underline{e}_i\otimes\underline{e}_j \tag{7}$$

Eq. (6) becomes

$$\frac{\mathrm{d}}{\mathrm{d}t}(\underline{\mathrm{d}M}.\underline{\mathrm{d}M'})=2\,\underline{\mathrm{d}M}.\underline{\underline{d}}\,(\underline{x},t).\underline{\mathrm{d}M'}=2\,d_{ij}\mathrm{d}x_i\mathrm{d}x_j\,. \tag{8}$$

The tensor $\underline{\underline{d}}(\underline{x},t)$ is the **strain rate** tensor.

With $\underline{\mathrm{d}M}=\underline{\mathrm{d}M'}=\underline{e}_1\mathrm{d}s$ in Eq. (8) we obtain the **rate of extension** of any infinitesimal material vector $\underline{\mathrm{d}M}$

$$\frac{\mathrm{d}}{\mathrm{d}t}(\mathrm{d}s)=d_{11}(\underline{x},t)\,\mathrm{d}s. \tag{9}$$

The rate of angular distortion of two orthogonal infinitesimal material vectors $\underline{\mathrm{d}M}_1=\underline{e}_1\mathrm{d}s_1$ and $\underline{\mathrm{d}M}_2=\underline{e}_2\mathrm{d}s_2$ is $\dot{\theta}$, such that $\frac{\mathrm{d}}{\mathrm{d}t}(\underline{\mathrm{d}M}_1.\underline{\mathrm{d}M}_2)=\dot{\theta}\,\mathrm{d}s_1\,\mathrm{d}s_2$, as shown in Figure 2. From Eq. (8) we obtain:

$$\dot{\theta}=2\,d_{12}(\underline{x},t)\,. \tag{10}$$

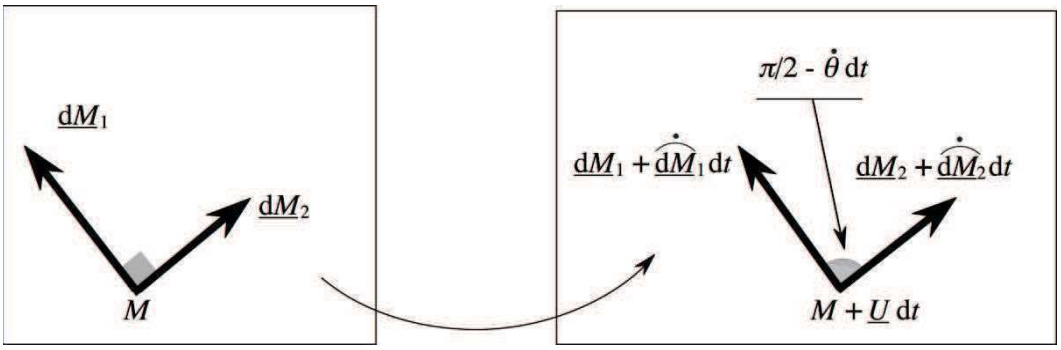

Figure 2. Rate of angular distortion of two orthogonal material vectors

Since $\underline{\underline{d}}(\underline{x},t)$ is a symmetric Euclidean tensor the eigenvectors of its associated linear mapping are real and mutually orthogonal. They define the **principal axes** of the tensor. In the orthonormal basis of its principal axes, $\underline{\underline{d}}(\underline{x},t)$ is written

$$\underline{\underline{d}}(\underline{x},t)=d_1(\underline{x},t)\,\underline{e}_1\otimes\underline{e}_1+d_2(\underline{x},t)\,\underline{e}_2\otimes\underline{e}_2+d_3(\underline{x},t)\,\underline{e}_3\otimes\underline{e}_3 \tag{11}$$

and it follows from Eq. (10) that a triad of infinitesimal material vectors attached to the material point M remains orthogonal in the infinitesimal transformation between t and $(t+\mathrm{d}t)$ while its orientation is conserved.

[3] The symbol " $^{\mathrm{t}}$ "denotes the transpose of the concerned tensor.

The **rate of volume dilatation** is easily obtained considering such a triad of infinitesimal material vectors along the principal axes of $\underline{\underline{d}}(\underline{x},t)$ (Figure 3)

$$\frac{\mathrm{d}}{\mathrm{d}t}(\mathrm{d}\Omega) = \mathrm{tr}\,\underline{\underline{d}}(\underline{x},t)\,\mathrm{d}\Omega = \mathrm{div}\,\underline{U}(\underline{x},t)\,\mathrm{d}\Omega\,. \tag{12}$$

As a consequence, an evolution in which there is no volume change at time t (isochoric evolution) is characterised by the zero divergence condition:

$$\mathrm{div}\,\underline{U}(\underline{x},t) = 0. \tag{13}$$

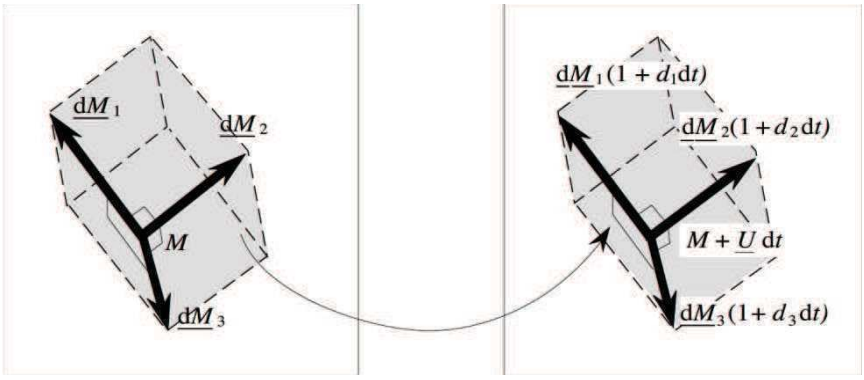

Figure 3. Triad of material vectors along the principal axes of $\underline{\underline{d}}(\underline{x},t)$

1.3 Conservation of mass

The mass of a system is obtained as the integral on the volume Ω of a finite volume density which is the mass per unit volume

$$\mathcal{M} = \int_\Omega \rho(\underline{x},t)\,\mathrm{d}\Omega = \int_\Omega \mathrm{d}m \tag{14}$$

where $\mathrm{d}m$ appears as the mass of the infinitesimal material element with volume $\mathrm{d}\Omega$.

According to the fundamental principle of mass conservation in classical mechanics, the total derivative of $\mathcal{M}$ with respect to time must be zero. It yields the **continuity equation** in the global form:

$$\frac{\mathrm{d}}{\mathrm{d}t}\mathcal{M} = \frac{\mathrm{d}}{\mathrm{d}t}\int_\Omega \rho(\underline{x},t)\,\mathrm{d}\Omega = \int_\Omega \frac{\mathrm{d}}{\mathrm{d}t}(\mathrm{d}m) = 0 \tag{15}$$

and, in the case of continuous and continuously differentiable fields ρ and $\underline{U}$, the local form

$$\frac{\partial \rho}{\partial t}(\underline{x},t) + \mathrm{div}\,\rho(\underline{x},t)\underline{U}(\underline{x},t) = 0 \tag{16}$$

If these fields are just piecewise continuous and continuously differentiable, the continuity equation must also be expressed on any discontinuity surface Σ with normal $\underline{n}$ and propagation velocity $\underline{W}$:

$$[\![\rho(\underline{U} - \underline{W})]\!].\underline{n} = 0 \tag{17}$$

with $[\![\ ]\!]$ the jump of the concerned quantity when crossing Σ in the direction of $\underline{n}$.

2 Dynamics

2.1 Quantity of acceleration

The acceleration of the particle at point M is denoted $\underline{a}(\underline{x},t)$. The quantity of acceleration of the material element with volume $\mathrm{d}\Omega$ and mass $\mathrm{d}m$ is

(18) $$\underline{a}(\underline{x},t)\,\mathrm{d}m = \rho(\underline{x},t)\,\underline{a}(\underline{x},t)\,\mathrm{d}\Omega .$$

2.2 External forces

External forces acting on the system are modelled by volume densities of forces (body forces) acting within the volume Ω and surface densities of forces acting on its boundary $\partial\Omega$.

More precisely, the **body forces** are described by a density per unit mass $\underline{F}(\underline{x},t)$ in such a way that the infinitesimal body force acting on the element $\mathrm{d}\Omega$ at point M is given by

(19) $$\underline{F}(\underline{x},t)\,\mathrm{d}m = \rho(\underline{x},t)\,\underline{F}(\underline{x},t)\,\mathrm{d}\Omega .$$

The **surface forces** are defined at each point of $\partial\Omega$ by a surface density $\underline{T}(\underline{x},t)$ and the infinitesimal force acting on the surface element $\mathrm{d}a$ is

(20) $$\underline{\mathrm{d}f}(\underline{x},t) = \underline{T}(\underline{x},t)\,\mathrm{d}a .$$

2.3 Internal forces: the Cauchy stress tensor

The following presentation adopts the classical viewpoint historically introduced by Cauchy [9].

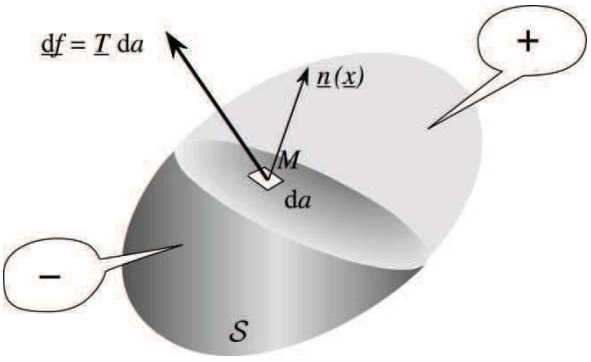

Figure 4. Internal contact forces modelled by the stress vector

The fundamental hypothesis is that the only internal forces in the system S are contact forces between its constituent particles. At any point M within Ω, consider a surface element $\mathrm{d}a$ with normal $\underline{n}(\underline{x})$: it is assumed that the forces exerted by the particles infinitely close to $\mathrm{d}a$ on the (+) side on the particles infinitely close to $\mathrm{d}a$ on the (-) side can be modelled by a force acting at M and proportional to $\mathrm{d}a$ (Figure 4)

(21) $$\underline{\mathrm{d}f} = \underline{T}(\underline{x},t,\underline{n}(\underline{x}))\,\mathrm{d}a .$$

The vector $\underline{T}(\underline{x},t,\underline{n}(\underline{x}))$ is the **stress vector** acting at point M on the facet $\mathrm{d}a$ with normal $\underline{n}(\underline{x})$ at time t.

Through the "small tetrahedron" argument illustrated in Figure 5 it is proven that $\underline{T}(\underline{x},t,\underline{n}(\underline{x}))$ is a **linear function** of $\underline{n}(\underline{x})$ through a second rank tensor $\underline{\underline{\sigma}}(\underline{x},t)$:

$$\begin{cases} \underline{T}(\underline{x},t,\underline{n}(\underline{x})) = \underline{\underline{\sigma}}(\underline{x},t).\underline{n}(\underline{x}) \\ \underline{\underline{\sigma}}(\underline{x},t) = \sigma_{ij}(\underline{x},t)\,\underline{e}_i \otimes \underline{e}_j \end{cases} \tag{22}$$

The tensor $\underline{\underline{\sigma}}(\underline{x},t)$ is the **Cauchy stress tensor** at point M at time t.

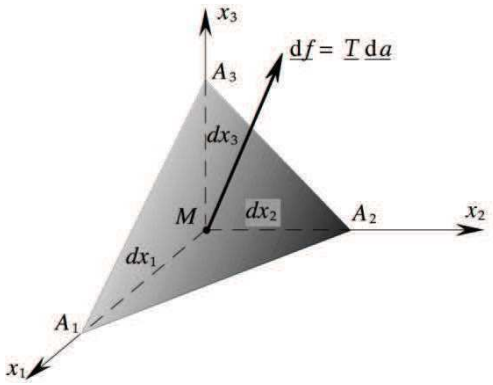

Figure 5. The small tetrahedron argument

Then, the "small parallelepiped" argument, illustrated in Figure 6, is used to prove the **symmetry** of $\underline{\underline{\sigma}}(\underline{x},t)$

$$\sigma_{ij}(\underline{x},t) = \sigma_{ji}(\underline{x},t). \tag{23}$$

2.4 Equation of motion

Through the same small parallelepiped argument the equation of motion is obtained in its explicit form in orthonormal Cartesian coordinates:

$$\begin{cases} \dfrac{\partial \sigma_{xx}}{\partial x} + \dfrac{\partial \sigma_{xy}}{\partial y} + \dfrac{\partial \sigma_{xz}}{\partial z} + \rho(F_x - a_x) = 0 \\ \dfrac{\partial \sigma_{yx}}{\partial x} + \dfrac{\partial \sigma_{yy}}{\partial y} + \dfrac{\partial \sigma_{yz}}{\partial z} + \rho(F_y - a_y) = 0 \\ \dfrac{\partial \sigma_{zx}}{\partial x} + \dfrac{\partial \sigma_{zy}}{\partial y} + \dfrac{\partial \sigma_{zz}}{\partial z} + \rho(F_z - a_z) = 0 \end{cases} \tag{24}$$

This vector equation can be written

$$\forall M \in \Omega,\ \mathrm{div}\,\underline{\underline{\sigma}}(\underline{x},t) + \rho(\underline{x},t)\left(\underline{F}(\underline{x},t) - \underline{a}(\underline{x},t)\right) = 0 \tag{25}$$

where

$$\mathrm{div}\,\underline{\underline{\sigma}}(\underline{x},t) = \frac{\partial \sigma_{ij}}{\partial x_j}(\underline{x},t)\,\underline{e}_i\,. \tag{26}$$

It is the **field equation of motion** that must be satisfied at any point inside Ω.

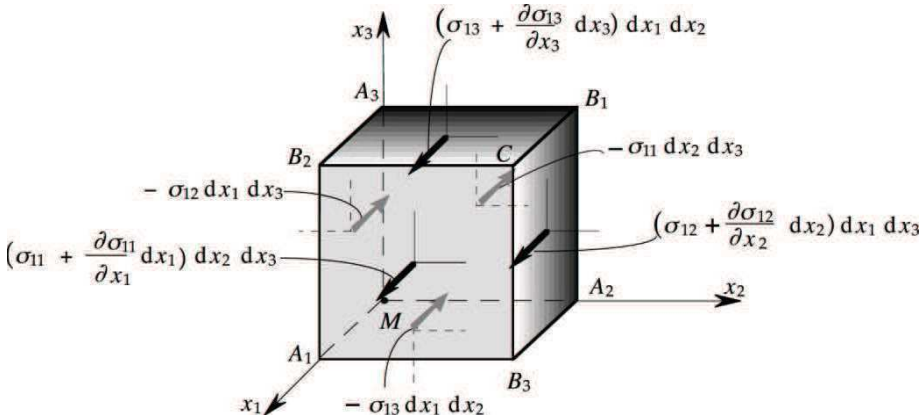

Figure 6. The small parallelepiped argument

The explicit form of the equation of motion in cylindrical coordinates is also of great practical importance:

$$(27)\qquad \begin{cases} \dfrac{\partial \sigma_{rr}}{\partial r} + \dfrac{1}{r}\dfrac{\partial \sigma_{r\theta}}{\partial \theta} + \dfrac{\partial \sigma_{rz}}{\partial z} + \dfrac{\sigma_{rr} - \sigma_{\theta\theta}}{r} + \rho(F_r - a_r) = 0 \\ \dfrac{\partial \sigma_{\theta r}}{\partial r} + \dfrac{1}{r}\dfrac{\partial \sigma_{\theta\theta}}{\partial \theta} + \dfrac{\partial \sigma_{yz}}{\partial z} + 2\dfrac{\sigma_{r\theta}}{r} + \rho(F_\theta - a_\theta) = 0 \\ \dfrac{\partial \sigma_{zr}}{\partial r} + \dfrac{1}{r}\dfrac{\partial \sigma_{z\theta}}{\partial \theta} + \dfrac{\partial \sigma_{zz}}{\partial z} + \rho(F_z - a_z) = 0 \end{cases}$$

At the boundary of the system, the equation of motion can be interpreted as expressing the equilibrium between the surface external forces acting on the surface element da on its external side and the surface contact internal forces acting on this same element (Figure 7) on its internal side. Hence the boundary equilibrium equation is written

$$(28)\qquad \forall M \in \partial\Omega,\ \underline{\underline{\sigma}}(\underline{x},t).\underline{n}(\underline{x}) = \underline{T}(\underline{x},t)\,.$$

In other words, the stress vector $\underline{T}(\underline{x},t,-\underline{n}(\underline{x}))$ acting on da with normal $-\underline{n}(\underline{x})$ equilibrates the surface external force acting on the same element.

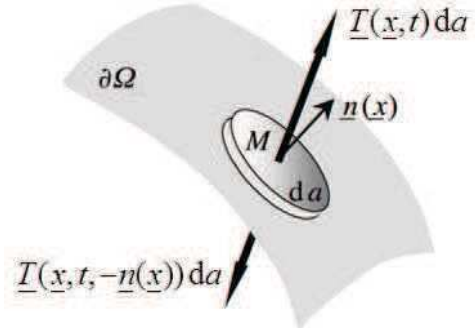

Figure 7. Stress vector on the boundary of S

2.5 Discontinuity of the Cauchy stress field

The Cauchy stress tensor field must be piecewise continuous and continuously differentiable. The equation of motion should also be expressed on the jump surfaces $\Sigma_{\underline{\underline{\sigma}}}$ of this stress field in the form of a jump equation (Figure 8).

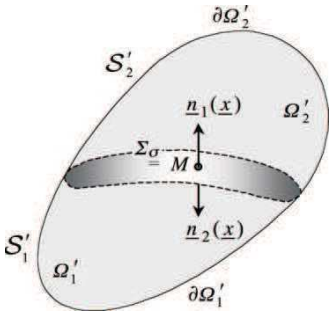

Figure 8. Cauchy stress field discontinuous on $\Sigma_{\underline{\underline{\sigma}}}$

Provided there is no surface density of external forces and no discontinuity of the velocity field (shock wave) on $\Sigma_{\underline{\underline{\sigma}}}$ the equation of motion on that surface is written:

(29) $$\forall M \in \Sigma_{\underline{\underline{\sigma}}},\ [\![\underline{\underline{\sigma}}(\underline{x},t)]\!].\underline{n}(\underline{x},t) = 0$$

which means that across a discontinuity surface of the stress field, **the stress vector** acting on the facet tangent to that surface **is continuous**.

Figure 9 illustrates a demonstration of this result, following the spirit of the small tetrahedron and small parallelepiped arguments. The jump surface is split into two parallel surfaces Σ_1 and Σ_2 separated by an infinitesimal distance λ: the fundamental law of mechanics applied to the small parallelepiped region limited by these two surfaces, to order zero in λ, yields:

(30) $$\underline{\underline{\sigma}}^2(\underline{x},t).\underline{n}(\underline{x})\,\mathrm{d}a - \underline{\underline{\sigma}}^1(\underline{x},t).\underline{n}(\underline{x})\,\mathrm{d}a = 0\,.$$

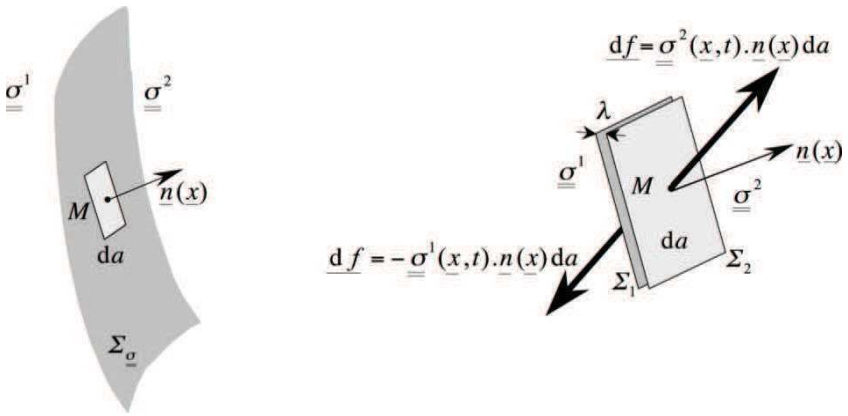

Figure 9. Discontinuous stress field: small parallelepiped argument

It is worth noting that, from a mathematical point of view, Eq. (29) is actually the jump equation associated with Eq. (25) as a conservation law; one may also say that Eq. (29) is embedded in Eq. (25) within the framework of the theory of distributions.

If a surface density of external forces or a discontinuity of the velocity field (shock wave) exists on $\Sigma_{\underline{\underline{\sigma}}}$, Eq. (29) is modified. The corresponding jump equations for Eq. (25) can be obtained mathematically through the theory of distributions or be easily established through the same demonstration as above in Figure 9 (*v.z.* [6]).

2.6 Local analysis of stresses

At point M, Eq. (22) defines the linear map which determines the stress vector $\underline{T}(\underline{x},t,\underline{n})$ for any facet with normal $\underline{n}$ passing through this point.

From the stress vector we define the normal stress σ acting on the facet as the component of $\underline{T}(\underline{x},t,\underline{n})$ along $\underline{n}$; the component $\underline{\tau}$ in the plane of the facet is the tangential stress or shear stress (Figure 10)

(31) $$\underline{T}(\underline{x},t,\underline{n}) = \sigma(\underline{x},t,\underline{n})\,\underline{n} + \underline{\tau}(\underline{x},t,\underline{n}).$$

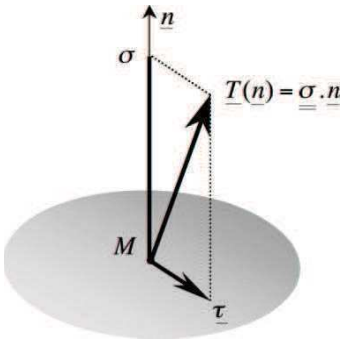

Figure 10. Normal stress and shear stress

From the symmetry of the Euclidean tensor $\underline{\underline{\sigma}}(\underline{x},t)$ it follows that the three eigenvectors of the linear mapping defined by Eq. (22) are real and mutually orthogonal. They define the principal axes of $\underline{\underline{\sigma}}(\underline{x},t)$. The corresponding principal values of $\underline{\underline{\sigma}}$ are the principal stresses $\sigma_1, \sigma_2, \sigma_3$.

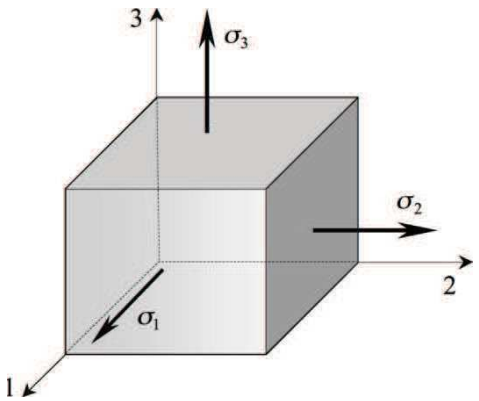

Figure 11. Stress vectors on facets normal to the principal axes of $\underline{\underline{\sigma}}$

Relative to an orthonormal basis arranged to coincide with the principal axes, $\underline{\underline{\sigma}}(\underline{x},t)$ is written

(32) $$\underline{\underline{\sigma}}(\underline{x},t)=\sigma_1(\underline{x},t)\,\underline{e}_1\otimes\underline{e}_1+\sigma_2(\underline{x},t)\,\underline{e}_2\otimes\underline{e}_2+\sigma_3(\underline{x},t)\,\underline{e}_3\otimes\underline{e}_3\,.$$

For a facet orthogonal to a principal axis the stress vector is purely normal (there is no shear stress on such a facet) and its magnitude is equal to the corresponding principal stress (Figure 11). Mathematically speaking, this is a characteristic property of the principal axes.

3 The theory of virtual work

3.1 Virtual velocity fields

Virtual motions of the system S are defined by vector fields $\underline{\hat{U}}$ of **virtual velocities** given on Ω and $\partial\Omega$ which are required to be **piecewise continuous and continuously differentiable**. The same symbol $\underline{\hat{U}}$ is used to denote the virtual motion defined by a virtual velocity field $\underline{\hat{U}}$. It is essential to note that the set of the virtual motions of the system is a **vector space**.

Regarding the terminology, one should not be confused by the words "velocity" and "motion". As a matter of fact, real velocity fields of the system obviously generate a subset of the virtual motion vector space because, beside the regularity conditions, they must comply with imposed boundary conditions, constitutive laws, etc. From a mathematical point of view, the virtual velocity fields will be used as **test functions** in the **duality processes**.

In the same way as for the real velocity field we define the virtual strain rate field $\underline{\underline{\hat{d}}}$ from the gradient of $\underline{\hat{U}}$

(33) $$\underline{\underline{\hat{d}}}(\underline{x})=\frac{1}{2}\left(\underline{\underline{\operatorname{grad}\hat{U}}}(\underline{x})+{}^{t}\,\underline{\underline{\operatorname{grad}\hat{U}}}(\underline{x})\right).$$

If $\Sigma_{\underline{\hat{U}}}$ is a jump surface for the field $\underline{\hat{U}}$, the discontinuity at point M following the outward normal $\underline{n}$ is denoted $[\![\underline{\hat{U}}(\underline{x})]\!]=\underline{\hat{U}}^{2}(\underline{x})-\underline{\hat{U}}^{1}(\underline{x})$ (Figure 12).

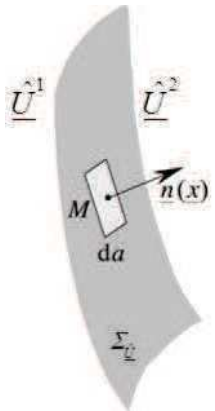

Figure 12. Discontinuous virtual velocity field

3.2 Theorem/Principle of virtual work

The divergence theorem

The divergence theorem for a piecewise continuous and continuously differentiable vector field $\underline{V}$ defined in Ω and on $\partial\Omega$, with $\Sigma_{\underline{V}}$ denoting the jump surfaces is written

$$\int_{\Omega} \operatorname{div} \underline{V} \, \mathrm{d}\Omega + \int_{\Sigma_{\underline{V}}} [\![\underline{V}]\!] . \underline{n} \, \mathrm{d}\Sigma_{\underline{V}} = \int_{\partial\Omega} \underline{V} . \underline{n} \, \mathrm{d}a \,. \tag{34}$$

The same equation is valid for any Euclidean tensor field with the same differentiability conditions. As an example, let $\underline{\underline{T}}$ be a second rank Euclidean tensor field continuous and continuously differentiable in Ω, with $\Sigma_{\underline{\underline{T}}}$ denoting the jump surfaces, we have

$$\int_{\Omega} \operatorname{div} \underline{\underline{T}} \, \mathrm{d}\Omega + \int_{\Sigma_{\underline{\underline{T}}}} [\![\underline{\underline{T}}]\!] . \underline{n} \, \mathrm{d}\Sigma_{\underline{\underline{T}}} = \int_{\partial\Omega} \underline{\underline{T}} . \underline{n} \, \mathrm{d}a \tag{35}$$

where $\underline{\underline{T}} = T_{ij} \, \underline{e}_i \otimes \underline{e}_j$ and $\operatorname{div} \underline{\underline{T}} = \dfrac{\partial T_{ij}}{\partial x_j} \underline{e}_i$.

Theorem of virtual (rate of) work

As a particular application of Eq. (34) let us consider the case when $\underline{V} = \underline{\underline{\sigma}} . \hat{\underline{U}}$ where $\underline{\underline{\sigma}}$ is the Cauchy stress tensor field which satisfies Eqs (23), (25), (28) and (29), and $\hat{\underline{U}}$ is a virtual velocity field piecewise continuous and continuously differentiable. It is assumed that the fields $\hat{\underline{U}}$ and $\underline{\underline{\sigma}}$ have no common jump surface, $\Sigma_{\hat{\underline{U}}} \neq \Sigma_{\underline{\underline{\sigma}}}$.

Introducing ":" as the symbol for the doubly contracted product of two 2nd-rank tensors $\underline{\underline{t}}$ and $\underline{\underline{u}}$

$$\underline{\underline{t}} : \underline{\underline{u}} = t_{ij} \, u_{ji} \,, \tag{36}$$

the following identity is recalled

$$\operatorname{div} (\underline{\underline{\sigma}} . \hat{\underline{U}}) = \underline{\underline{\sigma}} : \underline{\underline{\operatorname{grad} \hat{U}}} + \hat{\underline{U}} . \operatorname{div} ({}^{\mathrm{t}}\underline{\underline{\sigma}}) \,, \tag{37}$$

and it is observed that, in consideration of the symmetry of $\underline{\underline{\sigma}}$, it may be written

$$\operatorname{div} (\underline{\underline{\sigma}} . \hat{\underline{U}}) = \underline{\underline{\sigma}} : \hat{\underline{\underline{d}}} + \hat{\underline{U}} . \operatorname{div} \underline{\underline{\sigma}} \tag{38}$$

with $\hat{\underline{\underline{d}}}$ defined by Eq. (33).

Applying the divergence theorem (34) we get

$$\int_{\Omega} \operatorname{div} (\underline{\underline{\sigma}} . \hat{\underline{U}}) \, \mathrm{d}\Omega + \int_{\Sigma_{\underline{\underline{\sigma}}} \cup \Sigma_{\hat{\underline{U}}}} [\![\underline{\underline{\sigma}} . \hat{\underline{U}}]\!] . \underline{n} \, \mathrm{d}\Sigma = \int_{\partial\Omega} (\underline{\underline{\sigma}} . \hat{\underline{U}}) . \underline{n} \, \mathrm{d}a \,. \tag{39}$$

Since $\Sigma_{\underline{\underline{\sigma}}}$ and $\Sigma_{\hat{\underline{U}}}$ are distinct from each other, the second term of the first hand of Eq. (39) can be split and reduces to the integral on $\Sigma_{\hat{\underline{U}}}$ in consideration of Eq. (29).

Combining Eqs (38) and (39) yields

$$\int_\Omega \underline{\underline{\sigma}} : \underline{\underline{\hat{d}}}\, \mathrm{d}\Omega + \int_{\Sigma_{\hat{U}}} (\underline{\underline{\sigma}}.[\![\underline{\hat{U}}]\!]).\underline{n}\, \mathrm{d}\Sigma = -\int_\Omega \underline{\hat{U}}.\mathrm{div}\,\underline{\underline{\sigma}}\, \mathrm{d}\Omega + \int_{\partial\Omega} (\underline{\underline{\sigma}}.\underline{\hat{U}}).\underline{n}\, \mathrm{d}a\,. \tag{40}$$

Taking Eq. (25) into account we finally obtain

$$\int_\Omega \underline{\underline{\sigma}} : \underline{\underline{\hat{d}}}\, \mathrm{d}\Omega + \int_{\Sigma_{\hat{U}}} (\underline{\underline{\sigma}}.[\![\underline{\hat{U}}]\!]).\underline{n}\, \mathrm{d}\Sigma = \int_\Omega \rho(\underline{F} - \underline{a}).\underline{\hat{U}}\ \mathrm{d}\Omega + \int_{\partial\Omega} \underline{T}.\underline{\hat{U}}\, \mathrm{d}a \tag{41}$$

which is valid whatever the virtual velocity field $\underline{\hat{U}}$ piecewise continuous and continuously differentiable with $\Sigma_{\hat{U}} \neq \Sigma_{\underline{\underline{\sigma}}}$.

Eq. (41) expresses the **theorem of virtual (rate of) work**.

Dual Statement

Given a second rank symmetric tensor field $\underline{\underline{\sigma}}$ defined in Ω and on $\partial\Omega$, let us assume that $\forall \underline{\hat{U}}$ a piecewise continuous and continuously differentiable field in Ω with $\Sigma_{\hat{U}} \neq \Sigma_{\underline{\underline{\sigma}}}$, the following equation holds

$$\int_\Omega \underline{\underline{\sigma}} : \underline{\underline{\hat{d}}}\, \mathrm{d}\Omega + \int_{\Sigma_{\hat{U}}} (\underline{\underline{\sigma}}.[\![\underline{\hat{U}}]\!]).\underline{n}\, \mathrm{d}\Sigma = \int_\Omega \rho\ (\underline{F} - \underline{a}).\underline{\hat{U}}\ \mathrm{d}\Omega + \int_{\partial\Omega} \underline{T}.\underline{\hat{U}}\, \mathrm{d}a\,, \tag{42}$$

then, the tensor field satisfies the equations of motion with the acceleration field $\underline{a}$, the body forces $\rho\underline{F}$ and the surface forces $\underline{T}$

$$\begin{cases} \forall M \in \Omega,\ \mathrm{div}\,\underline{\underline{\sigma}}(\underline{x},t) + \rho(\underline{x},t)(\underline{F}(\underline{x},t) - \underline{a}(\underline{x},t)) = 0 \\ \forall M \in \Sigma_{\underline{\underline{\sigma}}},\ [\![\underline{\underline{\sigma}}(\underline{x},t)]\!].\underline{n}(\underline{x},t) = 0 \\ \forall M \in \partial\Omega,\ \underline{\underline{\sigma}}(\underline{x},t).\underline{n}(\underline{x}) = \underline{T}(\underline{x},t). \end{cases} \tag{43}$$

Eq. (42) is the **dual** statement of the equations of motion. It can be rearranged to make the generic virtual rates of work more conspicuous:

$$\int_\Omega \rho\underline{F}.\underline{\hat{U}}\ \mathrm{d}\Omega + \int_{\partial\Omega} \underline{T}.\underline{\hat{U}}\, \mathrm{d}a - \int_\Omega \underline{\underline{\sigma}} : \underline{\underline{\hat{d}}}\, \mathrm{d}\Omega - \int_{\Sigma_{\hat{U}}} (\underline{\underline{\sigma}}.[\![\underline{\hat{U}}]\!]).\underline{n}\, \mathrm{d}\Sigma = \int_\Omega \rho\underline{a}.\underline{\hat{U}}\ \mathrm{d}\Omega \tag{44}$$

In the left-hand member of Eq. (44), the first two terms stand for the **virtual rate of work by the external forces** and the last two terms express the **virtual rate of work by the internal forces**. The right-hand member is the **virtual rate of work by the quantities of acceleration**.

Thence, the dual statement may be expressed in the form:

The sum of the virtual rate of work by the external forces and the virtual rate of work by the internal forces is equal to the virtual rate of work by the quantities of acceleration.

This statement may be taken as a basic principle for the modelling of external and internal forces (*e.g.* [6]).

4 Statically and Kinematically admissible fields

4.1 Volume and boundary data

Since the Yield Design approach is based upon the compatibility between equilibrium and resistance, only equilibrium problems will be considered from now on and we will refer to the equation of motion in its particular form corresponding to equilibrium ($\underline{a}=0$) and to the virtual work equation with zero virtual rate of work by the quantities of acceleration.

For such problems the data consist of volume data, with the given values of the body forces $\rho\underline{F}$ in Ω, and of boundary data which are given values either for the surface density of external forces $\underline{T}$ or for the velocity $\underline{U}$ on $\partial\Omega$. These boundary data take the following form (Figure 13):

Three mutually orthogonal components are given for the two vectors, $\underline{T}$ and $\underline{U}$.

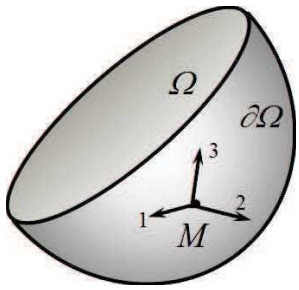

Figure 13. Boundary data

Introducing an index $i=1,2,3$ to denote the three directions of these orthogonal components, the known components are labelled by an upper index ^{d}:

$$\begin{cases} T_i^{d} & \text{on } S_{T_i} \\ U_i^{d} & \text{on } S_{U_i} \end{cases} \tag{45}$$

with

$$\begin{cases} S_{T_i} \cup S_{U_i} = \partial\Omega \\ S_{T_i} \cap S_{U_i} = \varnothing \end{cases}, \; i=1,2,3. \tag{46}$$

Note that the directions $i=1,2,3$ may vary from one point of $\partial\Omega$ to another.

4.2 Statically admissible stress fields

A stress field $\underline{\underline{\sigma}}$ is said to be statically admissible with the data $\rho\underline{F}$ in Ω and T_i^{d} on S_{T_i} if it is piecewise continuous and continuously differentiable and satisfies the equilibrium equations (25), (29), (28) with these data:

$$(47)\qquad \begin{cases} \operatorname{div} \underline{\underline{\sigma}}(\underline{x}) + \rho\, \underline{F}(\underline{x}) = 0 \text{ in } \Omega \\ [\![\underline{\underline{\sigma}}(\underline{x})]\!] . \underline{n}(\underline{x}) = 0 \text{ on } \Sigma_{\underline{\underline{\sigma}}} \\ \sigma_{ij} n_j = T_i^{\mathrm{d}} \text{ on } S_{T_i} \end{cases}$$

4.3 Kinematically admissible virtual velocity fields

A virtual velocity field $\underline{\hat{U}}$ is said to be kinematically admissible with the data U_i^{d} on S_{U_i} if it is piecewise continuous and continuously differentiable and such that:

$$(48)\qquad \hat{U}_i(\underline{x}) = U_i^{\mathrm{d}}(\underline{x}) \text{ on } S_{U_i} .$$

4.4 The virtual work equation

Let $\underline{\underline{\sigma}}$ be such a statically admissible stress field and $\underline{\hat{U}}$ a kinematically admissible virtual velocity field with the data $\rho \underline{F}$ in Ω and $T_i^{\mathrm{d}}, U_i^{\mathrm{d}}$ on $\partial\Omega$. Taking Eq. (46) into account, the virtual work equation (44) takes the form

$$(49)\qquad \int_\Omega \underline{\underline{\sigma}} : \underline{\underline{\hat{d}}}\, \mathrm{d}\Omega + \int_{\Sigma_{\underline{\hat{U}}}} (\underline{\underline{\sigma}} . [\![\underline{\hat{U}}]\!]) . \underline{n}\, \mathrm{d}\Sigma = \int_\Omega \rho \underline{F} . \underline{\hat{U}}\, \mathrm{d}\Omega + \sum_i \int_{S_{T_i}} T_i^{\mathrm{d}} \hat{U}_i\, \mathrm{d}a + \sum_i \int_{S_{U_i}} T_i(\underline{\underline{\sigma}}) U_i^{\mathrm{d}}\, \mathrm{d}a .$$

In this equation, the right-hand side is the virtual (rate of) work by **all the external forces in equilibrium with** $\underline{\underline{\sigma}}$ in the virtual velocity field $\underline{\hat{U}}$. It is denoted $\mathcal{P}_{\mathrm{e}}(\underline{\underline{\sigma}}, \underline{\hat{U}})$

$$(50)\qquad \mathcal{P}_{\mathrm{e}}(\underline{\underline{\sigma}}, \underline{\hat{U}}) = \int_\Omega \rho \underline{F} . \underline{\hat{U}}\, \mathrm{d}\Omega + \sum_i \int_{S_{T_i}} T_i^{\mathrm{d}} \hat{U}_i\, \mathrm{d}a + \sum_i \int_{S_{U_i}} T_i(\underline{\underline{\sigma}}) U_i^{\mathrm{d}}\, \mathrm{d}a .$$

Note that the left-hand side of Eq. (49) is the opposite of the virtual rate of work by the internal forces due to the presence of the minus signs in Eq. (44) where this virtual work is defined.

REFERENCES

[1] CHADWICK, P. (1999) – *Continuum Mechanics: Concise Theory and Problems*. Dover Publ. Inc., New York.

[2] CHUNG, T. J. (1996) – *Applied Continuum Mechanics*. Cambridge University Press, Cambridge UK.

[3] FUNG, Y. C. (1994) – *A first course in Continuum Mechanics*. 3rd ed. Prentice Hall, Englewood Cliffs, N.J.

[4] MALVERN, L. E. (1969) – *Introduction to the Mechanics of a Continuous Medium*. Prentice Hall, Englewood Cliffs, N.J.

[5] MASE, G. E. (1970) – *Theory and Problems of Continuum Mechanics*. Schaum's outline series, McGraw-Hill, New York.

[6] SALENÇON, J. (2001) – *Handbook of Continuum Mechanics*. Springer-Verlag, Berlin, Heidelberg, New York.

[7] TRUESDELL, C. (1966) – *The Elements of Continuum Mechanics*. Springer, Berlin, Heidelberg.

[8] ZIEGLER, F. (1991) – *Mechanics of Solids and Fluids*. Springer, Vienna.

[9] CAUCHY, A. (1829) – *Exercices de Mathématiques.* Œuvres complètes d'Augustin Cauchy, 1829; 2nd edition, 2nd series, Vol. 9, Gauthier-Villars, Paris, 1891

Chapter IV

Primal approach
Of the theory of Yield Design

Settlement of the problem

Potentially safe loads

Comments

Some usual isotropic strength criteria

References

PRIMAL APPROACH
Of the theory of Yield Design

This Chapter presents the theory of Yield Design in its primal approach directly derived from the basic principle of mathematical compatibility between the equilibrium equations of the system under the prescribed loads in the given geometry with the resistance of its constituent materials. It leads to the definition of the domain of potentially safe loads. This domain is convex as a consequence of the convexity of the strength domains of the constituent materials, which makes the determination of interior estimates much easier. For the relevance of the concept of potentially safe loads to practical applications, the deformations necessary to mobilize the given resistances must be physically compatible.

1 Settlement of the problem

1.1 Geometrical data

The system under consideration is defined by its volume Ω with boundary $\partial\Omega$. This generic definition of the given geometry includes the case, most frequent, when the system actually consists of several subsystems related to each other through interfaces which are also considered as parts of the system.

1.2 Loading mode of the system

The pattern of the data for the Yield Design problem is as described in Chapter III (§ 4.1): body forces defined throughout the volume Ω of the system and boundary data defined on the surface $\partial\Omega$. The specificity is now that these data are prescribed through the use of loading parameters in the following way.

For any set of data for the problem under consideration,

let $\underline{\underline{\sigma}}$ be a Statically Admissible (S. A.) stress field with these data,

let $\underline{\hat{U}}$ be a Kinematically Admissible (K. A.) virtual velocity field with these data,

then the virtual (rate of) work by all the external forces in equilibrium with $\underline{\underline{\sigma}}$ in the virtual velocity field $\underline{\hat{U}}$ is written

(1) $$\mathcal{P}_e(\underline{\underline{\sigma}},\underline{\hat{U}}) = \underline{Q}(\underline{\underline{\sigma}}).\underline{q}(\underline{\hat{U}})$$

where the vectors $\underline{Q}(\underline{\underline{\sigma}}) = (Q_1(\underline{\underline{\sigma}}),...Q_n(\underline{\underline{\sigma}}))$ and $\underline{q}(\underline{\hat{U}}) = (q_1(\underline{\hat{U}}),...q_n(\underline{\hat{U}}))$ are linear **functions of $\underline{\underline{\sigma}}$ and $\underline{\hat{U}}$ respectively**.

The vector $\underline{Q}(\underline{\underline{\sigma}}) = (Q_1(\underline{\underline{\sigma}}), \ldots Q_n(\underline{\underline{\sigma}}))$ is the loading vector or **the load** of the system. Its components are the **loading parameters.** The vector $\underline{q}(\underline{\hat{U}}) = (q_1(\underline{\hat{U}}), \ldots q_n(\underline{\hat{U}}))$ is the **generalized virtual velocity** of the system.

It follows that the virtual work equation (III, 49) is written

$$(2) \qquad \begin{cases} \forall \underline{\underline{\sigma}} \text{ S. A. with } \underline{Q}(\underline{\underline{\sigma}}), \\ \forall \underline{\hat{U}} \text{ K. A. with } \underline{q}(\underline{\hat{U}}), \\ \int_\Omega \underline{\underline{\sigma}} : \underline{\underline{\hat{d}}} \, \mathrm{d}\Omega + \int_{\Sigma_{\underline{\hat{U}}}} (\underline{\underline{\sigma}} . [\![\underline{\hat{U}}]\!]) . \underline{n} \, \mathrm{d}\Sigma = \underline{Q}(\underline{\underline{\sigma}}) . \underline{q}(\underline{\hat{U}}) \end{cases}$$

with

$$(3) \qquad \begin{cases} \underline{\underline{\sigma}} \mapsto \underline{Q}(\underline{\underline{\sigma}}) \text{ linear} \\ \underline{\hat{U}} \mapsto \underline{q}(\underline{\hat{U}}) \text{ linear.} \end{cases}$$

Figure 1 presents a simple 2-dimensional example that will help understanding this definition.

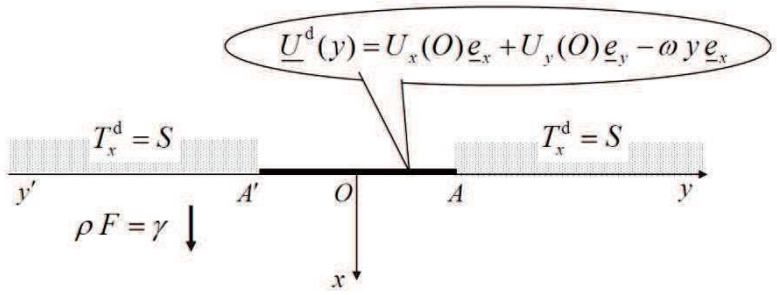

Figure 1. Indentation of a half space by a rigid plate

In this example the volume Ω of the system consists of the half space $x \geq 0$, the rigid plate $A'A = 2a$ acting on this half space, and the interface between these two elements. The boundary $\partial\Omega$ of the system is made up of the boundary of the half space at infinity $(x \to \infty, y \to \pm\infty)$, the surface of the half space on both sides of the plate $(x = 0, |y| > a)$, and the upper surface of the plate.

The body forces in the half space are vertical uniform $\rho F \underline{e}_x = \gamma \underline{e}_x$ where γ is a parameter.

Regarding the boundary data:

- At infinity $(x \to \infty, y \to \pm\infty)$ the velocity is prescribed: the medium is motionless, $\underline{U}^{\mathrm{d}} = 0$;
- On the surface of the half space on both sides of the plate $(x = 0, |y| > a)$, a uniform density of downward vertical surface forces is prescribed, $T_x^{\mathrm{d}} = S$ where S is a parameter;

- The plate being rigid, the corresponding boundary conditions on its upper surface refer to the velocities and take the form of a rigid body motion depending on three parameters $U_x(O), U_y(O), \omega$:

(4) $$\underline{U}^{\mathrm{d}}(y) = U_x(O)\,\underline{e}_x + U_y(O)\,\underline{e}_y - \omega\, y\, \underline{e}_x .$$

With these data, for any stress field $\underline{\underline{\sigma}}$ S. A. and any virtual velocity field $\underline{\hat{U}}$ K. A., the virtual (rate of) work by all the external forces in equilibrium with $\underline{\underline{\sigma}}$ is written

(5) $$\begin{aligned}\mathcal{P}_{\mathrm{e}}(\underline{\underline{\sigma}}, \underline{\hat{U}}) = \gamma \int_{\Omega} \hat{U}_x(\underline{x})\,\mathrm{d}\Omega + S\int_{y'A'\cup Ay} \hat{U}_x(0,y)\,\mathrm{d}y \\ + N(\underline{\underline{\sigma}})\,U_x(O) + T(\underline{\underline{\sigma}})\,U_y(O) + M(\underline{\underline{\sigma}})\,\omega\end{aligned}$$

with

(6) $$\begin{cases} N(\underline{\underline{\sigma}}) = \int_{A'A} -\sigma_{xx}\,\mathrm{d}y \\ T(\underline{\underline{\sigma}}) = \int_{A'A} -\sigma_{xy}\,\mathrm{d}y \\ M(\underline{\underline{\sigma}}) = \int_{A'A} y\,\sigma_{xx}\,\mathrm{d}y \end{cases}$$

It comes out from Eq. (5) that $\mathcal{P}_{\mathrm{e}}(\underline{\underline{\sigma}}, \underline{\hat{U}})$ is the product of two 5-dimension vectors $\underline{Q}(\underline{\underline{\sigma}})$ and $\underline{q}(\underline{\hat{U}})$, as in Eq. (1), with

(7) $$Q_1(\underline{\underline{\sigma}}) = \gamma,\ Q_2(\underline{\underline{\sigma}}) = S,\ Q_3(\underline{\underline{\sigma}}) = N(\underline{\underline{\sigma}}),\ Q_4(\underline{\underline{\sigma}}) = T(\underline{\underline{\sigma}}),\ Q_5(\underline{\underline{\sigma}}) = M(\underline{\underline{\sigma}})$$

and

(8) $$\begin{cases} q_1(\underline{\hat{U}}) = \int_{\Omega} \hat{U}_x(\underline{x})\,\mathrm{d}\Omega,\ q_2(\underline{\hat{U}}) = \int_{y'A'\cup Ay} \hat{U}_x(0,y)\,\mathrm{d}y \\ q_3(\underline{\hat{U}}) = U_x(O),\ q_4(\underline{\hat{U}}) = U_y(O),\ q_5(\underline{\hat{U}}) = \omega. \end{cases}$$

It is worth pointing out that the two first components of the loading vector $\underline{Q}(\underline{\underline{\sigma}})$ come straight from the parametric data on the forces while the three last ones are defined by duality from the parametric data on the velocities. Conversely, the two first components of the generalized velocity of the system are the dual quantities of the corresponding parametric data on the forces.

1.3 Resistance of the constituent material

The third set of data for the Yield Design problem refers to the resistance of the constituent material of the system.

At any point M of the system, a domain $G(\underline{x})$ is given in the 6-dimension vector space of the stress tensor $\underline{\underline{\sigma}}(\underline{x})$, which defines the stress states that comply with the resistance of the constituent material at that point:

(9) $$\underline{\underline{\sigma}}(\underline{x}) \in G(\underline{x}) \subset \mathbb{R}^6$$

with the following assumptions

(10) $$\underline{\underline{\sigma}}(\underline{x}) = 0 \in G(\underline{x})$$

and $G(\underline{x})$ **convex**

(11) $$\underline{\underline{\sigma}}^1(\underline{x}) \in G(\underline{x}),\ \underline{\underline{\sigma}}^2(\underline{x}) \in G(\underline{x}) \Rightarrow \forall \lambda \in [0,1],\ \lambda \underline{\underline{\sigma}}^1(\underline{x}) + (1-\lambda)\underline{\underline{\sigma}}^2(\underline{x}) \in G(\underline{x}).$$

$G(\underline{x})$ is commonly defined by means of a **convex** scalar function[1] of the tensor $\underline{\underline{\sigma}}(\underline{x})$

(12) $$f(\underline{x}, \underline{\underline{\sigma}}(\underline{x})) \le 0 \Leftrightarrow \underline{\underline{\sigma}}(\underline{x}) \in G(\underline{x})$$

with

(13) $$\begin{cases} f(\underline{x}, 0) \le 0 \\ \forall \lambda \in [0,1],\ f(\lambda \underline{\underline{\sigma}}^1 + (1-\lambda)\underline{\underline{\sigma}}^2) \le \lambda f(\underline{\underline{\sigma}}^1) + (1-\lambda) f(\underline{\underline{\sigma}}^2) \end{cases}.$$

The boundary of the **strength domain** $G(\underline{x})$ is thus defined by $f(\underline{x}, \underline{\underline{\sigma}}(\underline{x})) = 0$, which is commonly named the **criterion of resistance** of the material; the same terminology may be used for the function $f(\underline{x}, \underline{\underline{\sigma}}(\underline{x}))$ itself without ambiguity. The conditions (10) and (11) are met by all the criteria of resistance that are implemented in usual practice, whether they come directly from experimental results or are the design criteria prescribed by construction codes.

Being a material function, $f(\underline{x}, \underline{\underline{\sigma}}(\underline{x}))$ must be invariant through the group of symmetries of the material [3] at the considered point. In the case of an isotropic material, it takes the form of a function of the principal invariants of the tensor $\underline{\underline{\sigma}}(\underline{x})$, a symmetric function of the principal stresses.

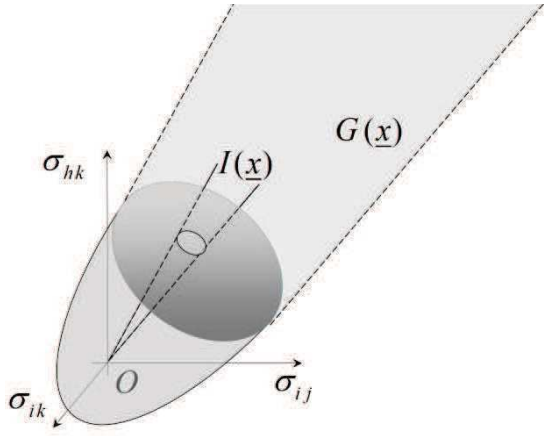

Figure 2. Domain $G(\underline{x})$

The usual pattern for $G(\underline{x})$ is to be bounded in $\mathbb{R}^6$ but with the possibility of extension to infinity in some directions (this being the model for a very high resistance). In such cases the convexity of $G(\underline{x})$ implies that all the directions of extension to infinity form a convex cone $I(\underline{x})$ (Figure 2).

[1] *Cf.* [1, 2].

When the material is modelled as a perfectly rigid solid, the domain $G(\underline{x})$ obviously extends to infinity for all directions in $\mathbb{R}^6$.

1.4 The Question

With the data listed above, the Yield Design problem takes the same form as in chapter II, with the question to be answered:

Given the geometry of the system (§ 1.1), given the n*-parameter loading mode (§ 1.2), determine whether a given load* $\underline{\underline{Q}}$ *can be sustained by the system complying with the resistance criteria (§ 1.3) of the constituent material.*

This question may again be stated in terms of "*stability*":

Is the system "stable" under the load $\underline{\underline{Q}}$ *?*

2 Potentially safe loads

2.1 Domain K

A necessary condition for the system to be stable under the load $\underline{\underline{Q}}$ is the existence of a stress field $\underline{\underline{\sigma}}$ S. A. with $\underline{\underline{Q}}$ and such that Eq. (9) be satisfied at any point in Ω:

$$\exists \underline{\underline{\sigma}} \begin{cases} \underline{\underline{\sigma}} \text{ S. A. with } \underline{\underline{Q}} \\ \underline{\underline{\sigma}}(\underline{x}) \in G(\underline{x}) \ \forall M \in \Omega. \end{cases} \tag{14}$$

Since Eq. (14) is only a necessary condition, the concerned loads $\underline{\underline{Q}}$ will be called **potentially safe** loads. They generate a domain K in the *n*-dimension loading space of the system

$$\underline{\underline{Q}}(\underline{\underline{\sigma}}) \in K \Leftrightarrow \exists \underline{\underline{\sigma}} \begin{cases} \underline{\underline{\sigma}} \text{ S. A. with } \underline{\underline{Q}}(\underline{\underline{\sigma}}) \\ \underline{\underline{\sigma}}(\underline{x}) \in G(\underline{x}) \ \forall M \in \Omega \end{cases} \tag{15}$$

2.2 Mathematical properties of the domain K

From Eq. (15) we derive simple and important properties of the domain K which are transmitted from the local level of the material to the global level of the system thanks to the linearity in Eq. (3):

- **The zero load is potentially safe**

$$\underline{\underline{Q}} = 0 \in K \tag{16}$$

as a consequence of Eq. (10), since the stress field $\underline{\underline{\sigma}} = 0$ equilibrates $\underline{\underline{Q}} = 0$.

- **The domain K is convex in $\mathbb{R}^n$**

It is a consequence of the convexity of $G(\underline{x})$ and of the linearity in Eq. (3): if $\underline{\underline{\sigma}}^1$ and $\underline{\underline{\sigma}}^2$ satisfy Eq. (15) with $\underline{Q}^1$ and $\underline{Q}^2$ respectively, then $\forall \lambda \in [0,1]$, $\lambda \underline{\underline{\sigma}}^1 + (1-\lambda)\underline{\underline{\sigma}}^2$ satisfies Eq. (15) with $\lambda \underline{Q}^1 + (1-\lambda)\underline{Q}^2$.

From this second result, it follows that the boundary of K is a surface in $\mathbb{R}^n$ which separates the potentially safe loads from the **certainly unsafe loads** outside K for which the necessary condition (15) is not satisfied. Due to this specificity among the potentially safe loads, the loads on the boundary of K are called **extreme loads.**

It may result from Eq. (15), in some very specific cases, that K is not bounded in the n-dimension loading space of the system. In such a case, due to the convexity of K, the directions of extension to infinity form a convex cone.

2.3 Interior approach of the domain K

Eq. (15) is the definition of the domain K. It also provides the construction method of this domain through a static approach. Any stress field $\underline{\underline{\sigma}}$ satisfying the left-hand side of Eq. (15) determines a potentially safe load. This process is made much more efficient by taking advantage of the convexity of K. Once k potentially safe loads $\underline{Q}^\ell$ have been obtained, taking the **convex hull** of these loads, as shown in Figure 3, provides an **interior approach** of the boundary of K or, briefly said, an interior approach of K. In this process the goal will be to extend the interior approach as far as suited to practical applications.

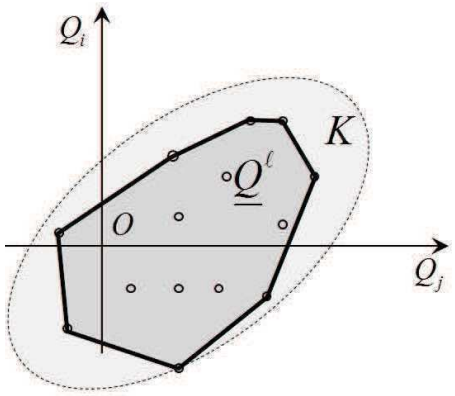

Figure 3. Interior approach of K

In the case of one positive loading parameter, the interior approach provides lower bound estimates for the extreme load Q^* of the system (Figure 4):

$$Q(\underline{\underline{\sigma}}) \le Q^* \Leftrightarrow \exists \underline{\underline{\sigma}} \begin{cases} \underline{\underline{\sigma}} \text{ S. A. with } Q(\underline{\underline{\sigma}}) \\ \underline{\underline{\sigma}}(\underline{x}) \in G(\underline{x}) \ \forall M \in \Omega \end{cases} \tag{17}$$

In this case, extending the interior approach results in maximising $\underline{Q}(\underline{\underline{\sigma}})$ in Eq. (17).

Figure 4. Interior approach of K in the case of one positive loading parameter

More generally the same result holds when a radial loading mode is considered, *i.e.* when the loading parameters of the problem vary proportionally to a single **positive** parameter λ which may stand for some "safety coefficient" of a given load $\underline{Q}^{\mathrm{d}}$. The interior approach provides a lower bound for the extreme value λ^* of this coefficient and results in a maximisation process:

$$\exists \underline{\underline{\sigma}} \begin{cases} \underline{\underline{\sigma}} \text{ S. A. with } \lambda \underline{Q}^{\mathrm{d}} \\ \underline{\underline{\sigma}}(\underline{x}) \in G(\underline{x}) \ \forall M \in \Omega \end{cases} \Leftrightarrow \lambda \le \lambda^*. \tag{18}$$

3 Comments

3.1 Permanent loads

At a first glance the theory just presented, where the loading mode depends on n parameters, seems to exclude the possibility of permanent loads acting on the system. Such loads can easily be taken into account by considering that they depend on a complementary fictitious loading parameter Q_{f}, by implementing the theory with the $(n+1)$ parameters and then by fixing Q_{f} at its prescribed value $Q_{\mathrm{f}}^{\,0}$. The domain of potentially safe loads for $(Q_1, Q_2, \ldots Q_n)$ is the section of the domain determined for $(Q_1, Q_2, \ldots Q_n, Q_{\mathrm{f}})$ by the plane $Q_{\mathrm{f}} = Q_{\mathrm{f}}^{\,0}$. It is still convex but it may happen that it does not include the load $\underline{Q} = (Q_1, Q_2, \ldots Q_n) = 0$ (Figure 5).

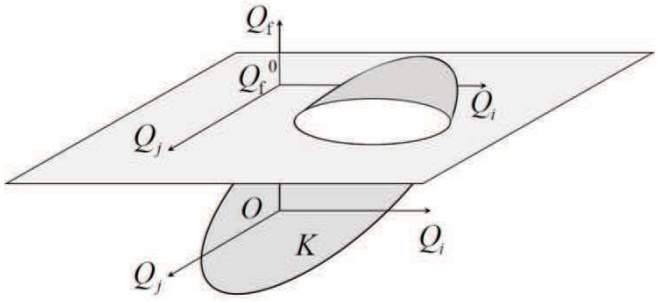

Figure 5. Taking permanent loads into account

The case of the "genuine" variable loads depending on one single positive loading parameter deserves special attention because, in the same way as in Figure 5, it may happen that the zero load does not fall within the segment of the potentially safe loads. Thence the interior approach will still provide a lower bound for the higher extreme load but an upper bound for the lower extreme load.

This is actually the case for "active" and "passive" pressure calculations in Soil mechanics for instance.

Systematically referring to the general formulation (Figure 3) makes it easier to avoid misunderstandings in such circumstances, especially when "safety coefficients" are concerned.

3.2 Convexity of $G(\underline{x})$

Convexity of the domain of resistance of the material has been assumed through Eq. (11). As already said, this property is commonly satisfied by the criteria of resistance that are implemented practically, at least for isotropic materials. The case of anisotropic materials has been studied by numerous authors (*e.g.* [4-7]) using different approaches.

As an example, Tristán-López [7], for the application of the Yield Design approach to soil mechanics practical problems (bearing capacity of strip footings [8], slope stability…), starting from the experimental analyses carried out by Bishop [4] for over-consolidated clays, obtained a domain of resistance on the stress tensor which was not convex but only **star-shaped** with respect to $\underline{\underline{\sigma}} = 0$, *i.e.* such that

$$\underline{\underline{\sigma}}(\underline{x}) \in G(\underline{x}) \Rightarrow \forall \lambda \in [0,1],\ \lambda\, \underline{\underline{\sigma}}(\underline{x}) \in G(\underline{x}) . \tag{19}$$

This affects neither the definition (15) of domain K nor the principle of the interior approach but, in this case, the implementation can only benefit from the fact that the domain K itself is proved to be **star-shaped** with respect to $\underline{Q} = 0$ (the property is conveyed from the local level to the global level in the same way as for convexity).

This is, by far, less efficient than in the "convex case" as it appears in Figure 6.

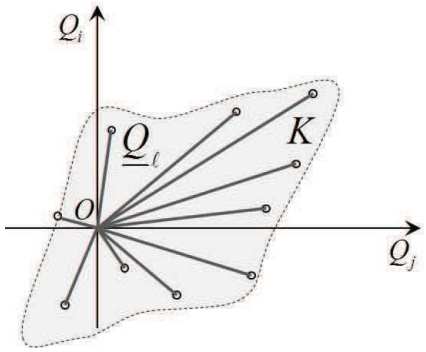

Figure 6. Interior approach of K in the case of a star-shaped $G(\underline{x})$

Moreover, as it will be underscored in Chapter VII (§ 3.1) and Chapter VIII (§ 2.5), the convexity of K as a consequence of $G(\underline{x})$ being convex $\forall M \in \Omega$ is essential for the practical implementation of the Yield Design approach to the dimensioning of systems or structures.

3.3 Constituent materials of the system

The description given in § 1.1 encompasses the case when the system Ω consists of several subsystems $\Omega_1, \Omega_2, ...\Omega_k$ connected to each other through interfaces. The stress vector $\underline{T}(\underline{n})$ acting on such an interface Σ is continuous when crossing the surface from one subsystem to the other (Figure 7). The interface itself plays the role of a constituent material for the whole system due to the fact that $\underline{T}(\underline{n})$ must comply with a condition of resistance which sets the "contact condition" between the two concerned subsystems such as perfect bonding, friction, cohesion, smoothness…

The condition of resistance of the interface is defined by a convex domain $\mathcal{G}(\underline{x})$ assigned to the vector $\underline{T}(\underline{n})$ at point M. When the interface is isotropic, $\mathcal{G}(\underline{x})$ concerns only the normal stress σ and the modulus of the tangential stress $|\underline{\tau}|$ on Σ at point M.

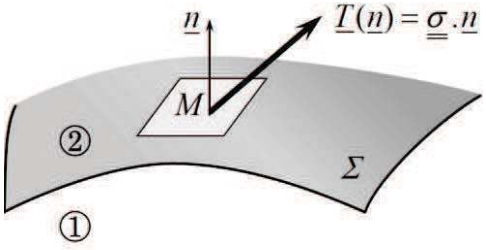

Figure 7. Interface between two subsystems

As a consequence, at point M, the stress field $\underline{\underline{\sigma}}$ must comply with the criteria of resistance of the constituent material on both sides of Σ and with the criterion of resistance of the interface itself on Σ:

$$(20) \qquad \begin{cases} \underline{\underline{\sigma}}^1(\underline{x}) \in G^1(\underline{x}) \\ \underline{\underline{\sigma}}^2(\underline{x}) \in G^2(\underline{x}) \\ \underline{\underline{\sigma}}^1(\underline{x}).\underline{n}(\underline{x}) = \underline{\underline{\sigma}}^2(\underline{x}).\underline{n}(\underline{x}) \in \mathcal{G}(\underline{x}) \end{cases}$$

Note that the last line in Eq. (20) defines a convex cylindrical domain for $\underline{\underline{\sigma}}^1(\underline{x})$ and $\underline{\underline{\sigma}}^2(\underline{x})$.

3.4 The relevance of the concept of potentially safe loads

The first analysis of the relevance of the concept of **potentially safe** loads which was made on the introductory example (Chapter II, section 3) led to the general conclusion that the words "potential" and "potentially" are the consequence of the restricted set of data of the Yield Design problem: the concept of potentially safe loads is the best answer that can be given to the question stated in Section 1.4.

As a positive consequence it must be retained that the Yield Design approach and the concepts of potentially safe loads, extreme loads and certainly unsafe loads are valid whatever the missing data such as the full description of the constitutive law of the

constituent material, the self-equilibrated initial state of stress, the loading path and the loading history, once the geometrical data of the system are given. This makes them particularly useful for back-calculations in post collapse analyses in the absence of sufficient data for modelling the entire process which resulted in the failure of a system.

If the constitutive law of the constituent material is known to be linear elastic and perfectly plastic, obeying the principle of maximum plastic work [9], the quasi-static elastoplastic evolution problem can be solved. A fundamental theorem established by Moreau [10] states that, in the absence of geometry changes, the solution to this problem exists as long as $\underline{Q} \in K$, with K defined by Eq. (15). Consequently, the potentially safe loads are now **certainly safe** loads, whatever the self-equilibrated initial state of stress and whatever the loading path and the loading history. The extreme loads are the **limit** loads of the system actually and the Yield Design approach will be termed **Limit analysis**. The interior approach of Limit analysis makes it possible to estimate the limit loads directly without solving the elastoplastic quasi-static evolution problem [11].

Retaining the linear elastic constitutive law for the material, without more information about its behaviour when its limit of resistance is reached, the significance of the extreme load depends on such data as the loading path and the initial stress state. In the case of a radial loading path (the Q_i being proportional to each other), it is proven that a self-equilibrated stress of state can always be determined such that the extreme load on the considered loading path starting from this initial stress state is the limit load reached after a fully elastic response of the system along this loading path.

Apart from these mathematical statements, more physical considerations can be developed from the long lasting experience of practical implementations of the theory. The relevance of the concept of extreme load is essentially dependent on the ductility of the material once its limit of resistance is reached, and on the **physical compatibility** of the deformations of the material which are necessary to mobilize the assumed resistances within the assumption of no geometry changes [12].

One must also bear in mind that the limits of resistance (strength criteria) which appear in the data are most often imposed by regulations or codes and are not necessarily associated with a constitutive law, all the more so since they refer to conventional values of the resistance parameters which are derived from the physical ones through partial safety coefficients (factors).

Finally, as already remarked in Chapter II (section 3), the assumption that **geometry changes remain negligible** during the whole loading process must be checked systematically. A striking example is given by the problem of the quasi-static expansion of a spherical (or cylindrical cavity) subjected to an increasing internal pressure in an indefinite homogeneous medium with Tresca's strength criterion [13-15].

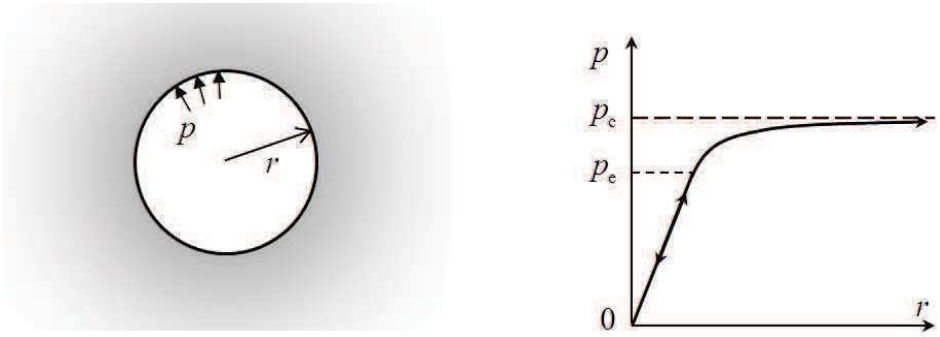

Figure 8. Expansion of a cavity in an indefinite elastoplastic medium

If no geometry changes are taken into account, it is shown that the pressure can increase indefinitely: the extreme load is infinite. But, following the geometry changes, *i.e.* the increase of the radius of the cavity, brings out the existence of a finite asymptotic critical value for the internal pressure (Figure 8).

This result, also valid for a material obeying Coulomb's strength criterion, is the theoretical basis of the pressuremeter test in geotechnical engineering.

4 Some usual isotropic strength criteria

4.1 3-D isotropic materials

- ***The Tresca criterion***

(21) $$f(\underline{\underline{\sigma}}) = \sup\left\{ \sigma_i - \sigma_j - \sigma_0 \,\middle|\, i,j = 1,2,3 \right\},$$

where σ_0 is the resistance of the material under simple tension. The resistance under simple compression is equal to $-\sigma_0$ and the resistance under simple shear is $\sigma_0 / 2$.[2]

- ***The von Mises criterion***

(22) $$f(\underline{\underline{\sigma}}) = \sqrt{\frac{1}{6}\left((\sigma_1 - \sigma_2)^2 + (\sigma_2 - \sigma_3)^2 + (\sigma_3 - \sigma_1)^2\right)} - k,$$

where k is the resistance of the material under simple shear. The resistance under pure tension is $k\sqrt{3}$; under pure compression it is equal to $-k\sqrt{3}$.

- ***Comments on these two criteria***

It is easily observed that these two criteria do not depend on the value of the first invariant I_1 of the tensor $\underline{\underline{\sigma}}$

(23) $$I_1 = \mathrm{tr}\,\underline{\underline{\sigma}} = \sigma_1 + \sigma_2 + \sigma_3.$$

[2] $f(\underline{\underline{\sigma}})$ can also be written as a function of the principal invariants of $\underline{\underline{\sigma}}$, but since it is only piecewise continuously differentiable this expression is not a closed form one.

It means that the resistance of the material is not affected by the addition of an isotropic, tensile or compressive, stress tensor. The corresponding domains $G(\underline{x})$ are, respectively, a prism and a circular cylinder in $(\sigma_1,\sigma_2,\sigma_3)$ Cartesian coordinates.

This model is usually accepted with regard to isotropic compressive stresses, at least for current pressures.

For tensile isotropic stresses, it is questionable due to the decohesion of the material when the normal stress on a facet at point M reaches a limit value T. To take this phenomenon into account, a tension cut-off may be introduced in the expression of the criteria.

- ***Tresca's and von Mises' criteria with tension cut-off***

The expressions of these criteria are derived from Eqs (21) and (22) with the limitation on the normal stress. For Tresca's criterion with tension cut-off we get:

$$f(\underline{\underline{\sigma}}) = \sup\left\{ \sigma_i - \sigma_j - \sigma_0,\ \sigma_i - T \,\middle|\, i,j = 1,2,3 \right\} \tag{24}$$

In $(\sigma_1,\sigma_2,\sigma_3)$ Cartesian coordinates, the domain $G(\underline{x})$ is now the preceding prism truncated by the three planes $\sigma_i = T,\ i = 1,2,3$ as shown in Figure 9.

For the von Mises criterion with tension cut-off (25), the geometrical representation is similar.

$$f(\underline{\underline{\sigma}}) = \sup\left\{ \sqrt{\frac{1}{6}\left((\sigma_1-\sigma_2)^2+(\sigma_2-\sigma_3)^2+(\sigma_3-\sigma_1)^2\right)} - k,\ \sigma_i - T \,\middle|\, i = 1,2,3 \right\}. \tag{25}$$

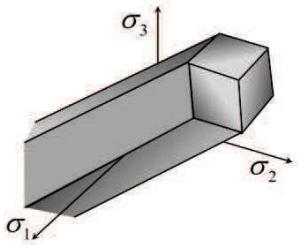

Figure 9. Tresca's criterion with tension cut-off

- ***Coulomb's criterion***

For frictional and cohesive materials Coulomb's criterion is written

$$f(\underline{\underline{\sigma}}) = \sup\left\{ \sigma_i(1+\sin\phi) - \sigma_j(1-\sin\phi) - 2C\cos\phi \,\middle|\, i,j = 1,2,3 \right\}, \tag{26}$$

with ϕ the friction angle and C the cohesion of the material.

This criterion is clearly dependent on the value of $\mathrm{tr}\,\underline{\underline{\sigma}}$. The corresponding domain $G(\underline{x})$ extends to infinity: it is represented geometrically in $(\sigma_1,\sigma_2,\sigma_3)$ Cartesian coordinates by a pyramid.

$G(\underline{x})$ is bounded in the directions of the tensile stresses but allows some tensions which are sometimes considered as not reliable for practical applications. Coulomb's criterion with tension cut-off is then considered.

- ***Coulomb's criterion with tension cut-off***

The Coulomb strength criterion with zero tension cut-off (Figure 10) is derived from Eq. (26) in the same way as Eq. (24).

(27) $$f(\underline{\underline{\sigma}}) = \sup\left\{ \sigma_i(1+\sin\phi) - \sigma_j(1-\sin\phi) - 2C\cos\phi,\ \sigma_i - T \,\middle|\, i,j = 1,2,3 \right\}$$

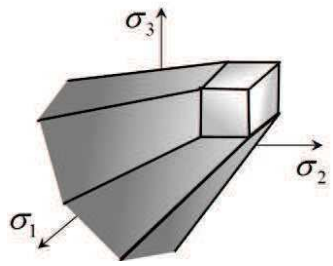

Figure 10. Coulomb's criterion with tension cut-off

The Tresca and Coulomb criteria with zero tension cut-off, $T = 0$ in Eqs (24) and (27), at first, and then small but not zero tension cut-off, have been introduced and implemented by Drucker, Chen and co-workers [16-18] to deal with some stability analysis problems in soil mechanics such as the critical height of a free standing vertical bank and also to model the resistance of concrete and rock as constituent materials.
More recently, the Tresca criterion with zero tension cut-off has been used as a conservative model in earthquake engineering problems for the determination of the bearing capacity of surface footings subjected to eccentric inclined loads [19-21].

- ***The Drucker-Prager criterion***

This criterion for frictional and cohesive materials is expressed as a closed form function of the principal invariants of $\underline{\underline{\sigma}}$. Its relation to the Coulomb criterion is similar to that of von Mises's criterion to Tresca's one.

(28) $$f(\underline{\underline{\sigma}}) = \sqrt{\frac{1}{6}\left((\sigma_1-\sigma_2)^2 + (\sigma_2-\sigma_3)^2 + (\sigma_3-\sigma_1)^2\right)} - \frac{3\sin\phi}{\sqrt{3(3+\sin^2\phi)}}\left(\frac{C}{\tan\phi} - \frac{1}{3}\operatorname{tr}\underline{\underline{\sigma}}\right)$$

- ***Comments***

As it can be seen easily from Eqs (21) and (26), Coulomb's criterion reduces to Tresca's criterion when $\phi = 0$ and $C \neq 0$. Obviously also, when $T \to \infty$, Tresca's and Coulomb's criteria with tension cut-off (24) and (27) simplify to the original Tresca's and Coulomb's strength conditions.

4.2 Isotropic interfaces

- ***The smooth interface***

With the notations introduced in § 3.3, the domain of resistance $\mathcal{G}(\underline{x})$ reduces to $\sigma \le 0$ (no tension) and $|\underline{\tau}| = \tau = 0$ (no friction):

(29) $$f(\underline{T}) = \sup\{\sigma, \tau\}.$$

- ***The Tresca interface***

This condition is also called the interface with layer friction. The normal stress must be non-tensile and the tangential stress is limited to a fixed value k_i:

(30) $$f(\underline{T}) = \sup\{\sigma, \tau - k_i\}.$$

- ***The Coulomb interface***

It is ***the*** historical condition. The normal stress must be non-tensile and the limit for the tangential stress is a linear function of the normal stress:

(31) $$f(\underline{T}) = \tau + \sigma \tan\phi_i$$

where ϕ_i is the friction angle of the interface.

- ***Fully rough interface***

The normal stress must be non-tensile and the tangential stress is not limited:

(32) $$f(\underline{T}) = \sigma.$$

- ***The interface with perfect bonding***

This interface is a model similar to the perfectly rigid solid (§ 1.3): the domain of resistance $\mathcal{G}(\underline{x})$ extends to infinity in any direction. No limit is imposed on the components (σ, τ) of the stress vector $\underline{T}(\underline{n})$

REFERENCES

[1] YANG, W. H. (1980) – A Generalized von Mises Criterion for Yield and Fracture. *Journal of Applied Mechanics, Transactions ASME,* **47**, 2, 297-300.

[2] YANG, W. H. (1980) – A Useful Theorem for Constructing Convex Yield Functions. *Journal of Applied Mechanics, Transactions ASME,* **47**, 2, 301-303.

[3] WINEMAN, A. S. & PIPKIN, A. C. (1964) – Material symmetry restrictions on constitutive equations. *Archive for Rational Mechanics and Analysis*, **17**, 184-214.

[4] BISHOP, A. W. (1966) – The strength of soils as engineering materials. *6th Rankine lecture. Géotechnique,* **16**, 2, 91-130.

[5] BOEHLER, J.-P. & SAWCZUK, A. (1970) – Équilibre limite des sols anisotropes. *Journal de Mécanique,* **9**, 1, 5-33.

[6] NOVA, R. & SACCHI, G. A. (1979) – A Generalized Failure Condition for Orthotropic Solids. *Proceedings of the International colloquium CNRS 295, Mechanical Behaviour of Anisotropic Solids*, Villard de Lans, 1979, Martinus Nidjoff, Boston, MA, 1982, pp. 623-641.

[7] TRISTÁN-LÓPEZ, A. (1981) – *Stabilité d'ouvrages en sols anisotropes*. Th. Dr Eng. École nationale des ponts et chaussées, Paris.

[8] SALENÇON, J. & TRISTÁN-LÓPEZ, A. (1981) – Force portante des semelles filantes sur sols cohérents anisotropes homogènes. *Comptes Rendus de l'Académie des sciences de Paris*, **292**, II, 1097-1102.

[9] HILL, R. (1948) – A variational principle of maximum plastic work in classical plasticity. *Quarterly Journal of Mechanics and Applied Mathematics*, **1**, 18-28.

[10] MOREAU, J. J. (1971) – *Rafle par un convexe variable*. Séminaire d'analyse convexe, Montpellier, France.

[11] SALENÇON, J. (2000) – *de l'Élastoplasticité au Calcul à la rupture*. Éditions de l'École polytechnique publ., Palaiseau, France.

[12] JEWELL, R. A. (1988) – Compatibility, serviceability and design factors for reinforced soil walls. *Proceedings of the International Symposium on Theory and Practice of Earth Reinforcement,* Fukuoka, Japan. Balkema publ., pp. 611-616.

[13] MANDEL, J. (1966) – *Cours de Mécanique des milieux continus.* Vol. II. Gauthier-Villars, Paris, pp. 736-748.

[14] SALENÇON, J. (1966) - Expansion quasi-statique d'une cavité à symétrie sphérique ou cylindrique dans un milieu élastoplastique. *Annales des Ponts et Chaussées*, **III**, 175-187.

[15] SALENÇON, J. (1969) - Contraction quasi-statique d'une cavité à symétrie sphérique ou cylindrique dans un milieu élastoplastique. *Annales des Ponts et Chaussées*, **IV**, 231-236.

[16] DRUCKER, D. C. (1969) – Limit analysis of two and three dimensional soil mechanics problems. *Journal of the Mechanics and Physics of Solids*, **1**, 4, 217-226

[17] CHEN, W. F. & DRUCKER, D. C. (1969) – Bearing capacity of concrete blocks or rock. *Journal of the Engineering Mechanics. Division, ASCE,* **95**, (EM4), 955-978.

[18] CHEN, W. F. (1975) – *Limit Analysis and Soil Plasticity*, Elsevier.

[19] SALENÇON, J. & PECKER, A. (1995) – Ultimate bearing capacity of shallow foundations under inclined and eccentric loads. Part II: purely cohesive soil without tensile strength. *European Journal of Mechanics*, A, **14**, n°3, 377-396.

[20] CHATZIGOGOS, C. T., PECKER, A. & SALENÇON, J. (2007) – Seismic bearing capacity of a circular footing on heterogeneous cohesive soil. *Soils and Foundations*, **47**(4), 783-797.

[21] SALENÇON, J., CHATZIGOGOS, C. T. & PECKER, A. (2009) – Seismic bearing capacity of circular footings: A Yield Design approach. *Journal of Mechanics of Materials and Structures (JoMMS)*, **4,** 2, 427-440.

Chapter V

Dual approach
Of the theory of Yield Design

A static exterior approach

A kinematic necessary condition

The π functions

π functions for usual isotropic strength criteria

References

DUAL APPROACH
Of the theory of Yield Design

The dual approach of the theory of Yield Design is based upon the dual definition of the domain of resistance of the constituent material through the concept of maximum resisting work in a virtual velocity field. A kinematic necessary condition for the potentially safe loads is thus established where kinematically admissible virtual velocity fields are used as test functions for the compatibility between equilibrium and resistance. It yields a sufficient condition for the certainly unsafe loads, which provides the basis for an exterior approach of the domain K.

1 A static exterior approach

The static interior approach presented in Chapter IV provides an estimate "from inside" of the boundary of the convex K or, in other words, lower bound estimates for the extreme loads of the system. If, for practical applications, the exact determination of K is, most often, not necessary (nor really meaningful), on the other hand the determination of an estimate "from outside" of the boundary of K, *i.e.* "upper bounds" for the extreme loads, will be a highly valuable result. This calls for an **exterior approach** of K.

From the definition of the convex K given by Eq. (15) in Chapter IV, the outside of K is generated by the **certainly unsafe loads** that are the loads for which Equilibrium and Resistance are **not** mathematically compatible:

$$\underline{\underline{Q}} \notin K \Leftrightarrow \nexists\, \underline{\underline{\sigma}} \begin{cases} \underline{\underline{\sigma}} \text{ S.A. with } \underline{\underline{Q}} \\ \underline{\underline{\sigma}}(\underline{x}) \in G(\underline{x}),\ \forall M \in \Omega \end{cases} \tag{1}$$

Implementing this static definition to prove that a given load $\underline{\underline{Q}}$ is certainly unsafe requires an exhaustive exploration of all the stress fields statically admissible with $\underline{\underline{Q}}$ and the proof that none of them complies with the condition of resistance. Despite its difficulty, this procedure turns out to be feasible in some cases, a typical example of which is the famous Coulomb's wedge approach for the stability analysis of a slope or a retaining wall [1, 2].

The governing idea is to start from the definition of K and to derive a necessary condition on $\underline{Q}$ such that Equilibrium and Resistance be compatible. In order for the method to be practically applicable, this condition should not refer to the stress field anymore and must refer only to the load $\underline{Q}$ itself and to the resistance of the constituent material. Such a condition usually results from a smart combination of the global equilibrium equations of the system with the condition of resistance: this is precisely the case when performing a stability analysis *"à la Coulomb"* or with Coulomb's analysis of the bearing capacity of a pillar [1].

The condition so obtained is **weaker** than the definition of K: it is a **necessary** condition for a load to be potentially safe. With $\underline{R}$ as a symbolic notation for the strength characteristics of the constituent materials[1] we can write this necessary condition in the form:

(2) $$\underline{Q} \in K \Rightarrow \mathcal{F}(\underline{Q}, \underline{R})$$

where $\mathcal{F}(\underline{Q}, \underline{R})$ stands for the necessary condition being fulfilled.

It follows from Eq. (2) that if the condition $\mathcal{F}(\underline{Q}, \underline{R})$ is not satisfied by a load $\underline{Q}^\ell$ this load is certainly unsafe and contributes to an exterior approach of K (Figure 1); we write:

(3) $$\cancel{\mathcal{F}(\underline{Q}^\ell, \underline{R})} \Rightarrow \underline{Q}^\ell \notin K .$$

Moreover, if an interior approach of K is already available (at least $\underline{Q} = 0$), it follows from the convexity of K that the infinite cone, opposite to the cone with summit $\underline{Q}^\ell$ and the interior approach as a base, is exterior to K, as shown in Figure 1a.

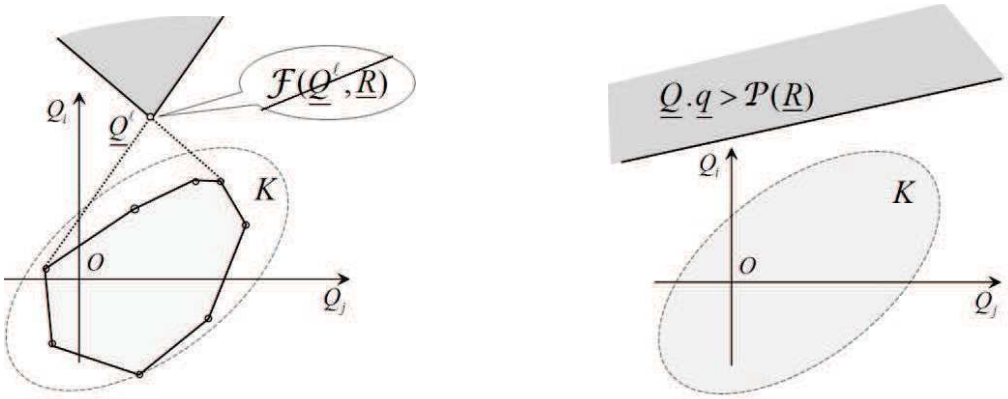

a) b)

Figure 1. Static exterior approach of K

It commonly happens that the condition $\mathcal{F}(\underline{Q}, \underline{R})$ appears in the form of a scalar inequality between a linear form in $\underline{Q}$ and a scalar function of $\underline{R}$

[1] This notation will be made more explicit in Chapter VII and even more in Chapter VIII.

(4) $$\mathcal{F}(\underline{Q},\underline{R}) \Leftrightarrow \underline{Q}.\underline{q} \le \mathcal{P}(\underline{R}),$$

where $\mathcal{P}(\underline{R})$ is non-negative since $\underline{Q}=0$ is a potentially safe load. In such a case, the half-space defined by

(5) $$\underline{Q}.\underline{q} > \mathcal{P}(\underline{R})$$

is exterior to K, as shown in Figure 1b.

As said previously, the difficulty of this static exterior approach lies in finding out and writing down a non-trivial necessary condition in the form of Eq. (2) which can be used in practice and lead to significant results. Also, the logical implications which have just been explained through Eqs (2) and (3) are sometimes difficult to follow when the calculations involved become too intricate. For these reasons, with the same goal of constructing an exterior approach of K, we will look for a necessary condition, in the form of Eq. (2), that can be obtained systematically.

2 A kinematic necessary condition

The rationale starts from the definition of K

(6) $$\underline{Q} \in K \Leftrightarrow \exists \underline{\underline{\sigma}} \begin{cases} \underline{\underline{\sigma}} \text{ S. A. with } \underline{Q} \\ \underline{\underline{\sigma}}(\underline{x}) \in G(\underline{x}) \ \forall M \in \Omega \end{cases}$$

Since $\underline{\underline{\sigma}}$ in Eq. (6) is statically admissible with $\underline{Q}$, it follows from the virtual work equation (Chapter IV, § 1.2) that the virtual (rate of) work by $\underline{Q}$ in any virtual velocity field $\underline{\hat{U}}$ kinematically admissible for the problem is equal to the opposite[2] of the virtual (rate of) work by the stress field $\underline{\underline{\sigma}}$

(7) $$\begin{cases} \forall \underline{\hat{U}} \ \text{ K. A.} \\ \underline{Q}.\underline{q}(\underline{\hat{U}}) = \int_\Omega \underline{\underline{\sigma}} : \underline{\underline{\hat{d}}} \, \mathrm{d}\Omega + \int_{\Sigma_{\underline{\hat{U}}}} (\underline{\underline{\sigma}}.[\![\underline{\hat{U}}]\!]).\underline{n} \, \mathrm{d}\Sigma. \end{cases}$$

Since $\underline{\underline{\sigma}}$ complies with the strength criterion, each integral in the right-hand side of Eq. (7) admits an upper bound built up from the upper bounds $\pi(\underline{x},\underline{\underline{\hat{d}}}(\underline{x}))$ and $\pi(\underline{x},\underline{n}(\underline{x}),[\![\underline{\hat{U}}(\underline{x})]\!])$ of the quantities to be integrated:

(8) $$\pi(\underline{x},\underline{\underline{\hat{d}}}(\underline{x})) = \operatorname{Sup}\left\{ \underline{\underline{\sigma}}' : \underline{\underline{\hat{d}}}(\underline{x}) \,\middle|\, \underline{\underline{\sigma}}' \in G(\underline{x}) \right\}$$

(9) $$\pi(\underline{x},\underline{n}(\underline{x}),[\![\underline{\hat{U}}(\underline{x})]\!]) = \operatorname{Sup}\left\{ (\underline{\underline{\sigma}}'.[\![\underline{\hat{U}}(\underline{x})]\!]).\underline{n}(\underline{x}) \,\middle|\, \underline{\underline{\sigma}}' \in G(\underline{x}) \right\}.$$

Thus, summing up the above equations it comes out that the virtual work by a potentially safe load $\underline{Q}$ in any kinematically admissible virtual velocity field $\underline{\hat{U}}$ admits an upper bound which is derived from the strength condition of the constituent material only:

[2] Remember the minus sign in the definition of the virtual rate of work by the internal forces (Chapter III, Eq. (44)).

$$(10)\qquad \underline{Q}\in K \Rightarrow \begin{cases} \forall \underline{\hat{U}} \text{ K. A.} \\ \underline{Q}.\underline{q}(\underline{\hat{U}}) \le \int_{\Omega} \pi\left(\underline{x},\underline{\underline{\hat{d}}}(\underline{x})\right)\mathrm{d}\Omega + \int_{\Sigma_{\underline{\hat{U}}}} \pi\left(\underline{x},\underline{n}(\underline{x}),[\![\underline{\hat{U}}(\underline{x})]\!]\right)\mathrm{d}\Sigma. \end{cases}$$

For any kinematically admissible virtual velocity field $\underline{\hat{U}}$, Eq. (10) provides a **necessary** condition in the form of Eq. (4). Symbolically we can write

$$(11)\qquad \mathcal{F}(\underline{Q},\underline{R}) \Leftrightarrow \begin{cases} \forall \underline{\hat{U}} \text{ K. A.} \\ \underline{Q}.\underline{q}(\underline{\hat{U}}) \le \int_{\Omega} \pi\left(\underline{x},\underline{\underline{\hat{d}}}(\underline{x})\right)\mathrm{d}\Omega + \int_{\Sigma_{\underline{\hat{U}}}} \pi\left(\underline{x},\underline{n}(\underline{x}),[\![\underline{\hat{U}}(\underline{x})]\!]\right)\mathrm{d}\Sigma \end{cases}$$

and an exterior approach of K will be obtained (Figure 2) in the form of Eq. (5):

$$(12)\quad \forall \underline{\hat{U}} \text{ K. A., } \underline{Q}.\underline{q}(\underline{\hat{U}}) > \int_{\Omega} \pi\left(\underline{x},\underline{\underline{\hat{d}}}(\underline{x})\right)\mathrm{d}\Omega + \int_{\Sigma_{\underline{\hat{U}}}} \pi\left(\underline{x},\underline{n}(\underline{x}),[\![\underline{\hat{U}}(\underline{x})]\!]\right)\mathrm{d}\Sigma \Rightarrow Q \notin K .$$

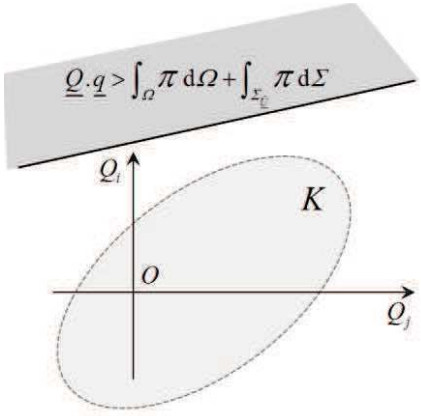

Figure 2. Kinematic exterior approach of K

The evident cornerstone of this method is the introduction of the π **functions** with the kinematically admissible virtual velocity fields as **test functions** for the compatibility between Equilibrium and Resistance. In order to assess the relevance and the efficiency of the exterior approach so obtained it is necessary to go deeper into the mathematical properties of the π functions while looking at their mechanical significance for a better understanding.

3 The π functions

3.1 Support function of $G(\underline{x})$

Two π functions have been introduced through Eqs (8) and (9). It is easy to see that there is only one function involved since, due to the symmetry of $\underline{\underline{\sigma}}'$, we have

$$(13)\qquad \begin{aligned} (\underline{\underline{\sigma}}'.[\![\underline{\hat{U}}(\underline{x})]\!]).\underline{n}(\underline{x}) &= \underline{\underline{\sigma}}':([\![\underline{\hat{U}}(\underline{x})]\!]\otimes\underline{n}(\underline{x})) \\ &= \underline{\underline{\sigma}}':\frac{1}{2}([\![\underline{\hat{U}}(\underline{x})]\!]\otimes\underline{n}(\underline{x})+\underline{n}(\underline{x})\otimes[\![\underline{\hat{U}}(\underline{x})]\!]), \end{aligned}$$

hence

(14) $$\pi(\underline{x},\underline{n}(\underline{x}),[\![\hat{\underline{U}}(\underline{x})]\!]) = \frac{1}{2}\pi(\underline{x},[\![\hat{\underline{U}}(\underline{x})]\!]\otimes\underline{n}(\underline{x}) + \underline{n}(\underline{x})\otimes[\![\hat{\underline{U}}(\underline{x})]\!]).$$

We will now focus our attention on $\pi(\underline{x},\hat{\underline{\underline{d}}}(\underline{x}))$.

From the mathematical point of view, the definition (8) of the function $\pi(\underline{x},\hat{\underline{\underline{d}}}(\underline{x}))$ is that of the **support function** of the convex $G(\underline{x})$ in the theory of convex analysis: the properties of that function are classical within that context [3]. Since here is not the place to develop such a theory we shall restrict ourselves to the results which are relevant to the theory of Yield Design.

3.2 Maximum resisting (rate of) work

To make the presentation more lively we will make use of the geometrical representations of $G(\underline{x})$ in $\mathbb{R}^6$ (the linear space of $\underline{\underline{\sigma}}(\underline{x})$) which we shall consider as an Euclidean space with the doubly contracted product ":" as the scalar product of the geometrical representation of $\underline{\underline{\sigma}}(\underline{x})$ with the geometrical representation of $\hat{\underline{\underline{d}}}(\underline{x})$.

As it was already discussed in Chapter III (§ 3.2) the quantity $(-\underline{\underline{\sigma}}:\hat{\underline{\underline{d}}})$ is classically named the volume density of the virtual work by the internal forces (the stresses) in the virtual velocity field $\hat{\underline{U}}$.To name the quantity $\underline{\underline{\sigma}}:\hat{\underline{\underline{d}}}$ we refer to Eq. (III, 44) which shows that in the case of equilibrium (no virtual work by the quantities of acceleration) the corresponding virtual work equilibrates the virtual work by the external forces. Therefore we will call this quantity the volume density of the **virtual resisting work** by the stresses in the virtual velocity field $\hat{\underline{U}}$.

Hence comes out the interpretation of the function $\pi(\underline{x},\hat{\underline{\underline{d}}}(\underline{x}))$: it is the volume density of the **maximum resisting work by a stress tensor complying with the condition of resistance** in the virtual velocity field $\hat{\underline{U}}$.

This leads to the geometrical illustration of the calculation of $\pi(\underline{x},\hat{\underline{\underline{d}}}(\underline{x}))$ (Figure 3). Given $\hat{\underline{\underline{d}}}(\underline{x})$, looking for the maximum value of $\underline{\underline{\sigma}}':\hat{\underline{\underline{d}}}(\underline{x})$ under the constraint $\underline{\underline{\sigma}}'\in G(\underline{x})$ amounts to looking for the point(s) on the boundary of $G(\underline{x})$ where the outward normal is collinear to $\hat{\underline{\underline{d}}}(\underline{x})$. Let $\underline{\underline{\sigma}}^*$ be one such point (Figure 3a), then

(15) $$\pi(\underline{x},\hat{\underline{\underline{d}}}(\underline{x})) = \underline{\underline{\sigma}}^*:\hat{\underline{\underline{d}}}(\underline{x}).$$

Since $G(\underline{x})$ is convex, Eq. (15) is single valued even in the case of multiple points on the boundary of $G(\underline{x})$ where the outward normal is collinear with $\hat{\underline{\underline{d}}}(\underline{x})$ (this occurs when $G(\underline{x})$ is not strictly convex).

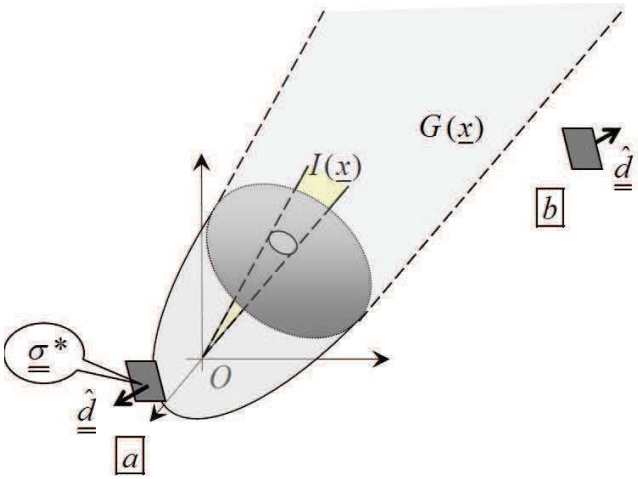

Figure 3. Maximum resisting (rate of) work

Regarding $\underline{\underline{\sigma}}^*$ two circumstances may be encountered.

- If $G(\underline{x})$ is **bounded** in all directions in $\mathbb{R}^6$

  $\underline{\underline{\sigma}}^*$ exists and is finite for any given value of $\hat{\underline{\underline{d}}}(\underline{x})$

  $$\pi(\underline{x}, \hat{\underline{\underline{d}}}(\underline{x})) = \underline{\underline{\sigma}}^* : \hat{\underline{\underline{d}}}(\underline{x}) \text{ is } \textbf{finite.}$$

- If $G(\underline{x})$ is **not bounded** in the directions of the convex cone $I(\underline{x})$

  For any given value of $\hat{\underline{\underline{d}}}(\underline{x})$ lying within the convex cone orthogonal to $I(\underline{x})$ ($\boxed{a}$ in Figure 3), $\underline{\underline{\sigma}}^*$ exists and is finite, thence

  $$\pi(\underline{x}, \hat{\underline{\underline{d}}}(\underline{x})) = \underline{\underline{\sigma}}^* : \hat{\underline{\underline{d}}}(\underline{x}) \text{ is } \textbf{finite.}$$

  For those values of $\hat{\underline{\underline{d}}}(\underline{x})$ which do not belong to that cone, looking for $\underline{\underline{\sigma}}^*$ shows that it is impossible to find a point at a finite distance where the outward normal is collinear with $\hat{\underline{\underline{d}}}(\underline{x})$: it follows that the value of $\underline{\underline{\sigma}}' : \hat{\underline{\underline{d}}}(\underline{x})$ under the constraint $\underline{\underline{\sigma}}' \in G(\underline{x})$ does not admit any upper bound ($\boxed{b}$ in Figure 3). Therefore $\pi(\underline{x}, \hat{\underline{\underline{d}}}(\underline{x}))$ is **infinite**:

(16) $$\pi(\underline{x}, \hat{\underline{\underline{d}}}(\underline{x})) = +\infty.$$

3.3 Mathematical properties of the π function

From its definition the π function has the following properties.

- $\pi(\underline{x}, \hat{\underline{\underline{d}}}(\underline{x}))$ is **non-negative** due to the fact that $\underline{\underline{\sigma}}(\underline{x}) = 0 \in G(\underline{x})$

(17) $$\forall \hat{\underline{\underline{d}}}(\underline{x}),\ \pi(\underline{x}, \hat{\underline{\underline{d}}}(\underline{x})) \geq 0.$$

- $\pi(\underline{x}, \hat{\underline{\underline{d}}}(\underline{x}))$ is **positively homogeneous with degree 1**

(18) $$\forall \underline{\underline{\hat{d}}}(\underline{x}), \forall \alpha \geq 0,\ \pi(\underline{x}, \alpha \underline{\underline{\hat{d}}}(\underline{x})) = \alpha \pi(\underline{x}, \underline{\underline{\hat{d}}}(\underline{x})).$$

This result is due to the fact that both $\underline{\underline{\hat{d}}}(\underline{x})$ and $\alpha \underline{\underline{\hat{d}}}(\underline{x})$ correspond either to the same $\underline{\underline{\sigma}}^*$ in Eq. (15) or to Eq. (16).

- $\pi(\underline{x}, \underline{\underline{\hat{d}}}(\underline{x}))$ is a **convex function** of $\underline{\underline{\hat{d}}}(\underline{x})$

(19) $$\forall \underline{\underline{\hat{d}}}^1, \forall \underline{\underline{\hat{d}}}^2, \forall \lambda \in [0,1],\ \pi(\underline{x}, \lambda \underline{\underline{\hat{d}}}^1 + (1-\lambda)\underline{\underline{\hat{d}}}^2) \leq \lambda \pi(\underline{x}, \underline{\underline{\hat{d}}}^1) + (1-\lambda)\pi(\underline{x}, \underline{\underline{\hat{d}}}^2).$$

This comes from the fact that, if $(\underline{\underline{\sigma}}^*)^1$, $(\underline{\underline{\sigma}}^*)^2$ and $\underline{\underline{\sigma}}^*$ are associated in Eq. (15) with $\underline{\underline{\hat{d}}}^1$, $\underline{\underline{\hat{d}}}^2$ and $\underline{\underline{\hat{d}}} = (\lambda \underline{\underline{\hat{d}}}^1 + (1-\lambda)\underline{\underline{\hat{d}}}^2)$, the definition of the π functions yields $\pi(\underline{x}, \underline{\underline{\hat{d}}}^1) = (\underline{\underline{\sigma}}^*)^1 : \underline{\underline{\hat{d}}}^1 \geq \underline{\underline{\sigma}}^* : \underline{\underline{\hat{d}}}^1$ and $\pi(\underline{x}, \underline{\underline{\hat{d}}}^2) = (\underline{\underline{\sigma}}^*)^1 : \underline{\underline{\hat{d}}}^2 \geq \underline{\underline{\sigma}}^* : \underline{\underline{\hat{d}}}^2$. The proof also holds when $\pi(\underline{x}, \underline{\underline{\hat{d}}}^1)$ or $\pi(\underline{x}, \underline{\underline{\hat{d}}}^2)$ is infinite.

3.4 Dual definition of $G(\underline{x})$

The geometrical illustration given in Figure 3 shows that, for all $\underline{\underline{\hat{d}}}(\underline{x})$ in the convex cone orthogonal to $I(\underline{x})$, Eq. (20) is the equation of the tangent plane to $G(\underline{x})$ with outward normal $\underline{\underline{\hat{d}}}(\underline{x})$

(20) $$\underline{\underline{\sigma}} : \underline{\underline{\hat{d}}}(\underline{x}) - \pi(\underline{x}, \underline{\underline{\hat{d}}}(\underline{x})) = 0.$$

The planes defined by this equation are all the planes which are tangent to $G(\underline{x})$ at a finite distance. Since $G(\underline{x})$ is convex, it follows from the definitions (15) and (16) of $\pi(\underline{x}, \underline{\underline{\hat{d}}}(\underline{x}))$ for any $\underline{\underline{\hat{d}}}(\underline{x}) \in \mathbb{R}^6$, that

(21) $$\underline{\underline{\sigma}}(\underline{x}) \in G(\underline{x}) \Leftrightarrow \forall \underline{\underline{\hat{d}}}(\underline{x}) \in \mathbb{R}^6,\ \underline{\underline{\sigma}}(\underline{x}) : \underline{\underline{\hat{d}}}(\underline{x}) - \pi(\underline{x}, \underline{\underline{\hat{d}}}(\underline{x})) \leq 0.$$

It thus appears, as noted in [4], that all information included in $G(\underline{x})$ through the strength criterion $f(\underline{x}, \underline{\underline{\sigma}}(\underline{x}))$ is encompassed in the volume density of the maximum resisting work $\pi(\underline{x}, \underline{\underline{\hat{d}}}(\underline{x}))$.

Conversely, assume that a function $\pi(\underline{x}, \underline{\underline{\hat{d}}}(\underline{x}))$ which satisfies the conditions (17) and (18) is given for any $\underline{\underline{\hat{d}}}(\underline{x}) \in \mathbb{R}^6$, then Eq. (22) generates a convex domain $G(\underline{x})$ in $\mathbb{R}^6$, which contains the origin:

(22) $$\underline{\underline{\sigma}}(\underline{x}) : \underline{\underline{\hat{d}}}(\underline{x}) - \pi(\underline{x}, \underline{\underline{\hat{d}}}(\underline{x})) \leq 0, \forall \underline{\underline{\hat{d}}}(\underline{x}) \in \mathbb{R}^6 \Leftrightarrow \underline{\underline{\sigma}}(\underline{x}) \in G(\underline{x}).$$

If the given function $\pi(\underline{x}, \underline{\underline{\hat{d}}}(\underline{x}))$ is convex, then $\pi(\underline{x}, \underline{\underline{\hat{d}}}(\underline{x}))$ is the maximum resisting work for $G(\underline{x})$.

This is the **dual definition** of the convex $G(\underline{x})$. Note that from the data of $\pi(\underline{x}, \underline{\underline{\hat{d}}}(\underline{x}))$ a strength criterion can easily be derived in the form

(23) $$f(x,\underline{\underline{\sigma}}(x)) = \sup\left\{ \underline{\underline{\sigma}}(\underline{x}):\underline{\underline{\hat{d}}}(\underline{x}) - \pi\left(\underline{x},\underline{\underline{\hat{d}}}(\underline{x})\right) \le 0 \;\middle|\; \underline{\underline{\hat{d}}}(\underline{x}) \in \mathbb{R}^6, \mathrm{tr}\left(\underline{\underline{\hat{d}}}(\underline{x})\right)^2 = 1 \right\}.$$

3.5 π functions for interfaces

As it was pointed out in Chapter IV (§ 3.3) the constituent materials of the system include the interfaces between the different subsystems $\Omega_1, \Omega_2, \ldots \Omega_k$ which constitute Ω. For this particular material the strength condition is on the stress vector $\underline{T}(\underline{n})$ acting at point M on the interface: it is given through a convex domain $\mathcal{G}(\underline{x})$. The dual quantity of $\underline{T}(\underline{n})$ in the expression of the virtual resisting work by the internal forces is the virtual velocity jump in the interface when crossing it in the direction indicated by $\underline{n}(\underline{x})$:

(24) $$\underline{\hat{V}}(\underline{x}) = [\![\underline{\hat{U}}_{\mathrm{i}}(\underline{x})]\!] = \underline{\hat{U}}_{\mathrm{i}}^{2}(\underline{x}) - \underline{\hat{U}}_{\mathrm{i}}^{1}(\underline{x}).$$

In this equation, the subscript "i" indicates that the jump which is considered takes place in the interface itself, notwithstanding any other virtual velocity jump which might occur in Ω_1 or in Ω_2 at the same point M.

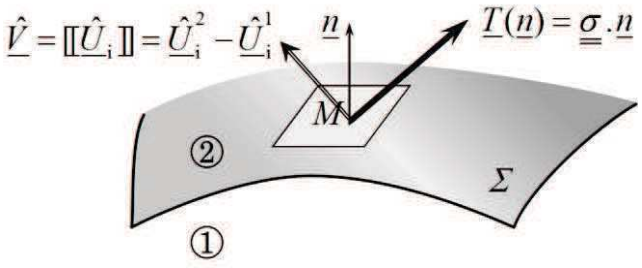

Figure 4. Virtual velocity jump when crossing an interface

The π function corresponding to $\underline{\hat{V}}$ is defined by:

(25) $$\pi\left(\underline{x},\underline{\hat{V}}(\underline{x})\right) = \sup\left\{ \underline{T'}.\,\underline{\hat{V}}(\underline{x}) \;\middle|\; \underline{T'} \in \mathcal{G}(\underline{x}) \right\}.$$

4 π functions for usual isotropic strength criteria

4.1 3-D isotropic materials

- ***The Tresca criterion***

$$f(\underline{\underline{\sigma}}) = \sup\left\{ \sigma_i - \sigma_j - \sigma_0 \;\middle|\; i,j = 1,2,3 \right\}$$

(26) $$\begin{cases} \pi\left(\underline{\underline{\hat{d}}}\right) = +\infty \;\text{ if }\; \mathrm{tr}\,\underline{\underline{\hat{d}}} \neq 0 \\ \pi\left(\underline{\underline{\hat{d}}}\right) = \dfrac{\sigma_0}{2}\left(\left|\hat{d}_1\right| + \left|\hat{d}_2\right| + \left|\hat{d}_3\right|\right) \;\text{ if }\; \mathrm{tr}\,\underline{\underline{\hat{d}}} = 0 \end{cases}$$

(27)
$$\begin{cases} \pi(\underline{n},[\![\underline{\hat{U}}]\!]) = +\infty \ \text{ if } [\![\underline{\hat{U}}]\!].\underline{n} \neq 0 \\ \pi(\underline{n},[\![\underline{\hat{U}}]\!]) = \dfrac{\sigma_0}{2}\left|[\![\underline{\hat{U}}]\!]\right| \ \text{ if } [\![\underline{\hat{U}}]\!].\underline{n} = 0 \end{cases}$$

- ***The von Mises criterion***

$$f(\underline{\underline{\sigma}}) = \sqrt{\frac{1}{6}\left((\sigma_1-\sigma_2)^2+(\sigma_2-\sigma_3)^2+(\sigma_3-\sigma_1)^2\right)} - k$$

(28)
$$\begin{cases} \pi(\underline{\underline{\hat{d}}}) = +\infty \ \text{ if } \operatorname{tr}\underline{\underline{\hat{d}}} \neq 0 \\ \pi(\underline{\underline{\hat{d}}}) = k\sqrt{2\operatorname{tr}(\underline{\underline{\hat{d}}})^2} \ \text{ if } \operatorname{tr}\underline{\underline{\hat{d}}} = 0 \end{cases}$$

(29)
$$\begin{cases} \pi(\underline{n},[\![\underline{\hat{U}}]\!]) = +\infty \ \text{ if } [\![\underline{\hat{U}}]\!].\underline{n} \neq 0 \\ \pi(\underline{n},[\![\underline{\hat{U}}]\!]) = k\left|[\![\underline{\hat{U}}]\!]\right| \ \text{ if } [\![\underline{\hat{U}}]\!].\underline{n} = 0 \end{cases}$$

- ***Coulomb's criterion***

$$f(\underline{\underline{\sigma}}) = \sup\left\{\sigma_i(1+\sin\phi)-\sigma_j(1-\sin\phi)-2C\cos\phi \,\middle|\, i,j=1,2,3\right\}$$

(30)
$$\begin{cases} \pi(\underline{\underline{\hat{d}}}) = +\infty \ \text{ if } \operatorname{tr}\underline{\underline{\hat{d}}} < (\left|\hat{d}_1\right|+\left|\hat{d}_2\right|+\left|\hat{d}_3\right|)\sin\phi \\ \pi(\underline{\underline{\hat{d}}}) = \dfrac{C}{\tan\phi}\operatorname{tr}\underline{\underline{\hat{d}}} \ \text{ if } \operatorname{tr}\underline{\underline{\hat{d}}} \geq (\left|\hat{d}_1\right|+\left|\hat{d}_2\right|+\left|\hat{d}_3\right|)\sin\phi \end{cases}$$

(31)
$$\begin{cases} \pi(\underline{n},[\![\underline{\hat{U}}]\!]) = +\infty \ \text{ if } [\![\underline{\hat{U}}]\!].\underline{n} < \left|[\![\underline{\hat{U}}]\!]\right|\sin\phi \\ \pi(\underline{n},[\![\underline{\hat{U}}]\!]) = \dfrac{C}{\tan\phi}[\![\underline{\hat{U}}]\!].\underline{n} \ \text{ if } [\![\underline{\hat{U}}]\!].\underline{n} \geq \left|[\![\underline{\hat{U}}]\!]\right|\sin\phi \end{cases}$$

- ***The Drucker-Prager criterion***

$$f(\underline{\underline{\sigma}}) = \sqrt{\frac{1}{6}\left((\sigma_1-\sigma_2)^2+(\sigma_2-\sigma_3)^2+(\sigma_3-\sigma_1)^2\right)} - \frac{3\sin\phi}{\sqrt{3(3+\sin^2\phi)}}\left(\frac{C}{\tan\phi}-\frac{1}{3}\operatorname{tr}\underline{\underline{\sigma}}\right)$$

(32)
$$\begin{cases} \pi(\underline{\underline{\hat{d}}}) = +\infty \ \text{ if } \operatorname{tr}\underline{\underline{\hat{d}}} < \sqrt{\dfrac{2\sin^2\phi}{3+\sin^2\phi}\left(3\operatorname{tr}(\underline{\underline{\hat{d}}})^2-(\operatorname{tr}\underline{\underline{\hat{d}}})^2\right)} \\ \pi(\underline{\underline{\hat{d}}}) = \dfrac{C}{\tan\phi}\operatorname{tr}\underline{\underline{\hat{d}}} \ \text{ if } \operatorname{tr}\underline{\underline{\hat{d}}} \geq \sqrt{\dfrac{2\sin^2\phi}{3+\sin^2\phi}\left(3\operatorname{tr}(\underline{\underline{\hat{d}}})^2-(\operatorname{tr}\underline{\underline{\hat{d}}})^2\right)} \end{cases}$$

(33)
$$\begin{cases} \pi(\underline{n},[\![\underline{\hat{U}}]\!]) = +\infty \ \text{ if } [\![\underline{\hat{U}}]\!].\underline{n} < \left|[\![\underline{\hat{U}}]\!]\right|\sin\phi \\ \pi(\underline{n},[\![\underline{\hat{U}}]\!]) = \dfrac{C}{\tan\phi}[\![\underline{\hat{U}}]\!].\underline{n} \ \text{ if } [\![\underline{\hat{U}}]\!].\underline{n} \geq \left|[\![\underline{\hat{U}}]\!]\right|\sin\phi \end{cases}$$

- ***Tresca's criterion with tension cut-off***

$$f(\underline{\underline{\sigma}}) = \sup\left\{\sigma_i - \sigma_j - \sigma_0,\ \sigma_i - T \,\middle|\, i,j = 1,2,3\right\}$$

(34)
$$\begin{cases} \pi(\underline{\underline{\hat{d}}}) = +\infty \ \text{ if } \operatorname{tr}\underline{\underline{\hat{d}}} < 0 \\ \pi(\underline{\underline{\hat{d}}}) = \dfrac{\sigma_0}{2}\left(\left|\hat{d}_1\right| + \left|\hat{d}_2\right| + \left|\hat{d}_3\right| - \operatorname{tr}\underline{\underline{\hat{d}}}\right) + T \operatorname{tr}\underline{\underline{\hat{d}}} \ \text{ if } \operatorname{tr}\underline{\underline{\hat{d}}} \geq 0 \end{cases}$$

(35)
$$\begin{cases} \pi(\underline{n}, [\![\underline{\hat{U}}]\!]) = +\infty \ \text{ if } [\![\underline{\hat{U}}]\!].\underline{n} < 0 \\ \pi(\underline{n}, [\![\underline{\hat{U}}]\!]) = \dfrac{\sigma_0}{2}\left(\left|[\![\underline{\hat{U}}]\!]\right| - [\![\underline{\hat{U}}]\!].\underline{n}\right) + T\,[\![\underline{\hat{U}}]\!].\underline{n} \ \text{ if } [\![\underline{\hat{U}}]\!].\underline{n} \geq 0 \end{cases}$$

Note that this includes the tension cut-off criterion

(36)
$$f(\underline{\underline{\sigma}}) = \sup\left\{\sigma_i - T \,\middle|\, i,j = 1,2,3\right\}$$

with

(37)
$$\begin{cases} \pi(\underline{\underline{\hat{d}}}) = +\infty \ \text{ if } \operatorname{tr}\underline{\underline{\hat{d}}} \neq \left|\hat{d}_1\right| + \left|\hat{d}_2\right| + \left|\hat{d}_3\right| \\ \pi(\underline{\underline{\hat{d}}}) = T \operatorname{tr}\underline{\underline{\hat{d}}} \ \text{ if } \operatorname{tr}\underline{\underline{\hat{d}}} = \left|\hat{d}_1\right| + \left|\hat{d}_2\right| + \left|\hat{d}_3\right| \end{cases}$$

(38)
$$\begin{cases} \pi(\underline{n}, [\![\underline{\hat{U}}]\!]) = +\infty \ \text{ if } [\![\underline{\hat{U}}]\!].\underline{n} \neq \left|[\![\underline{\hat{U}}]\!]\right| \\ \pi(\underline{n}, [\![\underline{\hat{U}}]\!]) = T\,[\![\underline{\hat{U}}]\!].\underline{n} \ \text{ if } [\![\underline{\hat{U}}]\!].\underline{n} = \left|[\![\underline{\hat{U}}]\!]\right| \end{cases}$$

- ***Coulomb's criterion with tension cut-off***

$$f(\underline{\underline{\sigma}}) = \sup\left\{\sigma_i(1+\sin\phi) - \sigma_j(1-\sin\phi) - 2C\cos\phi,\ \sigma_i - T \,\middle|\, i,j = 1,2,3\right\}$$

(39)
$$\begin{cases} \pi(\underline{\underline{\hat{d}}}) = +\infty \ \text{ if } \operatorname{tr}\underline{\underline{\hat{d}}} < \left(\left|\hat{d}_1\right| + \left|\hat{d}_2\right| + \left|\hat{d}_3\right|\right)\sin\phi \\ \pi(\underline{\underline{\hat{d}}}) = C\left(\left|\hat{d}_1\right| + \left|\hat{d}_2\right| + \left|\hat{d}_3\right| - \operatorname{tr}\underline{\underline{\hat{d}}}\right)\tan\left(\dfrac{\pi}{4} + \dfrac{\phi}{2}\right) \\ \qquad\qquad + \dfrac{T}{1-\sin\phi}\left(\operatorname{tr}\underline{\underline{\hat{d}}} - \left(\left|\hat{d}_1\right| + \left|\hat{d}_2\right| + \left|\hat{d}_3\right|\right)\sin\phi\right) \\ \text{if } \operatorname{tr}\underline{\underline{\hat{d}}} \geq \left(\left|\hat{d}_1\right| + \left|\hat{d}_2\right| + \left|\hat{d}_3\right|\right)\sin\phi \end{cases}$$

(40)
$$\begin{cases} \pi(\underline{n}, [\![\underline{\hat{U}}]\!]) = +\infty \ \text{ if } [\![\underline{\hat{U}}]\!].\underline{n} < \left|[\![\underline{\hat{U}}]\!]\right|\sin\phi \\ \pi(\underline{n}, [\![\underline{\hat{U}}]\!]) = C\left(\left|[\![\underline{\hat{U}}]\!]\right| - [\![\underline{\hat{U}}]\!].\underline{n}\right)\tan\left(\dfrac{\pi}{4} + \dfrac{\phi}{2}\right) \\ \qquad\qquad + \dfrac{T}{1-\sin\phi}\left([\![\underline{\hat{U}}]\!].\underline{n} - \left|[\![\underline{\hat{U}}]\!]\right|\sin\phi\right) \\ \text{if } [\![\underline{\hat{U}}]\!].\underline{n} \geq \left|[\![\underline{\hat{U}}]\!]\right|\sin\phi \end{cases}$$

- ***Comments***

Making $k = \sigma_0 / 2$ in Eqs (27) and (29), which amounts to taking the resistance of the material under simple shear as a reference, it comes out that the expressions of the π functions for the velocity jumps are identical for the Tresca criterion and the von Mises criterion. Also, when plane strain virtual strain rates are considered Eqs (26) and (28) yield the same result. Kinematic exterior approaches with plane strain kinematically admissible virtual velocity fields will thus be identical with these two criteria. The same relationship is valid between the Coulomb criterion and the Drucker-Prager criterion: with the expression adopted here (Chapter IV, Eq. (28)) for this latter criterion the correspondence is straightforward. It also holds between the Tresca criterion with tension cut-off and the von Mises criterion with tension cut-off, the Coulomb criterion with tension cut-off and the Drucker-Prager criterion with tension cut-off.

It was noted in Chapter IV (section 4.1) directly from the expressions of $f(\underline{\underline{\sigma}})$ that, as expected, the Tresca and Coulomb criteria with tension cut-off reduce to the original Tresca and Coulomb criteria when $T \to 0$. This appears also on the expressions of the π functions. When $T \to 0$, finite values for the corresponding π functions in Eqs (34) and (35) are only obtained when $\mathrm{tr}\,\hat{\underline{\underline{d}}}$ and $[\![\underline{\hat{U}}]\!].\underline{n}$ are set to zero and these values are identical to those obtained from Eqs (26) and (27). The same reasoning holds for the Coulomb criterion.

4.2 Isotropic interfaces

The virtual velocity jump is split into its normal component $\hat{V}_n = \underline{\hat{V}}.\underline{n}$ and its component tangent to the interface $\underline{\hat{V}}_t$.

- ***The smooth interface***

$$f(\underline{T}) = \sup\{\sigma, \tau\}$$

(41)
$$\begin{cases} \pi(\underline{\hat{V}}) = +\infty \ \text{ if } \underline{\hat{V}}.\underline{n} < 0 \\ \pi(\underline{\hat{V}}) = 0 \ \text{ if } \underline{\hat{V}}.\underline{n} \geq 0 \end{cases}$$

- ***The Tresca interface***

$$f(\underline{T}) = \sup\{\sigma, \tau - k_{\mathrm{i}}\}$$

(42)
$$\begin{cases} \pi(\underline{\hat{V}}) = +\infty \ \text{ if } \underline{\hat{V}}.\underline{n} < 0 \\ \pi(\underline{\hat{V}}) = k_{\mathrm{i}} \left| \underline{\hat{V}}_t \right| \ \text{ if } \underline{\hat{V}}.\underline{n} \geq 0 \end{cases}$$

- ***The Coulomb interface***

$$f(\underline{T}) = \tau + \sigma \tan\phi_i$$

$$\text{(43)} \qquad \begin{cases} \pi(\underline{\hat{V}}) = +\infty \ \text{ if } \underline{\hat{V}}.\underline{n} < \left|\underline{\hat{V}}_t\right| \tan\phi_i \\ \pi(\underline{\hat{V}}) = 0 \ \text{ if } \underline{\hat{V}}.\underline{n} \geq \left|\underline{\hat{V}}_t\right| \tan\phi_i \end{cases}$$

- ***Fully rough interface***

$$f(\underline{T}) = \sigma$$

$$\text{(44)} \qquad \begin{cases} \pi(\underline{\hat{V}}) = +\infty \ \text{ if } \underline{\hat{V}}.\underline{n} < \left|\underline{\hat{V}}\right| \\ \pi(\underline{\hat{V}}) = 0 \ \text{ if } \underline{\hat{V}}.\underline{n} = \left|\underline{\hat{V}}\right| \end{cases}$$

- ***The interface with perfect bonding***

No limit is imposed to (σ, τ).

$$\text{(45)} \qquad \pi(\underline{\hat{V}}) = +\infty \ \ \forall \underline{\hat{V}} \neq 0 .$$

REFERENCES

[1] COULOMB, C.-A. (1773) – Essai sur une application des règles de *Maximis* et *Minimis* à quelques problèmes de statique relatifs à l'architecture. *Mémoires de Mathématique et de Physique présentés à l'Académie Royale des Sciences*, **7**, 1776, pp. 343-382. (English translation: Note on an application of the rules of maximum and minimum to some statical problems relevant to architecture, [2], pp. 41-74).

[2] HEYMAN, J. (1972) – *Coulomb's Memoir on Statics. An Essay in the History of Civil Engineering*, Cambridge University Press.

[3] MOREAU, J.-J. (1966) – *Fonctionnelles convexes*. Séminaire Jean Leray, n° 2 (1966-1967), 1-108[3].

[4] PRAGER, W. (1955) – Théorie générale des états d'équilibre limite. *Journal de Mathématiques P ures et Appliquées*, **34**, 395-406.

[3] http://archive.numdam.org/ARCHIVE/SJL/SJL_1966-1967_2/SJL_1966-1967_2_1_0/SJL_1966-1967_2_1_0.pdf.

Chapter VI

Kinematic
Exterior approach

Equation of the kinematic exterior approach

Relevant virtual velocity fields

One domain, two approaches

References

KINEMATIC EXTERIOR APPROACH

The kinematic exterior approach of the theory of Yield Design states that, for any kinematically admissible virtual velocity field, if the virtual work by a given load exceeds the maximum resisting work, then this load is certainly unsafe. Using such virtual velocity fields, it is possible to draw a convex exterior estimate of the domain K. The efficiency of the method relies on the choice of the kinematically admissible virtual velocity fields which should be "relevant" with respect to the condition of resistance of the constituent material in order that the maximum resisting work be finite. The maximum resisting work, a functional of the kinematically admissible virtual velocity fields, is the support function of the convex domain of potentially safe loads for which it provides the dual definition.

1 Equation of the kinematic exterior approach

The implementation of the kinematic necessary condition presented in Chapter V to obtain an estimate "from outside" of the domain K proceeds from the construction of kinematically admissible virtual velocity fields. These vector fields are piecewise continuous and continuously differentiable and satisfy the boundary conditions on the velocity for the multi-parameter loading mode. From Eq. (10) in Chapter V, any such virtual velocity field $\underline{\hat{U}}$ contributes to the exterior approach of the domain K by excluding an entire half-space in the loading space of the system:

$$(1) \quad \forall \underline{\hat{U}} \text{ K. A., } K \subset \left\{ \underline{\underline{Q}}.\underline{q}(\underline{\hat{U}}) - \int_{\Omega} \pi\left(\underline{x}, \underline{\underline{\hat{d}}}(\underline{x})\right) \mathrm{d}\Omega - \int_{\Sigma_{\underline{\hat{U}}}} \pi\left(\underline{x}, \underline{n}(\underline{x}), [\![\underline{\hat{U}}(\underline{x})]\!]\right) \mathrm{d}\Sigma \leq 0 \right\}.$$

In this equation the sum of the integrals of the π functions in Ω and on $\Sigma_{\underline{\hat{U}}}$ appears as the maximum resisting (rate of) work in the considered virtual velocity field for the whole system, which will be denoted by $\mathcal{P}_{\mathrm{mr}}(\underline{\hat{U}})$

$$(2) \qquad \mathcal{P}_{\mathrm{mr}}(\underline{\hat{U}}) = \int_{\Omega} \pi\left(\underline{x}, \underline{\underline{\hat{d}}}(\underline{x})\right) \mathrm{d}\Omega + \int_{\Sigma_{\underline{\hat{U}}}} \pi\left(\underline{x}, \underline{n}(\underline{x}), [\![\underline{\hat{U}}(\underline{x})]\!]\right) \mathrm{d}\Sigma.$$

Eq. (1) takes the final form

$$(3) \qquad \forall \underline{\hat{U}} \text{ K. A., } K \subset \left\{ \underline{\underline{Q}}.\underline{q}(\underline{\hat{U}}) - \mathcal{P}_{\mathrm{mr}}(\underline{\hat{U}}) \leq 0 \right\}$$

which is the **fundamental equation of the kinematic exterior approach**.

This equation is meaningful whenever the inequality $\underline{Q}.\underline{q}(\hat{\underline{U}}) - \mathcal{P}_{\text{mr}}(\hat{\underline{U}}) \leq 0$ is non-trivial, *i.e.* not identically fulfilled.

It is clear that from the construction of several kinematically admissible virtual velocity fields a convex surface is obtained in the loading space $\mathbb{R}^n$ which is an estimate "from outside" of the boundary of K and which provides "upper bounds" for the extreme loads (Figure 1). For a given value of $\underline{q}(\hat{\underline{U}})$, the corresponding estimate is all the more valuable that the value of $\mathcal{P}_{\text{mr}}(\hat{\underline{U}})$ is lower.

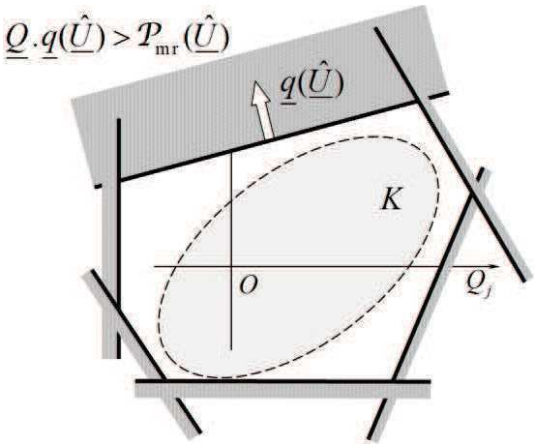

Figure 1. Kinematic exterior approach of K

In the case of one positive loading parameter the exterior approach provides upper bound estimates for the extreme load Q^* of the system (Figure 2) and results in a minimization process on $\mathcal{P}_{\text{mr}}(\hat{\underline{U}})$:

(4) $$\forall \hat{\underline{U}} \text{ K. A. such that } q(\hat{\underline{U}}) > 0, \quad Q^* \leq \frac{\mathcal{P}_{\text{mr}}(\hat{\underline{U}})}{q(\hat{\underline{U}})}.$$

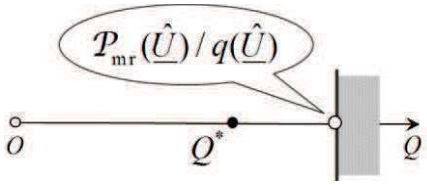

Figure 2. Kinematic exterior approach in the case of one positive loading parameter

In the same way, in the case of a radial loading mode when all loading parameters vary proportionally to one positive parameter λ standing for a "safety coefficient" of a given load $\underline{Q}^{\text{d}}$ (*cf.* Chapter IV, § 2.3), the kinematic exterior approach provides an upper bound for the extreme value λ^* of this coefficient

(5) $$\forall \hat{\underline{U}} \text{ K. A. such that } \underline{Q}^{\text{d}}.\underline{q}(\hat{\underline{U}}) > 0, \quad \lambda^* \leq \frac{\mathcal{P}_{\text{mr}}(\hat{\underline{U}})}{\underline{Q}^{\text{d}}.\underline{q}(\hat{\underline{U}})}.$$

Again, as in Chapter IV (§ 3.1), special attention should be paid to the case when "genuine" variable loads are acting together with permanent loads. For the reason already given, after the definition of any "safety coefficient" has been clearly stated, systematically referring to the fundamental equation of the kinematic exterior approach (3) leads to the correct result straightforwardly.

2 Relevant virtual velocity fields

2.1 Definition

In order to save time when implementing Eq. (3) it is worth observing that, since $\underline{Q}.\underline{q}(\underline{\hat{U}})$ is linear and $\mathcal{P}_{\text{mr}}(\underline{\hat{U}})$ positively homogeneous with degree 1 with respect to $\underline{\hat{U}}$, it is no use considering collinear kinematically admissible virtual velocity fields $(\alpha\underline{\hat{U}},\ \alpha>0)$, only one of them is sufficient.

As stated earlier, for the method to be efficient the inequality $(\underline{Q}.\underline{q}(\underline{\hat{U}})-\mathcal{P}_{\text{mr}}(\underline{\hat{U}})\le 0)$ must be non-trivial.

- A first condition is obvious:

(6) $$\underline{Q}.\underline{q}(\underline{\hat{U}})\neq 0\ .$$

It means that the kinematically admissible virtual velocity fields should be chosen in such a way as to have the external forces work actually.

- The second condition relates to $\mathcal{P}_{\text{mr}}(\underline{\hat{U}})$:

(7) $$\mathcal{P}_{\text{mr}}(\underline{\hat{U}})<+\infty\ .$$

It means that, as test functions, the kinematically admissible virtual velocity fields must explore the compatibility between equilibrium and resistance in the directions where the resistance of the material develops a finite maximum resisting work.

Kinematically admissible virtual velocity fields which comply with these two conditions will be called **relevant virtual velocity fields**.

Recalling the definition of $\mathcal{P}_{\text{mr}}(\underline{\hat{U}})$ it follows that, since the π functions are non-negative, Eq. (7) implies that each integral in Eq. (2) is finite

(8) $$\int_{\Omega}\pi\left(\underline{x},\underline{\underline{\hat{d}}}(\underline{x})\right)\mathrm{d}\Omega<+\infty\ ,$$

(9) $$\int_{\Sigma_{\underline{\hat{U}}}}\pi\left(\underline{x},\underline{n}(\underline{x}),[\![\underline{\hat{U}}(\underline{x})]\!]\right)\mathrm{d}\Sigma<+\infty$$

and, finally, that each π function takes a finite value everywhere in Ω and on $\Sigma_{\underline{\hat{U}}}$ respectively

(10) $$\pi(\underline{x}, \underline{\underline{\hat{d}}}(\underline{x})) < +\infty \text{ in } \Omega,$$

(11) $$\pi(\underline{x}, \underline{n}(\underline{x}), [\![\underline{\hat{U}}(\underline{x})]\!]) < +\infty \text{ on } \Sigma_{\underline{\hat{U}}}.$$

Eqs (10) and (11) mean that the virtual velocity field $\underline{\hat{U}}$ must be chosen in such a way that $\underline{\underline{\hat{d}}}(\underline{x})$ and $([\![\underline{\hat{U}}(\underline{x})]\!] \otimes \underline{n}(\underline{x}) + \underline{n}(\underline{x}) \otimes [\![\underline{\hat{U}}(\underline{x})]\!])$ be normal to the boundary of $G(\underline{x})$ at a finite distance.

This kind of normality rule must not be confounded with a constitutive law, whatever its formal similarity with the flow rule of plastic materials obeying the principle of maximum plastic work [1]. As it has been underscored before it is **the mathematical rule** derived from the strength criterion in the **dual definition** of $G(\underline{x})$: the relevance condition is just due to the fact that $G(\underline{x})$ is not bounded in some directions.
Unfortunately this confusion is quite frequent and begets misunderstandings regarding the status of Yield Design kinematic analyses.

2.2 Relevance conditions for usual isotropic strength criteria

- ***Tresca's and von Mises' criteria***

The relevance conditions are identical for these two criteria. This comes from the fact that they are not bounded within the same convex cone $I(\underline{x})$ which is reduced to the directions of isotropic stress tensors $\underline{\underline{\sigma}} = \sigma \underline{\underline{1}}$. From Eqs (26-29) in Chapter V we derive the conditions on $\underline{\underline{\hat{d}}}$ and on $[\![\underline{\hat{U}}]\!]$ with respect to $\Sigma_{\underline{\hat{U}}}$

(12) $$\begin{cases} \operatorname{tr} \underline{\underline{\hat{d}}} = 0 \\ [\![\underline{\hat{U}}]\!].\underline{n} = 0. \end{cases}$$

There should be **no volume change** in relevant virtual velocity fields. The second line in Eq. (12) means that the virtual velocity jump must be **tangent** to the jump surface.

- ***Coulomb's criterion***

The relevance conditions follow from Eqs (30, 31) in Chapter V:

(13) $$\begin{cases} \operatorname{tr} \underline{\underline{\hat{d}}} \geq (\left|\hat{d}_1\right| + \left|\hat{d}_2\right| + \left|\hat{d}_3\right|) \sin\phi \\ [\![\underline{\hat{U}}]\!].\underline{n} \geq \left|[\![\underline{\hat{U}}]\!]\right| \sin\phi. \end{cases}$$

They show that relevant virtual velocity fields should cause a **positive volume change**, the minimum dilatancy of which is given by the first line in Eq. (13). The consequence for $[\![\underline{\hat{U}}]\!]$ with respect to $\Sigma_{\underline{\hat{U}}}$ is that the virtual velocity jump cannot be tangent to the jump surface but must **make an angle at least equal to ϕ with** $\Sigma_{\underline{\hat{U}}}$ as shown in Figure 3.

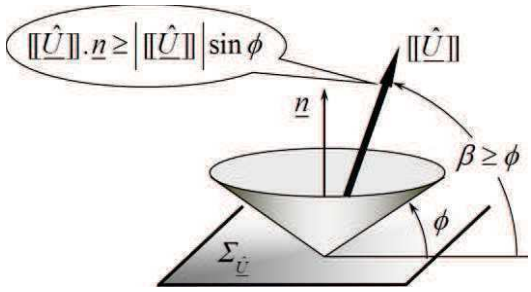

Figure 3. Relevant virtual velocity jump in the case of Coulomb's criterion

- ***Tresca's and von Mises criteria with tension cut-off***

The relevance conditions are the same for these two criteria: **non negative** virtual volume change.

(14)
$$\begin{cases} \operatorname{tr} \underline{\underline{\hat{d}}} \geq 0 \\ [\![\underline{\hat{U}}]\!].\underline{n} \geq 0. \end{cases}$$

- ***Coulomb's criterion with tension cut-off***

The relevant virtual velocity fields are the same as for the original Coulomb's criterion:

(15)
$$\begin{cases} \operatorname{tr} \underline{\underline{\hat{d}}} \geq (\left|\hat{d}_1\right| + \left|\hat{d}_2\right| + \left|\hat{d}_3\right|) \sin\phi \\ [\![\underline{\hat{U}}]\!].\underline{n} \geq \left|[\![\underline{\hat{U}}]\!]\right| \sin\phi. \end{cases}$$

- ***Smooth interface and Tresca's interface***

The condition of relevance proceeds from Eqs (41, 42) in Chapter V:

(16)
$$\underline{\hat{V}}.\underline{n} \geq 0\,.$$

- ***Coulomb's interface***

From Eq. (43) in Chapter V we get:

(17)
$$\underline{\hat{V}}.\underline{n} \geq \left|\underline{\hat{V}}_t\right| \tan\phi_i$$

The velocity jump $\underline{\hat{V}}$ in the interface must make an angle at least equal to ϕ_i with the interface Σ (Figure 4).

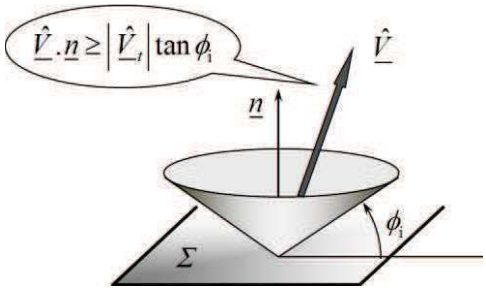

Figure 4. Relevant virtual velocity jump in a Coulomb's interface

- ***Fully rough interface***

The condition of relevance comes from Eq. (V, 44):

(18) $$\underline{\hat{V}}.\underline{n} = \left| \underline{\hat{V}} \right|,$$

which states that relevant virtual velocity jumps should be collinear to the outward normal to the interface.

- ***Interface with perfect bounding***

From Eq. (V, 45) the condition of relevance is just:

(19) $$\underline{\hat{V}} = 0.$$

2.3 Implementation of the relevance condition

When the kinematic exterior approach is performed analytically, the relevance condition is taken into account in the construction of the kinematically admissible virtual velocity fields.

For instance, if the relevance condition is given by Eq. (12), plane strain virtual velocity fields satisfying the zero divergence condition for two-dimensional problems can be derived from a scalar potential or obtained through the analytical integration of the Geiringer equations (*cf.* [2]) on a mesh of orthogonal characteristic lines. The same method, based on the counterpart of the Geiringer equations [3], is also used when the relevance condition is Eq. (13). The kinematically admissible virtual velocity fields obtained through these methods are relevant *stricto sensu*. The integration along the characteristic lines can also be carried out numerically.

For three-dimensional problems, similar methods are used in the case of axial symmetry, while highly sophisticated analytical approaches have been recently proposed for the construction of planar but non-plane strain virtual velocity fields [4, 5].

With the development of finite element methods the relevance condition may be taken into account through penalty[1] or dualisation methods (*e.g.* [6, 7]).

Taking the same examples as before, let us consider first the case when Eq. (12) is the relevance condition for instance with the von Mises strength criterion. The dualisation method consists in writing Eqs (V, 28, 29) which give the explicit values of $\pi(\underline{\underline{\hat{d}}})$ and $\pi(\underline{n},[\![\underline{\hat{U}}]\!])$, in the equivalent forms

(20) $$\begin{cases} \pi(\underline{\underline{\hat{d}}}) = \sup_{p\in\mathbb{R}} \left\{ k\sqrt{2\,\mathrm{tr}\,(\underline{\underline{\hat{d}}})^2} - p\,\mathrm{tr}\,\underline{\underline{\hat{d}}} \right\} \\ \pi(\underline{n},[\![\underline{\hat{U}}]\!]) = \sup_{p\in\mathbb{R}} \left\{ k\left|[\![\underline{\hat{U}}]\!]\right| - p[\![\underline{\hat{U}}]\!].\underline{n} \right\} \end{cases}$$

and letting the maximisation process on the field p to be performed numerically together with the minimisation of $\mathcal{P}_{\mathrm{mr}}(\underline{\hat{U}})$ in the fundamental equation (3).

[1] Relaxing the relevance mathematical constraint and adding the product of the constraint by its (high) "price" to the expression of the π function.

In the case of Eq. (13) with the Coulomb strength criterion, the method is quite similar with the following expressions to be introduced in Eq. (2) for $\mathcal{P}_{\rm mr}(\underline{\hat{U}})$:

$$(21)\qquad \begin{cases} \pi(\underline{\underline{\hat{d}}}) = \sup_{p\in\mathbb{R}^+} \left\{ \dfrac{C}{\tan\phi}\,\mathrm{tr}\,\underline{\underline{\hat{d}}} - p\left(\mathrm{tr}\,\underline{\underline{\hat{d}}} - (\left|\hat{d}_1\right| + \left|\hat{d}_2\right| + \left|\hat{d}_3\right|)\sin\phi\right) \right\} \\ \pi(\underline{n}, [\![\underline{\hat{U}}]\!]) = \sup_{p\in\mathbb{R}^+} \left\{ \dfrac{C}{\tan\phi}[\![\underline{\hat{U}}]\!].\underline{n} - p\left([\![\underline{\hat{U}}]\!].\underline{n} - \left|[\![\underline{\hat{U}}]\!]\right|\sin\phi\right) \right\}. \end{cases}$$

3 One domain, two approaches

3.1 Dual approach of the convex K

From its definition (2) and the properties of the the π functions, the functional $\mathcal{P}_{\rm mr}(\underline{\hat{U}})$ is obviously non-negative, positively homogeneous with degree 1 and convex with respect to the kinematically admissible virtual velocity fields $\underline{\hat{U}}$. Thence, in the same way as $\pi(\underline{x}, \underline{\underline{\hat{d}}}(\underline{x}))$ in Eq. (V, 22), $\mathcal{P}_{\rm mr}(\underline{\hat{U}})$ defines the convex domain $\boldsymbol{K}$ in $\mathbb{R}^n$ for which it is the support function through Eq. (22):

$$(22)\qquad \underline{Q} \in \boldsymbol{K} \Leftrightarrow \forall \underline{\hat{U}}\ \text{K. A.},\ \underline{Q}.\underline{q}(\underline{\hat{U}}) - \mathcal{P}_{\rm mr}(\underline{\hat{U}}) \le 0.$$

It follows that Eq. (3) can simply be written:

$$(23)\qquad K \subset \boldsymbol{K}.$$

Since $\mathcal{P}_{\rm mr}(\underline{\hat{U}})$ originates from the support function of $G(\underline{x})$, it is quite natural to expect that $\mathcal{P}_{\rm mr}(\underline{\hat{U}})$ is the support function of K, and that Eq. (23) is an identity.

The answer is positive. The mathematical proof was given by Frémond and Friaà [8], clarifying the mathematical features of the problem and pointing out the specific role played by the position of the zero stress state $(\underline{\underline{\sigma}}(\underline{x}) = 0)$ inside or on the boundary of $G(\underline{x})$.

This result proves that Eq. (22) is in fact **the dual definition** of K:

$$(24)\qquad \underline{Q} \in K \Leftrightarrow \forall \underline{\hat{U}}\ \text{K. A.},\ \underline{Q}.\underline{q}(\underline{\hat{U}}) - \mathcal{P}_{\rm mr}(\underline{\hat{U}}) \le 0,$$

which may also be written

$$(25)\qquad K = \bigcap_{\underline{\hat{U}}\ \text{K. A.}} \left\{ \underline{Q}.\underline{q}(\underline{\hat{U}}) - \mathcal{P}_{\rm mr}(\underline{\hat{U}}) \le 0 \right\}.$$

Although it does not modify the practical application of the kinematic exterior approach as sketched in Figure 1, this result states that the minimizing process on $\mathcal{P}_{\rm mr}(\underline{\hat{U}})$ for any given value of $\underline{q}(\underline{\hat{U}})$ converges to the exact determination of K.

3.2 Static interior approach combined with the kinematic exterior one

As a consequence of the preceding result it may happen that, by performing the static interior approach and the kinematic exterior one independently from each other, the following circumstances are encountered.

- *Through the static interior approach*
  A load $\underline{Q}(\underline{\underline{\sigma}})$ is proven to be potentially safe

(26)
$$\exists\, \underline{\underline{\sigma}} \begin{cases} \underline{\underline{\sigma}} \text{ S.A. with } \underline{Q}(\underline{\underline{\sigma}}) \\ \underline{\underline{\sigma}}(\underline{x}) \in G(\underline{x}),\ \forall M \in \Omega \end{cases}$$

- *Through the kinematic exterior approach*
  A half-space in $\mathbb{R}^n$ is proven to be exterior or tangent to K

(27)
$$\underline{\hat{U}} \text{ K. A. } \Rightarrow K \subset \left\{ \underline{Q}.\underline{q}(\underline{\hat{U}}) - \mathcal{P}_{\text{mr}}(\underline{\hat{U}}) \le 0 \right\}$$

- *And*
  $\underline{Q}(\underline{\underline{\sigma}})$ is such that its virtual work equilibrates the maximum resisting work in the virtual velocity field $\underline{\hat{U}}$ in Eq. (27):

(28)
$$\underline{Q}(\underline{\underline{\sigma}}).\underline{q}(\underline{\hat{U}}) - \mathcal{P}_{\text{mr}}(\underline{\hat{U}}) = 0\,.$$

Consequently we derive that (Figure 5)

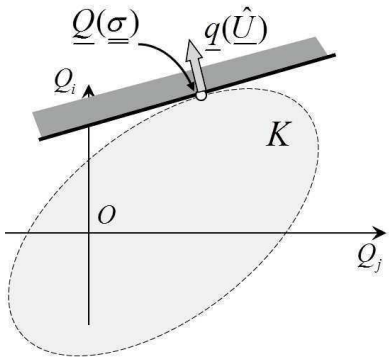

Figure 5. Combining the static interior approach and the kinematic exterior one

- $\underline{Q}(\underline{\underline{\sigma}})$ is situated on the boundary of K: it is an extreme load.
- The plane with equation $\underline{Q}(\underline{\underline{\sigma}}).\underline{q}(\underline{\hat{U}}) - \mathcal{P}_{\text{mr}}(\underline{\hat{U}}) = 0$ is tangent to K at point $\underline{Q}(\underline{\underline{\sigma}})$.

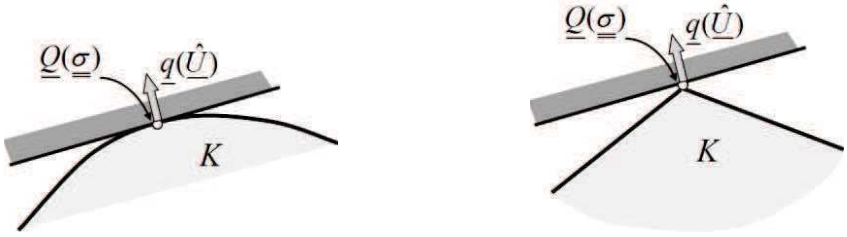

Figure 6. Regular or singular point on the boundary of K

Thus $\underline{q}(\underline{\hat{U}})$ is an outward normal to K at point $\underline{Q}(\underline{\underline{\sigma}})$, which may be a regular or a singular point (Figure 6).

Moreover, despite the fact that the statically admissible field $\underline{\underline{\sigma}}$ in Eq. (26) and the kinematically admissible virtual velocity field $\underline{\hat{U}}$ in Eq. (27) have been constructed independently, they come out as being associated to each other. Actually, reversing the rationale developed in Chapter V (Section 2), applying the virtual work equation to Eq. (28) and writing $\mathcal{P}_{\text{mr}}(\underline{\hat{U}})$ in its explicit form (2) we get:

$$(29)\quad \int_{\Omega} \underline{\underline{\sigma}} : \underline{\underline{\hat{d}}}\, \mathrm{d}\Omega + \int_{\Sigma_{\underline{\hat{U}}}} (\underline{\underline{\sigma}}.[\![\underline{\hat{U}}]\!]).\underline{n}\, \mathrm{d}\Sigma - \int_{\Omega} \pi\left(\underline{x}, \underline{\underline{\hat{d}}}(\underline{x})\right) \mathrm{d}\Omega - \int_{\Sigma_{\underline{\hat{U}}}} \pi\left(\underline{x}, \underline{n}(\underline{x}), [\![\underline{\hat{U}}(\underline{x})]\!]\right) \mathrm{d}\Sigma = 0 .$$

From the definition of the π functions this equality is satisfied only if

$$(30)\quad \underline{\underline{\sigma}}(\underline{x}).\underline{\underline{\hat{d}}}(\underline{x}) = \pi\left(\underline{x}, \underline{\underline{\hat{d}}}(\underline{x})\right) \text{ in } \Omega ,$$

$$(31)\quad \underline{\underline{\sigma}}(\underline{x}).[\![\underline{\hat{U}}(\underline{x})]\!].\underline{n}(\underline{x}) = \pi\left(\underline{x}, \underline{n}(\underline{x}), [\![\underline{\hat{U}}(\underline{x})]\!]\right) \text{ on } \Sigma_{\underline{\hat{U}}} .$$

It follows that at any point in Ω (resp. $\Sigma_{\underline{\hat{U}}}$) where $\underline{\underline{\hat{d}}}(\underline{x})$ (resp. $[\![\underline{\hat{U}}(\underline{x})]\!]$) is not equal to zero we have

$$(32)\quad \underline{\underline{\sigma}}(\underline{x}) = \underline{\underline{\sigma}}^{*}(\underline{x})$$

where $\underline{\underline{\sigma}}^{*}(\underline{x})$ is one stress state associated with $\underline{\underline{\hat{d}}}(\underline{x})$ (resp. $[\![\underline{\hat{U}}(\underline{x})]\!]$) in Eq. (V, 15).

In the case when $G(\underline{x})$ is **strictly convex** $\forall M \in \Omega$, this "association theorem" implies that all stress fields $\underline{\underline{\sigma}}$ satisfying Eq. (26) when $\underline{Q}$ is an extreme load will **coincide** wherever $\underline{\underline{\hat{d}}}(\underline{x}) \neq 0$ or $[\![\underline{\hat{U}}(\underline{x})]\!] \neq 0$ in any kinematically admissible virtual velocity field verifying Eq. (27). The result includes the case of non-collinear kinematically admissible virtual velocity fields satisfying Eq. (27), with $\underline{Q}$ being either a regular or a singular point on the boundary of K (*e.g.* [9]).

If the circumstances enunciated at the beginning of this paragraph are encountered with a stress field $\underline{\underline{\sigma}}$ satisfying Eq. (26) and a virtual velocity field $\underline{\hat{U}}$ satisfying Eq.(27), these associated fields are said to build up a **complete solution** to the Yield Design problem. An example will be given in Chapter XI (§ 4.2).

3.3 General comments

The primal approach of the theory of Yield Design has settled the problem and introduced the concept of potentially safe loads from the necessary condition for "stability" that Equilibrium and Resistance must be mathematically compatible. It has logically led to the static interior approach of the convex domain K which calls for the construction of statically admissible stress fields complying with the condition of resistance of the constituent material. The implementation of this method suffers two main drawbacks for practical applications:

- The fields to be constructed are symmetric tensor fields (6 piecewise continuous and continuously differentiable scalar fields) that must verify the 3 partial differential equations of equilibrium (Chapter III, § 2.4) and the boundary condition on the external forces, within the multi-parameter loading mode;
- The stress field must be constructed in the **entire** volume of the system.

This explains why, most often, when implementing the static interior approach only makes use of simple such stress fields, unless sophisticated mathematical methods, such as the method of characteristics for plane or axisymmetric problems [10-26], or efficient numerical procedures can be used [27-38]. The ever-present requirement of the complete construction of the stress field in its entire extension should always be carefully checked for the validity of the lower bounds so obtained[2].

In consideration of these difficulties, the dual approach of the theory of Yield Design is a real **step forward**.

- The kinematic exterior approach only requires the construction of kinematically admissible virtual velocity fields (only 3 piecewise continuous and continuously differentiable scalar fields) which must verify the boundary conditions on the velocity within the multi-parameter loading mode.
- The fundamental equation of the kinematic exterior approach can be written systematically since the expression of the maximum resisting work is available at the same time as the strength criterion.
- Moreover, the concept of relevant virtual velocity field provides guidelines for designing efficient kinematically admissible virtual velocity fields. As shown in Figure 1, a few well chosen kinematically admissible virtual velocity fields may be sufficient for providing a good convex exterior estimate of the domain K.
- Finally, it is worth noting that this estimate is affirmative as regards instability, which makes it most valuable for back calculations.

At first glance, the two approaches of the Yield Design theory could appear as a mere mathematical transposition of the common practice of ancient builders according to which (using the present concepts)

- If a stress field in equilibrium with the loads and complying with the resistance of the constituent material can be found, the system will be certainly stable
- If a velocity field can be found where the work by the external forces exceeds the work by the resisting forces, the system will be certainly unstable.

We have already seen that the first statement is not true and must be corrected by substituting “potentially” to “certainly”.

But the second statement is not true either. The difficulty lies in the definition of the work by the resisting forces in a velocity field which is implicitly assumed to be a real one, since these forces are only known through the limits they are assigned. It follows that complementary assumptions are introduced in order to conciliate the use of

[2] As a matter of fact it is very seldom satisfied.

"real" velocity fields with the condition of resistance. Examples have been given (*e.g.* [39]) showing that the two statements are not consistent with each other and can lead to contradictory results. Let us recall once more that the kinematic exterior approach is only valid in the form it has been presented here with kinematically admissible **virtual** velocity fields and with the **maximum resisting work** derived from the **dualisation** of the strength condition.

Some final comments may now be added to what has been written in Chapter IV (§ 3.2) regarding the **convexity** assumption for the strength condition of the constituent material. As a matter of fact, assuming for instance that this domain is star-shaped with respect to the origin, the rationale developed in Section 2 of Chapter V can be completely reproduced:

- the same kinematical necessary condition will be established,
- π functions defined and computed
- and the same kinematic approach can be performed.

The important point then is that the π functions involved are but the dual definition of the convex hull of the strength condition. Therefore this kinematic approach refers to the dual definition of the domain of potentially safe loads with this convex hull as a strength condition, which encompasses the convex hull of the actual star-shaped domain of potentially safe loads.

REFERENCES

[1] HILL, R. (1948) – A variational principle of maximum plastic work in classical plasticity. *Quarterly Journal of Mechanics and Applied Mathematics*, **1**, 18-28.

[2] GEIRINGER, H. (1953) – Some recent results in the theory of an ideal plastic body. *Advances in Applied Mechanics,* Academic Press, New York.

[3] SALENÇON, J. (1977) – *Applications of the Theory of Plasticity in Soil Mechanics*. John Wiley and sons, Chichester.

[4] PUZRIN, A. M. & RANDOLPH, M. F. (2003) – New planar velocity fields for upper bound limit analysis. *International Journal of Solids and Structures,* **40**, (13-14), 3603-3619.

[5] RANDOLPH, M. F. & PUZRIN, A. M. (2003) – Upper bound limit analysis of circular foundations on clay under general loading. *Géotechnique*, **53**, 9, 785-796.

[6] DELBECQ, J.M., FRÉMOND, M., PECKER, A, & SALENÇON, J. (1977) – Éléments finis en plasticité et viscoplasticité. *Journal de Mécanique Appliquée*, **1**, n°3, 1977, 267-304.

[7] FRÉMOND, M. & SALENÇON, J. (1973) – Limit analysis by finite-element method. *Proceedings of the Symposium on the Role of Plasticity in Soil Mechanics*, Cambridge (UK), Sept. 1973, (PALMER A. C. ed.), pp. 297-308.

[8] FRÉMOND, M. & FRIAÀ, A. (1978) – Analyse limite. Comparaison des méthodes statique et cinématique. *Comptes Rendus de l'Académie des sciences de Paris*, **286**, A, 107-110.

[9] SALENÇON, J. (1968) – Étude d'une classe de solutions cinématiques pour le problème du poinçonnement d'un demi-plan non homogène. *Comptes Rendus de l'Académie des sciences de Paris,* **267**, A, 171-173.

[10] BEREZANCEW, B. G. (1952) – *Axisymmetric Problem of the Theory of Limiting Equilibrium of a Granular Medium.* [in Russian], Gostekhizdat, Moscow (1952).

[11] HILL, R. (1950) – *The mathematical theory of plasticity.* Clarendon Press, Oxford.

[12] HOULSBY, G. T. & WROTH, C. P. (1982) – Direct solution of plasticity problems in soils by the method of characteristics. *Proceedings of the 4th International Conference on Numerical Methods in Geomechanics, Edmonton*, **3**, pp. 1059-1071.

[13] KÖTTER, W. T. (1903) – Die Bestimmung des Druckes an den gekrümmten Gleitflächen, eine Aufgabe aus der Lehre vom Erddruck. *Berliner Akademie Bericht,* 229-233.

[14] KÖTTER, W. T. (1909) – Über den Druck von Sand gegen Öffnungsverschlüsse im horizontalen Boden kastenförmiger Gefäße. *Berliner Akademie Bericht*, 493-510.

[15] LAU, C. K. & BOLTON, M. D. (2011) – The bearing capacity of footings on granular soils. I: numerical analysis. *Géotechnique*, **61**, 8, 627-638.

[16] MARTIN, C. M. (2005) – Exact bearing capacity calculations using the method of characteristics. *Proceedings of the 11th International Conference. on Computer Methods and Advances in Geomechanics,* **4**, pp. 441-450.

[17] MASSAU, J. (1899) – Mémoire sur l'intégration graphique des équations aux dérivées partielles ; chap. IV: équilibre des terres sans cohésion. *Annales de l'Association des Ingénieurs de l'École de Gand*, 1899; Édition du centenaire, Comité national de mécanique, Brussels, Mons, 1952.

[18] MATAR, M. & SALENÇON, J. (1979) – Capacité portante des semelles filantes. *Revue Française de Géotechnique*, **9**, 1979, 51-76.

[19] MICHALOWSKI, R. L. & YOU L. (1998) – Non-symmetrical limit loads on strip footings. *Soils and Foundations*, **38**, 4, 195-203.

[20] MICHALOWSKI, R. L. & DRESCHER A. (2009) – Three-dimensional stability analysis of slopes and excavations. *Géotechnique*, **59**, 10, 839-850.

[21] SALENÇON, J. (1974) – Bearing capacity of a footing on a purely cohesive soil with linearly varying shear strength. *Géotechnique*, **24**, n°3, 1974, 443-446.

[22] SALENÇON, J., FLORENTIN, P. & GABRIEL, Y. (1976) – Capacité portante globale d'une fondation sur un sol non homogène. *Géotechnique*, **26**, n°2, 1976, 351-370.

[23] SALENÇON, J. & MATAR, M. (1982) – Capacité portante des fondations superficielles circulaires. *Journal de Mécanique Théorique et Appliquée*, **1**, n°2, 1982, 237-267.

[24] SOKOLOVSKI, V. V. (1955) – *Theorie der Plastizität*. VEB Verlag Technik, Berlin.

[25] SOKOLOVSKI, V. V. (1960) – *Statics of Soil Media*. Butterworths Scientific Publications, London.

[26] SOKOLOVSKI, V. V. (1965) – *Statics of Granular Media*. Pergamon Press, Oxford.

[27] ANDERHEGGEN, E. & KNÖPFEL, H. (1972) – Finite element limit analysis using linear programming. *Int. J. of Solids and Structures*, **8**, 1413-1431.

[28] KAMMOUN, Z., PASTOR, F., SMAOUI, H. & PASTOR, J. (2010) – Large satic problem in numerical analysis: a decomposition approach. *Int. J. for Numerical and Analytical Methods in Geomechanics*, **34**, 18, 1960-1980.

[29] KRABBENHOFT, K. & DAMKILDE, L. (2003) – A general optimization algorithm for lower bound limit analysis. *International Journal for Numerical Methods in Engineering*, **56**, 165-184.

[30] KRABBENHOFT, K., LYAMIN, A. V., HIJAJ, M. & SLOAN, M. W. (2005) – A new discontinuous upper bound analysis formulation. *International Journal for Numerical Methods in Engineering*, **63**, 1069-1088.

[31] LYAMIN, A. V. & SLOAN, M. W. (2002) – Lower bound limit analysis using nonlinear programming. *International Journal for Numerical Methods in Engineering*, **55**, 573-611.

[32] LYAMIN, A. V. & SLOAN, M. W. (2002) – Upper bound limit analysis using linear finite elements and non-linear programming. *International Journal for Numerical and Analytical Methods in Geomechanics*, **26**, 181-216.

[33] LYSMER, J. (1970) – Limit analysis of plane problems in soil mechanics. *Journal of the Soil Mechanics and Foundations Division, ASCE*, **96**, 1311-1334.

[34] MAKRODIMOPOULOS, A. & MARTIN, C. M. (2006) – Lower bound limit analysis of cohesive-frictional materials using second-order cone programming. *International Journal for Numerical Methods in Engineering*, **66**, 4, 604-634.

[35] MAKRODIMOPOULOS, A. & MARTIN, C. M. (2007) – Upper bound limit using simplex strain element and second-order cone programming. *International Journal for Numerical and Analytical Methods in Geomechanics*, **31**, 835-865.

[36] MAKRODIMOPOULOS, A. & MARTIN, C. M. (2008) – Upper bound limit using discontinuous quadratic displacement fields. *Communications in Numerical Methods in Engineering*, **24**, 11, 911-927.

[37] MARTIN, C. M. (2011) – The use of adaptive finite-element limit analysis to reveal slip-line fields. *Géotechnique Letters*, **1**, 2, 23-29.

[38] PASTOR, F., LOUTE, E. & PASTOR, J. (2009) – Limit analysis and convex programming: A decomposition approach of the kinematic mixed method. *International Journal for Numerical Methods in Engineering*, **78**, 254-274.

[39] SALENÇON, J. (1972) – Un exemple de non-validité de la théorie classique des charges limites pour un système non standard. *Proceedings of the International Symposium on the Foundations of Plasticity*, Warsaw, 1972. *Problems of Plasticity*, A. Sawczuck ed. Noordhoff, Leyden, 1974, pp. 432-439.

Chapter VII

Ultimate Limit State Design From the theory of Yield Design

Basic principles of Ultimate Limit State Design
Revisiting the Yield Design theory in the context of ULSD
The Yield Design theory applied to ULSD
References

ULTIMATE LIMIT STATE DESIGN
From the theory of Yield Design

With the explicit introduction of Resistance parameters to define the strength conditions of the constituent materials, the theory of Yield Design is completed as the fundamental basis of Ultimate Limit State Design. The equation of the kinematic exterior approach provides an unambiguous scalar expression for the symbolic inequality of ULSD where the "effects" are clearly identified as the virtual work by the design loads on the one side and as the maximum resisting work by the design resistances on the other. It makes it easy to handle the partial factors on the loads, either "unfavourable" or "favourable" to equilibrium, and on the resistances, and also to define a partial factor for model uncertainties.

1 Basic principles of Ultimate Limit State Design

The basic principles of Ultimate Limit State Design (ULSD) have been announced in Chapter I (§ 2.2) in the terms used by Krebs Ovesen [1]:

"*The design criterion is simply to design for equilibrium* [under the design loads] *in the design limit state of failure. The design criterion could be expressed in the following way:*

(1) $$R_{\mathrm{d}} \geq S_{\mathrm{d}}".$$

This means that the *design load effect* S_{d} should be inferior to the *effect of the design resistances* R_{d}.

The simplicity of this statement relies on two requirements:

- A clear distinction between the **loads** or **active forces** on one side and the **resistances** on the other side is made in such a way that
- Their "effects" can be defined in a scalar form independently from each other.

These conditions being fullfilled, **design** values of the quantities involved are introduced which are derived from the "actual" or conventional data through the application of **partial factors**.

For the resistances, each partial factor (for material property) is a divisor, >1, applied to the value of each conventional strength characteristic.

For the active forces (permanent and variable actions), the partial factor is a multiplier for each independent load, >1 for a load which is unfavourable to equilibrium and <1 for a favourable one.

In the case of statically determined systems the symbolic inequality in Eq. (1) is easily transformed into a mathematical expression by taking the strength criterion of the constituent material as a scalar measure of the "effects". For each design load combination the strength criterion must be checked at any point in the system in order to enforce that its value does not exceed the limit assigned by the design values of the resistance. Obviously this procedure cannot be used in the general case. Apart from this major difficulty, it also appears that, depending on the mathematical form of the strength criterion, making the distinction between unfavourable and favourable loads can prove quite tricky!

2 Revisiting the Yield Design theory in the context of ULSD

2.1 Resistance parameters

The similarity between the principles of ULSD and the fundamental basis of the Yield Design theory, "Compatiblity between Equilibrium and Resistance", has already been underscored in Chapter I. Now, with reference to the definition of the potentially safe loads given in Chapter IV, it is possible to be more precise.

Regarding the loads, the multi-parameter loading mode in the Yield Design theory is perfectly suited to ULSD: all the independent external loads which appear in the different design load combinations, including the permanent loads, are assigned a loading parameter. Each parameter Q_i is a function of the corresponding partial factor. Symbolically these partial factors on the actions will be denoted $\underline{\Gamma}_Q$.

As for the resistances, the strength domains of the constituent materials of the system are defined through **resistance parameters** [2] (*e.g.* ϕ, C, σ_0,…). These parameters will now be denoted symbolically by $\underline{R}$, which is a function of the partial factors for material property denoted $\underline{\Gamma}_R$; the strength domain of the material at point M is $G(\underline{x},\underline{R})$.

2.2 Potentially safe loads

The concept of potentially safe loads remains unchanged but, in order to make the dependence on the strength parameters more apparent, its definition is now written:

$$\underline{Q}(\underline{\underline{\sigma}}) \in K(\underline{R}) \Leftrightarrow \exists \underline{\underline{\sigma}} \begin{cases} \underline{\underline{\sigma}} \text{ S. A. with } \underline{Q}(\underline{\underline{\sigma}}) \\ \underline{\underline{\sigma}}(\underline{x}) \in G(\underline{x},\underline{R}) \ \forall M \in \Omega \end{cases}. \tag{2}$$

In the same way $\underline{R}$ also appears in the definition of the volume density of maximum resisting work at M

$$\pi(\underline{x},\underline{R},\underline{\underline{\hat{d}}}(\underline{x})) = \text{Sup}\left\{ \underline{\underline{\sigma}}' : \underline{\underline{\hat{d}}}(\underline{x}) \,\middle|\, \underline{\underline{\sigma}}' \in G(\underline{x},\underline{R}) \right\} \tag{3}$$

and the maximum resisting work in a virtual velocity field is

$$\mathcal{P}_{\mathrm{mr}}(\hat{\underline{U}},\underline{R}) = \int_{\Omega} \pi\left(\underline{x},\underline{R},\hat{\underline{\underline{d}}}(\underline{x})\right)\mathrm{d}\Omega + \int_{\Sigma_{\hat{\underline{U}}}} \pi\left(\underline{x},\underline{R},\underline{n}(\underline{x}),[\![\hat{\underline{U}}(\underline{x})]\!]\right)\mathrm{d}\Sigma\,. \tag{4}$$

The fundamental equation of the kinematic exterior approach becomes[1] (Figure 1):

$$\forall \hat{\underline{U}} \text{ K. A., } K(\underline{R}) \subset \left\{ \underline{Q}.\underline{q}(\hat{\underline{U}}) - \mathcal{P}_{\mathrm{mr}}(\hat{\underline{U}},\underline{R}) \le 0 \right\}. \tag{5}$$

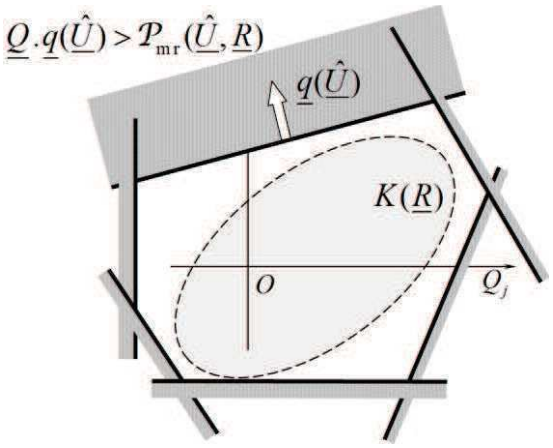

Figure 1. Kinematic exterior approach of $K(\underline{R})$

3 The Yield Design theory applied to ULSD

3.1 Static approach of ULSD

With this modified definition of the potentially safe loads which takes into account the specificaties of the ULSD problem, the statement of the design criterion of ULSD in Section 1 can be written

For each design load combination, the design criterion is expressed by the following equation

$$\underline{Q}(\underline{\Gamma}_Q) \in K\left(\underline{R}(\underline{\Gamma}_R)\right). \tag{6}$$

The left-hand member of this equation means that each load Q_i of the design load combination is considered with its design values obtained with both partial factors corresponding to the "unfavourable" and "favourable" cases ($\Gamma^{\mathrm{u}}_{Q_i}$ and $\Gamma^{\mathrm{f}}_{Q_i}$).

The right-hand member is the convex domain of the potentially safe loads for the design values of the resistance parameters with the partial factor $\underline{\Gamma}_R$ consistent with the considered design load combination, *i.e.* taking into account the fact that the partial factors for material properties may depend on the considered design load combination.

This is illustrated in Figure 2 where it appears that, since each load is to be considered with its two partial factors, the left-hand side in Eq. (6) is represented by a

[1] To be compared with Eq. (5) in Chapter V.

hyper-cube in $\mathbb{R}^n$ which must be included in the convex domain $K(\underline{R}(\underline{\Gamma}_R))$. It is worth noting that the convexity of $K(\underline{R}(\underline{\Gamma}_R))$ justifies the fact that only the partial factors for "favourable" and "unfavourable" loads need being introduced.

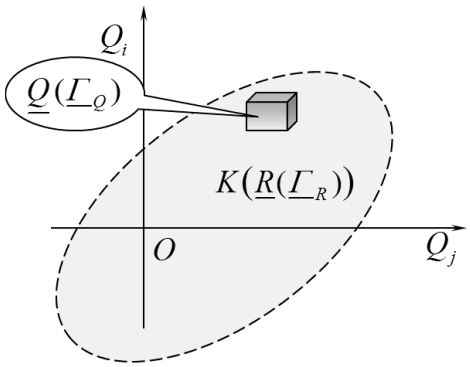

Figure 2. Static approach of ULSD

3.2 Kinematic approach of ULSD

Eq. (6) does not meet the goal of giving a scalar quantification to Eq. (1) that could be easily implemented in practice. Since Eq. (5), the modified form of the fundamental equation of the kinematic approach, is a scalar inequality where the left-hand side member only deals with the design loads while the right-hand side member only concerns the design resistances, it offers a possibility for such an identification.

More precisely, given a design load combination, let $\hat{\underline{U}}$ be a kinematically admissible virtual velocity field.

- The right-hand side member of Eq. (5) is obtained directly from Eq. (4) with the design values of the resistance parameters consistent with the considered design load combination.
- The left-hand side member is the expression of the virtual work by this load combination in the virtual velocity field. The distinction between "unfavourable" loads and "favourable" ones is self-apparent from the sign of the contribution of each load to this virtual work
  - a load Q_i is "unfavourable to equilibrium" if $Q_i q_i > 0$ [2]: it is then assigned the partial factor $\Gamma_{Q_i}^{\mathrm{u}}$;
  - it is "favourable to equilibrium" if $Q_i q_i < 0$ and it is assigned the partial factor $\Gamma_{Q_i}^{\mathrm{f}}$.

It follows that, from the practical point of view, the implementation of Eq. (5) can be easily performed through a computer code.

Going back to the terminology introduced in Eq. (1), we may say now that, in the kinematically virtual velocity field $\hat{\underline{U}}$, the left-hand side member of Eq. (5) represents the **design load effect** and the right-hand side member is the **design resistance effect**.

[2] No summation on repeated indices here.

Recalling now that the inequality in Eq. (5) must be checked over all kinematically admissible virtual velocity fields, the explicit scalar expression of Eq. (1) will be written:

$$S_{\mathrm{d}} \le R_{\mathrm{d}} \Leftrightarrow \forall \hat{\underline{U}} \ \text{K. A.}, \ \underline{\underline{Q}}(\underline{\Gamma}_Q).\underline{q}(\hat{\underline{U}}) \le \mathcal{P}_{\mathrm{mr}}(\hat{\underline{U}}, \underline{\underline{R}}(\underline{\Gamma}_R)). \tag{7}$$

In this equation the equivalence sign is a consequence of the dual definition of the potentially safe loads given in Chapter VI (§ 3.1).

3.3 Partial factor for model uncertainties

In practice, in the same way as for Eq. (2), it is quite exceptional that an exhaustive exploration of all kinematically admissible virtual velocity fields be performed. Only a class of such virtual velocity fields is usually considered in order to maintain a good balance between the intellectual and computational investments compared with the relevance of the data and the method. The results obtained through such a limited procedure are taken into account in the Ultimate Limit State Design of the considered system with the adjunction of a multiplying partial factor $\Gamma_{\mathrm{M}} > 1$ applied to the virtual work by the loads in Eq. (7). This factor depends on the class C_{M} of kinematically admissible virtual velocity fields which are implemented. Then Eq. (7) becomes

$$S_{\mathrm{d}} \le R_{\mathrm{d}} \Leftrightarrow \forall \hat{\underline{U}} \ \text{K. A.} \in C_{\mathrm{M}}, \ \Gamma_{\mathrm{M}} \underline{\underline{Q}}(\underline{\Gamma}_Q).\underline{q}(\hat{\underline{U}}) \le \mathcal{P}_{\mathrm{mr}}(\hat{\underline{U}}, \underline{\underline{R}}(\underline{\Gamma}_R)). \tag{8}$$

Γ_{M} is called the partial factor for **model uncertainties**; it may also encompass other "uncertain" aspects of the adopted modelling.

3.4 As a conclusion

The kinematic exterior approach of the theory of Yield Design is the fundamental basis which yields the scalar quantification of the symbolic formulation of ULSD to be implemented easily in practical circumstances. As a cornerstone, it appeals to the kinematically admissible virtual velocity fields as test functions to define the effect of the design loads and the effect of the design resistances.

The comparison between the virtual work by the design loads and the maximum resisting work by the design resistances should be carried out on the whole set of kinematically admissible velocity fields. In each such velocity field the distinction between the loads which are "unfavourable to equilibrium" and those which are "favourable" comes out automatically from the sign of their virtual work.

It must be emphasized that it is essential for the consistency of the method that the correct mathematical definition of the maximum resisting work, derived only from the strength condition of the constituent material through the mathematical dualisation process, be used in this approach [3, 4].

REFERENCES

[1] OVESEN, N. K. (1989) – General Report, session 30: Codes and Standards. *Proceedings of the 12th International Conference on Soil Mechanics and Foundation Engineering,* Balkema, Rotterdam, pp. 2751-2764.

[2] SAVE, M. & PRAGER, W. (1985) – *Structural Optimization.* Vol. 1, *Optimality Criteria*. Plenum Press, New York, London.

[3] SALENÇON, J. (1994) – Approche théorique du calcul aux états limites ultimes. *Les grands systèmes des sciences et de la technologie*, J. Horowitz et J.L. Lions ed., Masson, Paris, pp. 701-722.

[4] SIMON, B. (2009) – Yield design calculation of earth retaining structures. *Ground Engineering*, **49**, 2, 20-25

Chapter VIII

Optimality and probability approaches of Yield Design

Optimal dimensioning and probabilistic approach
Domain of potential stability
Optimal dimensioning
Probabilistic approach of Yield Design
References

OPTIMALITY AND PROBABILITY APPROACHES Of Yield Design

In the Yield Design theory, the loads applied to a system and the resistances of its constituent materials play symmetric roles in the equations to be satisfied for potential stability. Given a set of prescribed loads, the potential stability of the system defines the potentially safe dimensionings. Optimal dimensioning requires minimising a given objective function on the convex domain of potentially safe dimensionings and leads to linear or convex programming problems. When the prescribed loads and the assumed resistances are given a stochastic character, the question of potential stability receives a probabilistic answer. The interior approach and, essentially, the kinematic exterior approach provide lower and upper bound estimates for the probability of stability and for the probability of collapse.

1 Optimal dimensioning and probabilistic approach

The concept of Resistance parameters was explicitly introduced in Chapter VII in order to point out the direct relationship between ULSD and the theory of Yield Design as its theoretical basis. As a major outcome it provides an unambiguous significance for the fundamental inequality of ULSD which can be quantified taking into account the partial factors on the loads and the resistances, and the partial factor for model uncertainties.

Within this framework one may say that Yield Design is used to analyse the stability of a system which is completely defined in a deterministic way, since the uncertainties on the loads and on the resistances are supposed to be accounted for through the corresponding partial factors. As regards optimality in the dimensioning of the considered system, it may obviously be looked for by performing the Yield Design stability analysis in an iterative way while varying the values of the resistance parameters in a trial-and-error process.

Since optimality (*e.g.* [1]) and probability approaches have been largely studied in the past – usually referring to "plastic design" – the objective here is to sketch out the main fundamental results of the theory of Yield Design when optimality and probability approaches are concerned:

- **Optimal dimensioning** of a system in a given geometry, from the resistance of the constituent elements point of view[1], under a given set of loads;

[1] From now on, the word "dimensioning" will only be used from the resistance of the constituent elements point of view in a given geometric design.

- **Probabilistic approach** in the case of stochastic resistance- and/or loading parameters, leading to a consistent definition of the probability of stability of a system within the Yield Design framework.

2 Domain of potential stability

2.1 Resistance parameters

It is now necessary to be more precise regarding the definition of the resistance parameters introduced in Chapter VII (§ 2.1). We assume that the volume Ω of the system under consideration can be divided into m distinct zones Ω_j, with no overlapping, such that, in each zone Ω_j, the resistance of the constituent material, which may be inhomogeneous, is proportional to the resistance parameter $R_j \geq 0$

$$\begin{cases} \Omega = \Omega_1 \cup \Omega_2 \cup ... \ \Omega_m \\ \Omega_j \cap \Omega_k = \varnothing, \ \forall \ j \neq k \in (1,...m) \end{cases} \tag{1}$$

and the strength condition is written

$$\forall \underline{x} \in \Omega_j, \ \underline{\underline{\sigma}}(\underline{x}) \in G_j(\underline{x}, R_j) = R_j \, G_j(\underline{x}). \tag{2}$$

Each $G_j(\underline{x})$ exhibits the same mathematical properties as $G(\underline{x})$ in Chapter IV (§ 1.3), namely: $0 \in G_j(\underline{x})$ and convexity[2].

The "vector" $\underline{R} = (R_1,...R_m)$ is an element of $(\mathbb{R}_+)^m$.

As a consequence of Eq. (2) we have

$$\begin{cases} \pi \left(\underline{x}, R_j, \underline{\underline{\hat{d}}}(\underline{x}) \right) = R_j \, \pi_j \left(\underline{x}_j, \underline{\underline{\hat{d}}}(\underline{x}) \right) \\ \pi \left(\underline{x}, R_j, \underline{n}(\underline{x}), [\![\underline{\hat{U}}(\underline{x})]\!] \right) = R_j \, \pi_j \left(\underline{x}, \underline{n}(\underline{x}), [\![\underline{\hat{U}}(\underline{x})]\!] \right) \end{cases} \tag{3}$$

where the functions π_j refer to the strength domain $G_j(\underline{x})$.

In consistence with Eqs (2) and (4) in Chapter VII we write

$$\forall M \in \Omega, \ \underline{\underline{\sigma}}(\underline{x}) \in G(\underline{x}, \underline{R}) \Leftrightarrow \forall \Omega_j, \ \forall M \in \Omega_j, \ \underline{\underline{\sigma}}(\underline{x}) \in G_j(\underline{x}, R_j) \tag{4}$$

and

$$\mathcal{P}_{\text{mr}}(\underline{\hat{U}}, \underline{R}) = \sum_j R_j \int_{\Omega_j} \pi_j \left(\underline{x}, \underline{\underline{\hat{d}}}(\underline{x}) \right) \mathrm{d}\Omega_j + \sum_j R_j \int_{(\Sigma_{\underline{\hat{U}}})_j} \pi_j \left(\underline{x}, \underline{n}(\underline{x}), [\![\underline{\hat{U}}(\underline{x})]\!] \right) \mathrm{d}\Sigma_j , \tag{5}$$

with the discontinuities of the virtual velocity field at the interface between two adjacent zones Ω_j and Ω_k being treated as in Chapter V (§ 3.5).

---

[2] There is obviously no summation on repeated indices in Eq. (2). The presentation encompasses the case when the strength domain in a given zone Ω_j is the intersection of two or more convex domains $G_j^{\ell}(\underline{x}, R_j^{\ell})$ each of them being characterised by its own resistance parameter R_j^{ℓ} as in Eq. (2).

Introducing $\underline{r}(\underline{\hat{U}}) = (r_1, \ldots r_m)$ defined by

$$r_j(\underline{\hat{U}}) = \int_{\Omega_j} \pi_j\left(\underline{x}, \underline{\underline{\hat{d}}}(\underline{x})\right) \mathrm{d}\Omega_j + \int_{(\Sigma_{\underline{\hat{U}}})_j} \pi_j\left(\underline{x}, \underline{n}(\underline{x}), [\![\underline{\hat{U}}(\underline{x})]\!]\right) \mathrm{d}\Sigma_j \tag{6}$$

we get for Eq. (5) the simplified form

$$\mathcal{P}_{\mathrm{mr}}(\underline{\hat{U}}, \underline{R}) = \underline{R}.\underline{r}(\underline{\hat{U}}). \tag{7}$$

2.2 Potentially safe dimensionings

As stated in Chapter VII (§ 2.2), potential stability of the system within the Yield Design framework amounts to writing:

$$\underline{Q}(\underline{\underline{\sigma}}) \in K(\underline{R}) \Leftrightarrow \exists \underline{\underline{\sigma}} \begin{cases} \underline{\underline{\sigma}} \text{ S. A. with } \underline{Q}(\underline{\underline{\sigma}}) \\ \underline{\underline{\sigma}}(\underline{x}) \in G(\underline{x}, \underline{R}) \ \forall M \in \Omega \end{cases} \tag{8}$$

Conversely, a load $\underline{Q}$ being given, any dimensioning of the system defined by $\underline{R}$ such that Eq. (8) is satisfied is a **potentially safe dimensioning**[3] of the system for this load $\underline{Q}$.

This definition generates a domain $D(\underline{Q})$ in $(\mathbb{R}_+)^m$

$$\underline{Q} \in K(\underline{R}) \subset \mathbb{R}^n \Leftrightarrow \underline{R} \in D(\underline{Q}) \subset (\mathbb{R}_+)^m. \tag{9}$$

Obviously the domain $D(\underline{Q})$ is not bounded when $R_j \to +\infty$:

$$\underline{R}^\ell \in D(\underline{Q}) \Rightarrow \underline{R} \in D(\underline{Q}), \ \forall \underline{R} \geq \underline{R}^\ell \tag{10}$$

with the definition

$$\underline{R} \geq \underline{R}^\ell \Leftrightarrow \forall j = 1, \ldots m, \ R_j \geq R_j^\ell .^4 \tag{11}$$

From the convexity of the $G_j(\underline{x})$ it follows that $D(\underline{Q})$ is also **convex** in $(\mathbb{R}_+)^m$:

let $\underline{R}^1 \in D(\underline{Q})$ and $\underline{R}^2 \in D(\underline{Q})$ be two potentially safe dimensionings and let $\underline{\underline{\sigma}}^1$ and $\underline{\underline{\sigma}}^2$ be two stress fields satisfying Eq. (8) with $\underline{R}^1$ and $\underline{R}^2$ respectively. Consider the stress field $\underline{\underline{\sigma}} = \lambda \underline{\underline{\sigma}}^1 + (1-\lambda)\underline{\underline{\sigma}}^2, \lambda \in [0,1]$. It is statically admissible with $\underline{Q}$, and we have in any Ω_j

$$\frac{\underline{\underline{\sigma}}(\underline{x})}{\lambda R_j^1 + (1-\lambda) R_j^2} = \frac{\lambda R_j^1}{\lambda R_j^1 + (1-\lambda) R_j^2} \frac{\underline{\underline{\sigma}}^1(\underline{x})}{R_j^1} + \frac{(1-\lambda) R_j^2}{\lambda R_j^1 + (1-\lambda) R_j^2} \frac{\underline{\underline{\sigma}}^2(\underline{x})}{R_j^2} \tag{12}$$

which may be written

---

[3] The adverb "potentially" retains the same meaning as for the loads in the general theory of Yield Design.

[4] Conversely, $K(\underline{R}^\ell) \subset K(\underline{R}), \ \forall \underline{R} \geq \underline{R}^\ell$.

(13) $$\frac{\underline{\underline{\sigma}}(\underline{x})}{\lambda R_j^1+(1-\lambda)R_j^2}=\mu\,\frac{\underline{\underline{\sigma}}^1(\underline{x})}{R_j^1}+(1-\mu)\,\frac{\underline{\underline{\sigma}}^2(\underline{x})}{R_j^2},\ \mu\in[0,1]$$

where both $\frac{\underline{\underline{\sigma}}^1(\underline{x})}{R_j^1}$ and $\frac{\underline{\underline{\sigma}}^2(\underline{x})}{R_j^2}$ are members of $G_j(\underline{x})$.

Hence, since $G_j(\underline{x})$ is convex, $\frac{\underline{\underline{\sigma}}(\underline{x})}{\lambda R_j^1+(1-\lambda)R_j^2}$ is also a member of $G_j(\underline{x})$, $\forall j=1,...m$, which proves that $\underline{Q}\in K\left(\lambda\underline{R}^1+(1-\lambda)\underline{R}^2\right)$ and, therefore, that $D(\underline{Q})$ is convex (Figure 1).

The dimensionings at the boundary of $D(\underline{Q})$ are the **extreme dimensionings**[5] for the system under the load $\underline{Q}$ while the internal ones are **conservative** from the Yield Design point of view.

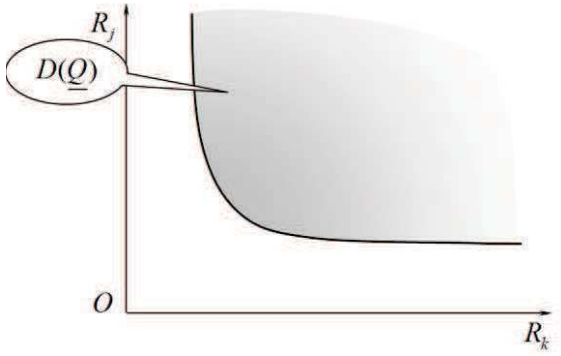

Figure 1. Domain $D(\underline{Q})$ of potentially safe dimensionings

2.3 Interior approach

Eqs (8) and (9) provide the interior approach of $D(\underline{Q})$ straightforwardly:

(14) $$\underline{R}\in D(\underline{Q})\Leftrightarrow\exists\underline{\underline{\sigma}}\begin{cases}\underline{\underline{\sigma}}\text{ S. A. with }\underline{Q}\\ \underline{\underline{\sigma}}(\underline{x})\in G(\underline{x},\underline{R})\ \forall M\in\Omega\end{cases}$$

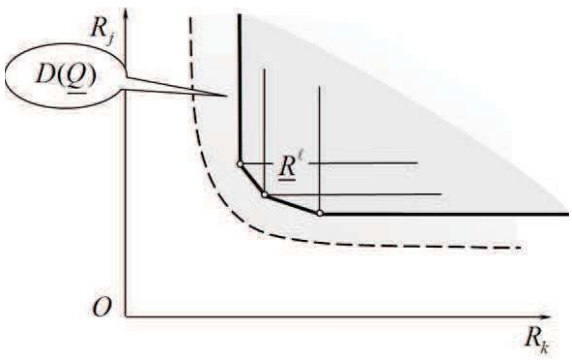

Figure 2. Interior approach of $D(\underline{Q})$

[5] With the same meaning as for the extreme loads.

Taking advantage of Eq. (10) and the convexity of $D(\underline{Q})$ the interior approach obtained from k potentially safe dimensionings $\underline{R}^{\ell}$ is the convex hull of the convex cones $\underline{R} \geq \underline{R}^{\ell}$, with the definition (11), as shown in Figure 2.

The interior approach is obviously **conservative** and calls for **minimisation** processes on $\underline{R}^{\ell}$ in order to improve the estimate of $D(\underline{Q})$ so obtained.

2.4 Kinematic exterior approach

With Eq. (7), the fundamental equation of the kinematic exterior approach of $K(\underline{R})$ takes the form

$$\forall \underline{\hat{U}} \text{ K. A., } K(\underline{R}) \subset \left\{ \underline{Q}.\underline{q}(\underline{\hat{U}}) - \underline{R}.\underline{r}(\underline{\hat{U}}) \leq 0 \right\} \tag{15}$$

which, conversely, yields the kinematic exterior approach of $D(\underline{Q})$

$$\forall \underline{\hat{U}} \text{ K. A., } D(\underline{Q}) \subset \left\{ \underline{Q}.\underline{q}(\underline{\hat{U}}) - \underline{R}.\underline{r}(\underline{\hat{U}}) \leq 0 \right\} \tag{16}$$

as presented in Figure 3. It is worth noting that in this kinematic exterior approach is obviously **non conservative**. Improving the estimate of $D(\underline{Q})$ is obtained through a **maximisation** process performed on $\underline{Q}.\underline{q}(\underline{\hat{U}})$ with $\underline{r}(\underline{\hat{U}})$ being fixed. When an extreme dimensioning is reached, $\underline{r}(\underline{\hat{U}})$ is an inward normal to $D(\underline{Q})$.

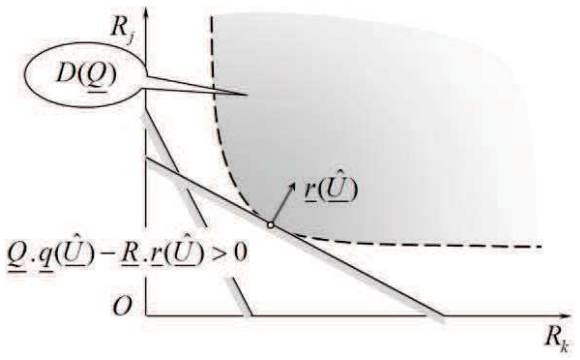

Figure 3. Kinematic exterior approach of $D(\underline{Q})$

Under the same mathematical conditions as for $K(\underline{R})$ given by Frémond and Friaà [2] it can be established that Eq. (16) is the dual definition of $D(\underline{Q})$:

$$\underline{R} \in D(\underline{Q}) \Leftrightarrow \forall \underline{\hat{U}} \text{ K. A., } \underline{Q}.\underline{q}(\underline{\hat{U}}) - \underline{R}.\underline{r}(\underline{\hat{U}}) \leq 0 \tag{17}$$

which may also be written

$$D(\underline{Q}) = \bigcap_{\underline{\hat{U}} \text{ K. A.}} \left\{ \underline{Q}.\underline{q}(\underline{\hat{U}}) - \underline{R}.\underline{r}(\underline{\hat{U}}) \leq 0 \right\}. \tag{18}$$

2.5 Potential stability under a set of loads

Most often the system under consideration must be dimensioned in order to sustain a prescribed set of loads $(\underline{Q}^1,\underline{Q}^2,...\underline{Q}^k)$. The corresponding domain of potentially safe dimensionings is denoted $D(\underline{Q}^1,\underline{Q}^2,...\underline{Q}^k)$. Obviously it is just the intersection of the individual $D(\underline{Q}^\ell)$, $\ell=1...k$, (Figure 4)

(19) $$D(\underline{Q}^1,\underline{Q}^2,...\underline{Q}^k)=D(\underline{Q}^1)\cap D(\underline{Q}^2)...\cap D(\underline{Q}^k).$$

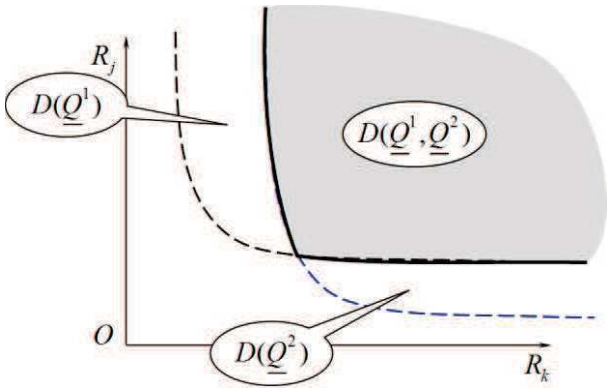

Figure 4. Domain of potentially safe dimensionings in the case of two loads

Hence, the intersection of interior approaches of $D(\underline{Q}^\ell)$, $\ell=1...k$ obtained as in Figure 2 yields an interior approach for $D(\underline{Q}^1,\underline{Q}^2,...\underline{Q}^k)$.

The kinematic exterior approach of $D(\underline{Q}^1,\underline{Q}^2...\underline{Q}^k)$ follows from Eq. (16) which must be satisfied for all the loads of the considered set:

(20) $$\forall \underline{\hat{U}} \text{ K. A., } D(\underline{Q}^1,\underline{Q}^2,...\underline{Q}^k)\subset\left\{\underline{Q}^\ell.\underline{q}(\underline{\hat{U}})-\underline{R}.\underline{r}(\underline{\hat{U}})\le 0\right\},\ \ell=1...k$$

or, in other words

(21) $$\forall \underline{\hat{U}} \text{ K. A., } D(\underline{Q}^1,\underline{Q}^2,...\underline{Q}^k)\subset\left\{\sup_{\ell=1...k}\underline{Q}^\ell.\underline{q}(\underline{\hat{U}})-\underline{R}.\underline{r}(\underline{\hat{U}})\le 0\right\}.$$

It is worth noting that, due to the convexity of $K(\underline{R})$, any dimensioning that is potentially safe for $(\underline{Q}^1,\underline{Q}^2,...\underline{Q}^k)$ is potentially safe for all the loads within the convex hull of $(\underline{Q}^1,\underline{Q}^2,...\underline{Q}^k)$. This property is essential for practical applications, since it proves (again) that only the maximum "favourable" and "unfavourable" external loads need being regarded (*cf.* Chapter VII, Figure 2).

2.6 Domain of potential stability of a system

From the definition of $D(\underline{Q})$ it is apparent that $K(\underline{R})$ and $D(\underline{Q})$ are just two sides of the same mathematical concept which expresses the potential stability of the considered system under a given load with a given set of resistance parameters, as illustrated by the two approaches in the preceding paragraphs,. This calls for the

introduction of the space $\{\underline{Q}\}\times\{\underline{R}\}=\mathbb{R}^n\times(\mathbb{R}_+)^m$, as in [3-5], with the **domain of stability of the system** being denoted $\mathcal{K}$:

$$(\underline{Q},\underline{R})\in\mathcal{K}\subset\mathbb{R}^n\times(\mathbb{R}_+)^m \Leftrightarrow \exists\underline{\underline{\sigma}}\begin{cases}\underline{\underline{\sigma}}\text{ S. A. with }\underline{Q}\\ \underline{\underline{\sigma}}(\underline{x})\in G(\underline{x},\underline{R})\ \forall M\in\Omega\end{cases} \tag{22}$$

equivalent to the dual definition[6]

$$(\underline{Q},\underline{R})\in\mathcal{K}\subset\mathbb{R}^n\times(\mathbb{R}_+)^m \Leftrightarrow \forall\hat{\underline{U}}\ \text{K. A.},\ \underline{Q}.\underline{q}(\hat{\underline{U}})-\underline{R}.\underline{r}(\hat{\underline{U}})\le 0\ . \tag{23}$$

From these definitions it is clear that $\mathcal{K}$ proceeds from the geometric data of the system, the loading mode (Chapter IV, § 1.2) and the parametric description of the strength conditions of the constituent material through Eqs (1) and (2). Symbolically $\mathcal{K}$ may be represented as a pair of kitchen scales checking that the "resistance effect" exceeds the "load effect" following the ULSD terminology (Figure 5).

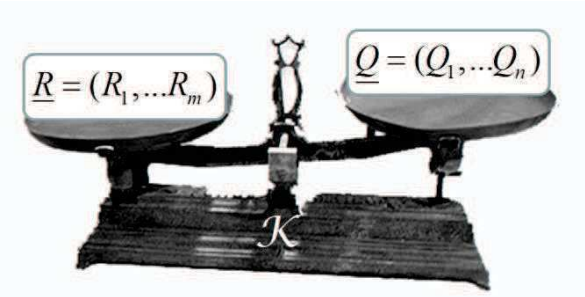

Figure 5. Symbolic interpretation of $\mathcal{K}$

From the mathematical properties of the $G_j(\underline{x})$ it comes out easily that $\mathcal{K}$ is a cone with apex O in $\mathbb{R}^n\times(\mathbb{R}_+)^m$

$$(\underline{Q},\underline{R})\in\mathcal{K}\Rightarrow(\alpha\underline{Q},\alpha\underline{R})\in\mathcal{K},\ \forall\alpha\ge 0 \tag{24}$$

and also that $\mathcal{K}$ is convex

$$(\underline{Q}^1,\underline{R}^1)\in\mathcal{K},(\underline{Q}^2,\underline{R}^2)\in\mathcal{K}\Rightarrow\lambda(\underline{Q}^1,\underline{R}^1)+(1-\lambda)(\underline{Q}^2,\underline{R}^2)\in\mathcal{K},\ \forall\lambda\in[0,1]. \tag{25}$$

The proof of Eq. (25) is similar to Eqs (12) and (13) with the stress fields $\underline{\underline{\sigma}}^1$ and $\underline{\underline{\sigma}}^2$ satisfying Eq. (8) with $(\underline{Q}^1,\underline{R}^1)$ and $(\underline{Q}^2,\underline{R}^2)$ respectively[7].

The interior approach of $\mathcal{K}$ is the direct consequence of Eq. (22). The kinematic exterior approach is derived from Eq. (23) and results in the dual definition:

$$\mathcal{K}=\bigcap_{\hat{\underline{U}}\ \text{K. A.}}\left\{\underline{Q}.\underline{q}(\hat{\underline{U}})-\underline{R}.\underline{r}(\hat{\underline{U}})\le 0\right\} \tag{26}$$

The definition of $\mathcal{K}$ encompasses all the results established for $K(\underline{R})$ and $D(\underline{Q})$ as shown in Figure 6

[6] From now on the conditions established by Frémond and Friaà [1] are supposed to be fulfilled.

[7] As a matter of fact, the proof in § 2.2 is just a particular case of the present one with $\underline{Q}=\underline{Q}^1=\underline{Q}^2$.

- For a given value $\underline{R}^{\mathrm{d}}$ of $\underline{R}$, $K(\underline{R}^{\mathrm{d}})$ is the projection onto $\left\{\underline{Q}\right\}=\mathbb{R}^n$ of the intersection of $\mathcal{K}$ with $\underline{R}=\underline{R}^{\mathrm{d}}$.
- For a given value $\underline{Q}^{\mathrm{d}}$ of $\underline{Q}$, $D(\underline{Q}^{\mathrm{d}})$ is the projection onto $\left\{\underline{R}\right\}=(\mathbb{R}_+)^m$ of the intersection of $\mathcal{K}$ with $\underline{Q}=\underline{Q}^{\mathrm{d}}$.

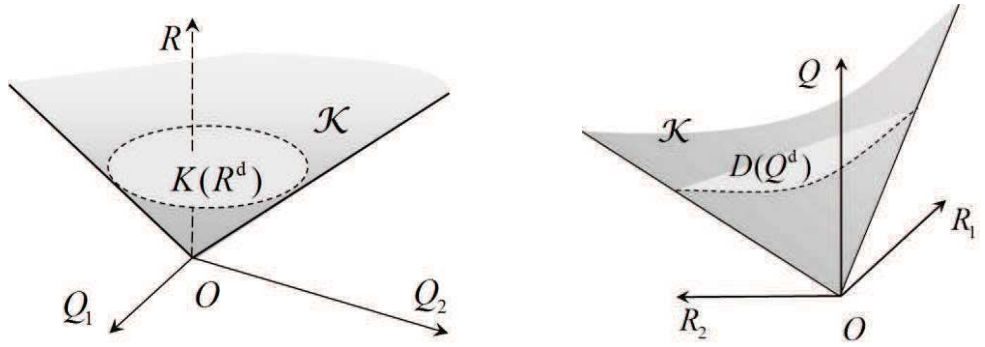

Figure 6. Geometric representation of $\mathcal{K}$, $K(\underline{R}^{\mathrm{d}})$ and $D(\underline{Q}^{\mathrm{d}})$ in the cases $(n=2,\ m=1)$ and $(n=1,\ m=2)$

3 Optimal dimensioning

3.1 Introductory remarks

Many research and practical papers have been devoted to the optimal dimensioning of systems, especially in the case of structures such as those presented in Chapter IX. They are either related to elastic design codes or based upon considerations similar to the Yield Design arguments presented in the preceding Section (*e.g.* [5]). These ones are usually referred to as *Plastic optimal design* due to the fact that they are principally concerned with structures made of metal beams or plates and that ductility is part of the necessary conditions for the relevance of potentially safe loads as it was pointed out in Chapter II (Section 3) and Chapter IV (§ 3.4).

The main objective of this Section is to provide some guidelines for reading the abundant literature on the topic, bearing in mind that it will not cover the case of structures for which the dimensioning depends on scalar fields, such as plates or slabs with varying thickness.

3.2 Optimal dimensioning based upon potential stability

Section 2 has brought out the definition of $D(\underline{Q})$ and $D(\underline{Q}^1,\underline{Q}^2,\ldots\underline{Q}^k)$ together with their interior and kinematic exterior approaches. Not surprisingly, it turned out that $D(\underline{Q})$ and $D(\underline{Q}^1,\underline{Q}^2,\ldots\underline{Q}^k)$ are not bounded in $(\mathbb{R}_+)^m$. This implies that any decision based upon the knowledge of the potentially safe dimensionings requires the introduction of a criterion in the form of some "economic" or "objective" function of $\underline{R}$, in order to determine the dimensioning or pre-dimensioning of the considered

system that will be retained. **Minimum weight** dimensioning[8] (or design) is one such criterion, often encountered as a particular and simplified case of **Minimum cost**.

As a first step it is commonly assumed that the economic function is linear and increases with $\underline{R}$:

$$\phi(\underline{R}) = \underline{C}.\underline{R}, \quad \underline{C} \in (\mathbb{R}_+)^m . \tag{27}$$

Looking for the optimal dimensioning among the potentially safe ones amounts to finding the extreme dimensioning where $\underline{C}$ is an inward normal to the boundary of $D(\underline{Q})$ or $D(\underline{Q}^1, \underline{Q}^2 ... \underline{Q}^k)$ as shown in Figure 7. Note that the optimality for $(\underline{Q}^1, \underline{Q}^2 ... \underline{Q}^k)$ means optimality for any load within the convex hull of $(\underline{Q}^1, \underline{Q}^2 ... \underline{Q}^k)$.

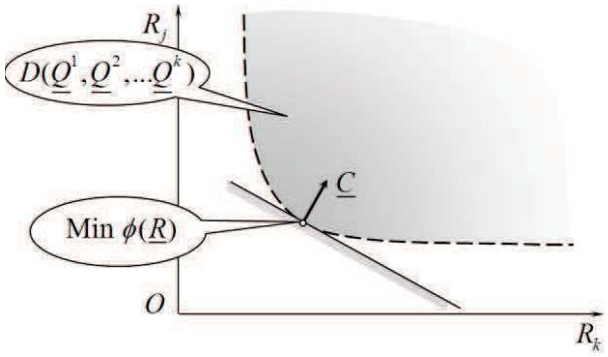

Figure 7. Optimal dimensioning in the case of a linear objective function

From the mathematical point of view it is a **convex programing** problem for which various solving techniques are available (*e.g.* [6, 7]).

In some cases, such as when dealing with frames or trusses, the boundary of the convex $D(\underline{Q})$ or $D(\underline{Q}^1, \underline{Q}^2 ... \underline{Q}^k)$ happens to be made of segments of lines and the problem is reduced to a simpler **linear programming** one (*e.g.* [8-14]).

When comparing Figure 7 with Figure 3 one cannot fail to note a formal similarity which can be summarized in the following form: for a given linear objective function, the optimal dimensioning is obtained when the gradient of the objective function is collinear with the gradient of the maximum resisting work with respect to $\underline{R}$.

Despite its non-conservative character, the kinematic exterior approach is most commonly used to estimate $D(\underline{Q})$ or $D(\underline{Q}^1, \underline{Q}^2, ... \underline{Q}^k)$. Then, it comes out from the above statement that, for optimality purposes, it is only necessary to consider the relevant virtual kinematically admissible velocity fields $\underline{\hat{U}}$ for which $\underline{r}(\underline{\hat{U}})$ is collinear with $\underline{C}$.

These considerations are the transcription in this particular case of classical convex programming results which received practical applications in the numerical methods that were developed for optimal plastic design). Beside the

[8] Minimum *mass* would be more correct.

case of linear objective functions they remain valid for convex objective functions[9] and can even be applied if the objective function is just weakly concave as in the following paragraph (Figure 8).

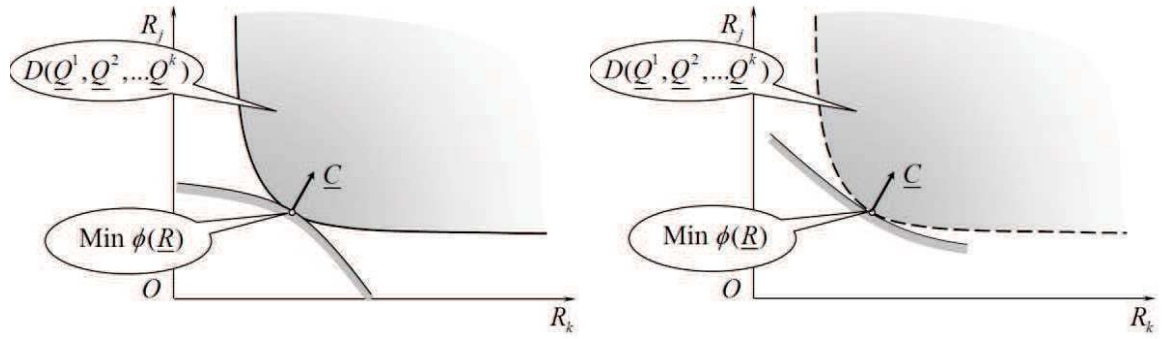

Figure 8. Optimal dimensioning in the case of a convex or a weakly concave objective function

3.3 Additional remarks

As a matter of fact, as observed by various authors, the objective function is seldom linear with respect to $\underline{R}$. For instance, when metal frames or structures are concerned, only commercial beam sections are available within shape-series such as **U**-, **L**-, or **T**-shaped sections, etc. Although the sections within one series are not exactly geometrically similar, their masses follow a (concave) law of the form [15]

(28) $$\phi(\underline{R}) = \sum_{j=1\ldots m} C_j R_j^{2/3}$$

or, according to [16]

(29) $$\phi(\underline{R}) = \sum_{j=1\ldots m} C_j R_j^{0,6} \ .$$

In such cases, if the mass of the structure is taken as the proper objective function[10], one strategy when looking for the optimal dimensioning can be to linearize $\phi(\underline{R})$ about a feasible value of $\underline{R}$ in a trial-and-error process. Also, since the range of practically available sections within one shape-series is not a continuum, it only allows discrete values of $\underline{R}$ to be taken into account when looking for the optimal dimensioning; this may be done again in a trial-and-error process or through some penalty method [17-19].

[9] $\forall \lambda \in (0,1),\ \phi(\lambda \underline{R}^1 + (1-\lambda)\underline{R}^2) \leq \lambda \phi(\underline{R}^1) + (1-\lambda)\phi(\underline{R}^2)$

[10] Note that the complexity of the structure (joints, etc.) is also part of the cost.

4 Probabilistic approach of Yield Design

4.1 Introductory remarks

For efficiency sake in their everyday practical implementations, structural design codes are shaped into a deterministic pattern where the variability of the loads applied to the system and the variability of the resistance characteristics of the constituent materials are accounted for through the corresponding "partial" factors.

The Yield Design framework also offers the possibility to introduce a probabilistic approach as an alternative way to deal

- with the statistic observations about the occurrence of the prescribed load levels and load combinations on the one side
- and, on the other side, with the stochastic distributions of the material resistance characteristics in the range within their assumed maximum and minimum values.

As for Section 3, the objectives of the present Section are just to provide some guidelines when making a way in the relevant literature (*e.g.* [20-22]). Therefore mathematical "technicalities" will be avoided – not meaning that they should be disregarded – but one should keep in mind that a probabilistic approach assumes, as a cornerstone, that the events taken into consideration are **properly defined** and that they can actually receive a **relevant stochastic treatment**.

4.2 Settlement of the probabilistic Yield Design problem

The Yield Design problem is still defined on the given geometry of the system, within the multi-parameter loading mode framework and with the Resistance parameters defined as in § 2.1. But the question to be answered will be modified from the original one (Chapter IV, § 1.4) due to the fact that the loading parameters and/or the Resistance parameters are **stochastic** variables defined in the following ways.

Stochastic loading parameters

The loading vector $\underline{Q}$ is given in the loading space $\left\{\underline{Q}\right\}=\mathbb{R}^n$ through a probability law and we denote by $\mu_{\underline{Q}}$ the corresponding probability measure.

This means that if $\mathbb{A}$ is a part of $\left\{\underline{Q}\right\}=\mathbb{R}^n$ the probability for $\underline{Q}$ to fall in $\mathbb{A}$ is $\mu_{\underline{Q}}(\mathbb{A})$

$$\forall \mathbb{A}\subset\mathbb{R}^n,\ \text{prob}\left\{\underline{Q}\in\mathbb{A}\right\}=\mu_{\underline{Q}}(\mathbb{A}) \tag{30}$$

with the properties (Figure 9)

$$\begin{cases}\forall \mathbb{A}\subset\mathbb{R}^n,\ \mu_{\underline{Q}}(\mathbb{A})\geq 0\\ \mu_{\underline{Q}}(\mathbb{R}^n)=1.\end{cases} \tag{31}$$

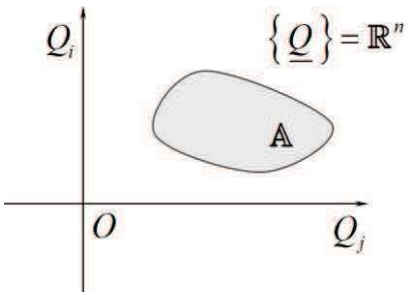

Figure 9. Stochastic modelling of the loading parameters

The measure $\mu_{\underline{Q}}$ may be defined by a probability density function $f(\underline{Q})$ such that Eq. (31) be satisfied; in such a case

$$\begin{cases} f(\underline{Q}) = f(Q_1, Q_2, \ldots Q_n) \\ \mu_{\underline{Q}}(\mathbb{A}) = \int_{\mathbb{A}} \mathrm{d}\mu_{\underline{Q}} = \int_{\mathbb{A}} f(\underline{Q})\, \mathrm{d}Q_1 \mathrm{d}Q_2 \ldots \mathrm{d}Q_n \end{cases}. \tag{32}$$

It could also happen that only a set of discrete values $\underline{Q}^1, \underline{Q}^2, \ldots \underline{Q}^p$ be feasible for $\underline{Q}$, in which case $\mu_{\underline{Q}}$ would be reduced to the corresponding Dirac measures:

$$\mu_{\underline{Q}} = \alpha^1 \delta_{\underline{Q}^1} + \alpha^2 \delta_{\underline{Q}^2} + \ldots \alpha^p \delta_{\underline{Q}^p}, \ \alpha^1, \alpha^2, \ldots \alpha^p > 0, \ \alpha^1 + \alpha^2 + \ldots \alpha^p = 1. \tag{33}$$

If the components of the loading vector are stochastically independent[11], each of them with its own probability law μ_{Q_i}, we have:

$$\mu_{\underline{Q}} = \mu_{Q_1}\, \mu_{Q_2} \ldots \mu_{Q_n}. \tag{34}$$

Stochastic Resistance parameters

The resistance "vector" $\underline{R}$ is given in $\{\underline{R}\} = (\mathbb{R}_+)^m$ through a probability law with $\mu_{\underline{R}}$ as a probability measure to account for the physical scattering of the values of the resistance parameters between their assumed maximum and minimum values

$$\forall \mathbb{B} \subset (\mathbb{R}_+)^m, \ \mathrm{prob}\{\underline{R} \in \mathbb{B}\} = \mu_{\underline{R}}(\mathbb{B}) \tag{35}$$

with

$$\begin{cases} \forall \mathbb{B} \subset (\mathbb{R}_+)^m, \ \mu_{\underline{R}}(\mathbb{B}) \geq 0 \\ \mu_{\underline{R}}(\mathbb{R}_+)^m = 1. \end{cases} \tag{36}$$

The resistance parameters are usually stochastically independent[12].

[11] This case is seldom encountered in practice: for instance, maximum values of the loading parameters do not usually occur simultaneously.

[12] Note that the framework for the resistance parameters defined in § 2.1 does not apply to the resistance parameters C and ϕ in Coulomb's criterion for which this assertion would not hold.

4.3 Probability of stability of a system

Since the data of the Yield Design problem are given a stochastic character the question to be answered now receives a probabilistic formulation:

What is the probability of (potential) stability of the system under the given stochastic loading with the given stochastic resistance parameters?

Stochastic loads with deterministic resistances

Let us consider first the case when only the load $\underline{Q}$ is stochastic while the resistance parameter is deterministic with the value $\underline{R}^{\mathrm{d}}$. From the very definition of the (potential) stability of the system it comes out that the stochastic event the probability of which must be assessed is that $\underline{Q}$ **fall in** $K(\underline{R}^{\mathrm{d}})$. Hence the probability of stability[13] of the system is just

$$P_{\mathrm{s}}(\mu_{\underline{Q}}, \underline{R}^{\mathrm{d}}) = \mu_{\underline{Q}}[K(\underline{R}^{\mathrm{d}})] \tag{37}$$

and the probability of collapse is the complement to 1

$$P_{\mathrm{c}}(\mu_{\underline{Q}}, \underline{R}^{\mathrm{d}}) = 1 - P_{\mathrm{s}}(\mu_{\underline{Q}}, \underline{R}^{\mathrm{d}}) = 1 - \mu_{\underline{Q}}[K(\underline{R}^{\mathrm{d}})]. \tag{38}$$

It follows from Eq. (30) that any **interior approach** of $K(\underline{R}^{\mathrm{d}})$ yields a **lower bound for** $P_{\mathrm{s}}(\mu_{\underline{Q}}, \underline{R}^{\mathrm{d}})$.

Conversely, any **exterior approach** provides an **upper bound for** $P_{\mathrm{s}}(\mu_{\underline{Q}}, \underline{R}^{\mathrm{d}})$ and a **lower bound for** $P_{\mathrm{c}}(\mu_{\underline{Q}}, \underline{R}^{\mathrm{d}})$:

$$\forall \hat{\underline{U}} \text{ K. A.}, \; P_{\mathrm{s}}(\mu_{\underline{Q}}, \underline{R}^{\mathrm{d}}) \le \mu_{\underline{Q}} \left\{ \underline{Q}.\underline{q}(\hat{\underline{U}}) - \underline{R}^{\mathrm{d}}.\underline{r}(\hat{\underline{U}}) \le 0 \right\} \tag{39}$$

$$\forall \hat{\underline{U}} \text{ K. A. } P_{\mathrm{c}}(\mu_{\underline{Q}}, \underline{R}^{\mathrm{d}}) \ge \mu_{\underline{Q}} \left\{ \underline{Q}.\underline{q}(\hat{\underline{U}}) - \underline{R}^{\mathrm{d}}.\underline{r}(\hat{\underline{U}}) > 0 \right\} \tag{40}$$

and, recalling the dual definition of $K(\underline{R}^{\mathrm{d}})$,

$$P_{\mathrm{s}}(\mu_{\underline{Q}}, \underline{R}^{\mathrm{d}}) = \mu_{\underline{Q}} \left[\bigcap_{\hat{\underline{U}} \text{ K. A.}} \left\{ \underline{Q}.\underline{q}(\hat{\underline{U}}) - \underline{R}^{\mathrm{d}}.\underline{r}(\hat{\underline{U}}) \le 0 \right\} \right] \tag{41}$$

$$P_{\mathrm{c}}(\mu_{\underline{Q}}, \underline{R}^{\mathrm{d}}) = \mu_{\underline{Q}} \left[\bigcup_{\hat{\underline{U}} \text{ K. A.}} \left\{ \underline{Q}.\underline{q}(\hat{\underline{U}}) - \underline{R}^{\mathrm{d}}.\underline{r}(\hat{\underline{U}}) > 0 \right\} \right]. \tag{42}$$

Since the kinematic exterior approach is the most commonly used when trying to estimate the probability of stability (or of collapse) of a system it is very important to understand the consequences of these two equations. For instance, Eq. (42) implies that if several kinematically admissible virtual velocity fields $\hat{\underline{U}}^1, \hat{\underline{U}}^2 \ldots$ are implemented in the kinematic exterior approach, the best value to be retained as the lower bound for $P_{\mathrm{c}}(\mu_{\underline{Q}}, \underline{R}^{\mathrm{d}})$ **is not** the maximum of the corresponding values of

[13] From now on the adjective "potential" will be dropped for simplified wording.

$\mu_{\underline{Q}}\left\{ \underline{Q}.\underline{q}(\hat{\underline{U}}) - \underline{R}^{\mathrm{d}}.\underline{r}(\hat{\underline{U}}) > 0 \right\}$ **but results from the second hand** of Eq. (42) which yields a higher value than each of them

$$P_{\mathrm{c}}(\underline{Q},\mu_{\underline{R}}) \geq \mu_{\underline{R}}\left[\bigcup_{\hat{\underline{U}}^1,\,\hat{\underline{U}}^2,\ldots \text{K. A.},} \left\{ \underline{Q}.\underline{q}(\hat{\underline{U}}^p) - \underline{R}.\underline{r}(\hat{\underline{U}}^p) > 0 \right\} \right] \tag{43}$$

This remark is all the more important that usually the checking of the dimensioning of a system is (fortunately) concerned only with very low values of $P_{\mathrm{c}}(\mu_{\underline{Q}},\underline{R}^{\mathrm{d}})$ and therefore an error in the estimate of this probability may result in dramatic consequences.

Deterministic loads with stochastic resistances

In the same way as above we consider the case of a deterministic set of prescribed loads $(\underline{Q}^1,\underline{Q}^2,\ldots\underline{Q}^k)$ with a stochastic dimensioning defined as in § 4.2. From the definition given in § 2.5 we can state that the probability of stability of the system is the probability that the dimensioning $\underline{R}$ **fall in** $D(\underline{Q}^1,\underline{Q}^2,\ldots\underline{Q}^k)$:

$$P_{\mathrm{s}}(\underline{Q}^1,\underline{Q}^2,\ldots\underline{Q}^k,\mu_{\underline{R}}) = \mu_{\underline{R}}[D(\underline{Q}^1,\underline{Q}^2,\ldots\underline{Q}^k)] \tag{44}$$

and

$$P_{\mathrm{c}}(\underline{Q}^1,\underline{Q}^2,\ldots\underline{Q}^k,\mu_{\underline{R}}) = 1 - P_{\mathrm{s}}(\underline{Q}^1,\underline{Q}^2,\ldots\underline{Q}^k,\mu_{\underline{R}}) = 1 - \mu_{\underline{R}}[D(\underline{Q}^1,\underline{Q}^2,\ldots\underline{Q}^k)]. \tag{45}$$

As in the preceding paragraph, any **interior approach** of $D(\underline{Q}^1,\underline{Q}^2,\ldots\underline{Q}^k)$ results in a **lower bound for** $P_{\mathrm{s}}(\underline{Q}^1,\underline{Q}^2,\ldots\underline{Q}^k,\mu_{\underline{R}})$ and the **kinematic exterior approach** follows from Eq. (21) to give a **lower bound for** $P_{\mathrm{c}}(\underline{Q}^1,\underline{Q}^2,\ldots\underline{Q}^k,\mu_{\underline{R}})$

$$\forall \hat{\underline{U}} \text{ K. A., } P_{\mathrm{c}}(\underline{Q}^1,\underline{Q}^2,\ldots\underline{Q}^k,\mu_{\underline{R}}) \geq \mu_{\underline{R}}\left\{ \sup_{\ell=1\ldots k} \underline{Q}^{\ell}.\underline{q}(\hat{\underline{U}}) - \underline{R}.\underline{r}(\hat{\underline{U}}) > 0 \right\} \tag{46}$$

and

$$P_{\mathrm{c}}(\underline{Q}^1,\underline{Q}^2,\ldots\underline{Q}^k,\mu_{\underline{R}}) = \mu_{\underline{R}}\left[\bigcup_{\hat{\underline{U}} \text{ K. A.}} \left\{ \sup_{\ell=1\ldots k} \underline{Q}^{\ell}.\underline{q}(\hat{\underline{U}}) - \underline{R}.\underline{r}(\hat{\underline{U}}) > 0 \right\} \right] \tag{47}$$

with the same comments as for Eq. (42).

Stochastic loads with stochastic resistances

From these two particular cases it is now easy to understand that, when both the loading vector and the resistance vector are stochastic variables, the probability of stability of the system is defined and obtained by referring to the domain of potential stability $\mathcal{K} \subset \mathbb{R}^n \times (\mathbb{R}_+)^m$ (§ 2.6). The probability of stability of the system is the probability that $(\underline{Q},\underline{R})$ fall in $\mathcal{K}$. With $\mu_{\underline{Q},\underline{R}}$ the joint probability measure for $(\underline{Q},\underline{R})$ in $\mathbb{R}^n \times (\mathbb{R}_+)^m$

$$P_{\mathrm{s}}(\mu_{\underline{Q},\underline{R}}) = \mu_{\underline{Q},\underline{R}}(\mathcal{K}). \tag{48}$$

Since it has been implicitly assumed in § 4.2 that $\underline{Q}$ and $\underline{R}$ are stochastically independent variables, their joint probability measure is the product $\mu_{\underline{Q},\underline{R}} = \mu_{\underline{Q}} \times \mu_{\underline{R}}$ and Eq. (48) can be written explicitly

$$P_s(\mu_{\underline{Q},\underline{R}}) = \mu_{\underline{Q},\underline{R}}(\mathcal{K}) = \begin{cases} \int_{(\mathbb{R}_+)^m} \mu_{\underline{Q}}(K(\underline{R}))\, \mathrm{d}\mu_{\underline{R}} \\ \int_{\mathbb{R}^n} \mu_{\underline{R}}(D(\underline{Q}))\, \mathrm{d}\mu_{\underline{Q}} \end{cases} \tag{49}$$

and, in the case of probability density functions $f(\underline{Q})$ and $g(\underline{R})$

$$P_s(\mu_{\underline{Q},\underline{R}}) = \mu_{\underline{Q},\underline{R}}(\mathcal{K}) = \begin{cases} \int_{(\mathbb{R}_+)^m} g(\underline{R})\, \mathrm{d}R_1 \ldots \mathrm{d}R_m \int_{K(\underline{R})} f(\underline{Q})\, \mathrm{d}Q_1 \ldots \mathrm{d}Q_n \\ \int_{\mathbb{R}^n} f(\underline{Q})\, \mathrm{d}Q_1 \ldots \mathrm{d}Q_n \int_{D(\underline{Q})} g(\underline{R})\, \mathrm{d}R_1 \ldots \mathrm{d}R_m \,. \end{cases} \tag{50}$$

Lower bounds for the probability of stability and for the probability of collapse are obtained, as in the particular cases examined previously, through the interior approach and the kinematic exterior approach respectively. The corresponding equations are similar to those written above – for instance we get Eq.(51) for the kinematic exterior approach – although their practical implementation may prove to be somewhat cumbersome

$$P_c(\mu_{\underline{Q}}, \underline{R}) \geq \mu_{\underline{Q},\underline{R}} \left[\bigcup_{\hat{\underline{U}} \text{ K. A.}} \left\{ \underline{Q}.\underline{q}(\hat{\underline{U}}) - \underline{R}.\underline{r}(\hat{\underline{U}}) > 0 \right\} \right] \tag{51}$$

4.4 Additional comments

The literature about probabilistic Yield Design approaches has been essentially devoted to the case of stochastic resistance parameters, not taking into account stochastic loading parameters at the same time. As it was mentioned earlier, practical applications aim at checking the reliability of the considered system and look for high levels for the probability of stability ($P_s(\underline{Q}^1, \underline{Q}^2 \ldots \underline{Q}^k, \mu_{\underline{R}}) \simeq 1$) and, conversely, very low levels for the probability of collapse ($P_c(\underline{Q}^1, \underline{Q}^2 \ldots \underline{Q}^k, \mu_{\underline{R}}) \simeq 0$).

Various research papers (*e.g.* [23-25]), often based upon the use of Monte Carlo methods, have drawn the attention onto the fact that the results obtained at very low probability levels depend strongly on the initial choices for the probability laws of the resistance parameters and of the load combinations. They are highly sensitive to the "Tail behaviour" of these laws when the minimum values of the resistance parameters or the extreme values of the loads are concerned ("rare events"). From this point of view, the Gumbel probability density functions [26], the Weibull ones [27, 28] and, more generally, the extreme value probability laws have often been (heuristically, *cf.* [29]) considered as good candidates for such stochastic modelling.

Consequently, for practical applications, in this case as in other similar ones, one should not take the values obtained for the very low probability levels as absolute results but only as ranking indicators when dimensioning a system.

As stated by Bouleau [29], *"Any attempt to allow a specific numerical value to the probability of a rare event is suspect, unless the physical laws governing the corresponding phenomenon are explicitly and exhaustively known…This does not mean that the use of probabilities or probabilistic concepts should be rejected from construction codes since such an approach can lead to a better expression of certain design rules."*[14]

REFERENCES

[1] SAVE, M. & PRAGER, W. (1985) – *Structural Optimization. Volume I. Optimality criteria.* Plenum Press, New York, London.

[2] FRÉMOND, M. & FRIAÀ, A. (1978) – Analyse limite. Comparaison des méthodes statique et cinématique. *Comptes Rendus de l'Académie des sciences de Paris*, **286**, A, 107-110.

[3] GAVARINI, C. & VENEZIANO, D. (1971) – On the safety domain of structures. *1st Italian national Conference on Theoretical and Applied Mechanics,* Udine, Italy.

[4] SALENÇON, J. (1975) – Optimisation des structures par le calcul aux états limites. *Les méthodes d'optimisation dans la construction*. Séminaire UTI-CISCO, 1973, Eyrolles, Paris, pp. 117-124.

[5] SALENÇON, J. (1983) – *Calcul à la rupture et analyse limite*. Presses de l'École Nationale des Ponts et Chaussées publ., Paris, 1983.

[6] GAVARINI, C. (1973) – Applications de la programmation mathématique à l'analyse limite des structures. *Revue française d'automatique, d'informatique et de recherche opérationnelle*, **7**, V3, 55-68.

[7] GAVARINI, C. (1968) – Calcolo a rottura e programmazione non-lineare. *Rendiconti Istituto Lombardo di Scienze e Lettere*, **A**, **102**, 329-342.

[8] DORN, W. S. & GREENBERG, H. J. (1957) – Linear programming & plastic limit analysis of structures. *Quarterly of Applied Mathematics*, **15**, 155-167.

[9] CHARNES, A., LEMKE, C. E. & ZIENKIEWICZ, O. C. (1959) – Virtual work, linear programming and plastic limit analysis. *Proceedings of the Royal Society*, **A**, **251**, 110-116.

[10] HOSKIN, B. C. (1960) – *Limit analysis, limit design and linear programming*. Aeronautical Research Laboratories, Melbourne, Report ARL/SM.274.

[14] "Un principe épistémologique se dégage : toute démarche attribuant une valeur numérique précise pour la probabilité d'un phénomène rare est suspecte, sauf si les lois physiques régissant le phénomène sont explicitement et exhaustivement connues… Ceci ne signifie pas que l'usage de probabilités ou de concepts probabilistes soit pour autant à rejeter des règlements de construction, dans la mesure ou un tel langage peut permettre une expression plus fine de certaines règles de conception."

[11] CERADINI, G. & GAVARINI, C. (1965) – Calcolo a rottura e programmazione lineare. *Giornale del Genio Civile*, **12**, 48-64.

[12] GAVARINI, C. (1966) – I teoremi fondamentali del calcolo a rottura e la dualita in programmazione lineare. *Ingegneria Civile*, **18**, 48-64.

[13] GAVARINI, C. (1966) – Plastic analysis of structures and duality in linear programming. *Meccanica*, **1**, 3-4, 95-97.

[14] MUNRO, J. & SMITH, D. L. (1972) – Linear programming duality in plastic analysis and synthesis. *Proceedings of the International Symposium on Computer-aided Structural Design*, vol. 1, Warwick Univ.

[15] LESCOUARCH, Y. & BROZZETTI, J. (1972) – Dimensionnement optimal des poutres.. *Proceedings of the Symposium on «Méthodes de calcul aux états limites des structures à barres»* CTICM, pp. 407-455.

[16] HEYMAN, J. (1975) – Les principes du calcul plastique. *Séminaire UTI-CISCO*, 1973, Eyrolles, Paris, pp. 85-109.

[17] TOAKLEY, A. R. (1968) – Optimum design using available sections. *Journal of the. Structural Division, Proc. ASCE*, **94**, 1219-1241.

[18] RINGERTZ, U. T. (1988) – On methods for discrete structural optimization. *Engineering Optimization*, **13**, 1, 47-64.

[19] YADAVAL, R. S. S. & GURUJEE C. S. (1997) - Optimal design of trusses using available sections. *Journal of Structural Engineering*, ASCE, **123**, 685-688.

[20] AUGUSTI, G. & BARATTA, A. (1972) – Theory of probability and limit analysis of structures under multi-parameter loading. *Symposium on the Foundations of Plasticity*, Warsaw, Aug. 30 - Sept. 2, A. SAWCZUK ed., Nordhoff, Leyden, pp. 347-364.

[21] SACCHI, G. (1973) – Étude probabiliste des structures élastoplastiques. *Proceedings of the Symposium, «Calcul aux états limites des structures à barres»*. CTICM, UTI-CISCO, Eyrolles, Paris, 1975, 117-124.

[22] GAVARINI, C. (1977) – Aspect probabiliste de la rupture. *Symp. Évolutions et théories modernes en élasticité et plasticité,* Saint-Rémy-lès-Chevreuse, 12-15 dec. 1977, CISCO, pp. 131-157.

[23] PARIMI, S. R. & COHN, M. Z. (1978) – Optimal solutions in probabilistic structural design. *Journal de Mécanique Appliquée*, **2**, 1, 47-92.

[24] CARMASOL, A. (1983) – *Approche probabiliste du calcul à la rupture*. Dr Eng. Th. École nationale des ponts et chaussées, Paris.

[25] CARMASOL, A. & SALENÇON, J. (1985) – Une approche probabiliste du dimensionnement des structures par le calcul à la rupture. *Journal de Mécanique Théorique et Appliquée*, **4**, 3, 305-321.

[26] GUMBEL, E. J. (1958) – *Statistics of extremes*. Columbia Univ. Press, New-York.

[27] WEIBULL, W. (1939) – *A Statistical Theory of the Strength of Materials*. Ingeniörsvetenskapsakademiens Handlingar, **151**, Generalstabens Litografiska Anstalts Förlag, Stockholm.

[28] WEIBULL, W. (1951) – A statistical distribution function of wide applicability. *J. Appl. Mech.*, **18**, 293-297.

[29] BOULEAU, N. (1991) – Splendeurs et misères des lois de valeurs extrêmes. *Revue Risques*, **4**, 85-92. *Halshs.archives-ouvertes.fr/docs/00/05/65/72/PDF/c.15.pdf.*

Chapter IX

Yield Design of structures

The curvilinear one-dimensional continuum
Implementation of the Yield Design theory
Typical strength criteria
Final comments
References

YIELD DESIGN OF STRUCTURES

The Chapter is devoted to the implementation of the Yield Design theory in the case of structures made of slender elements, addressed within the curvilinear one-dimensional continuum framework. The kinematics is defined by velocity distributor fields which describe the rigid body motion of the microstructure attached at any point of the director curve while the external and internal forces are represented by the corresponding wrench fields. The constituent elements are held together by joints and connected to the external world by supports. The implementation of the interior approach proceeds directly from the strength criteria of the elements, the joints and the supports. The kinematic exterior approach is based on the construction of kinematically admissible virtual motions defined by velocity distributor fields.

1 The curvilinear one-dimensional continuum

In a similar way as in Chapter III we recall now the curvilinear one-dimensional continuum model. Following the classic pattern, we first define the external and internal forces and write down the equilibrium equations, and then we introduce the virtual velocity fields and state the virtual work theorem/principle. An alternative presentation based upon the virtual work principle as a starting point may be found in [1].

1.1 Geometric description of the model

The curvilinear one-dimensional continuum is a mechanical model built to represent slender elements subjected to concentrated or distributed forces and moments. Taking advantage of the geometric specificity introduced by the slenderness of the considered elements, the model refers, for the geometric description of a typical system S, to a **director curve** (C).

A system S is described geometrically on an arc AB of the director curve (C). As a continuum, it is constituted of "particles". Since the model aims at squeezing a three-dimensional slender element onto a one-dimensional description, a particle P is no more a kind of "diluted material point" with the volume $\mathrm{d}\Omega$, only characterised by its position, as it used to be in the classical three-dimensional continuum [1]. It is now described as a "diluted material point" with length $\mathrm{d}s$ and with a **transverse microstructure**. This microstructure may be represented, in the considered reference configuration, by a plane surface element orthogonal to the director curve at the point P (Figure 1).

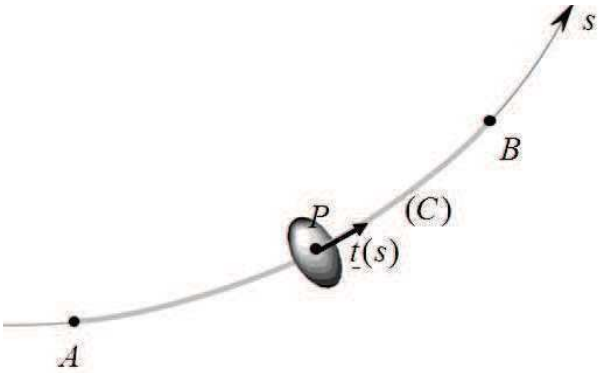

Figure 1. The particle at the point P

1.2 Kinematics

The velocity field

The particle at the point P, with the length ds along $\underline{t}(s)$ the tangent vector to (C), is characterised by its position s on (C) and by the orientation of the transverse microstructure. The evolution of the system at a given instant of time t is described, from the geometrical point of view, by the velocity of the generic point P of (C) denoted by $\underline{U}(s)$ and the angular velocity of its micro-structure denoted by $\underline{\Omega}(s)$ given for all the particles on AB.

The **movement of the particle** P in the one-dimensional model is the rigid body motion defined by these two vectors attached to the particle P. The general expression of the corresponding velocity field in $\mathbb{R}^3$ is

(1) $$\forall M \in \mathbb{R}^3,\ \underline{U}(M) = \underline{U}(s) + \underline{\Omega}(s) \wedge \underline{PM},$$

where the symbol " $\wedge$ " denotes the external product of two vectors.

To describe such a rigid body velocity field the concept of **velocity distributor** has been introduced (*e.g.* [1]). Eq. (1) is the explicit definition of the velocity field generated by the **velocity distributor** $\{\mathbb{U}(s)\}$ which describes the movement of the **particle**

(2) $$\{\mathbb{U}(s)\} = \{\, P,\ \underline{U}(s),\ \underline{\Omega}(s)\}$$

with the characteristic property

(3) $$\forall \underline{PQ} \in \mathbb{R}^3,\ \{\mathbb{U}(s)\} = \{\, P,\ \underline{U}(s),\ \underline{\Omega}(s)\} = \left\{ Q,\ \underline{U}(s) + \underline{\Omega}(s) \wedge \underline{PQ},\ \underline{\Omega}(s)\right\}.$$

In order to comply with the concept of a continuous medium, in the same way as for the classical three-dimensional continuum, the fields $\underline{U}(s)$ and $\underline{\Omega}(s)$ are **piecewise continuous and continuously differentiable** on AB.

Any rigid body motion of the system S (resp. subsystem S') is characterised by the rigid body of the current particle P being constant on AB (resp. $A'B'$): in such a case, the system (resp. subsystem) is not deformed. Deformation is the result of the **variation** of the rigid body motion of the particles along the director curve.

The **strain rate** of the one-dimensional continuum at the point P is the derivative, with respect to s, of the rigid body motion attached to the particle P, *i.e.* the derivative of the velocity distributor $\{\mathbb{U}(s)\}$ with respect to s.

The expression of this derivative is obtained from the comparison of the rigid body velocity fields attached to two adjacent particles P and $P+\underline{\mathrm{d}P}$. From Eq. (1) we get through the characteristic property (3), the point M being fixed,

$$\forall M \in \mathbb{R}^3,\ \frac{\mathrm{d}}{\mathrm{d}s}\underline{\underline{U}}(M) = \frac{\mathrm{d}}{\mathrm{d}s}\underline{U}(s) - \underline{\underline{\Omega}}(s)\wedge\underline{t}(s) + \frac{\mathrm{d}}{\mathrm{d}s}\underline{\underline{\Omega}}(s)\wedge\underline{PM} \tag{4}$$

and then the strain rate of the one-dimensional continuum at the point P is written

$$\frac{\mathrm{d}}{\mathrm{d}s}\{\mathbb{U}(s)\} = \{\mathbb{D}(s)\} = \left\{ P,\ \frac{\mathrm{d}}{\mathrm{d}s}\underline{U}(s) - \underline{\underline{\Omega}}(s)\wedge\underline{t}(s),\ \frac{\mathrm{d}}{\mathrm{d}s}\underline{\underline{\Omega}}(s) \right\}. \tag{5}$$

It means that the rigid body motion of the particle $P+\underline{\mathrm{d}P}$ with respect to the particle P is defined by the translation with vector

$$\left(\frac{\mathrm{d}}{\mathrm{d}s}\underline{U}(s) - \underline{\underline{\Omega}}(s)\wedge\underline{t}(s)\right)\mathrm{d}s \tag{6}$$

and the rotation

$$\frac{\mathrm{d}}{\mathrm{d}s}\underline{\underline{\Omega}}(s)\,\mathrm{d}s\,. \tag{7}$$

From Eq. (6) we can easily identify the **rate of stretch of the director curve** at the point P from the component of the translation vector along $\underline{t}(s)$

$$D(s) = \frac{\mathrm{d}\underline{\underline{U}}}{\mathrm{d}s}.\underline{t}(s). \tag{8}$$

To interpret the component orthogonal to the director curve

$$\frac{\mathrm{d}}{\mathrm{d}s}\underline{U}(s) - D(s)\underline{t}(s) - \underline{\underline{\Omega}}(s)\wedge\underline{t}(s) \tag{9}$$

more easily we observe that if the microstructure is represented by a plane surface element orthogonal to the director curve at the point P in the reference configuration, the rotation rate of the director curve is equal to $\underline{t}(s)\wedge\frac{\mathrm{d}}{\mathrm{d}s}\underline{U}(s)$ while the rotation rate of the microstructure is $\underline{\underline{\Omega}}(\underline{s})$. Let $\Omega_t(s) = \underline{\underline{\Omega}}(s).\underline{t}(s)$ denote the tangential component of $\underline{\underline{\Omega}}(\underline{s})$, then

$$\underline{t}(s)\wedge\frac{\mathrm{d}}{\mathrm{d}s}\underline{U}(s) - \left(\underline{\underline{\Omega}}(s) - \Omega_t(s)\underline{t}(s)\right) \tag{10}$$

is the **rate of angular distortion** of the microstructure with respect to the director curve. In the particular case when the condition

$$\underline{t}(s)\wedge\frac{\mathrm{d}}{\mathrm{d}s}\underline{U}(s) - \left(\underline{\underline{\Omega}}(s) - \Omega_t(s)\underline{t}(s)\right) = 0 \tag{11}$$

equivalent to

$$\frac{\mathrm{d}}{\mathrm{d}s}\underline{U}(s) - D(s)\underline{t}(s) - \underline{\Omega}(s) \wedge \underline{t}(s) = 0 \tag{12}$$

holds as an internal constraint on the model it implies that the microstructure remains orthogonal to the director curve (C) in the evolution of the system. Eq. (11) is known as the **Navier-Bernoulli condition**. With this condition the velocity field of the particles is defined by the vector field $\underline{U}(s)$ and the scalar field $\Omega_t(s)$ which gives the torsion rate of the director curve while the rate of bending is

$$\underline{\Omega}(s) - \Omega_t(s)\underline{t}(s) = \underline{t}(s) \wedge \frac{\mathrm{d}}{\mathrm{d}s}\underline{U}(s) \ . \tag{13}$$

The Navier-Bernoulli condition is often introduced as a part of a constitutive law. It will appear in § 2.3 as a mathematical condition for the relevance of kinematically admissible virtual motions for specific strength criteria.

1.3 Dynamics

External forces

The external forces applied to a system AB are modelled by:

- A line density $\underline{f}(s)$ corresponding to the distributed forces acting on AB, so that the infinitesimal distributed force is $\underline{f}(s)\mathrm{d}s$ for the length element $\mathrm{d}s$.
- A line density $\underline{m}(s)$ corresponding to the distributed moments acting on AB, so that the infinitesimal distributed moment is $\underline{m}(s)\mathrm{d}s$ for the length element $\mathrm{d}s$ (in practice it is often equal to zero).
- At the endpoints A and B, which stand for the boundary of the system:
  a concentrated force $\underline{R}_A$ and a concentrated moment $\underline{H}_A$ at the point A;
  a concentrated force $\underline{R}_B$ and a concentrated moment $\underline{H}_B$ at the point B.
- Concentrated forces $\underline{F}_i$ and concentrated moments $\underline{M}_i$ applied at points P_i of AB will also be considered.

Internal forces

It is assumed that the particles of the system AB exert no action at a distance upon one another and that, at the point P, the particle of the system immediately downstream exerts on the particle immediately upstream, via the microstructure, contact forces which are reduced to a concentrated force $\underline{\mathcal{X}}(s)$ and a concentrated moment $\underline{\Gamma}(s)$.

These two vectors at the point P (Figure 2) define the **wrench of internal forces**

$$\left[\mathbb{X}(s)\right] = \left[P, \underline{\mathcal{X}}(s), \underline{\Gamma}(s)\right] \tag{14}$$

with the characteristic property

$$\forall \underline{PQ} \in \mathbb{R}^3, \left[\mathbb{X}(s)\right] = \left[P, \underline{\mathcal{X}}(s), \underline{\Gamma}(s)\right] = \left[Q, \underline{\mathcal{X}}(s), \underline{\Gamma}(s) + \underline{QP} \wedge \underline{\mathcal{X}}(s)\right]. \tag{15}$$

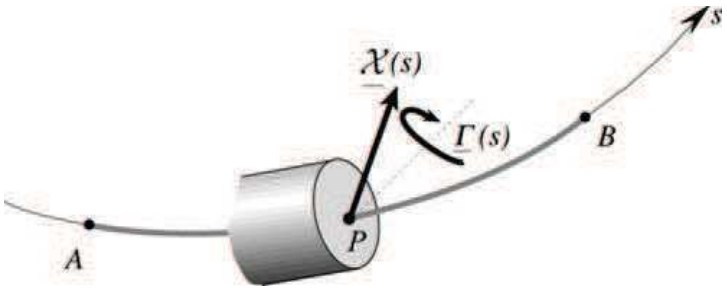

Figure 2. Wrench of internal forces at the point P

It is common practice to decompose the reduced elements $\underline{\mathcal{X}}(s)$ and $\underline{\Gamma}(s)$ at P into components along $\underline{t}(s)$ and in the plane of the orthogonal microstructure. We set

(16) $$\underline{\mathcal{X}}(s) = N(s)\underline{t}(s) + \underline{V}(s)$$

(17) $$\underline{\Gamma}(s) = T(s)\underline{t}(s) + \underline{\mathcal{M}}(s)$$

where $\underline{V}(s)$ and $\underline{\mathcal{M}}(s)$ lie in the plane orthogonal to (C). The terminology refers physically to the orthogonal microstructure, thus recalling the slender solid at the origin of the model (Figure 3):

- $N(s)$ is the **normal force** at P, which is tangent to the director curve
- $\underline{V}(s)$ is the **shearing force** at P, it is orthogonal to the director curve
- $T(s)$ is the **twisting moment** at P, tangent to the director curve
- $\underline{\mathcal{M}}(s)$ is the **bending moment** at P, orthogonal to the director curve.

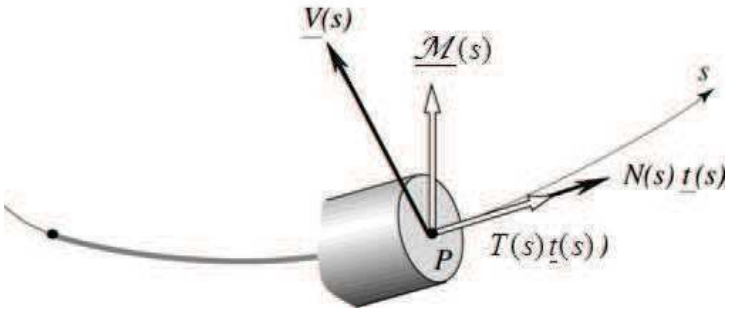

Figure 3. Normal force, shearing force, twisting moment and bending moment at P

Equilibrium equations

Taking advantage of the geometric simplicity of the model the differential equilibrium equations are classically obtained by writing down the fundamental law of Statics for the infinitesimal element at the point P (Figure 4). In the absence of a concentrated force or moment we get

(18)
$$\begin{cases} \forall P \in AB, \\ \dfrac{\mathrm{d}\underline{\mathcal{X}}(s)}{\mathrm{d}s} + \underline{f}(s) = 0 \\ \dfrac{\mathrm{d}\underline{\Gamma}(s)}{\mathrm{d}s} + \underline{t}(s) \wedge \underline{\mathcal{X}}(s) + \underline{m}(s) = 0 \end{cases}$$

and the boundary conditions at the endpoints

(19)
$$\begin{cases} \underline{\mathcal{X}}(s_A) = -\underline{R}_A, \quad \underline{\Gamma}(s_A) = -\underline{H}_A \\ \underline{\mathcal{X}}(s_B) = \underline{R}_B, \quad \underline{\Gamma}(s_B) = \underline{H}_B. \end{cases}$$

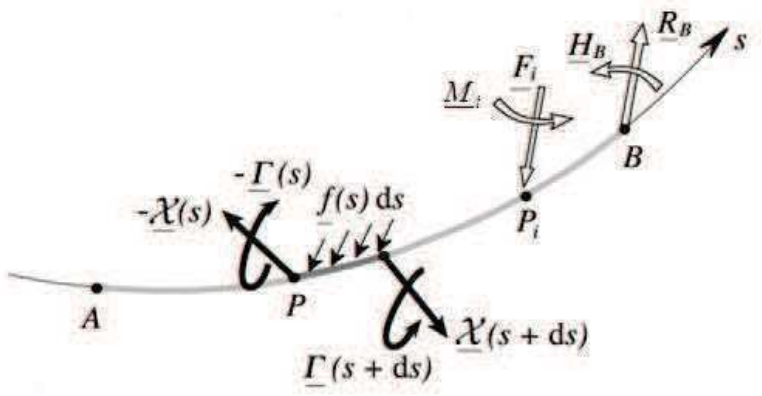

Figure 4. Differential Equilibrium equations

In the case of a concentrated force or moment at a point P_i

(20)
$$[\![\, \underline{\mathcal{X}}(s_i) \,]\!] = -\underline{F}_i, \quad [\![\, \underline{\Gamma}(s_i) \,]\!] = -\underline{M}_i.$$

These equations can be simplified by introducing the wrenches of the external forces:

- For the distributed forces and moments, the line density wrench

(21)
$$\left[\, \mathbb{f}(s) \,\right] = \left[P,\ \underline{f}(s),\ \underline{m}(s) \right]$$

- For the concentrated forces and moments

(22)
$$\left[\, \mathbb{F}(s_i) \,\right] = \left[\, P_i, \underline{F}_i, \underline{M}_i \,\right]$$

- For the endpoint forces and moments

(23)
$$\begin{cases} \left[\, \mathbb{R}_A \,\right] = \left[\, A, \underline{R}_A, \underline{H}_A \,\right] \\ \left[\, \mathbb{R}_B \,\right] = \left[\, B, \underline{R}_B, \underline{H}_B \,\right] \end{cases}$$

The derivative of $\left[\, \mathbb{X}(s) \right]$ comes easily from the characteristic property (15)

(24)
$$\frac{\mathrm{d}}{\mathrm{d}s}\left[\, \mathbb{X}(s) \,\right] = \left[P,\ \frac{\mathrm{d}}{\mathrm{d}s}\underline{\mathcal{X}}(s),\ \frac{\mathrm{d}}{\mathrm{d}s}\underline{\Gamma}(s) + \underline{t}(s) \wedge \underline{\mathcal{X}}(s) \right].$$

Hence, Eq. (18) takes the form of a single differential equation:

$$\begin{cases} \forall P \in AB, \\ \dfrac{\mathrm{d}}{\mathrm{d}s}\left[\mathbb{X}(s)\right] + \left[\mathbb{f}(s)\right] = 0. \end{cases} \tag{25}$$

The boundary conditions become

$$\begin{cases} \left[\mathbb{X}(s_A)\right] = -\left[\mathbb{R}_A\right] \\ \left[\mathbb{X}(s_B)\right] = \left[\mathbb{R}_B\right] \end{cases} \tag{26}$$

and the jump condition at the point P_i is written

$$\left[\!\left[\left[\mathbb{X}(s_i)\right]\right]\!\right] + \left[\mathbb{F}(s_i)\right] = 0. \tag{27}$$

Integrating the Equilibrium Equation

Eqs (25) and (27) integrate immediately with the boundary conditions (26). They determine the wrench of internal forces at the point P, either by downstream integration from P to the endpoint B or by upstream integration from P to the endpoint A. The equations are equivalent to each other, due to the global equilibrium of the system AB.

$$\begin{cases} \left[\mathbb{X}(s)\right] = \left[\mathbb{R}_B\right] + \displaystyle\int_{PB}\left[\mathbb{f}(s)\right]\mathrm{d}s + \sum_{s<s_i<s_B}\left[\mathbb{F}(s_i)\right] \\ \left[\mathbb{X}(s)\right] = -\left[\mathbb{R}_A\right] - \displaystyle\int_{AP}\left[\mathbb{f}(s)\right]\mathrm{d}s - \sum_{s_A<s_i<s}\left[\mathbb{F}(s_i)\right] \end{cases} \tag{28}$$

The internal force wrench at the point P is equal to the wrench of all external forces applied to the element downstream of P; it is also the opposite of the wrench of all external forces applied to the element upstream of P.

1.4 Theorem/Principle of virtual work

Virtual motions

The virtual motions of the system AB are defined in the same manner as the actual kinematics in § 1.2 with the virtual velocity distributor field $\left\{\hat{\mathbb{U}}(s)\right\} = \left\{P, \hat{\underline{U}}(s), \hat{\underline{\Omega}}(s)\right\}$, piecewise continuous and continuously differentiable on AB.

Virtual work by the external forces

The virtual (rate of) work by the external forces is written

$$\begin{aligned} \mathcal{P}_{\mathrm{e}} = {} & \underline{R}_A.\hat{\underline{U}}(s_A) + \underline{H}_A.\hat{\underline{\Omega}}(s_A) + \underline{R}_B.\hat{\underline{U}}(s_B) + \underline{H}_B.\hat{\underline{\Omega}}(s_B) \\ & + \sum_{s_A<s_i<s_B}\left(\underline{F}_i.\hat{\underline{U}}(s_i) + \underline{M}_i.\hat{\underline{\Omega}}(s_i)\right) \\ & + \int_{AB}\left(\underline{f}(s).\hat{\underline{U}}(s) + \underline{m}(s).\hat{\underline{\Omega}}(s)\right)\mathrm{d}s. \end{aligned} \tag{29}$$

The second hand of this equation is the sum of the scalar products of the applied forces by the virtual velocities and the scalar products of the applied moments by the virtual rotation rates of the microstructure. This is just the sum of the scalar products of the corresponding wrenches of forces by the virtual velocity distributors at the considered points so that Eq. (29) can be written in the more compact form

$$\mathcal{P}_e(\{\hat{\mathbb{U}}\}) = [\mathbb{R}_A].\{\hat{\mathbb{U}}(s_A)\} + [\mathbb{R}_B].\{\hat{\mathbb{U}}(s_B)\} + \sum_{s_A<s_i<s_B} [\mathbb{F}(s_i)].\{\hat{\mathbb{U}}(s_i)\} + \int_{AB} [\mathbb{f}(s)].\{\hat{\mathbb{U}}(s)\}\,ds. \tag{30}$$

The Virtual work equation

Taking advantage of the equilibrium equations (25)-(27), the second line of Eq. (30) can be integrated and we get the virtual work equation (31) where the two last terms of the first hand stand for the virtual (rate of) work by the internal forces taking into account the discontinuities of the virtual motion at points P_j which should not coincide with any point P_i where the wrench of internal forces is discontinuous:

$$\mathcal{P}_e(\{\hat{\mathbb{U}}\}) - \int_{AB} [\mathbb{X}(s)].\frac{d}{ds}\{\hat{\mathbb{U}}(s)\}\,ds - \sum_{s_A<s_j<s_B} [\mathbb{X}(s_j)].[\![\{\hat{\mathbb{U}}(s_j)\}]\!] = 0. \tag{31}$$

It states that, in the case of equilibrium, the sum of the virtual work by the external forces $\mathcal{P}_e$ with the virtual work by the internal forces $\mathcal{P}_i([\mathbb{X}],\{\hat{\mathbb{U}}\})$ is equal to zero. Explicitly:

$$\mathcal{P}_e(\{\hat{\mathbb{U}}\}) + \mathcal{P}_i([\mathbb{X}],\{\hat{\mathbb{U}}\}) = 0 \tag{32}$$

with

$$\begin{aligned}\mathcal{P}_i([\mathbb{X}],\{\hat{\mathbb{U}}\}) = &- \sum_{s_A<s_j<s_B} \underline{X}(s_j).[\![\underline{\hat{U}}(s_j)]\!] - \sum_{s_A<s_j<s_B} \underline{\Gamma}(s_j).[\![\underline{\hat{\Omega}}(s_j)]\!] \\ &- \int_{AB} \underline{X}(s).\left(\frac{d}{ds}\underline{\hat{U}}(s) - \underline{\hat{\Omega}}(s)\wedge\underline{t}(s)\right)ds \\ &- \int_{AB} \underline{\Gamma}(s).\frac{d}{ds}\underline{\hat{\Omega}}(s)\,ds.\end{aligned} \tag{33}$$

From Eq. (16) we may transform the second line of this equation as the sum of the virtual work by the normal force $-\int_{AB} N(s)D(s)\,ds$ and the virtual work by the shearing force

$$-\int_{AB} \underline{V}(s).\left(\frac{d}{ds}\underline{\hat{U}}(s) - \underline{\hat{\Omega}}(s)\wedge\underline{t}(s)\right)ds \tag{34}$$

It comes out from this expression that if the Navier-Bernoulli condition (12) is imposed to the virtual velocity field the shearing force does not contribute to the virtual work by the internal forces.

2 Implementation of the Yield Design theory

2.1 Settlement of the problem

Geometrical data

The settlement of the Yield Design problem within the framework of the one-dimensional continuum follows the same path as in Chapter IV. The geometric data have already been defined in § 1.1 for a one-dimensional element A_iB_i. In practice, the systems to be considered are made from assemblages of slender elements (frames, trusses…). These can be modelled as two- or three-dimensional **structures** built up from **one-dimensional members** held together by assembly **joints** (Figure 5). The geometric definition of the structure includes these joints. It also includes the supports of the structure.
As a consequence, the equilibrium equations of the structure consist of the equilibrium equation of each member, and of the equilibrium equation of each joint or support which states that **the wrench of *all forces* applied to it must be equal to zero**.

Figure 5. Solferino footbridge (Paris) showing structural elements (© Jean Salençon)

Loading mode

The loads are applied to the members of the structure in the form of distributed or concentrated wrenches, and also to the joints and supports in the form of concentrated wrenches.

The loading mode of the structure is a multi-parameter one, following the definition given in Chapter IV (§ 1.2).

Resistance of the constituent material

The counterpart of the Cauchy stress tensor in the general theory is now the wrench of internal forces $\left[\mathbb{X}(s)\right]$.

Regarding the one-dimensional members themselves, the resistance is defined at any point P of an element A_iB_i by a domain of resistance $G(s)$ for $\left[\mathbb{X}(s)\right]$ in $\mathbb{R}^6$, which is often specified through a strength criterion:

(35) $$\left[\mathbb{X}(s)\right] \in G(s) \subset \mathbb{R}^6 \Leftrightarrow f(\left[\mathbb{X}(s)\right]) \le 0.$$

As a rule, $G(s)$ is convex and includes the wrench $\left[\mathbb{X}(s)\right] = 0$. The explicit forms of $f(\left[\mathbb{X}(s)\right])$ in terms of the components $(N, \underline{V}, T, \underline{\mathcal{M}})$ of the reduced elements of $\left[\mathbb{X}(s)\right]$ are called **interaction formulae**. In practice, they rarely involve the whole set of the six scalar components of $(N, \underline{V}, T, \underline{\mathcal{M}})$, due to the specificities of each problem under exam (*cf.* § 2.2).

The resistance of the assembly joints and structural supports deserves special comments.

Consider a joint A where the oriented elements A_iB_i are connected (Figure 6). For each element, a convex strength condition is imposed by the joint, which concerns the wrench of forces exerted by the element on the joint and includes the zero wrench of forces, namely

(36) $$\left[\mathbb{X}(s_{A_i})\right] \in \mathcal{G}_{A_i} \Leftrightarrow f_{A_i}(\left[\mathbb{X}(s_{A_i})\right]) \le 0.$$

Thus, in the same way as for the interfaces in Chapter IV (§ 3.3), the wrench of internal forces has to comply with Eq. (36) and with the strength condition (35) of the element itself at the point A_i.

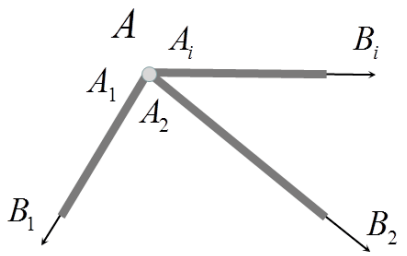

Figure 6. Strength conditions at an assembly joint

It is important to note that, at a given joint A, the type of the strength condition (36) imposed by the joint (§ 3.2) may differ from one element A_iB_i to the other.

The same procedure applies to a structural support but, since it is commonplace for structural supports to coincide geometrically with assembly joints in the model, it is important to have a clear view of the mechanical operation of the structure at the relevant joint and support in order to avoid any confusion (*cf.* § 3.3). As an example, in the case of Figure 7, the strength condition should be split into the strength condition at the assembly joint in the form of Eq. (36) and the strength condition of the structural support itself

(37) $$\left[\mathbb{X}(s_A)\right] \in \mathcal{G}_A \Leftrightarrow f_A(\left[\mathbb{X}(s_A)\right]) \le 0$$

As a matter of fact, structural supports are just particular cases of assembly joints, with specific strength criteria, which connect the structure to the external world with kinematic boundary data set to zero.

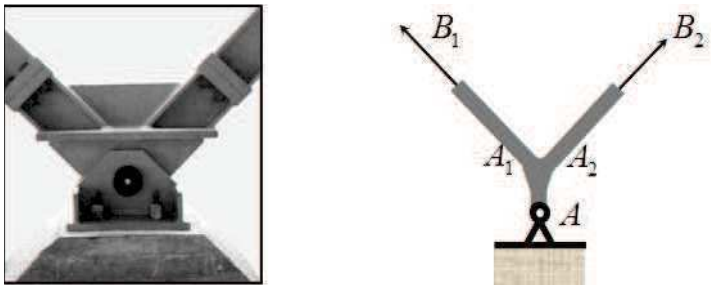

Figure 7. A rigid assembly joint on a fixed hinged support

2.2 Interior approach

Statically admissible internal force wrench fields

In a similar way as in Chapter IV an internal force field is said to be **statically admissible** (S. A.) for the problem with a given value of the load $\underline{Q}$ if it is a wrench field defined on the entire geometry of the system, piecewise continuous and continuously differentiable, which satisfies the equilibrium equations (25)-(27) in each one-dimensional element and the equilibrium equations of the assembly joints and structural supports[1], for this value of the load.

Interior approach of K

From the general theory (Chapter IV, section 2) we get the definition and the interior approach of the domain of potentially safe loads for the structure by substituting statically admissible internal force wrench fields for statically admissible stress fields in the corresponding equations

$$\underline{Q}([\mathbb{X}]) \in K \Leftrightarrow \exists [\mathbb{X}] \begin{cases} [\mathbb{X}] \text{ S. A. with } \underline{Q}([\mathbb{X}]) \\ [\mathbb{X}(s)] \in G(s) \ \forall A_i B_i, \forall P \in A_i B_i \\ [\mathbb{X}(s_{A_i})] \in \mathcal{G}_{A_i} \ \ \forall A_i \end{cases} \tag{38}$$

Potentially safe loads

From the convexity of $G(s)$ and $\mathcal{G}_{A_i}$ the domain K is convex as in the general theory. It also includes the zero load (Figure 8).

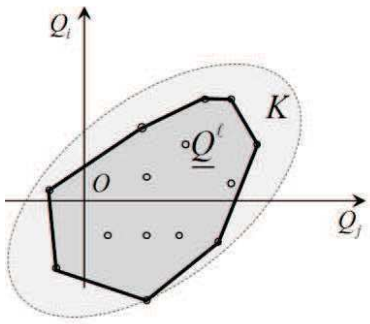

Figure 8. Interior estimate of K provided by the convex hull of potentially safe loads

[1] As already stated in § 2.1, the wrench of *all forces* applied to the joint or support must be equal to zero: this condition should not be mixed up with the strength condition.

As it has been noted previously, the explicit forms of the strength criteria which are used in practice seldom refer to the whole set of the six scalar components of $(N,\underline{V},T,\underline{\mathcal{M}})$. As a consequence the missing components of $[\mathbb{X}(s)]$ are unlimited. In other words, $G(s)$ is not bounded in the corresponding directions of the $\mathbb{R}^6$ space of the internal force wrenches. For instance, in the case of a plane structure loaded in its own plane Oxy, the Yield Design analysis is often carried out with $f([\mathbb{X}(s)])$ being restricted to $f(N,M_z)$, where M_z is the component of $\underline{\mathcal{M}}$ along the z axis[2], or even to $f(M_z)$ only. After such a simplified analysis has been performed, another one is usually made on the basis of the design so-obtained in order to check the compatibility with the complete strength criteria (*e.g.* taking the shearing force into account). Such a double-step procedure aims at taking the best advantage of the geometric simplicity of the one-dimensional continuum model.

2.3 Exterior approach

Kinematically admissible virtual motions

A virtual motion of the structure is defined by a virtual velocity distributor field $\{\hat{\mathbb{U}}(s)\} = \{P, \underline{\hat{U}}(s), \underline{\hat{\Omega}}(s)\}$ as in § 1.4. The domain of definition of this field consists of the constituent one-dimensional members A_iB_i of the structure, the joints connecting these members, and the supports of the structure.

In order to be **kinematically admissible** for the problem such a virtual motion must be piecewise continuous and continuously differentiable in the structure.

Virtual work equation for the structure

Let $[\mathbb{X}]$ be a statically admissible internal force wrench field in the structure and $\{\hat{\mathbb{U}}\}$ a kinematically admissible virtual motion of the structure.

The virtual work by the external forces in equilibrium with $[\mathbb{X}]$ in the virtual motion $\{\hat{\mathbb{U}}\}$ is developed by the corresponding wrenches of external forces applied to the constituent members, the assembly joints and to the structural supports. According to the multi-parameter loading mode, it takes the form

$$\mathcal{P}_e([\mathbb{X}],\{\hat{\mathbb{U}}\}) = \underline{Q}([\mathbb{X}]).\underline{q}(\{\hat{\mathbb{U}}\}). \tag{39}$$

The virtual work by the internal forces in the structures is developed in each oriented constituent member A_iB_i with the same expression as in Eq. (31), and in the joints and supports.

Recalling the notation $\{\hat{\mathbb{D}}(s)\} = \dfrac{\mathrm{d}}{\mathrm{d}s}\{\hat{\mathbb{U}}(s)\}$, we have:

[2] This is the case when Oxy is a plane of symmetry for the physical system modelled by the structure.

$$\mathcal{P}_i([\,\mathbb{X}\,],\{\hat{\mathbb{U}}\}) = -\sum_i \int_{A_iB_i} [\,\mathbb{X}(s)\,].\{\hat{\mathbb{D}}(s)\}\,\mathrm{d}s - \sum_j [\,\mathbb{X}(s_j)\,].[\![\{\hat{\mathbb{U}}(s_j)\}]\!] \\ -\sum_i [\,\mathbb{X}(s_{A_i})\,].[\![\{\hat{\mathbb{U}}(A_i)\}]\!] - \sum_i [\,\mathbb{X}(s_{B_i})\,].[\![\{\hat{\mathbb{U}}(B_i)\}]\!] \\ -\sum [\,\mathbb{X}(s_A)\,].\{\hat{\mathbb{U}}(s_A)\} \tag{40}$$

where the second line stands for the joints and supports, with the notations

$$\begin{cases} [\![\{\hat{\mathbb{U}}(A_i)\}]\!] = \{\hat{\mathbb{U}}(s_{A_i})\} - \{\hat{\mathbb{U}}(A)\} \\ [\![\{\hat{\mathbb{U}}(B_i)\}]\!] = \{\hat{\mathbb{U}}(B)\} - \{\hat{\mathbb{U}}(s_{B_i})\}, \end{cases} \tag{41}$$

and the third line stands for the structural supports.

Maximum resisting work

The maximum resisting work to be used in the kinematic exterior approach, as stated in the general theory, consists here

- of the contribution of each one-dimensional member itself, obtained as the upper bound of the right-hand side of the first line in Eq. (40) due to the strength condition (35),
- of the contribution at the joints and the supports, derived from the strength condition (36) as the upper bound of the second line,
- and of the contribution at the supports derived from the strength condition (37) as the upper bound of the third line.

We get

- for the line density of maximum resisting work in the first contribution

$$\pi(\{\hat{\mathbb{D}}(s)\}) = \sup\left\{[\,\mathbb{X}'\,].\{\hat{\mathbb{D}}(s)\} \,\middle|\, [\,\mathbb{X}'\,] \in G(s)\right\} \tag{42}$$

and for each virtual velocity jump

$$\pi([\![\{\hat{\mathbb{U}}(s_j)\}]\!]) = \sup\left\{[\,\mathbb{X}'\,].[\![\{\hat{\mathbb{U}}(s_j)\}]\!] \,\middle|\, [\,\mathbb{X}'\,] \in G(s_j)\right\}. \tag{43}$$

- For the second contribution

$$\begin{cases} \pi_{A_i}([\![\{\hat{\mathbb{U}}(A_i)\}]\!]) = \sup\left\{[\,\mathbb{X}'\,].[\![\{\hat{\mathbb{U}}(A_i)\}]\!] \,\middle|\, [\,\mathbb{X}'\,] \in \mathcal{G}_{A_i}\right\} \\ \pi_{B_i}([\![\{\hat{\mathbb{U}}(B_i)\}]\!]) = \sup\left\{[\,\mathbb{X}'\,].[\![\{\hat{\mathbb{U}}(B_i)\}]\!] \,\middle|\, [\,\mathbb{X}'\,] \in \mathcal{G}_{B_i}\right\}. \end{cases} \tag{44}$$

- For the third contribution

$$\pi_A(\{\hat{\mathbb{U}}(s_A)\}) = \sup\left\{[\,\mathbb{X}'\,].\{\hat{\mathbb{U}}(s_A)\} \,\middle|\, [\,\mathbb{X}'\,] \in \mathcal{G}_A\right\} \tag{45}$$

Finally the maximum resisting work for the structure is written

(46) $$\mathcal{P}_{\text{mr}}(\{\hat{\mathbb{U}}\}) = \sum_i \int_{A_iB_i} \pi(\{\hat{\mathbb{D}}(s)\})\,\mathrm{d}s + \sum_j \pi([\![\{\hat{\mathbb{U}}(s_j)\}]\!]) + \sum_i \pi_{A_i}([\![\{\hat{\mathbb{U}}(A_i)\}]\!]) + \sum_i \pi_{B_i}([\![\{\hat{\mathbb{U}}(B_i)\}]\!]) + \sum \pi_A(\{\hat{\mathbb{U}}(s_A)\}).$$

Fundamental equation and relevant virtual motions

The fundamental equation of the kinematic exterior approach is the counterpart of Eq. (3) in Chapter VI

(47) $$\forall \{\hat{\mathbb{U}}\} \text{ K. A., } K \subset \left\{ \underline{Q}.\underline{q}(\{\hat{\mathbb{U}}\}) - \mathcal{P}_{\text{mr}}(\{\hat{\mathbb{U}}\}) \le 0 \right\}.$$

The efficiency of this equation for the determination of an exterior approach of domain K requires $\mathcal{P}_{\text{mr}}(\{\hat{\mathbb{U}}\})$ being finite: $\{\hat{\mathbb{U}}\}$ must be a **relevant** kinematically admissible virtual motion of the structure (Chapter VI, § 2.1) complying with the conditions imposed by the unbounded directions of the strength criteria of the members, the joints and the supports.

3 Typical strength criteria

3.1 Interaction formulae

Wires

From the Yield Design viewpoint, wires are modelled as exhibiting **no resistance except to tension**.

The strength criterion is written

(48) $$[\,\mathbb{X}(s)\,] \in G(s) \Leftrightarrow \begin{cases} 0 \le N(s) \le N_0(s) \\ |\,\underline{V}(s)\,| = T(s) = |\,\underline{\mathcal{M}}(s)\,| = 0. \end{cases}$$

Hence

(49) $$\begin{cases} \pi(\{\hat{\mathbb{D}}(s)\}) = \sup\{\,0, N_0(s)\,\hat{D}(s)\,\} \\ \pi([\![\{\hat{\mathbb{U}}(s)\}]\!]) = \sup\{\,0, N_0(s)[\![\,\hat{\underline{U}}(s)]\!].\underline{t}(s)\,\}. \end{cases}$$

Normal bending (*cf.* § 2.2)

In the case of a plane structure loaded in its own plane Oxy a first Yield Design approach is often performed with strength criteria which depend on M_z only

(50) $$[\,\mathbb{X}(s)\,] \in G(s) \Leftrightarrow m^-(s) \le M_z(s) \le m^+(s)$$

where $m^+(s)$ and $m^-(s)$ are the **algebraic values** of the maximum resisting bending moment of the element in positive and negative bending respectively. This means that the components $(N(s), \underline{V}(s), T(s), \underline{\mathcal{M}}(s) - M_z\,\underline{e}_z)$ of $[\![\,\mathbb{X}(s)\,]\!]$, are **not bounded**.

Hence

$$(51)\qquad \begin{cases} \pi(\{\mathbb{D}(s)\}) = +\infty \\ \qquad \text{if } \dfrac{\mathrm{d}}{\mathrm{d}s}\underline{\hat{U}}(s) - \underline{\hat{\Omega}}(s) \wedge \underline{t}(s) \neq 0 \text{ or } \dfrac{\mathrm{d}\underline{\hat{\Omega}}(s)}{\mathrm{d}s} \wedge \underline{e}_z \neq 0 \\ \pi(\{\mathbb{D}(s)\}) = \sup\{\, m^-\hat{\chi}(s),\ m^+\hat{\chi}(s)\} \\ \qquad \text{if } \dfrac{\mathrm{d}}{\mathrm{d}s}\underline{\hat{U}}(s) - \underline{\hat{\Omega}}(s) \wedge \underline{t}(s) = 0 \text{ and } \dfrac{\mathrm{d}\underline{\hat{\Omega}}(s)}{\mathrm{d}s} = \hat{\chi}(s)\,\underline{e}_z \end{cases}$$

and

$$(52)\qquad \begin{cases} \pi([\![\,\{\hat{\mathbb{U}}(s)\}\,]\!]) = +\infty \\ \qquad \text{if } [\![\,\underline{\hat{U}}(s)\,]\!] \neq 0 \text{ or } [\![\,\underline{\hat{\Omega}}(s)\,]\!] \wedge \underline{e}_z \neq 0 \\ \pi([\![\,\{\hat{\mathbb{U}}(s)\}\,]\!]) = \sup\{\, m^-\hat{\theta}(s),\ m\hat{\theta}^+(s)\} \\ \qquad \text{if } [\![\,\underline{\hat{U}}(s)\,]\!] = 0 \text{ and } [\![\,\underline{\hat{\Omega}}(s)\,]\!] = \hat{\theta}(s)\,\underline{e}_z\,. \end{cases}$$

Practically, for such problems, this implies that kinematically admissible plane virtual motions in Oxy must satisfy the Navier-Bernoulli condition with zero virtual rate of stretch to be relevant.

Bending moment and axial load

The same case as above is now considered, taking into account the normal force in the strength criterion. The interaction formulae vary according to the shape and to the nature of the cross section of the original three-dimensional beam which is modelled as a one-dimensional medium.

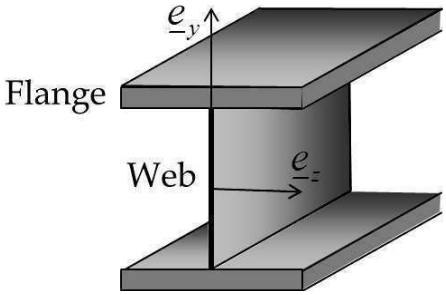

Figure 9. Ideal **I**-shaped section with vanishing web

As a **first example**, for a homogeneous ideal **I**-shaped section with vanishing web (Figure 9), the following interaction formula may be adopted

$$(53)\qquad [\![\,\mathbb{X}(s)\,]\!] \in G(s) \Leftrightarrow \left|\frac{M_z(s)}{m}\right| + \left|\frac{N(s)}{N_0}\right| - 1 \leq 0.$$

Hence, for the maximum resisting work

$$(54)\qquad \begin{cases} \pi(\{\mathbb{D}(s)\}) = +\infty \\ \qquad \text{if } \left(\dfrac{\mathrm{d}}{\mathrm{d}s}\underline{\hat{U}}(s) - \underline{\hat{\Omega}}(s)\wedge\underline{t}(s)\right)\wedge\underline{t}(s) \neq 0 \text{ or } \dfrac{\mathrm{d}\underline{\hat{\Omega}}(s)}{\mathrm{d}s}\wedge\underline{e}_z \neq 0 \\ \pi(\{\mathbb{D}(s)\}) = \sup\left\{ N_0\left|\hat{D}(s)\right|, m\left|\hat{\chi}(s)\right|\right\} \\ \qquad \text{if } \left(\dfrac{\mathrm{d}}{\mathrm{d}s}\underline{\hat{U}}(s) - \underline{\hat{\Omega}}(s)\wedge\underline{t}(s)\right)\wedge\underline{t}(s) = 0 \text{ and } \dfrac{\mathrm{d}\underline{\hat{\Omega}}(s)}{\mathrm{d}s} = \hat{\chi}(s)\,\underline{e}_z \end{cases}$$

and

$$(55)\qquad \begin{cases} \pi([\![\{\hat{\mathbb{U}}(s)\}]\!]) = +\infty \\ \qquad \text{if } [\![\underline{\hat{U}}(s)]\!]\wedge\underline{t}(s) \neq 0 \text{ or } [\![\underline{\hat{\Omega}}(s)]\!]\wedge\underline{e}_z \neq 0 \\ \pi([\![\{\hat{\mathbb{U}}(s)\}]\!]) = \sup\left\{ N_0\left|[\![\hat{U}(s)]\!]\right|, m\left|\hat{\theta}(s)\right|\right\} \\ \qquad \text{if } [\![\underline{\hat{U}}(s)]\!] = [\![\hat{U}(s)]\!]\,\underline{t}(s) \text{ and } [\![\underline{\hat{\Omega}}(s)]\!] = \hat{\theta}(s)\,\underline{e}_z . \end{cases}$$

As a consequence, kinematically admissible plane virtual motions in Oxy in order to be relevant, must satisfy the Navier-Bernoulli condition without any condition on the virtual rate of stretch.

As a **second example** we consider a rectangular cross section for which the following interaction formula is obtained when the constituent material is homogeneous and exhibits the same resistance in tension and compression

$$(56)\qquad [\,\mathbb{X}(s)\,]\in G(s) \Leftrightarrow \left|\frac{M_z(s)}{m}\right| + \left(\frac{N(s)}{N_0}\right)^2 - 1 \leq 0 .$$

The relevance conditions are the same as in Eqs (54)-(55) and the maximum resisting work is written

$$(57)\qquad \begin{cases} \pi(\{\mathbb{D}(s)\}) = \dfrac{4(m\hat{\chi})^2 + (N_0\hat{D})^2}{4\left|m\hat{\chi}\right|} \quad \text{if} \quad \left|\dfrac{N_0\hat{D}}{2m\hat{\chi}}\right| \leq 1 \\ \pi(\{\mathbb{D}(s)\}) = N_0\left|\hat{D}\right| \quad \text{if} \quad \left|\dfrac{N_0\hat{D}}{2m\hat{\chi}}\right| \geq 1 \end{cases}$$

$$(58)\qquad \begin{cases} \pi([\![\{\hat{\mathbb{U}}(s)\}]\!]) = \dfrac{4(m\hat{\theta})^2 + (N_0[\![\hat{U}]\!])^2}{4\left|m\hat{\theta}\right|} \quad \text{if} \quad \left|\dfrac{N_0[\![\hat{U}]\!]}{2m\hat{\theta}}\right| \leq 1 \\ \pi([\![\{\hat{\mathbb{U}}(s)\}]\!]) = N_0[\![\hat{U}]\!] \quad \text{if} \quad \left|\dfrac{N_0[\![\hat{U}]\!]}{2m\hat{\theta}}\right| \geq 1. \end{cases}$$

3.2 Assembly joints

Rigid joint (Figure 10)

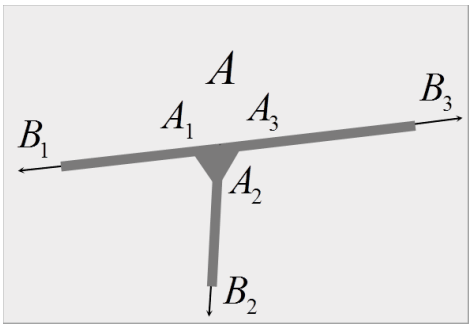

Figure 10. Rigid joint

When a member is connected to a rigid joint, no limitation is imposed to $\left[\mathbb{X}(s_{A_i}) \right]$ through Eq. (36). Hence, with the definition (41) for $[\![\{ \hat{\mathbb{U}}(A_i) \}]\!]$, we have for the maximum resisting work

(59) $$\pi_{A_i}([\![\{ \hat{\mathbb{U}}(A_i) \}]\!]) = +\infty .$$

Ball and socket joint

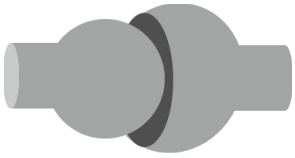

Figure 11. Ball and socket joint

This three-dimensional joint (Figure 11) requires the component $\underline{\Gamma}(s_{A_i})$ of $\left[\mathbb{X}(s_{A_i}) \right]$ to be equal to zero and does not impose any limitation on $\underline{\mathcal{X}}(s_{A_i})$

(60) $$\left[\mathbb{X}(s_{A_i}) \right] \in \mathcal{G}_{A_i} \Leftrightarrow \underline{\Gamma}(s_{A_i}) = 0 ,$$

from which we derive

(61) $$\begin{cases} \pi_{A_i}([\![\{ \hat{\mathbb{U}}(A_i) \}]\!]) = +\infty \ \text{ if } \ [\![\underline{\hat{U}}(A_i)]\!] \neq 0 \\ \pi_{A_i}([\![\{ \hat{\mathbb{U}}(A_i) \}]\!]) = 0 \ \text{ if } \ [\![\underline{\hat{U}}(A_i)]\!] = 0 . \end{cases}$$

The relevant virtual motions allow any virtual rotation jump between the member and the joint and no virtual velocity jump.

In addition to Eq. (60) a limitation may be set on $\underline{\mathcal{X}}(s_{A_i})$, with the corresponding changes on the relevance conditions and the expression of the maximum resisting work.

Pinned joint or axial joint (Figure 12)

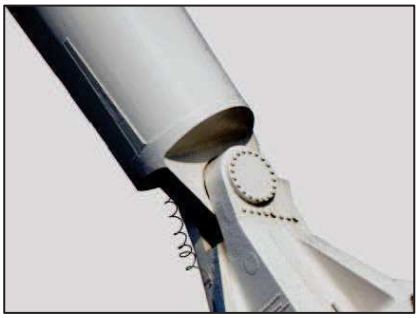

Figure 12. Pinned joint (*London Eye*. © Jean Salençon)

For a pinned joint parallel to $\underline{e}_z$ the strength criterion is less restrictive than Eq. (60) since it only concerns the component of $\underline{\Gamma}(s_{A_i})$ along $\underline{e}_z$

$$\left[\mathbb{X}(s_{A_i})\right] \in \mathcal{G}_{A_i} \Leftrightarrow \underline{\Gamma}(s_{A_i}).\underline{e}_z = 0 ; \tag{62}$$

therefore

$$\begin{cases} \pi_{A_i}([\![\left\{\hat{\mathbb{U}}(A_i)\right\}]\!]) = +\infty \ \text{ if } \ [\![\underline{\hat{U}}(A_i)]\!] \neq 0 \text{ or } [\![\underline{\hat{\Omega}}(A_i)]\!] \wedge \underline{e}_z \neq 0 \\ \pi_{A_i}([\![\left\{\hat{\mathbb{U}}(A_i)\right\}]\!]) = 0 \ \text{ if } \ [\![\underline{\hat{U}}(A_i)]\!] = 0 \text{ and } [\![\underline{\hat{\Omega}}(A_i)]\!] = \hat{\theta}(A_i)\underline{e}_z. \end{cases} \tag{63}$$

The relevant virtual motions allow any virtual rotation jump parallel to the axis of the joint and no virtual velocity jump.

In the same way as for the previous joint, in addition to Eq. (62) a limitation may also be set on $\underline{\mathcal{X}}(s_{A_i})$.

Other types of joints

More sophisticated strength criteria for the joints can be treated in the same way as above, such as a non-symmetric pinned joint where

$$\left[\mathbb{X}(s_{A_i})\right] \in \mathcal{G}_{A_i} \Leftrightarrow \gamma^- \leq \underline{\Gamma}(s_{A_i}).\underline{e}_z \leq 0 \tag{64}$$

and therefore

$$\begin{cases} \pi_{A_i}([\![\left\{\hat{\mathbb{U}}(A_i)\right\}]\!]) = +\infty \ \text{ if } \ [\![\underline{\hat{U}}(A_i)]\!] \neq 0 \text{ or } [\![\underline{\hat{\Omega}}(A_i)]\!] \wedge \underline{e}_z \neq 0 \\ \pi_{A_i}([\![\left\{\hat{\mathbb{U}}(A_i)\right\}]\!]) = \sup\left\{\gamma^- \hat{\theta}(A_i), 0\right\} \ \text{ if } \ [\![\underline{\hat{U}}(A_i)]\!] = 0 \text{ and } [\![\underline{\hat{\Omega}}(A_i)]\!] = \hat{\theta}(A_i)\underline{e}_z. \end{cases} \tag{65}$$

It is also recalled that the strength criterion at a given joint may differ from one connected member to the other.

3.3 Structural supports

The strength conditions for the supports concern the endpoints where the structure is connected to the external world. Following the procedure exposed in § 2.1 and sketched in Figure 7 a structural support is only concerned with two elements: the external world on the one side, which will be conventionally considered as the upstream side, and the corresponding endpoint of the structure on the other, considered as the downstream side[3].

Fixed bilateral structural supports

Fixed rigid (or built-in), ball and socket, or axial supports (Figure 13) are governed by the same strength conditions on $\left[\mathbb{X}(s_A)\right]$ and the same expressions for the maximum resisting work densities on $\left\{\hat{\mathbb{U}}(s_A)\right\}$ as their counterpart assembly joints (Eqs (60) to (65)).

Figure 13. Fixed built-in and axial structural supports

Movable bilateral supports

A movable bilateral support such as the axial support in Figure 14 differs from the corresponding fixed one by setting bounds to the horizontal component of $\left[\mathbb{X}(s_A)\right]$. The strength condition is written

$$\left[\mathbb{X}(s_A)\right] \in \mathcal{G}_A \Leftrightarrow \begin{cases} \underline{\Gamma}(s_A).\underline{e}_z = 0 \\ L^- \le \underline{\mathcal{X}}(s_A).\underline{e}_x \le L^+ \end{cases} \tag{66}$$

with L^+ and L^- the algebraic values of the limits set to the horizontal component of $\left[\mathbb{X}(s_A)\right]$.

The maximum resisting work density is

$$\begin{cases} \pi_A(\left\{\hat{\mathbb{U}}(s_A)\right\}) = +\infty \\ \qquad\qquad \text{if } \underline{\hat{U}}(s_A) \wedge \underline{e}_x \neq 0 \text{ or } \underline{\hat{\Omega}}(s_A) \wedge \underline{e}_z \neq 0 \\ \pi_A(\left\{\hat{\mathbb{U}}(s_A)\right\}) = \sup\left\{ L^- \hat{U}_x(s_A), L^+ \hat{U}_x(s_A) \right\} \\ \qquad\qquad \text{if } \underline{\hat{U}}(s_A) = \hat{U}_x(s_A)\,\underline{e}_x \text{ and } \underline{\hat{\Omega}}(s_A) = \hat{\theta}(s_A)\,\underline{e}_z. \end{cases} \tag{67}$$

[3] The opposite convention may obviously be adopted.

Figure 14. Movable pinned support and fixed unilateral support

Unilateral structural supports

Within the framework of the Yield Design theory, unilateral supports are just particular cases of movable structural supports with a unilateral mathematical constraint on $\left[\,\mathbb{X}(s_A)\,\right]$.

For instance, Figure 14 presents a fixed unilateral support such that

$$\left[\,\mathbb{X}(s_A)\,\right] \in \mathcal{G}_A \Leftrightarrow \underline{\mathcal{X}}(s_A).\underline{e}_y \le 0 \text{ and } \underline{\Gamma}(s_A) = 0. \tag{68}$$

Hence

$$\begin{cases} \pi_A(\{\hat{\mathbb{U}}(s_A)\}) = +\infty \text{ if } \underline{\hat{U}}(s_A).\underline{e}_y < 0 \\ \pi_A(\{\hat{\mathbb{U}}(s_A)\}) = 0 \text{ if } \underline{\hat{U}}(s_A).\underline{e}_y \ge 0. \end{cases} \tag{69}$$

4 Final comments

The Yield Design approach within the one-dimensional continuum framework is currently applied to the analysis of frames and trusses. Many theoretical works (*e.g.* [2-15]) have been devoted to such applications from the numerical point of view in relation with linear programming and convex programming, applying the duality and Kuhn-Tucker theorems. The principal goal was to increase the efficiency of the algorithms for the minimisation process in the kinematic exterior approach and in the dualised implementation of a genuine static interior approach [16].

The approach is convenient for the Yield Design analysis of beams and arches with the introduction of the appropriate interaction formulae according to the constituent material (homogeneous or non-homogeneous; steel, reinforced or pre-stressed concrete, etc.) and depending on the cross section shape (**I**-shaped section, solid-webbed girder, box girder, etc.)

The one-dimensional curvilinear model is also the basis for crude and simplified Yield Design analyses of masonry vaults or arches as sketched in Figure 15. The problem is two-dimensional. Along the director curve drawn through the voussoirs, the strength criterion of the constituent stone material must be satisfied, often in the form of a limitation on the compressive normal force:

$$-N_0 \le \underline{N}(s) \le 0\,, \tag{70}$$

with the corresponding maximum resisting work

$$\pi\left(\{\hat{\mathbb{U}}(s)\}\right) = \sup\left\{-N_0\,\hat{D}(s), 0\right\}. \tag{71}$$

The strength criterion of the joints between the voussoirs, applies only to the points of the director curve where the joints are located and takes the form of a Coulomb friction condition on the components of $\underline{\mathcal{X}}(s)$ together with the bending moment M_z being restricted to zero.

Let $\underline{e}_X(s)$ be the unit vector normal to the joint and $\underline{e}_Y(s)$ the tangent to the joint in the plane of the director curve, the strength criterion of the joint is the counterpart of Eq. (IV, 31)

$$f([\![\,\mathbb{X}(s)\,]\!]) \le 0 \Leftrightarrow \left|\,\underline{\mathcal{X}}(s).\underline{e}_Y(s)\,\right| + \underline{\mathcal{X}}(s).\underline{e}_X(s)\tan\phi_j \le 0 \tag{72}$$

and the maximum resisting work to be implemented in the kinematic exterior approach at the specific points where the joints are located is the counterpart of Eq. (V, 40)

$$\begin{cases} \pi([\![\{\hat{\mathbb{U}}(s)\}]\!]) = +\infty \ \text{ if } \ [\![\,\hat{\underline{U}}(s)\,]\!].\underline{e}_X(s) < \left|\,[\![\,\hat{\underline{U}}(s)\,]\!].\underline{e}_Y(s)\,\right|\tan\phi_j \\ \pi([\![\{\hat{\mathbb{U}}(s)\}]\!]) = 0 \ \text{ if } \ [\![\,\hat{\underline{U}}(s)\,]\!].\underline{e}_X(s) \ge \left|\,[\![\,\hat{\underline{U}}(s)\,]\!].\underline{e}_Y(s)\,\right|\tan\phi_j . \end{cases} \tag{73}$$

Quite often, the director curve turns out to be orthogonal to the joints, $\underline{e}_X(s) = \underline{t}(s)$, so that Eq. (72) is concerned with the normal force $N(s)$ and the shearing force $V(s)$.

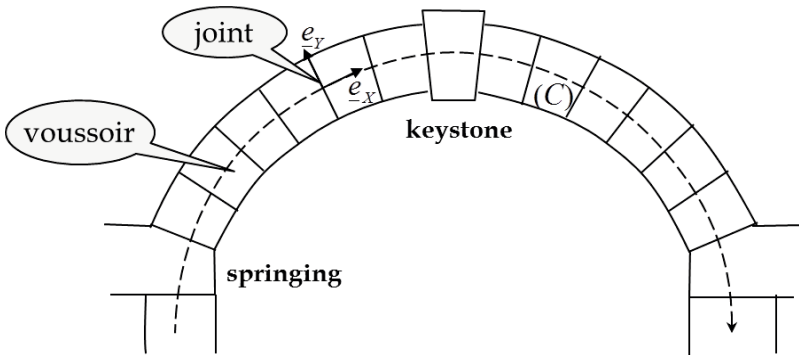

Figure 15. A masonry vault

Detailed reviews of the methods for the stability analysis of masonry vaults will be found for instance in the comprehensive surveys by Heyman and Benvenuto and in historical references (*cf.* [17-31]).

REFERENCES

[1] SALENÇON, J. (2001) – *Handbook of Continuum Mechanics*. Springer-Verlag, Berlin, Heidelberg, New York.

[2] CHARNES, A. & GREENBERG, H. J. (1951) – Plastic collapse and linear programming. *Bulletin of the American Mathematical Society*, **57**, 480.

[3] NEAL, B. G. & SYMONDS, P. S. (1950-51) – The calculation of collapse loads for framed structures. *Journal of the Institution of Civil Engineers*, **35**, 21.

[4] ENGLISH, J. M. (1954) – Design of frames by relaxation of yield hinges. *Transactions of the American Society of Civil Engineers*, **119**, 1143.

[5] HORNE, M. R. (1954) – A moment distribution method for the analysis and design of structures by the plastic theory. *Proceedings of the Institution of Civil Engineers*, **3**, (part 3), 51.

[6] DORN, W. S. & GREENBERG, H. J. (1957) – Linear programming & plastic limit analysis of structures. *Quarterly of Applied Mathematics*, **15**, 155.

[7] HEYMAN, J. (1957) – *Plastic design of portal frames*. Cambridge University Press.

[8] HEYMAN, J. (1959) – Automatic analysis of steel framed structures under fixed and varying loads. *Proceedings of the Institution of Civil Engineers*,**12**, 39.

[9] CHARNES, A., LEMKE, C. E. & ZIENKIEWICZ, O. C. (1959) – virtual work, linear programming and plastic limit analysis. *Proceedings of the Royal Society*, **A**, **251**, 110-116.

[10] HOSKIN, B. C. (1960) – *Limit analysis, limit design and linear programming*. Aeronautical Research Laboratories, Melbourne, Report ARL/SM.274.

[11] CERADINI, G. & GAVARINI, C. (1965) – Calcolo a rottura e programmazione lineare. *Giornale Genio Civile*, **1-2**, 48-64.

[12] GAVARINI, C. (1966) – I teoremi fondamentali del calcolo a rottura e la dualita in programmazione lineare. *Ingegneria Civile*, **18**, 48-64.

[13] GAVARINI, C. (1966) – Plastic analysis of structures and duality in linear programming. *Meccanica*, **1**, 3-4, 95-97.

[14] GAVARINI, C. (1968) – Calcolo a rottura e programmazione non-lineare. *Rendiconti Istituto Lombardo di Scienze e Lettere*, **A**, **102**, 329-342.

[15] MUNRO, J. & SMITH, D. L. (1972) – Linear programming duality in plastic analysis and synthesis. *Proceedings International Symposium on Computer-aided Structural Design*, vol. 1, Warwick Univ.

[16] CROC, M., MICHEL, G. & SALENÇON, J (1971) – Application de la programmation mathématique au calcul à la rupture des structures. *International Journal of Solids and Structures,* **7**, 10, 1317-1332.

[17] COULOMB, C.-A. (1773) – *Essai sur une application des règles de* Maximis *et* Minimis *à quelques problèmes de statique relatifs à l'architecture.* Mémoire présenté à l'Académie Royale des sciences, Paris, **VII**, pp. 343-382.

[18] MÉRY, E. (1840) – Équilibre des voutes en berceau. *Annales des ponts et chaussées,* **I**, 50-70.

[19] DURAND-CLAYE, A. (1867) – Stabilité des voûtes en maçonnerie. *Annales des ponts et chaussées,***I**, 63-96.

[20] DURAND-CLAYE, A. (1880) – Stabilité des voûtes et des arcs. *Annales des ponts et chaussées,* **I**, 416-440.

[21] HEYMAN, J. (1966) – The stone skeleton. *International Journal of Solids and Structures,* **2**, 2, 249-279.

[22] HEYMAN, J. (1969) – The safety of masonry arches. *International Journal of Mechanical Sciences*, **11**, 363-385.

[23] HEYMAN, J. (1972) – *Coulomb's Memoir on Statics: an Essay in the History of Civil Engineering*. Cambridge (UK)

[24] HEYMAN, J. (1980) – The estimation of the strength of masonry arches. *Proceedings A.S.C.E.*, Part 2, **69**, 921-937.

[25] HEYMAN, J. (1982) – *The Masonry Arch.* Ellis Horwood Ltd, John Wiley, Chichester (UK).

[26] HEYMAN, J. (1998) – *Structural Analysis*. 3rd ed., Prentice Hall, Upper Saddle River, N.J.

[27] BENVENUTO, E. (1981) – *La scienza delle costruzioni e il suo sviluppo storico*. Edizione Sansoni, Florence.

[28] BENVENUTO, E. (1991) – *An introduction to the History of Structural mechanics*. *Part II: Vaulted Structures and Elastic Systems*. Springer-Verlag.

[29] DELBECQ, J.-M. (1981) – Analyse de la stabilité des voûtes en maçonnerie de Charles-Augustin Coulomb à nos jours. *Annales des ponts et chaussées,* **19**, 36-43.

[30] DELBECQ, J.-M. (1982) – Analyse de la stabilité des voûtes en maçonnerie par le calcul à la rupture. *Journal de Mécanique Appliquée* **1**, 1, 91-121.

[31] ALTA, D., BARSOTTI, R. & BENNATTI, S. (2012) – Equilibrium of Pointed, Circular and Elliptical Masonry Arches Bearing Vertical Walls. *Journal of Structural Engineering*, *ASCE,* **118**, 7, 880-888, July 2012.

Chapter X

Yield Design of plates
The model

Modelling plates as two-dimensional continua

Dynamics

Theorem/Principle of virtual work

Plate model derived from the three-dimensional continuum

References

YIELD DESIGN of PLATES
The model

Yield Design analysis of thin plane structural elements (plates, thin slabs…) subjected to bending is performed on a two-dimensional mechanical model built upon a director sheet with the adjunction of a transverse microstructure. The kinematics is defined by velocity distributor fields which describe the rigid body motion of the microstructure attached at any point of the sheet. The external forces are described by wrench fields of distributed forces and moments. The internal forces are represented by the symmetric two-dimensional tensor of membrane forces, with the corresponding in-plane Equilibrium equations, and the two-dimensional shear force vector field and internal moment tensor field, with the out-of-plane Equilibrium equations.

1 Modelling plates as two-dimensional continua

1.1 Geometric description of the model

The two-dimensional modelling of plates (and thin slabs) proceeds from the specificity of the geometric characteristics of these structural elements which are plane and slender. The model is described as a two-dimensional continuum built on a **plane director sheet** (D) in the $\mathbb{R}^3$ Euclidean geometric space [1].

A system S is described geometrically on a surface S of the director sheet (D) and it is modelled as a set of **particles.** In a similar way as in Chapter IX, since the model stands as the result of the smashing onto the director sheet (D) of the three-dimensional plate or slab, a particle P is now described as a "diluted material point" with surface $\mathrm{d}S$ and the adjunction of a **transverse microstructure**. In a general approach, this microstructure stands for the volume element orthogonal to (D) at the point P: it is represented, in the reference configuration, by a segment of a line orthogonal to (D) at the point P (Figure 1).

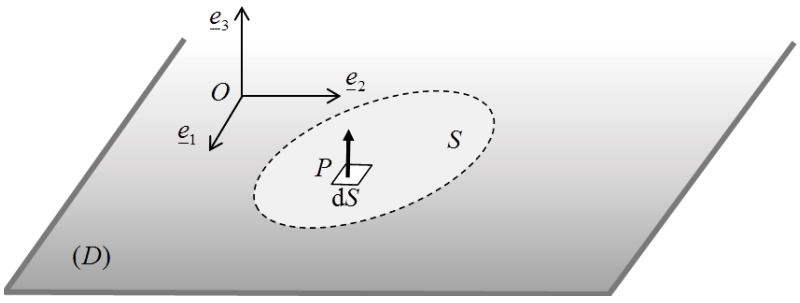

Figure 1. The particle at point P with its associated microstructure

From the comparison of these introductory words with § 1.1 in Chapter IX it can be anticipated that some aspects of this two-dimensional model will be similar to the one-dimensional model studied before, with the important difference that ordinary differential equations along the director curve will now be replaced by partial differential equations in the director sheet. This will require the introduction of tensor quantities and, from this latter point of view, similarities with the classical three-dimensional continuum model will also be encountered but with some new technicalities which may seem somewhat cumbersome at a first glance.

1.2 Kinematics

The velocity field

Let the position of the geometrical point P in the director sheet (D) be denoted $\underline{OP} = \underline{s} = x_i \, \underline{e}_i$, $i = 1,2$ where $(O, \underline{e}_1, \underline{e}_2)$ is the right-handed basis of an orthogonal Cartesian coordinate system in (D) with $\underline{e}_3$ the unit vector orthogonal to (D). The particle at the point P is geometrically characterised by its position $\underline{s}$ in (D) and by the orientation of the transverse microstructure.

From the geometric point of view, the evolution of the system at a given instant of time t is described by the movement of the particles: it is defined by the velocity of the generic point P in (D) denoted $\underline{U}(\underline{s})$ and the angular velocity of the associated microstructure denoted $\underline{\Omega}(\underline{s})$, given for all the particles in S.

The **movement of the particle** P in the two-dimensional model is the rigid body motion defined in $\mathbb{R}^3$ by the two vectors $\underline{U}(\underline{s})$ and $\underline{\Omega}(\underline{s})$ attached to the particle, with the general expression of the corresponding velocity field in $\mathbb{R}^3$

(1) $$\forall M \in \mathbb{R}^3, \; \underline{U}(M) = \underline{U}(\underline{s}) + \underline{\Omega}(\underline{s}) \wedge \underline{PM}.$$

It is generated by the **velocity distributor** $\{\mathbb{U}(\underline{s})\}$ as defined in Chapter IX (§ 1.2)

(2) $$\{\mathbb{U}(\underline{s})\} = \{ P, \underline{U}(\underline{s}), \underline{\Omega}(\underline{s}) \}.$$

Continuity of the medium implies that the fields $\underline{U}(\underline{s})$ and $\underline{\Omega}(\underline{s})$ are piecewise **continuous and continuously differentiable** in S.

The system is deformed when the rigid body motion of the particles varies over S. Comparing the velocity fields attached to two adjacent particles P and $P + \underline{\mathrm{d}s}$ in S we get

(3) $$\forall M \in \mathbb{R}^3, \; \mathrm{d}\underline{U}(M) = \underline{\underline{\partial U}}(\underline{s}) . \underline{\mathrm{d}s} - \underline{\Omega}(\underline{s}) \wedge \underline{\mathrm{d}s} + \left(\underline{\underline{\partial \Omega}}(\underline{s}) . \underline{\mathrm{d}s} \right) \wedge \underline{PM}$$

where **the point** M **is fixed**, and $\underline{\underline{\partial U}}(\underline{s})$ and $\underline{\underline{\partial \Omega}}(\underline{s})$ denote the gradients of the corresponding fields with respect to (x_1, x_2) in (D). These Euclidean tensors are elements of $\mathbb{R}^3 \otimes \mathbb{R}^2$, which means that they transform a vector in (D) into a vector in $\mathbb{R}^3$.

In consideration of the specific role played by the third dimension in the model it is convenient to split the fields $\underline{U}(\underline{s})$ and $\underline{\Omega}(\underline{s})$ as follows

$$(4)\qquad \begin{cases} \underline{U}(\underline{s}) = \underline{u}(\underline{s}) + w(\underline{s})\,\underline{e}_3 & \underline{u}(\underline{s}) \in (D),\ w(\underline{s}) \in \mathbb{R} \\ \underline{\Omega}(\underline{s}) = \underline{\omega}(\underline{s}) + \Omega_3(\underline{s})\,\underline{e}_3 & \underline{\omega}(\underline{s}) \in (D),\ \Omega_3(\underline{s}) \in \mathbb{R}. \end{cases}$$

Hence the gradients

$$(5)\qquad \begin{cases} \underline{\underline{\partial U}}(\underline{s}) = \underline{\underline{\partial u}}(\underline{s}) + \underline{e}_3 \otimes \underline{\partial w}(\underline{s}) & \underline{\underline{\partial u}}(\underline{s}) \in \mathbb{R}^2 \otimes \mathbb{R}^2 \\ \underline{\underline{\partial \Omega}}(\underline{s}) = \underline{\underline{\partial \omega}}(\underline{s}) + \underline{e}_3 \otimes \underline{\partial \Omega_3}(\underline{s}) & \underline{\underline{\partial \omega}}(\underline{s}) \in \mathbb{R}^2 \otimes \mathbb{R}^2. \end{cases}$$

In order to make the presentation simpler we shall restrict the two-dimensional modelling of plates to what is necessary and sufficient for the classical Yield Design analysis of plates subjected to bending. Thence, although the in-plane component $\underline{u}(\underline{s})$ of $\underline{U}(\underline{s})$ will be retained essentially for pedagogical reasons, the transverse component $\Omega_3(\underline{s})\,\underline{e}_3$ of $\underline{\Omega}(\underline{s})$ will be set to zero identically. This means that the strain rate exhibits no torsional component[1].

It follows that Eq. (3) takes the reduced form

$$(6)\qquad \forall M \in \mathbb{R}^3,\ \mathrm{d}\underline{U}(M) = \left(\underline{\underline{\partial u}}(\underline{s}) + \underline{e}_3 \otimes \underline{\partial w}(\underline{s})\right).\mathrm{d}\underline{s} - \underline{\omega}(\underline{s}) \wedge \mathrm{d}\underline{s} + \left(\underline{\underline{\partial \omega}}(\underline{s}).\mathrm{d}\underline{s}\right) \wedge \underline{PM}$$

showing that the rigid body motion of the particle $P + \mathrm{d}\underline{s}$ with respect to the particle P is defined by the translation with vector

$$(7)\qquad \left(\underline{\underline{\partial u}}(\underline{s}) + \underline{e}_3 \otimes \underline{\partial w}(\underline{s})\right).\mathrm{d}\underline{s} - \underline{\omega}(\underline{s}) \wedge \mathrm{d}\underline{s}$$

and the rotation

$$(8)\qquad \underline{\underline{\partial \omega}}(\underline{s}).\mathrm{d}\underline{s}.$$

The term $\underline{\underline{\partial u}}(\underline{s}).\mathrm{d}\underline{s}$ in Eq.(7) is just the two-dimensional counterpart of the term $\underline{\underline{\mathrm{grad}\,U}}.\mathrm{d}\underline{M}$ in Eq. (III, 5). The symmetric part of $\underline{\underline{\partial u}}(\underline{s})$ is the strain rate tensor of a classical two-dimensional continuum defined on (D).

As for the complement, $\underline{e}_3 \otimes \underline{\partial w}(\underline{s}).\mathrm{d}\underline{s} - \underline{\omega}(\underline{s}) \wedge \mathrm{d}\underline{s}$, we observe that since both terms are oriented along $\underline{e}_3$ Eq. (7) may also be written

$$(9)\qquad \underline{\underline{\partial u}}(\underline{s}).\mathrm{d}\underline{s} + \underline{e}_3 \otimes \left(\underline{\partial w}(\underline{s}) - \underline{e}_3 \wedge \underline{\omega}(\underline{s})\right).\mathrm{d}\underline{s}.$$

This equation recalls Eq. (IX, 9). Its second term is related to the rate of angular distortion of the microstructure with respect to the director sheet: the rotation rate of the normal to the director sheet at the point P is $-\underline{e}_3 \wedge \underline{\partial w}(\underline{s})$ while the rotation rate of the microstructure is just $\underline{\omega}(\underline{s})$. These two rotation rates are independent from each other as they proceed from $w(\underline{s})$ and $\underline{\omega}(\underline{s})$ respectively.

---

[1] A general presentation retaining the transverse component Ω_3 , although heavier, can be carried out up to the implementation of the Yield Design theory; then, assuming infinite resistance to torsion results in the $\hat{\Omega}_3$ component of the relevant virtual motions to be identically equal to zero.

Note that, in the particular case when the condition

$$\underline{\partial w}(\underline{s}) - \underline{e}_3 \wedge \underline{\omega}(\underline{s}) = 0, \tag{10}$$

which is known as the **Kirchhoff-Love condition,** is imposed to the model as an **internal constraint** it implies that the microstructure remains orthogonal to the director sheet (D) in the evolution of the system[2].

Finally, for the general model considered here, we write the gradient of the rigid body velocity field

$$\forall M \in \mathbb{R}^3,\ \underline{\underline{\partial U}}(M) = \underline{\underline{\partial u}}(\underline{s}) + \underline{e}_3 \otimes \left(\underline{\partial w}(\underline{s}) - \underline{e}_3 \wedge \underline{\omega}(\underline{s})\right) + \underline{\underline{\partial \omega}}(\underline{s}) \wedge \underline{PM}. \tag{11}$$

It defines the gradient of the velocity distributor (2) as the **tensorial distributor**

$$\partial\left\{\mathbb{U}(\underline{s})\right\} = \left\{ P,\ \underline{\underline{\partial u}}(\underline{s}) + \underline{e}_3 \otimes \left(\underline{\partial w}(\underline{s}) - \underline{e}_3 \wedge \underline{\omega}(\underline{s})\right),\ \underline{\underline{\partial \omega}}(\underline{s}) \right\}. \tag{12}$$

2 Dynamics

2.1 External forces

External forces are applied to a system $\mathcal{S}$ on the surface S and at the boundary denoted ∂S.

Surface forces

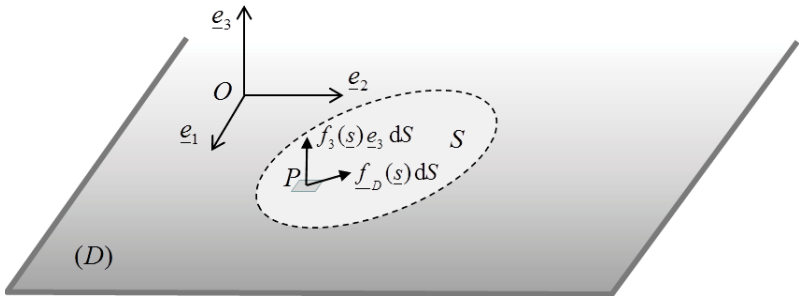

Figure 2. Distributed forces acting on the system

Surface forces are modelled by

- A surface density $\underline{f}(\underline{s})$ corresponding to the distributed external forces acting on S (Figure 2).
- This surface density can be split into its normal and tangential (in-plane) components with respect to (D). The infinitesimal distributed force is $\underline{f}(\underline{s})\,\mathrm{d}S$

$$\begin{cases} \underline{f}(\underline{s}) = \underline{f}_D(\underline{s}) + f_3(\underline{s})\underline{e}_3 \\ \underline{f}_D(\underline{s}) = f_1(\underline{s})\underline{e}_1 + f_2(\underline{s})\underline{e}_2 . \end{cases} \tag{13}$$

- Occasionally, an external moment surface density $\underline{h}_D(\underline{s})$, parallel to (D) will be considered.

[2] Note the similarity with the Navier-Bernoulli condition, Eqs (IX. 11, 12).

- Line densities of in-plane and out-of-plane external forces $\underline{\phi}_D(\underline{s})$ and $\phi_3(\underline{s})\underline{e}_3$, or external moments $\underline{\Gamma}_D(\underline{s})$ parallel to (D), will also be introduced[3].
- Concentrated external forces or concentrated external moments parallel to (D) will only be treated as limit cases of high surface densities on concentrated areas.

Boundary forces

Boundary forces are modelled by (Figure 3)

- A line density of force on ∂S: on the element $\mathrm{d}\ell$ with outward normal $\underline{n}(\underline{s})$ such that the distributed force is

(14) $$\underline{T}(\underline{s})\,\mathrm{d}\ell + R(\underline{s})\,\underline{e}_3\,\mathrm{d}\ell$$

where $\underline{T}(\underline{s})\,\mathrm{d}\ell$ denotes the in-plane component.

- A line density of moment on ∂S, with no component along $\underline{e}_3$[4]: on the element $\mathrm{d}\ell$ the distributed moment lies in (D) and is equal to

(15) $$\underline{H}(\underline{s})\,\mathrm{d}\ell\,.$$

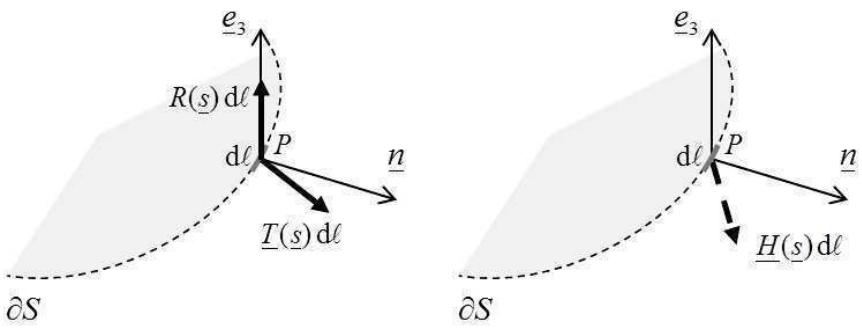

Figure 3. Boundary forces acting on the system

Note that, in order for the system to be in equilibrium, it is necessary that the external forces and moments comply with the global equilibrium equations in terms of resultant force and moment. It may be observed that all the distributed or concentrated external moments applied to the system are supposed to have no component along $\underline{e}_3$, consistently with the kinematic hypothesis.

2.2 Internal forces

It is assumed that the particles of the system $\mathcal{S}$ exert no action at a distance upon one another. At the point P, adjacent particles interact along an arc of a line $\mathrm{d}\ell$ with normal $\underline{n}(\underline{s})$ which defines the (+) and (-) sides as in Chapter III (§ 2.3). The **contact forces** exerted by the particle on the (+) side on the particle on the (-) side are proportional to $\mathrm{d}\ell$ and modelled as follows.

[3] Such forces may result from the connections of the system with other structural elements.
[4] No torsion of the modelled plate is assumed.

- A force proportional to $\mathrm{d}\ell$, with components $\underline{N}(\underline{s},\underline{n})\,\mathrm{d}\ell$ in the plane of (D) and $V(\underline{s},\underline{n})\,\mathrm{d}\ell$ along $\underline{e}_3$

(16) $$\underline{N}(\underline{s},\underline{n})\,\mathrm{d}\ell + V(\underline{s},\underline{n})\,\underline{e}_3\,\mathrm{d}\ell.$$

- A moment proportional to $\mathrm{d}\ell$ with no component along $\underline{e}_3$

(17) $$\underline{\Gamma}(\underline{s},\underline{n})\,\mathrm{d}\ell\,.$$

2.3 Equilibrium equations

Establishing the equilibrium equations for this model in the classical presentation refers to the same arguments as for the three-dimensional continuum model:

- The global equilibrium of a small triangle to prove the linear dependence on the orientation of the corresponding facet;
- The global equilibrium of a small parallelogram to establish the partial differential equations for the internal forces fields.

In-plane Equilibrium equations

Exactly as for the three-dimensional continuum, the global equilibrium of the forces applied to a small triangle in the plane of the director sheet (D) proves that $\underline{N}(\underline{s},\underline{n})$ is a linear function of $\underline{n}$ through a tensor $\underline{\underline{N}}(\underline{s})$

(18) $$\underline{N}(\underline{s},\underline{n}) = \underline{\underline{N}}(\underline{s}).\underline{n}.$$

Then the small parallelogram argument proves the symmetry of the second rank **membrane force** tensor $\underline{\underline{N}}(\underline{s})$ and yields the in-plane equilibrium equations

(19) $$\begin{cases} \underline{\underline{N}}(\underline{s}) = N_{ij}(\underline{s})\,\underline{e}_i \otimes \underline{e}_j \;\; i,j = 1,2 \\ N_{ij}(\underline{s}) = N_{ji}(\underline{s}) \\ \mathrm{div}\,\underline{\underline{N}}(\underline{s}) + \underline{f}_D(\underline{s}) = 0. \end{cases}$$

These in-plane equilibrium equations are completed by the boundary condition

(20) $$\underline{\underline{N}}(\underline{s}).\underline{n} = \underline{T}(\underline{s}).$$

In the case of a line density $\underline{\phi}_D(\underline{s})$ of in-plane external forces applied to the system along (L), the membrane force field is discontinuous when crossing (L) following its normal $\underline{n}$ and the corresponding jump equation is written

(21) $$[\![\underline{\underline{N}}(\underline{s})]\!].\underline{n}(\underline{s}) + \underline{\phi}_D(\underline{s}) = 0.$$

Eqs (19)-(21) provide the whole set of equations for the in-plane equilibrium of the model, which are independent of the out-of-plane problem to be examined now.

Out-of-plane Equilibrium equations

Shear forces

Global equilibrium[5] of the forces applied to a small triangle along $\underline{e}_3$ proves that the scalar $V(\underline{s},\underline{n})$ is a linear function of $\underline{n}$ through a vector $\underline{V}(\underline{s}) \in \mathbb{R}^2$

$$\begin{cases} \underline{V}(\underline{s}) = V_i(\underline{s})\,\underline{e}_i \;\; i=1,2 \\ V(\underline{s},\underline{n}) = \underline{V}(\underline{s}).\underline{n}. \end{cases} \tag{22}$$

The component $V_1(\underline{s})$ (resp. $V_2(\underline{s})$) of $\underline{V}(\underline{s})$ is the magnitude of the line density of shear force $V_1(\underline{s})\underline{e}_3$ on the facet with normal $\underline{e}_1$ (resp. $\underline{e}_2$) at point P. The vector $\underline{V}(\underline{s})$ is called the **shear force vector** although it is clear from Eq. (22) that it represents a **linear operator** and not a force (Figure 4).

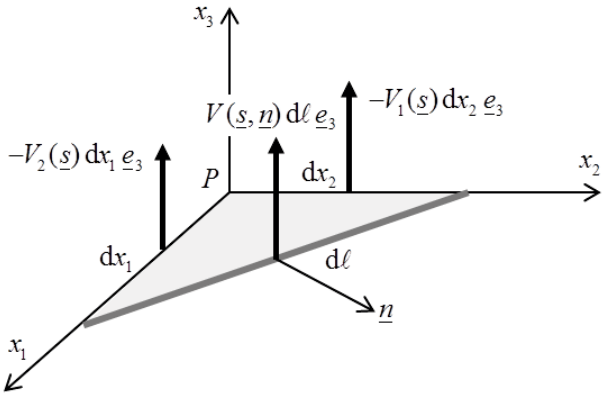

Figure 4. The small triangle argument applied to the shear forces

The global equilibrium of the forces applied to the small parallelogram along $\underline{e}_3$ (Figure 5) yields the partial derivative equation (23) for the shear force field

$$\mathrm{div}\,\underline{V}(\underline{s}) + f_3(\underline{s}) = 0\,. \tag{23}$$

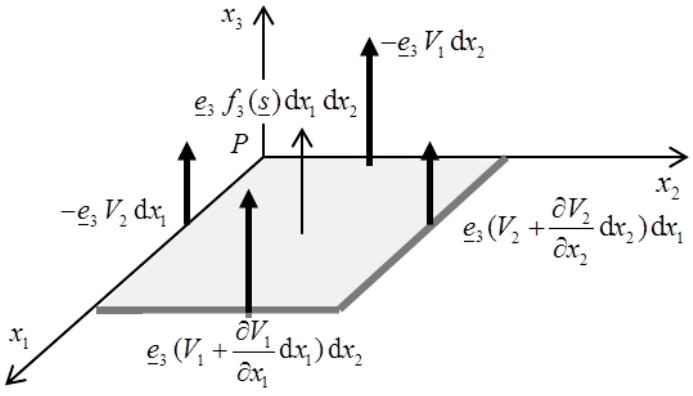

Figure 5. Global equilibrium of the small parallelogram along $\underline{e}_3$

[5] The contribution of the vertical component of the distributed forces is of second order.

The boundary condition for the shear force field follows from Eqs (14), (16) and (22). At the point P of ∂S with outward normal $\underline{n}(\underline{s})$

(24) $$\underline{V}(\underline{s}).\underline{n} = R(\underline{s}).$$

If a line density of vertical force $\phi_3(\underline{s})\underline{e}_3$ is applied along a line (L) in S, the shear force field is discontinuous and the jump equation when crossing this line following the normal $\underline{n}$ is:

(25) $$[\![\underline{V}(\underline{s})]\!].\underline{n}(\underline{s}) + \phi_3(\underline{s}) = 0\,.$$

Internal moments

In the same way as before, the global equilibrium of the moments applied to the small triangle proves that $\underline{\Gamma}(\underline{s},\underline{n})$ is a linear function of $\underline{n}$ through the second rank tensor $\underline{\underline{\Gamma}}(\underline{s}) \in \mathbb{R}^2 \otimes \mathbb{R}^2$ (Figure 6)

(26) $$\begin{cases} \underline{\underline{\Gamma}}(\underline{s}) = \Gamma_{ji}(\underline{s})\underline{e}_j \otimes \underline{e}_i \;\; i,j = 1,2 \\ \underline{\Gamma}(\underline{s},\underline{n}) = \underline{\underline{\Gamma}}(\underline{s}).\underline{n}. \end{cases}$$

The components $\Gamma_{11}(\underline{s})$ and $\Gamma_{21}(\underline{s})$ (resp. $\Gamma_{12}(\underline{s})$ and $\Gamma_{22}(\underline{s})$) of $\underline{\underline{\Gamma}}(\underline{s})$ are the components along $\underline{e}_1$ and $\underline{e}_2$ of $\underline{\Gamma}_1(\underline{s})$, the line density of internal moment on the facet with normal $\underline{e}_1$ (resp. $\underline{\Gamma}_2(\underline{s})$, $\underline{e}_2$) (Figure 6).

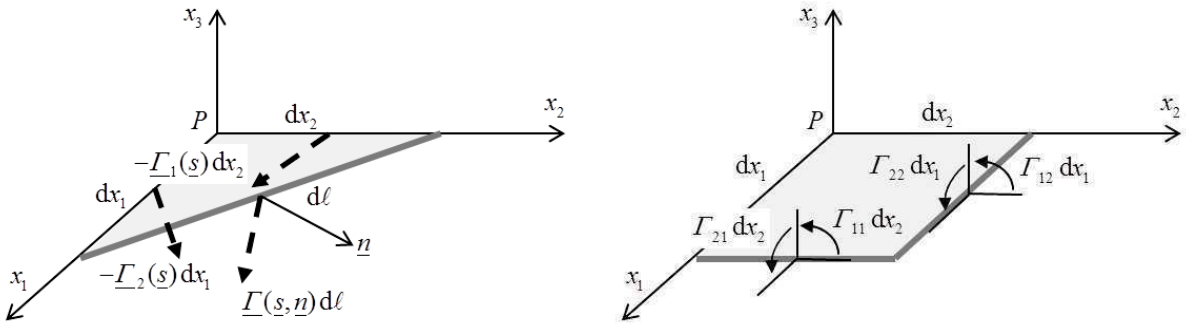

Figure 6. The small triangle argument applied to the moments. Components of $\underline{\underline{\Gamma}}(\underline{s})$

For the small parallelogram, the global equilibrium equation with respect to the moments is written (Figure 7)

(27) $$\frac{\partial \underline{\Gamma}_2}{\partial x_2} + \frac{\partial \underline{\Gamma}_1}{\partial x_1} + V_2\,\underline{e}_1 - V_1\,\underline{e}_2 + \underline{h}_D = 0$$

or, explicitly,

(28) $$\begin{cases} \dfrac{\partial \Gamma_{11}}{\partial x_1} + \dfrac{\partial \Gamma_{12}}{\partial x_2} + V_2 + h_1 = 0 \\ \dfrac{\partial \Gamma_{21}}{\partial x_1} + \dfrac{\partial \Gamma_{22}}{\partial x_2} - V_1 + h_2 = 0. \end{cases}$$

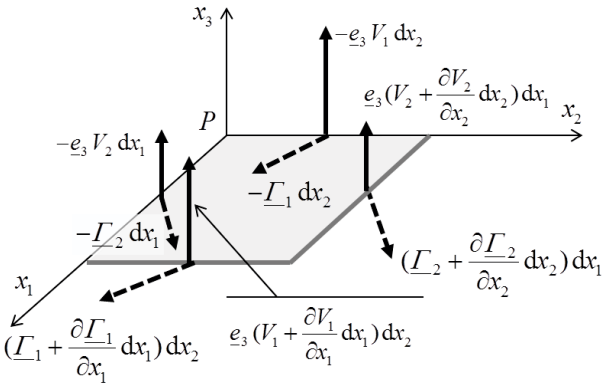

Figure 7. Global equilibrium of the small parallelogram

We observe that Eq. (28) can also be written in the expected form of a conservation law

(29) $$\operatorname{div}\underline{\underline{\Gamma}}(\underline{s})-\underline{e}_3\wedge\underline{V}(\underline{s})+\underline{h}_D(\underline{s})=0\,.$$

With the introduction of the second rank tensor $\underline{\underline{M}}(\underline{s})=\underline{e}_3\wedge\underline{\underline{\Gamma}}(\underline{s})$ defined by

(30) $$\forall\,\underline{n}\in\mathbb{R}^2,\ \underline{\underline{M}}(\underline{s}).\underline{n}=\underline{e}_3\wedge(\underline{\underline{\Gamma}}(\underline{s}).\underline{n})=\underline{e}_3\wedge\underline{\Gamma}(\underline{s},\underline{n})\,,$$

this equation takes the form[6]

(31) $$\operatorname{div}\underline{\underline{M}}(\underline{s})+\underline{V}(\underline{s})+\underline{m}_D(\underline{s})=0$$

with

(32) $$\underline{m}_D(\underline{s})=\underline{e}_3\wedge\underline{h}_D(\underline{s})\,.$$

The tensor $\underline{\underline{M}}(\underline{s})$ is the **tensor of internal moments**.

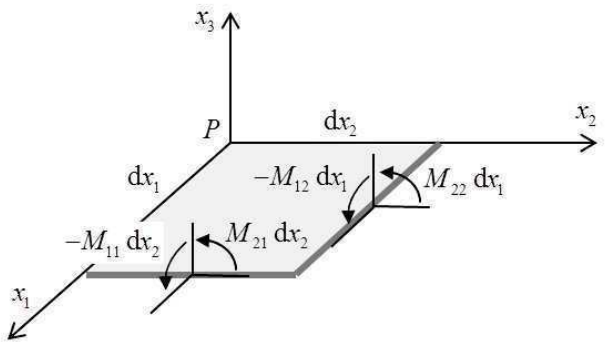

Figure 8. Components of the tensor of internal moments

The components of $\underline{\underline{M}}$ determined from Eq. (30) are shown in Figure 8

(33) $$\begin{cases} M_{11}=-\Gamma_{21} & M_{12}=-\Gamma_{22} \\ M_{21}=\Gamma_{11} & M_{22}=\Gamma_{12}\,. \end{cases}$$

[6] More justification for the introduction of tensor $\underline{\underline{M}}$ will appear in Section 4, when the two-dimensional model is derived from the original three-dimensional slender solid within the three-dimensional continuum mechanics framework

From the dimensional analysis viewpoint, they appear as forces, making the "moment" terminology somewhat misleading.

It is worth noting that **no symmetry** result can be established at this stage for the tensor $\underline{\underline{M}}$. Thence the explicit forms of Eq. (31) in Cartesian and polar coordinates are respectively

$$\begin{cases} \dfrac{\partial M_{xx}}{\partial x}+\dfrac{\partial M_{xy}}{\partial y}+V_x+(m_D)_x=0 \\ \dfrac{\partial M_{yx}}{\partial x}+\dfrac{\partial M_{yy}}{\partial y}+V_y+(m_D)_y=0 \end{cases} \tag{34}$$

$$\begin{cases} \dfrac{\partial M_{rr}}{\partial r}+\dfrac{1}{r}\dfrac{\partial M_{r\theta}}{\partial \theta}+\dfrac{M_{rr}-M_{\theta\theta}}{r}+V_r+(m_D)_r=0 \\ \dfrac{\partial M_{\theta r}}{\partial r}+\dfrac{1}{r}\dfrac{\partial M_{\theta\theta}}{\partial \theta}+\dfrac{M_{r\theta}+M_{\theta r}}{r}+V_\theta+(m_D)_\theta=0. \end{cases} \tag{35}$$

Together with the field equation (31) the internal moment field must comply with the boundary conditions which are derived from Eqs (17) and (30). At the point P of ∂S with outward normal $\underline{n}$

$$\begin{cases} \underline{\underline{M}}(\underline{s}).\underline{n}=\underline{e}_3\wedge\underline{H}(\underline{s}) \\ \underline{\underline{\Gamma}}(\underline{s}).\underline{n}=\underline{H}(\underline{s}). \end{cases} \tag{36}$$

Discontinuity of the internal moment tensor field occurs when a line density of external moment $\underline{\Gamma}_D(\underline{s})$ is applied to the system along a line (L) in S. The jump equations for the fields $\underline{\underline{M}}$ and $\underline{\underline{\Gamma}}$ are obtained from Eqs (29) and (31)

$$\begin{cases} [\![\underline{\underline{M}}(\underline{s})]\!].\underline{n}(\underline{s})+\underline{e}_3\wedge\underline{\Gamma}_D(\underline{s})=0 \\ [\![\underline{\underline{\Gamma}}(\underline{s})]\!].\underline{n}(\underline{s})+\underline{\Gamma}_D(\underline{s})=0. \end{cases} \tag{37}$$

3 Theorem/Principle of virtual work

3.1 Virtual motions

The virtual motions of the system $\mathcal{S}$ are defined in the same manner as the real kinematics described in § 1.2 through a velocity distributor

$$\left\{\hat{\mathbb{U}}(\underline{s})\right\}=\left\{P,\underline{\hat{U}}(\underline{s}),\underline{\hat{\Omega}}(\underline{s})\right\} \tag{38}$$

with the condition $\hat{\Omega}_3(\underline{s})=0$.

The fields $\underline{\hat{U}}(\underline{s})$ and $\underline{\hat{\Omega}}(\underline{s})$ are piecewise continuous and continuously differentiable in S. They are split into their in-plane and out-of-plane components according to Eq. (4) with similar notations.

3.2 The virtual work equation

With the description given above for the external forces – surface densities of tangential and normal forces, line densities of forces and in-plane moments in S and on ∂S – the virtual (rate of) work by the external forces in any virtual motion of the system takes the form

$$\begin{aligned}(39)\qquad \mathcal{P}_{\mathrm{e}}(\{\hat{\mathbb{U}}\}) = \mathcal{P}_{\mathrm{e}}(\underline{\hat{u}},\hat{w},\underline{\hat{\omega}}) &= \int_S \underline{f}_D(\underline{s}).\underline{\hat{u}}(\underline{s})\,\mathrm{d}S + \int_L \underline{\phi}_D(\underline{s}).\underline{\hat{u}}(\underline{s})\,\mathrm{d}L + \int_{\partial S} \underline{T}(\underline{s}).\underline{\hat{u}}(\underline{s})\,\mathrm{d}\ell \\ &+ \int_S f_3(\underline{s})\,\hat{w}(\underline{s})\,\mathrm{d}S + \int_L \phi_3(\underline{s})\,\hat{w}(\underline{s})\,\mathrm{d}L + \int_{\partial S} R(\underline{s})\,\hat{w}(\underline{s})\,\mathrm{d}\ell \\ &+ \int_S \underline{h}_D(\underline{s}).\underline{\hat{\omega}}(\underline{s})\,\mathrm{d}S + \int_L \underline{\Gamma}_D(\underline{s}).\underline{\hat{\omega}}(\underline{s})\,\mathrm{d}L + \int_{\partial S} \underline{H}(\underline{s}).\underline{\hat{\omega}}(\underline{s})\,\mathrm{d}\ell\,,\end{aligned}$$

which can be split in the form

$$(40)\qquad \mathcal{P}_{\mathrm{e}}(\{\hat{\mathbb{U}}\}) = \mathcal{P}_{\mathrm{e}}(\underline{\hat{u}}) + \mathcal{P}_{\mathrm{e}}(\hat{w},\underline{\hat{\omega}})$$

where $\mathcal{P}_{\mathrm{e}}(\underline{\hat{u}})$ stands for the first line of the right-hand member of Eq. (39).

Taking the in-plane equilibrium equations into account, $\mathcal{P}_{\mathrm{e}}(\underline{\hat{u}})$ transforms in the same way as for the three-dimensional continuum (*cf.* Chapter III, § 3.2)

$$\begin{aligned}(41)\qquad \mathcal{P}_{\mathrm{e}}(\underline{\hat{u}}) &= \int_S \underline{f}_D(\underline{s}).\underline{\hat{u}}(\underline{s})\,\mathrm{d}S + \int_L \underline{\phi}_D(\underline{s}).\underline{\hat{u}}(\underline{s})\,\mathrm{d}L + \int_{\partial S} \underline{T}(\underline{s}).\underline{\hat{u}}(\underline{s})\,\mathrm{d}\ell \\ &= \int_S \underline{\underline{N}}(\underline{s}):\underline{\underline{\partial}}\underline{\hat{u}}(\underline{s})\,\mathrm{d}S + \int_{L_{\underline{\hat{u}}}} \underline{n}(\underline{s}).\underline{\underline{N}}(\underline{s}).[\![\underline{\hat{u}}(\underline{s})]\!]\,\mathrm{d}L \\ &= -\mathcal{P}_{\mathrm{i}}(\underline{\hat{u}})\,.\end{aligned}$$

which is just the theorem of virtual work for the membrane (or in-plane) two-dimensional model.

The second line of Eq. (39) transforms similarly:

$$\begin{aligned}(42)\qquad &\int_S f_3(\underline{s})\,\hat{w}(\underline{s})\,\mathrm{d}S + \int_L \phi_3(\underline{s})\,\hat{w}(\underline{s})\,\mathrm{d}L + \int_{\partial S} R(\underline{s})\,\hat{w}(\underline{s})\,\mathrm{d}\ell = \\ &= \int_S \underline{V}(\underline{s}).\underline{\partial}\hat{w}(\underline{s})\,\mathrm{d}S + \int_{L_{\hat{w}}} \underline{V}(\underline{s}).[\![\hat{w}(\underline{s})]\!]\,\underline{n}(\underline{s})\,\mathrm{d}L\,.\end{aligned}$$

For the third line, we first recall the two following mathematical identities

$$(43)\qquad \mathrm{div}\,({}^{\mathrm{t}}\underline{\underline{\Gamma}}.\underline{\hat{\omega}}) = {}^{\mathrm{t}}\underline{\underline{\Gamma}}:\underline{\underline{\partial}}\underline{\hat{\omega}} + \underline{\hat{\omega}}.\mathrm{div}\,\underline{\underline{\Gamma}}$$

and

$$(44)\qquad \int_S \mathrm{div}\,({}^{\mathrm{t}}\underline{\underline{\Gamma}}.\underline{\hat{\omega}})\,\mathrm{d}S + \int_L \underline{\hat{\omega}}.[\![\underline{\underline{\Gamma}}]\!].\underline{n}\,\mathrm{d}L + \int_{L_{\underline{\hat{\omega}}}} [\![\underline{\hat{\omega}}]\!].\underline{\underline{\Gamma}}.\underline{n}\,\mathrm{d}L = \int_{\partial S} \underline{\hat{\omega}}.\underline{\underline{\Gamma}}.\underline{n}\,\mathrm{d}\ell\,,$$

an application of the divergence formula (*cf.* [2]).

Combining these two equations we get

$$(45)\qquad \int_{\partial S} \underline{\hat{\omega}}.\underline{\underline{\Gamma}}.\underline{n}\,\mathrm{d}\ell - \int_S \underline{\hat{\omega}}.\mathrm{div}\,\underline{\underline{\Gamma}}\,\mathrm{d}S = \int_S {}^{\mathrm{t}}\underline{\underline{\Gamma}}:\underline{\underline{\partial}}\underline{\hat{\omega}}\,\mathrm{d}S + \int_{L_{\underline{\hat{\omega}}}} [\![\underline{\hat{\omega}}]\!].\underline{\underline{\Gamma}}.\underline{n}\,\mathrm{d}L + \int_L \underline{\hat{\omega}}.[\![\underline{\underline{\Gamma}}]\!].\underline{n}\,\mathrm{d}L$$

and, taking Eqs (29), (36) and (37) into account,

$$(46)\quad \int_S \underline{h}_D(\underline{s}).\hat{\underline{\omega}}(\underline{s})\,\mathrm{d}S+\int_L \underline{\Gamma}_D(\underline{s}).\hat{\underline{\omega}}(\underline{s})\,\mathrm{d}L+\int_{\partial S}\underline{H}(\underline{s}).\hat{\underline{\omega}}(\underline{s})\,\mathrm{d}\ell =$$
$$=\int_S {}^{\mathrm{t}}\underline{\underline{\Gamma}}(\underline{s}):\underline{\underline{\partial}}\hat{\underline{\omega}}(\underline{s})\,\mathrm{d}S-\int_S \underline{V}(\underline{s}).(\underline{e}_3\wedge\hat{\underline{\omega}}(\underline{s}))\,\mathrm{d}S+\int_{L_{\hat{\underline{\omega}}}}[\![\hat{\underline{\omega}}(\underline{s})]\!].\underline{\underline{\Gamma}}(\underline{s}).\underline{n}(\underline{s})\,\mathrm{d}L.$$

Joining Eqs (42) and (46) together we get the expression of the virtual work by the internal forces in the out-of-plane two-dimensional model

$$(47)\quad \mathcal{P}_{\mathrm{i}}\{\hat{w},\hat{\underline{\omega}}\}=-\int_S {}^{\mathrm{t}}\underline{\underline{\Gamma}}(\underline{s}):\underline{\underline{\partial}}\hat{\underline{\omega}}(\underline{s})\,\mathrm{d}S-\int_{L_{\hat{\underline{\omega}}}}[\![\hat{\underline{\omega}}(\underline{s})]\!].\underline{\underline{\Gamma}}(\underline{s}).\underline{n}(\underline{s})\,\mathrm{d}L$$
$$-\int_S \underline{V}(\underline{s}).(\underline{\partial}\hat{w}(\underline{s})-\underline{e}_3\wedge\hat{\underline{\omega}}(\underline{s}))\,\mathrm{d}S-\int_{L_{\hat{w}}}\underline{V}(\underline{s}).[\![\hat{w}(\underline{s})]\!]\,\underline{n}(\underline{s})\,\mathrm{d}L.$$

With

$$(48)\quad \mathcal{P}_{\mathrm{e}}\{\hat{w},\hat{\underline{\omega}}\}=\int_S f_3(\underline{s})\,\hat{w}(\underline{s})\,\mathrm{d}S+\int_L \phi_3(\underline{s})\,\hat{w}(\underline{s})\,\mathrm{d}L+\int_{\partial S}R(\underline{s})\,\hat{w}(\underline{s})\,\mathrm{d}\ell$$
$$+\int_S \underline{h}_D(\underline{s}).\hat{\underline{\omega}}(\underline{s})\,\mathrm{d}S+\int_L \underline{\Gamma}_D(\underline{s}).\hat{\underline{\omega}}(\underline{s})\,\mathrm{d}L+\int_{\partial S}\underline{H}(\underline{s}).\hat{\underline{\omega}}(\underline{s})\,\mathrm{d}\ell,$$

the theorem of virtual work for the out-of-plane two-dimensional model is written

$\forall\,\hat{w},\hat{\underline{\omega}}$ piecewise continuous and continuously differentiable in S

$$(49)\quad \mathcal{P}_{\mathrm{e}}\{\hat{w},\hat{\underline{\omega}}\}+\mathcal{P}_{\mathrm{i}}\{\hat{w},\hat{\underline{\omega}}\}=0.$$

In Eq. (49), the virtual work by the internal forces $\mathcal{P}_{\mathrm{i}}\{\hat{w},\hat{\underline{\omega}}\}$ may also be expressed using the internal moment tensor $\underline{\underline{M}}$. For this purpose, it is convenient to introduce

$$(50)\quad \hat{\underline{v}}(\underline{s})=\underline{e}_3\wedge\hat{\underline{\omega}}(\underline{s})$$

which yields:

$$(51)\quad \mathcal{P}_{\mathrm{i}}\{\hat{w},\hat{\underline{v}}\}=-\int_S {}^{\mathrm{t}}\underline{\underline{M}}(\underline{s}):\underline{\underline{\partial}}\hat{\underline{v}}(\underline{s})\,\mathrm{d}S-\int_{L_{\hat{\underline{\omega}}}}[\![\hat{\underline{v}}(\underline{s})]\!].\underline{\underline{M}}(\underline{s}).\underline{n}(\underline{s})\,\mathrm{d}L$$
$$-\int_S \underline{V}(\underline{s}).(\underline{\partial}\hat{w}(\underline{s})-\hat{\underline{v}}(\underline{s}))\,\mathrm{d}S-\int_{L_{\hat{w}}}\underline{V}(\underline{s}).[\![\hat{w}(\underline{s})]\!]\,\underline{n}(\underline{s})\,\mathrm{d}L.$$

As a conclusion, the virtual work equation

$$(52)\quad \mathcal{P}_{\mathrm{e}}(\{\hat{\mathbb{U}}\})+\mathcal{P}_{\mathrm{i}}(\{\hat{\mathbb{U}}\})=0$$

is expressed by Eqs (41) and (49)-(51). Joining Eqs (41) and (47) or (51) together we get the complete expression for the virtual work by the internal forces $\mathcal{P}_{\mathrm{i}}(\{\hat{\mathbb{U}}\})$ in those virtual motions that exhibit no rotation rate about $\underline{e}_3$

$$(53)\quad \mathcal{P}_{\mathrm{i}}(\hat{\underline{u}},\hat{w},\hat{\underline{v}})=-\int_S \underline{\underline{N}}(\underline{s}):\underline{\underline{\partial}}\hat{\underline{u}}(\underline{s})\,\mathrm{d}S-\int_{L_{\hat{\underline{u}}}}\underline{n}(\underline{s}).\underline{\underline{N}}(\underline{s}).[\![\hat{\underline{u}}(\underline{s})]\!]\,\mathrm{d}L$$
$$-\int_S {}^{\mathrm{t}}\underline{\underline{M}}(\underline{s}):\underline{\underline{\partial}}\hat{\underline{v}}(\underline{s})\,\mathrm{d}S-\int_{L_{\hat{\underline{\omega}}}}[\![\hat{\underline{v}}(\underline{s})]\!].\underline{\underline{M}}(\underline{s}).\underline{n}(\underline{s})\,\mathrm{d}L$$
$$-\int_S \underline{V}(\underline{s}).(\underline{\partial}\hat{w}(\underline{s})-\hat{\underline{v}}(\underline{s}))\,\mathrm{d}S-\int_{L_{\hat{w}}}\underline{V}(\underline{s}).[\![\hat{w}(\underline{s})]\!]\,\underline{n}(\underline{s})\,\mathrm{d}L.$$

It is worth noting from Eq. (53) that in the particular case when the Kirchhoff-Love condition (10) is imposed to the virtual velocity field there is no contribution by the shear force vector to the virtual work by the internal forces (similar to the shear force not contributing to the virtual work by the internal forces under the Navier-Bernoulli condition in Chapter IX, § 1.4). At the same time, the Kirchhoff-Love condition implies that $\underline{\underline{\partial}}\hat{v}(\underline{s}) = \underline{\underline{\partial^2}}\hat{w}(\underline{s})$ which is a symmetric second rank tensor. It follows that in Eq. (53) only the symmetric part of tensor $\underline{\underline{M}}(\underline{s})$ contributes to the virtual work by the internal forces.

3.3 Tensorial wrench of internal forces

The gradient of the virtual velocity distributor $\left\{ \hat{\mathbb{U}} \right\}$ is the counterpart of the tensorial distributor defined in Eq. (12) for $\left\{ \mathbb{U} \right\}$. It is written

$$\partial\left\{\hat{\mathbb{U}}(\underline{s})\right\} = \left\{ P,\ \underline{\underline{\partial}}\hat{u}(\underline{s}) + \underline{e}_3 \otimes \partial\hat{w}(\underline{s}) - \underline{e}_3 \otimes \left(\underline{e}_3 \wedge \hat{\underline{\omega}}(\underline{s})\right),\ \underline{\underline{\partial}}\hat{\underline{\omega}}(\underline{s}) \right\}. \tag{54}$$

Concerning the internal forces, we first define the wrench of the densities of internal forces on the line element $\mathrm{d}\ell$ with normal $\underline{n}$ at the point P

$$\left[P,\ \underline{N}(\underline{s},\underline{n}) + \underline{e}_3 V(\underline{s},\underline{n}),\ \underline{\Gamma}(\underline{s},\underline{n})\right], \tag{55}$$

which depends linearly on $\underline{n}$ through the **tensorial wrench**

$$\begin{aligned} \left[\mathbb{X}(\underline{s})\right] &= \left[P,\ \underline{\underline{N}}(\underline{s}) + \underline{e}_3 \otimes \underline{V}(\underline{s}),\ \underline{\underline{\Gamma}}(\underline{s})\right] \\ &= \left[P,\ \underline{\underline{N}}(\underline{s}) + \underline{e}_3 \otimes \underline{V}(\underline{s}),\ -\underline{e}_3 \wedge \underline{\underline{M}}(\underline{s})\right] \end{aligned} \tag{56}$$

$$\begin{aligned} \left[\mathbb{X}(\underline{s})\right].\underline{n} &= \left[P,\ \underline{\underline{N}}(\underline{s}).\underline{n} + \left(\underline{e}_3 \otimes \underline{V}(\underline{s})\right).\underline{n},\ \underline{\underline{\Gamma}}(\underline{s}).\underline{n}\right] \\ &= \left[P,\ \underline{N}(\underline{s},\underline{n}) + \underline{e}_3 V(\underline{s},\underline{n}),\ \underline{\Gamma}(\underline{s},\underline{n})\right]. \end{aligned} \tag{57}$$

The doubly contracted product ${}^{\mathrm{t}}\left[\mathbb{X}(\underline{s})\right] : \partial\left\{\hat{\mathbb{U}}(\underline{s})\right\}$ is the duality product of these two quantities. Taking Eqs (50), (54), (56) and the symmetry of $\underline{\underline{N}}(\underline{s})$ into account, it is written

$$\begin{aligned} {}^{\mathrm{t}}\left[\mathbb{X}(\underline{s})\right] : \partial\left\{\hat{\mathbb{U}}(\underline{s})\right\} &= \underline{\underline{N}}(\underline{s}) : \underline{\underline{\partial}}\hat{u}(\underline{s}) + \underline{V}(\underline{s}).\partial\hat{w} - \underline{V}(\underline{s}).\hat{\underline{v}}(\underline{s}) + {}^{\mathrm{t}}\underline{\underline{\Gamma}}(\underline{s}) : \underline{\underline{\partial}}\hat{\underline{\omega}}(\underline{s}) \\ &= \underline{\underline{N}}(\underline{s}) : \underline{\underline{\partial}}\hat{u}(\underline{s}) + \underline{V}(\underline{s}).\underline{\partial}\hat{w} - \underline{V}(\underline{s}).\hat{\underline{v}}(\underline{s}) + {}^{\mathrm{t}}\underline{\underline{M}}(\underline{s}) : \underline{\underline{\partial}}\hat{\underline{v}}(\underline{s}). \end{aligned} \tag{58}$$

Hence the expression for $\mathcal{P}_{\mathrm{i}}\left(\left\{ \hat{\mathbb{U}} \right\}\right)$

$$\mathcal{P}_{\mathrm{i}}\left(\left\{ \hat{\mathbb{U}} \right\}\right) = -\int_S {}^{\mathrm{t}}\left[\mathbb{X}(\underline{s})\right] : \partial\left\{\hat{\mathbb{U}}(\underline{s})\right\} \mathrm{d}S - \int_{L_{\hat{\mathbb{U}}}} [\![\left\{\hat{\mathbb{U}}(\underline{s})\right\}]\!].\left[\mathbb{X}(\underline{s})\right].\underline{n}(\underline{s})\,\mathrm{d}L\,. \tag{59}$$

Eq. (59) is similar to its counterpart for micropolar three-dimensional media (*cf.* [2]).

With the wrenches of external forces defined in the same way as in Chapter IX (§ 1.3)

$$(60)\qquad \begin{cases} \left[\ \mathbb{f}(\underline{s})\ \right]=\left[\ P,\ \underline{f}(\underline{s}),\ \underline{h}_D(\underline{s})\ \right] \\ \left[\ \mathbb{F}(\underline{s})\ \right]=\left[\ P,\underline{\phi}_D(\underline{s})+\phi_3(\underline{s})\,\underline{e}_3,\underline{\Gamma}_D(\underline{s})\ \right] \\ \left[\ \mathbb{R}(\underline{s})\ \right]=\left[\ P,\underline{T}(\underline{s})+R(\underline{s})\,\underline{e}_3,\underline{H}(\underline{s})\ \right], \end{cases}$$

the virtual work by the external forces $\mathcal{P}_{\mathrm{e}}(\left\{\ \hat{\mathbb{U}}\ \right\})$ is written

$$(61)\qquad \mathcal{P}_{\mathrm{e}}(\left\{\ \hat{\mathbb{U}}\ \right\})=\int_S\left[\ \mathbb{f}(\underline{s})\ \right].\left\{\hat{\mathbb{U}}(\underline{s})\right\}\mathrm{d}S+\int_L\left[\ \mathbb{F}(\underline{s})\ \right].\left\{\hat{\mathbb{U}}(\underline{s})\right\}\mathrm{d}L+\int_{\partial S}\left[\ \mathbb{R}(\underline{s})\ \right].\left\{\hat{\mathbb{U}}(\underline{s})\right\}\mathrm{d}L\,.$$

The in-plane and out-of-plane Equilibrium equations take the form of a single conservation law

$$(62)\qquad \begin{cases} \forall P\in S\,, \\ \mathrm{div}\left[\ \mathbb{X}(\underline{s})\right]+\left[\ \mathbb{f}(\underline{s})\ \right]=0 \end{cases}$$

with the corresponding jump equation when crossing (L)

$$(63)\qquad [\![\left[\ \mathbb{X}(\underline{s})\right]]\!].\underline{n}(\underline{s})+\left[\ \mathbb{F}(\underline{s})\ \right]=0$$

and the boundary condition along ∂S

$$(64)\qquad \left[\ \mathbb{X}(\underline{s})\right].\underline{n}(\underline{s})=\left[\ \mathbb{R}(\underline{s})\ \right].$$

4 Plate model derived from the three-dimensional continuum

A particular case of the model is obtained through a "micro-macro" process starting from the three-dimensional continuum modelling of the original slender structural element, subjected to volume density forces and surface density boundary forces, which is smashed flat onto the director sheet (D) (*cf.* [3]).

4.1 Internal forces

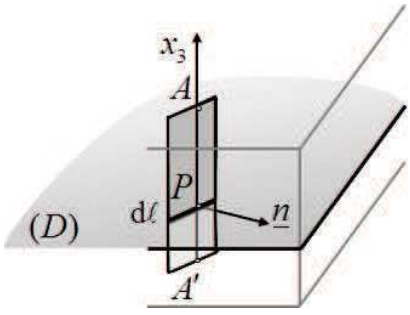

Figure 9. Smashing flat the three-dimensional facet onto the director sheet

More precisely, to perform this "micro-macro" process we consider in S the generic point P of the particle $P(\underline{s})$ and the facet $\mathrm{d}\ell$ with normal $\underline{n}$ within the two-dimensional plate model framework and we define the internal forces acting on this facet, namely $\underline{N}(\underline{s},\underline{n})\,\mathrm{d}\ell+V(\underline{s},\underline{n})\,\underline{e}_3\,\mathrm{d}\ell$ and $\underline{\Gamma}(\underline{s},\underline{n})\,\mathrm{d}\ell$, as the reduced elements, with respect to P, of the stresses acting on the three-dimensional facet with normal $\underline{n}$ defined, in the original solid, by $\mathrm{d}\ell$ and the transversal thickness $A'A$ (Figure 9).

Introducing the two-dimensional part of the tensor $\underline{\underline{\sigma}}(\underline{s},x_3)$ defined by

$$\underline{\underline{\sigma}}_D(\underline{s},x_3)=\sigma_{ij}(\underline{s},x_3)\,\underline{e}_i\otimes\underline{e}_j\ ,\ i,j=1,2\ , \tag{65}$$

we obtain the expressions of $\underline{N}(\underline{s},\underline{n})\,\mathrm{d}\ell+\underline{V}(\underline{s},\underline{n})\,\underline{e}_3\,\mathrm{d}\ell$ and $\underline{\Gamma}(\underline{s},\underline{n})\,\mathrm{d}\ell$

$$\begin{cases}\left(\underline{\underline{N}}(\underline{s}).\underline{n}+\underline{e}_3\,\underline{V}(\underline{s}).\underline{n}\right)\mathrm{d}\ell=\mathrm{d}\ell\displaystyle\int_{A'}^{A}\underline{\underline{\sigma}}_D(\underline{s},x_3).\underline{n}\,\mathrm{d}x_3+\mathrm{d}\ell\int_{A'}^{A}\underline{e}_3\,\sigma_{3i}(\underline{s},x_3)\,n_i\,\mathrm{d}x_3\\ \underline{\Gamma}(\underline{s}).\underline{n}\,\mathrm{d}\ell=\mathrm{d}\ell\displaystyle\int_{A'}^{A}x_3\,\underline{e}_3\wedge\left(\underline{\underline{\sigma}}(\underline{s},x_3).\underline{n}\right)\mathrm{d}x_3=\mathrm{d}\ell\int_{A'}^{A}x_3\,\underline{e}_3\wedge\left(\underline{\underline{\sigma}}_D(\underline{s},x_3).\underline{n}\right)\mathrm{d}x_3\,.\end{cases} \tag{66}$$

It follows from Eq. (66) that

$$\begin{cases}\underline{\underline{N}}(\underline{s})=\displaystyle\int_{A'}^{A}\underline{\underline{\sigma}}_D(\underline{s},x_3)\,\mathrm{d}x_3\\ \underline{V}(\underline{s})=\displaystyle\int_{A'}^{A}\sigma_{3i}(\underline{s},x_3)\,\underline{e}_i\,\mathrm{d}x_3\end{cases} \tag{67}$$

and

$$\underline{\underline{M}}(\underline{s})=\underline{e}_3\wedge\underline{\underline{\Gamma}}(\underline{s})=-\int_{A'}^{A}x_3\,\underline{\underline{\sigma}}_D(\underline{s},x_3)\,\mathrm{d}x_3\,. \tag{68}$$

The tensorial wrench of internal forces comes out as

$$\left[\,\mathbb{X}(\underline{s})\,\right]=\int_{A'}^{A}\left[P,\ \underline{\underline{\sigma}}_D(\underline{s},x_3)+\sigma_{3i}(\underline{s},x_3)\underline{e}_3\otimes\underline{e}_i,\ x_3\,\underline{e}_3\wedge\underline{\underline{\sigma}}_D(\underline{s},x_3)\right]\mathrm{d}x_3\ . \tag{69}$$

4.2 Equilibrium equations and External forces

Integrating the three-dimensional continuum equilibrium equations recalled in Chapter III with respect to x_3 brings out the equilibrium equations for the two-dimensional continuum, together with the expressions of the external forces.

- We first note that since $\underline{\underline{\sigma}}(\underline{s},x_3)$ and, consequently, $\underline{\underline{\sigma}}_D(\underline{s},x_3)$ are symmetric it follows from Eq. (67) that $\underline{\underline{N}}(\underline{s})$ is symmetric.
- It also implies through Eq. (68) that $\underline{\underline{M}}(\underline{s})$ **is symmetric**.
- Integrating the three-dimensional continuum equilibrium equations for the x_1 and x_2 coordinates with respect to x_3 results in Eq. (19)

  $$\mathrm{div}\,\underline{\underline{N}}(\underline{s})+\underline{f}_D(\underline{s})=0$$

  with

$$\begin{aligned}\underline{f}_D(\underline{s})=&\,\underline{e}_1\left(\sigma_{13}(\underline{s},A)-\sigma_{13}(\underline{s},A')\right)+\underline{e}_1\int_{A'}^{A}\rho(\underline{s},x_3)\,F_1(\underline{s},x_3)\,\mathrm{d}x_3\\&+\underline{e}_2\left(\sigma_{23}(\underline{s},A)-\sigma_{23}(\underline{s},A')\right)+\underline{e}_2\int_{A'}^{A}\rho(\underline{s},x_3)\,F_2(\underline{s},x_3)\,\mathrm{d}x_3\,.\end{aligned} \tag{70}$$

- Integrating the third equilibrium equation brings out Eq. (23)

  $$\mathrm{div}\,\underline{V}(\underline{s})+f_3(\underline{s})=0\,,$$

  where the external force surface density for the two-dimensional model is obtained from the data on the external forces for the three-dimensional problem

(71) $$f_3(\underline{s}) = \left(\sigma_{33}(\underline{s}, A) - \sigma_{33}(\underline{s}, A')\right) + \int_{A'}^{A} \rho(\underline{s}, x_3)\, F_3(\underline{s}, x_3)\, \mathrm{d}x_3 .$$

- The equilibrium equation (31) is obtained from the components of Eq. (72) along $\underline{e}_1$ and $\underline{e}_2$

(72) $$-\int_{A'}^{A} x_3 \left(\operatorname{div} \underline{\underline{\sigma}}(\underline{s}, x_3) + \rho(\underline{s}, x_3)\, \underline{F}(\underline{s}, x_3)\right) \mathrm{d}x_3 = 0 ,$$

we get

(73) $$\operatorname{div} \underline{\underline{M}}(\underline{s}) + \underline{V}(\underline{s}) + \underline{m}_D(\underline{s}) = 0$$

with the external moment surface density for the two-dimensional model derived from the data on the external forces for the three-dimensional problem:

(74) $$\underline{m}_D(\underline{s}) = -x_3(A)\left(\sigma_{13}(\underline{s}, A)\,\underline{e}_1 + \sigma_{23}(\underline{s}, A)\,\underline{e}_2\right) + x_3(A')\left(\sigma_{13}(\underline{s}, A')\,\underline{e}_1 + \sigma_{23}(\underline{s}, A')\,\underline{e}_2\right)$$
$$-\int_{A'}^{A} x_3\, \rho(\underline{s}, x_3)\left(F_1(\underline{s}, x_3)\,\underline{e}_1 + F_2(\underline{s}, x_3)\,\underline{e}_2\right) \mathrm{d}x_3 .$$

- The boundary equations are obtained in the same way. Referring to Eqs (14) and (15)

(75) $$\begin{cases} \underline{T}(\underline{s})\,\mathrm{d}\ell + R(\underline{s})\,\underline{e}_3\,\mathrm{d}\ell = \mathrm{d}\ell \int_{A'}^{A} \underline{\underline{\sigma}}(\underline{s}, x_3).\underline{n}\,\mathrm{d}x_3 \\ \underline{H}(\underline{s})\,\mathrm{d}\ell = \mathrm{d}\ell \int_{A'}^{A} x_3\, \underline{e}_3 \wedge (\underline{\underline{\sigma}}_D(\underline{s}, x_3).\underline{n})\,\mathrm{d}x_3 . \end{cases}$$

4.3 Virtual work approach

It thus appears that this "micro-macro" modelling process results in a particular form of the general model where, incidentally, the tensor of internal moments is proven to be **symmetric**.

Also Eqs (70), (71) and (74) give the explicit expressions of the surface densities of external forces and moments in the two-dimensional model: as it could be anticipated, $\underline{f}(\underline{s})\,\mathrm{d}S = \underline{f}_D(\underline{s})\,\mathrm{d}S + f_3(\underline{s})\,\underline{e}_3\,\mathrm{d}S$ and $\underline{h}_D(\underline{s})\,\mathrm{d}S = -\underline{e}_3 \wedge \underline{m}_D(\underline{s})\,\mathrm{d}S$ are just the **reduced elements of the wrench of all the external forces** applied to a vertical cylinder parallel to $A'A$ and with section $\mathrm{d}S$ in the original three-dimensional structural element (Figure 10). This means that $\left[\, \mathbb{f}(\underline{s}) \,\right]$ defined in Eq. (60) is just the wrench of all the volume and surface densities of external forces.

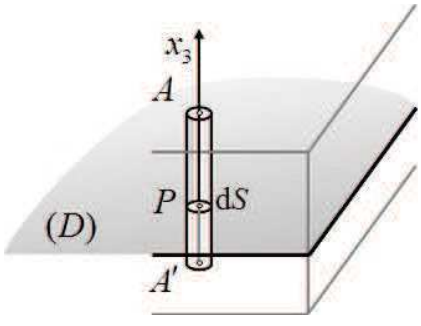

Figure 10. Cylindrical volume element in the three-dimensional solid

The same conclusion applies to the line densities of external forces along ∂S with respect to $[\,\mathbb{R}(\underline{s})\,]$.

The rationale of this modelling process may be more easily perceived through the virtual work theory.

Given the velocity distributor field $\left\{\hat{\mathbb{U}}(\underline{s})\right\} = \left\{\, P,\, \hat{\underline{u}}(\underline{s}) + \hat{w}(\underline{s})\,\underline{e}_3,\, \hat{\underline{\omega}}(\underline{s})\right\}$, with $\hat{\underline{u}}(\underline{s})$, $\hat{w}(\underline{s})$ and $\hat{\underline{\omega}}(\underline{s})$ continuous and continuously differentiable, consider the virtual velocity field defined **in the three-dimensional solid** in the following way.

At any point M the virtual velocity is written

(76) $$\hat{\underline{U}}(\underline{s}, x_3) = \hat{\underline{u}}(\underline{s}) + \hat{w}(\underline{s})\,\underline{e}_3 + \hat{\underline{\omega}}(\underline{s}) \wedge x_3\,\underline{e}_3$$

from which we derive the three-dimensional velocity gradient (with $\hat{\underline{v}} = \underline{e}_3 \wedge \hat{\underline{\omega}}$)

(77) $$\begin{aligned}\underline{\underline{\underline{\mathrm{grad}}}}\,\hat{\underline{U}}(\underline{s}, x_3) &= \underline{\underline{\partial}}\hat{\underline{u}}(\underline{s}) + \underline{e}_3 \otimes \underline{\partial w}(\underline{s}) + \hat{\underline{\omega}}(\underline{s}) \wedge (\underline{e}_3 \otimes \underline{e}_3) + x_3\,\underline{\underline{\partial}}\hat{\underline{\omega}}(\underline{s}) \wedge \underline{e}_3 \\ &= \underline{\underline{\partial}}\hat{\underline{u}}(\underline{s}) + \underline{e}_3 \otimes \underline{\partial w}(\underline{s}) - \hat{\underline{v}}(\underline{s}) \otimes \underline{e}_3 - x_3\,\underline{\underline{\partial}}\hat{\underline{v}}(\underline{s}).\end{aligned}$$

It follows that the virtual work by the internal forces takes the explicit form:

(78) $$\mathcal{P}_{\mathrm{i}}(\hat{\underline{U}}) = -\int_{S\times A'A} \underline{\underline{\sigma}}(\underline{s}, x_3) : \underline{\underline{\underline{\mathrm{grad}}}}\,\hat{\underline{U}}(\underline{s}, x_3)\,\mathrm{d}S\,\mathrm{d}x_3$$

with

(79) $$\begin{aligned}\int_{S\times A'A} \underline{\underline{\sigma}}(\underline{s}, x_3) : \underline{\underline{\underline{\mathrm{grad}}}}\,\hat{\underline{U}}(\underline{s}, x_3)\,\mathrm{d}S\,\mathrm{d}x_3 &= \int_{S\times A'A} \underline{\underline{\sigma}}_D(\underline{s}, x_3) : \underline{\underline{\partial}}\hat{\underline{u}}(\underline{s})\,\mathrm{d}S\,\mathrm{d}x_3 \\ &+ \int_{S\times A'A} \left(\sigma_{31}(\underline{s}, x_3)\frac{\partial \hat{w}}{\partial x_1}(\underline{s}) + \sigma_{32}(\underline{s}, x_3)\frac{\partial \hat{w}}{\partial x_2}(\underline{s})\right)\mathrm{d}S\,\mathrm{d}x_3 \\ &- \int_{S\times A'A} \left(\sigma_{31}(\underline{s}, x_3)\hat{v}_1(\underline{s}) + \sigma_{32}(\underline{s}, x_3)\hat{v}_2(\underline{s})\right)\mathrm{d}S\,\mathrm{d}x_3 \\ &- \int_{S\times A'A} x_3\,\underline{\underline{\sigma}}_D(\underline{s}, x_3) : \underline{\underline{\partial}}\hat{\underline{v}}(\underline{s})\,\mathrm{d}S\,\mathrm{d}x_3.\end{aligned}$$

Taking Eqs (67) and (68) into account, Eq. (79) becomes:

(80) $$\begin{aligned}\int_{S\times A'A} \underline{\underline{\sigma}}(\underline{s}, x_3) : \underline{\underline{\underline{\mathrm{grad}}}}\,\hat{\underline{U}}(\underline{s}, x_3)\,\mathrm{d}S\,\mathrm{d}x_3 &= \int_S \underline{\underline{N}}(\underline{s}) : \underline{\underline{\partial}}\hat{\underline{u}}(\underline{s})\,\mathrm{d}S \\ &+ \int_S \underline{V}(\underline{s}).\left(\underline{\partial}\hat{w}(\underline{s}) - \hat{\underline{v}}(\underline{s})\right)\mathrm{d}S + \int_S \underline{\underline{M}}(\underline{s}) : \underline{\underline{\partial}}\hat{\underline{v}}(\underline{s})\,\mathrm{d}S.\end{aligned}$$

In other words we have

(81) $$\mathcal{P}_{\mathrm{i}}(\hat{\underline{U}}) = \mathcal{P}_{\mathrm{i}}(\hat{\underline{u}}, \hat{w}, \hat{\underline{v}}) = \mathcal{P}_{\mathrm{i}}(\left\{\hat{\mathbb{U}}\right\}).$$

As for the virtual work by the external forces, it must be observed that the virtual velocity field defined by Eq.(76) is, at each point P, *i.e.* for each value of $\underline{s}$, a rigid body motion. Thence, the virtual work by the external forces $\mathcal{P}_{\mathrm{e}}(\hat{\underline{U}})$ is the integral over S and along ∂S of the product of the reduced elements of the external forces wrench at P by the reduced elements of the velocity distributor at the same point. From Eqs (70)-(71), (74)-(75) we get Eq. (82) which is identical to Eqs (39) and (61) in the case of no external force line densities over S:

(82) $$\mathcal{P}_{\mathrm{e}}(\hat{\underline{U}}) = \int_S \underline{f}_D(\underline{s}).\hat{\underline{u}}(\underline{s})\,\mathrm{d}S + \int_S f_3(\underline{s})\,\hat{w}(\underline{s})\,\mathrm{d}S + \int_S \underline{h}_D(\underline{s}).\hat{\underline{\omega}}(\underline{s})\,\mathrm{d}S$$
$$+ \int_{\partial S} \underline{T}(\underline{s}).\hat{\underline{u}}(\underline{s})\,\mathrm{d}\ell + \int_{\partial S} R(\underline{s})\,\hat{w}(\underline{s})\,\mathrm{d}\ell + \int_{\partial S} \underline{H}(\underline{s}).\hat{\underline{\omega}}(\underline{s})\,\mathrm{d}\ell,$$

This proves that the two-dimensional model and the original three-dimensional one are equivalent from the virtual work theory viewpoint in the velocity fields defined by Eq. (76). Considering piecewise continuous and continuously differentiable $\hat{\underline{u}}(\underline{s})$, $\hat{w}(\underline{s})$ and $\hat{\underline{\omega}}(\underline{s})$ fields leads to the same conclusion.

4.4 Final comments

The micro-macro process which has been presented here above may appear as a double-edged sword:

- On the one side it shows that there is no inconsistency between the three-dimensional continuum model and the modelling of plates as two-dimensional continua.
- But it may also lead to the idea that this two-dimensional modelling is dependent on the three-dimensional continuum and is just some kind of simplified by-product of it.

It is essential to retain that the general two-dimensional model presented in the preceding Sections is mechanically consistent in itself and is valid independently of the possibility of performing the "micro-macro" modelling process and also independently of any assumption about the mechanical behaviour of the constituent material.

Within the two-dimensional framework, data on the mechanical properties of the constituent material, such as its strength criterion or its constitutive law concerning $[\mathbb{X}(\underline{s})]$ and $\partial\{\mathbb{U}(\underline{s})\}$ will either proceed from experimental results at the global (macro) level or from the "micro-macro" analysis through Eqs (67), (68) and (80).

This will be the case in the following Chapter for the strength criteria of (metal) plates or (reinforced concrete) slabs.

REFERENCES

[1] HJELMSTAD, K. D. (1997) – *Fundamentals of Structural Mechanics.* Prentice-Hall, Upper Saddle River, NJ.

[2] SALENÇON, J. (2001) – *Handbook of Continuum Mechanics*. Springer-Verlag, Berlin, Heidelberg, New York.

[3] LUBLINER, J. – (1990) – *Plasticity Theory*. MacMillan Publ. Company, New York.

Chapter XI

Yield Design of plates Subjected to pure bending

The Yield Design problem
Implementation of the Yield Design theory
Strength criteria and π functions
Final comments
References

YIELD DESIGN of PLATES
Subjected to pure bending

The Yield Design analysis of plates subjected to bending is performed within the framework of the out-of-plane equilibrium equations and virtual work equation. In the case when the strength criterion only refers to the internal moment tensor the relevant virtual motions comply with the Kirchhoff-Love condition: they are defined by the continuous and piecewise continuously differentiable virtual transversal velocity field of the director sheet. A particularly important class of relevant virtual motions is obtained through the concept of hinge lines introduced by Johansen.

1 The Yield Design problem

1.1 General outline

"Plastic analysis" for metal plates [*e.g.* 1-4], "Yield line theory" for thin reinforced concrete slabs [*e.g.* 5-7], have been commonly used for the dimensioning of such structural elements subjected to pure bending due to the action of distributed or concentrated normal forces. The corresponding methods can here be presented jointly within the general framework of the Yield Design theory applied to the two-dimensional continuum plate modelling introduced in Chapter X.

It may be recalled that the in-plane and the out-of-plane Equilibrium equations of this two-dimensional continuum are independent of each other. Usually, at least in the pre-dimensioning stage, the strength criterion of the two-dimensional constituent material of the model only concerns the components $\underline{V}(\underline{s})$ and $\underline{\underline{M}}(\underline{s})$ of the tensorial wrench of internal forces, without any reference to the tensor of membrane forces $\underline{\underline{N}}(\underline{s})$. As already explained in Chapter IX (Section 2.2) this means that the membrane forces suffer no limitation: therefore the two-dimensional Yield Design analysis of plates subjected to pure bending will be performed within the only framework of the out-of-plane Equilibrium equations with the corresponding restricted expression of the equation of virtual work.

1.2 Settlement of the problem

Geometrical data

The Yield Design problem is defined on a system S with surface S and boundary ∂S in the plane director sheet (D). This geometric description encompasses the

supports which link the system to the external world defined as motionless. These supports are situated along ∂S and they are characterised mechanically by their strength condition which may be bilateral or unilateral, simple, rigid… as sketched in Figure 1 in the case of a built-in support.

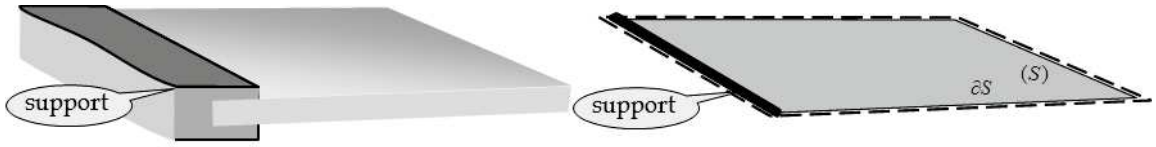

Figure 1. A plate with a built-in support

Loading mode

The external forces applied to the system consist of distributed loads and distributed moments; concentrated loads will be considered in § 4.1 as a limit case. The loading mode of the system is a multi-parameter one as described in Chapter IV (1.2).

Resistance of the constituent material

In the same way as for the curvilinear one-dimensional media studied in Chapter IX, the counterpart of the Cauchy stress tensor in the general theory is now the wrench of internal forces $\left[\mathbb{X}(\underline{s})\right]$. The resistance of the constituent material is thus defined through a domain $\mathcal{G}(\underline{s})$ which, in the case of pure bending, usually only refers to the component $\underline{\underline{M}}(\underline{s})$ of the tensorial wrench $\left[\mathbb{X}(\underline{s})\right]$, thus assuming no limitation to the shear force vector:

$$(1) \qquad \left[\mathbb{X}(\underline{s})\right] \in \mathcal{G}(\underline{s}) \Leftrightarrow f\left(\underline{s}, \underline{\underline{M}}(\underline{s})\right) \leq 0 \Leftrightarrow \underline{\underline{M}}(\underline{s}) \in G(\underline{s}) .$$

When the "micro-macro" modelling process presented in Chapter X (Section 4) is physically feasible, the strength criterion of the two-dimensional constituent material is derived from the strength domain of the three-dimensional continuum through an auxiliary Yield Design problem where the components of $\underline{\underline{M}}(\underline{s})$ play the role of loading parameters, recalling that in this process, consistently with the result established in Section X.4, $\underline{\underline{M}}(\underline{s})$ is symmetric with components given by Eq. (X. 66).

This is the case for instance for transversally homogeneous plates made of a material obeying the von Mises criterion or the Tresca criterion: the corresponding two-dimensional criteria for $\underline{\underline{M}}(\underline{s})$ comes out in the same form as the plane stress criteria of the three-dimensional medium (*cf.* § 3.1).

In other cases such as for thin reinforced concrete slabs, the strength criterion proceeds directly from (possibly heuristic) theoretical or experimental analyses at the macroscopic level (*cf.* §. 3.2).

As a matter of fact, although the symmetry of the tensor $\underline{\underline{M}}(\underline{s})$ has not been established in the general case, it turns out that the implementation of the Yield Design theory to this model has been performed within the symmetry assumption.

Therefore **symmetry of the tensor of internal moments will be assumed from now on:** $\underline{\underline{M}}(\underline{s}) = {}^{t}\underline{\underline{M}}(\underline{s})$.

For the supports with the notations of § 2.1 in Chapter X, considering the pure bending problem, the strength condition only sets limits onto $R(\underline{s})$, the out-of-plane component of the line density of external forces, and $\underline{H}(\underline{s})$, the in-plane distributed moment line density.

According to Eq. (64) in Chapter X, this results in a condition for $\left[\mathbb{X}(\underline{s})\right]$ in the form

$$\left[\mathbb{X}(\underline{s})\right].\underline{n}(\underline{s}) \in \mathcal{G}_s(\underline{s}) \Leftrightarrow f_s\left(\underline{s}, V(\underline{s},\underline{n}), \underline{\Gamma}(\underline{s},\underline{n})\right) \le 0 \tag{2}$$

which only concerns $V(\underline{s},\underline{n})$ and $\underline{\Gamma}(\underline{s},\underline{n})$ where $\underline{n}$ denotes the outward normal to the boundary of the system at the considered point.

2 Implementation of the Yield Design theory

2.1 Interior approach

The implementation of the interior approach strictly follows the same pattern as in the general theory (Chapter IV, Section 2). Statically admissible fields $\underline{V}(\underline{s})$ and $\underline{\underline{M}}(\underline{s})$ must be constructed in S which comply with the strength criteria of the constituent material and supports of the system.

Not surprisingly, performing the interior approach in order to obtain lower bounds for the extreme loads often requires some good academic skill, which explains why this method is not currently used in daily practice. The importance of such solutions is evident regarding the assessment of the Yield Design dimensioning of plates. A survey of the most important contributions in this field may be found in [8-11]: let us mention [12-17].

2.2 Exterior approach

Kinematically admissible virtual motions

Virtual motions of the considered two-dimensional model have been defined in Chapter X (§ 3.1) by means of piecewise continuous and continuously differentiable fields $\underline{\hat{u}}(\underline{s}), \hat{w}(\underline{s})$ and $\underline{\hat{\omega}}(\underline{s})$ on S in the form of a virtual velocity distributor field

$$\left\{\hat{\mathbb{U}}(\underline{s})\right\} = \left\{P, \underline{\hat{U}}(\underline{s}), \underline{\hat{\Omega}}(\underline{s})\right\} = \left\{P, \underline{\hat{u}}(\underline{s}) + \hat{w}(\underline{s})\underline{e}_3, \underline{\hat{\omega}}(\underline{s})\right\} . \tag{3}$$

Maximum resisting work for the system

Recalling the symmetry of $\underline{\underline{M}}(\underline{s})$ and that $\underline{\hat{v}}(\underline{s}) = \underline{e}_3 \wedge \underline{\hat{\omega}}(\underline{s})$, the resisting work by the internal forces in the system in a virtual motion (3) comes out from Eq. (X, 53) in S and along the discontinuity lines $L_{\hat{w}}$ and $L_{\underline{\hat{\omega}}}$, with the addition of the contribution of the supports along ∂S:

$$(4)\qquad -\mathcal{P}_{\mathrm{i}}(\hat{\underline{u}},\hat{w},\hat{\underline{v}}) = \int_S \underline{\underline{N}}(\underline{s}):\underline{\underline{\partial\hat{u}}}(\underline{s})\,\mathrm{d}S + \int_{L_{\hat{\underline{u}}}} \underline{n}(\underline{s}).\underline{\underline{N}}(\underline{s}).[\![\hat{\underline{u}}(\underline{s})]\!]\,\mathrm{d}L$$
$$+\int_S \underline{V}(\underline{s}).\left(\underline{\partial\hat{w}}(\underline{s}) - \hat{\underline{v}}(\underline{s})\right)\mathrm{d}S + \int_{L_{\hat{w}}+\partial S} \underline{V}(\underline{s}).[\![\hat{w}(\underline{s})]\!]\underline{n}(\underline{s})\,\mathrm{d}L$$
$$+\int_S \underline{\underline{M}}(\underline{s}):\underline{\underline{\partial\hat{v}}}(\underline{s})\,\mathrm{d}S + \int_{L_{\hat{\underline{\omega}}}+\partial S} [\![\hat{\underline{v}}(\underline{s})]\!].\underline{\underline{M}}(\underline{s}).\underline{n}(\underline{s})\,\mathrm{d}L.$$

The "external world" being assumed to be motionless, the jumps in the integrals related to the supports are $[\![\hat{w}(\underline{s})]\!] = -\hat{w}(\underline{s})$ and $[\![\hat{\underline{v}}(\underline{s})]\!] = \underline{e}_3 \wedge [\![\hat{\underline{\omega}}(\underline{s})]\!] = -\underline{e}_3 \wedge \hat{\underline{\omega}}(\underline{s})$ along ∂S.

The maximum resisting work in a given virtual motion of the system is obtained as the sum of the maximums of the integrals in Eq. (4) under the constraint of the strength criteria (1) and (2), which introduces the corresponding π functions:

$$(5)\qquad \begin{cases} \pi\left(\underline{\underline{\partial\hat{u}}}(\underline{s})\right) = +\infty \ \text{ if } \ \underline{\underline{\partial\hat{u}}}(\underline{s}) \neq 0 \\ \pi\left(\underline{\underline{\partial\hat{u}}}(\underline{s})\right) = 0 \ \text{ if } \ \underline{\underline{\partial\hat{u}}}(\underline{s}) = 0 \\ \pi\left(\underline{n}(\underline{s}),[\![\hat{\underline{u}}(\underline{s})]\!]\right) = +\infty \ \text{ if } \ [\![\hat{\underline{u}}(\underline{s})]\!] \neq 0 \\ \pi\left(\underline{n}(\underline{s}),[\![\hat{\underline{u}}(\underline{s})]\!]\right) = 0 \ \text{ if } \ [\![\hat{\underline{u}}(\underline{s})]\!] = 0 \end{cases}$$

$$(6)\qquad \begin{cases} \pi\left(\underline{\partial\hat{w}}(\underline{s}) - \hat{\underline{v}}(\underline{s})\right) = +\infty \ \text{ if } \ \underline{\partial\hat{w}}(\underline{s}) - \hat{\underline{v}}(\underline{s}) \neq 0 \\ \pi\left(\underline{\partial\hat{w}}(\underline{s}) - \hat{\underline{v}}(\underline{s})\right) = 0 \ \text{ if } \ \underline{\partial\hat{w}}(\underline{s}) - \hat{\underline{v}}(\underline{s}) = 0 \\ \pi\left(\underline{n}(\underline{s}),[\![\hat{w}(\underline{s})]\!]\right) = +\infty \ \text{ if } \ [\![\hat{w}(\underline{s})]\!] \neq 0 \\ \pi\left(\underline{n}(\underline{s}),[\![\hat{w}(\underline{s})]\!]\right) = 0 \ \text{ if } \ [\![\hat{w}(\underline{s})]\!] = 0 \end{cases}$$

$$(7)\qquad \begin{cases} \pi\left(\underline{\underline{\partial\hat{v}}}(\underline{s})\right) = \mathrm{Sup}\left\{ \underline{\underline{M'}}:\underline{\underline{\partial\hat{v}}}(\underline{s}) \,\middle|\, \underline{\underline{M'}} \in G(\underline{s}) \right\} \\ \pi\left(\underline{n}(\underline{s}),[\![\hat{\underline{v}}(\underline{s})]\!]\right) = \mathrm{Sup}\left\{ [\![\hat{\underline{v}}(\underline{s})]\!].\underline{\underline{M'}}.\underline{n}(\underline{s}) \,\middle|\, \underline{\underline{M'}} \in G(\underline{s}) \right\} \end{cases}$$

$$(8)\qquad \pi_{\mathrm{s}}([\![\hat{w}]\!],[\![\hat{\underline{\omega}}]\!]) = \mathrm{Sup}\left\{ V'[\![\hat{w}]\!] + \underline{\Gamma'}.[\![\hat{\underline{\omega}}]\!] \,\middle|\, (V',\underline{\Gamma'}) \in \mathcal{G}_{\mathrm{s}}(\underline{s}) \right\}.$$

Relevant virtual motions

The description of the relevant virtual motions of the system for the kinematic Yield Design exterior approach, as defined in Chapter VI (Section 2), follows from Eqs (5)-(8). In S the relevance conditions are:

$$(9)\qquad \begin{cases} \underline{\underline{\partial\hat{u}}}(\underline{s}) \equiv 0, \ \ [\![\hat{\underline{u}}(\underline{s})]\!] \equiv 0 \\ \underline{\partial\hat{w}}(\underline{s}) - \hat{\underline{v}}(\underline{s}) \equiv 0, \ \ [\![\hat{w}(\underline{s})]\!] \equiv 0. \end{cases}$$

In plain words this means that for a kinematically admissible virtual motion to be relevant for the strength condition (1) no virtual motion should occur in the plane of the director sheet and the Kirchhoff-Love condition must be identically satisfied [18]. It is clear that these mathematical conditions, just derived from the corresponding expressions of the π functions for the efficiency of the exterior approach, do not pertain to any constitutive equation as internal constraints.

Consequently, the relevant virtual motions of the system are defined in S by the **continuous** and **piecewise continuously differentiable scalar field** $\hat{w}(\underline{s})$ **only**.

It follows that in the relevant virtual motions the integrals of $\pi\left(\underline{\underline{\partial}}\hat{\underline{v}}(\underline{s})\right)$ and $\pi\left(\underline{n}(\underline{s}),[\![\,\hat{\underline{v}}(\underline{s})\,]\!]\right)$ in the expression of the maximum resisting work of the system will take the second line of Eq. (9) into account.

- Regarding $\pi\left(\underline{\underline{\partial}}\hat{\underline{v}}(\underline{s})\right)$ we get

$$\pi\left(\underline{\underline{\partial}}\hat{\underline{v}}(\underline{s})\right)=\mathrm{Sup}\left\{\underline{\underline{M}}'\colon \underline{\underline{\partial^2}}\hat{w}(\underline{s})\;\middle|\;\underline{\underline{M}}'\in G(\underline{s})\right\} \tag{10}$$

where $\underline{\underline{\partial^2}}\hat{w}(\underline{s})$ is the **virtual rate of curvature tensor** of the director sheet

$$\underline{\underline{\partial^2}}\hat{w}(\underline{s})=\underline{\underline{\hat{\chi}}}(\underline{s}) \tag{11}$$

and we write

$$\pi\left(\underline{\underline{\partial}}\hat{\underline{v}}(\underline{s})\right)=\pi\left(\underline{\underline{\hat{\chi}}}(\underline{s})\right)=\mathrm{Sup}\left\{\underline{\underline{M}}'\colon \underline{\underline{\hat{\chi}}}(\underline{s})\;\middle|\;\underline{\underline{M}}'\in G(\underline{s})\right\}. \tag{12}$$

- Regarding $\pi\left(\underline{n},[\![\,\hat{\underline{v}}\,]\!]\right)=\pi\left(\underline{n},[\![\,\underline{\underline{\partial}}\hat{w}\,]\!]\right)$

Define $\underline{t}(\underline{s})$, the unit tangential vector to $L_{\hat{\omega}}=L_{\underline{\underline{\partial}}\hat{w}}$ at the point P, in such a way that $\left(\underline{t}(\underline{s}),\,\underline{n}(\underline{s}),\,\underline{e}_3\right)$ be a right-handed triad. Since Eq. (9) states that $\hat{w}(\underline{s})$ is continuous we have, from Hadamard's compatibility condition along $L_{\hat{\omega}}=L_{\underline{\underline{\partial}}\hat{w}}$ (*cf.* [19])

$$[\![\,\hat{w}(\underline{s})\,]\!]=0\;\Rightarrow\;[\![\,\underline{\underline{\partial}}\hat{w}(\underline{s})\,]\!].\underline{t}(\underline{s})=0 \tag{13}$$

that is

$$[\![\,\hat{\underline{v}}(\underline{s})\,]\!]=[\![\,\underline{\underline{\partial}}\hat{w}(\underline{s})\,]\!]=\hat{\theta}(\underline{s})\,\underline{n}(\underline{s}) \tag{14}$$

and consequently, since $\hat{\underline{v}}(\underline{s})=\underline{e}_3\wedge\hat{\underline{\omega}}(\underline{s})$,

$$[\![\,\hat{\underline{\omega}}(\underline{s})\,]\!]=\hat{\theta}(\underline{s})\,\underline{t}(\underline{s}). \tag{15}$$

This means that the Kirchhoff-Love condition implies that the discontinuity of the virtual rotation rate is tangent to the discontinuity line (Figure 2).

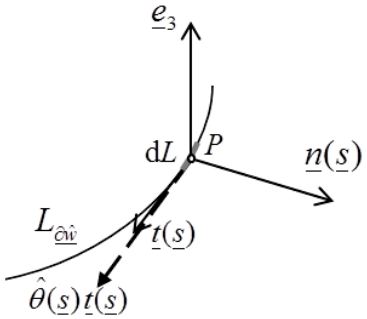

Figure 2. Relevant discontinuity of the virtual rotation rate

Hence $\pi(\underline{n}, [\![\underline{\hat{v}}]\!]) = \pi(\underline{n}, [\![\underline{\partial \hat{w}}]\!])$ becomes

$$\pi(\underline{n}(\underline{s}), [\![\underline{\hat{v}}(\underline{s})]\!]) = \pi(\underline{n}(\underline{s}), \hat{\theta}(\underline{s})) = \mathrm{Sup}\left\{ \hat{\theta}(\underline{s})\, \underline{\underline{M'}} : (\underline{n}(\underline{s}) \otimes \underline{n}(\underline{s})) \,\middle|\, \underline{\underline{M'}} \in G(\underline{s}) \right\}. \tag{16}$$

- Regarding the supports

the conditions of relevance will be studied in more details in § 3.3 depending on the explicit form of the strength criterion but they all include the condition:

$$[\![\underline{\hat{u}}(\underline{s})]\!] \equiv 0. \tag{17}$$

Finally the maximum resisting work in a relevant virtual motion of the system is given by:

$$\mathcal{P}_{\mathrm{mr}}(\hat{w}) = \int_S \pi(\underline{\underline{\hat{\chi}}}(\underline{s}))\, \mathrm{d}S + \int_{L_{\underline{\hat{\omega}}}} \pi(\underline{n}(\underline{s}), \hat{\theta}(\underline{s}))\, \mathrm{d}L + \int_{\partial S} \pi_{\mathrm{s}}([\![\hat{w}]\!], [\![\underline{\hat{\omega}}]\!])\, \mathrm{d}L. \tag{18}$$

3 Strength criteria and π functions

In view of the abundant literature devoted to the determination and formulation of the strength criteria for plates subjected to bending, this Section will concentrate on the presentation of the most commonly used criteria with the corresponding π functions to be implemented in the Yield Design approach. The reader may refer to such exhaustive textbooks as [8, 9] or [20] for extensive lists of references.

3.1 Metal plates

The Tresca and von Mises strength criteria for metal plates subjected to pure bending are derived from the three-dimensional strength criteria of the constituent material through the "micro-macro" modelling process described in Chapter X (Section 4).

In the case when the constituent material is homogeneous following the transverse direction $\underline{e}_3$, the director sheet is positioned as the medium plane of the plate. The three-dimensional stress state is a plane stress one. It is discontinuous when crossing the medium plane: above and below this plane the stress fields are constant opposite limit state fields with respect to the strength criterion (Figure 3).
The result for the two-dimensional strength criteria concerning $\underline{\underline{M}}(\underline{s})$ comes through Eq. (68) of Chapter X and has exactly the same form as the plane stress strength criteria of the three-dimensional constituent material.

The corresponding criteria are sometimes referred to as **Tresca Plates** and **von Mises Plates**.

From the Yield Design viewpoint these plates are **isotropic** and their strength criteria are symmetric functions of the principal internal moments M_1 and M_2 [1].

[1] Equivalently, they are functions of the invariants of the internal moment tensor but the corresponding formulation is rarely used in practice.

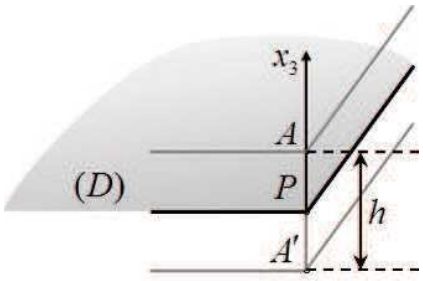

Figure 3. Director sheet for a homogeneous metal plate

Tresca Plates

The strength criterion is written

$$\underline{\underline{M}} \in G(\underline{s}) \Leftrightarrow f(\underline{s},\underline{\underline{M}}) = \mathrm{Sup}\left\{ |M_1|, |M_2|, |M_1 - M_2| \right\} - m_0(\underline{s}) \leq 0 \tag{19}$$

with $m_0(\underline{s}) = \sigma_0(\underline{s})\, h^2/4$, where $\sigma_0(\underline{s})$ is the resistance of the three-dimensional material under simple tension and h is the thickness of the plate (Figure 4).

The corresponding π functions are derived from Eq. (19) through Eqs (12) and (16)

$$\begin{cases} \pi(\underline{s},\underline{\underline{\hat{\chi}}}) = m_0(\underline{s})\,\mathrm{Sup}\left\{ |\hat{\chi}_1|, |\hat{\chi}_2|, |\hat{\chi}_1 + \hat{\chi}_2| \right\} \\ \pi(\underline{s},\underline{n},\hat{\theta}) = m_0(\underline{s}) \left| \hat{\theta} \right|. \end{cases} \tag{20}$$

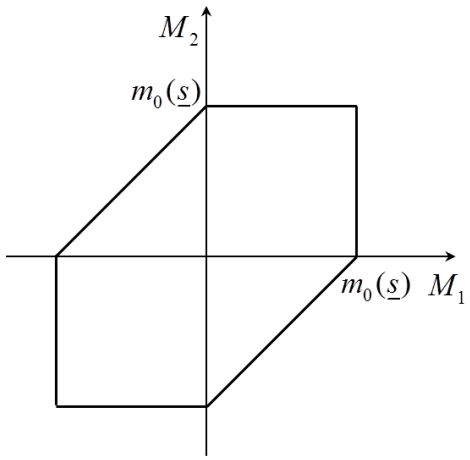

Figure 4. Tresca's strength criterion for plates subjected to pure bending

Von Mises Plates

The strength criterion is written (Figure 5):

$$\underline{\underline{M}} \in G(\underline{s}) \Leftrightarrow f(\underline{s},\underline{\underline{M}}) = {M_1}^2 + {M_2}^2 - M_1 M_2 - \frac{3}{4} {m_0}^2(\underline{s}) \leq 0, \tag{21}$$

with $m_0(\underline{s}) = \sigma_0(\underline{s})\, h^2/2\sqrt{3} = k(\underline{s})\, h^2/2$, where $\sigma_0(\underline{s})$ is the resistance under simple tension and $k(\underline{s})$ is the resistance under simple shear of the three-dimensional constituent material (*cf.* Chapter IV, § 4.1).

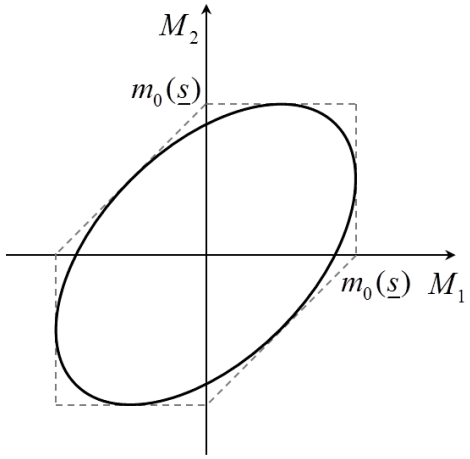

Figure 5. von Mises' strength criterion for plates subjected to pure bending

In the same way as above we get the corresponding π functions:

$$\begin{cases} \pi(\underline{s},\hat{\underline{\underline{\chi}}}) = m_0(\underline{s})\sqrt{\hat{\chi}_1^{\,2} + \hat{\chi}_2^{\,2} + \hat{\chi}_1\hat{\chi}_2} \\ \pi(\underline{s},\underline{n},\hat{\theta}) = m_0(\underline{s})\left|\hat{\theta}\right|. \end{cases} \tag{22}$$

3.2 Reinforced concrete slabs

Mechanical description

Figure 6 is a schematic representation of a concrete slab reinforced in two mutually orthogonal directions (x) and (y). In each direction, the reinforcement consists of two layers (upper and lower) of iron bars which are responsible for the resistance of the reinforced concrete as a composite constituent material under simple tension in the corresponding direction.

For the Yield Design analysis of such slabs subjected to pure bending, it is necessary to determine the strength criterion $f((\underline{s}),\underline{\underline{M}}(\underline{s}))$ for the reinforced concrete slab element as a constituent material. The most usual form was introduced by Johansen [4, 5] from experimental data and through a heuristic and theoretical approach, mostly from a virtual kinematics viewpoint.

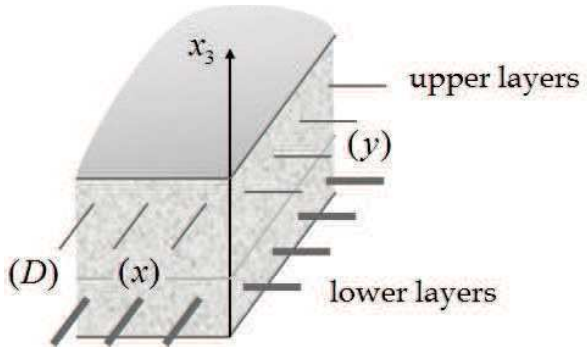

Figure 6. Reinforced concrete slab

Maximum resisting bending moments

Let us first consider at point P a relevant virtual jump of the rotation rate, in the form of Eq. (15), $[\![\, \underline{\hat{\omega}}(\underline{s}) \,]\!] = \hat{\theta}(\underline{s})\underline{t}(\underline{s})$, with $\underline{t}(\underline{s})$ along one of the reinforcement directions, namely (x) for example (Figure 7).

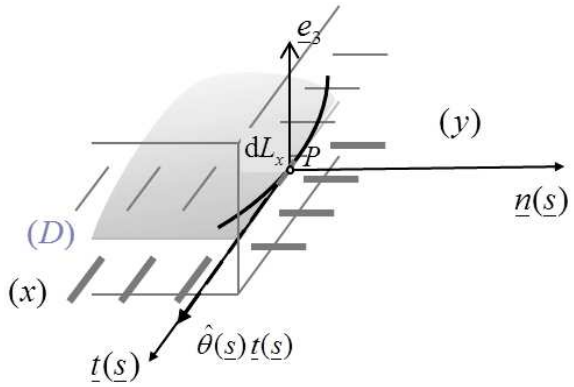

Figure 7. Rotation rate jump along a reinforcement direction

The maximum resisting bending moment that can be developed in this virtual motion is governed and determined by the resistance to traction generated by the reinforcement layers in the (y) direction:

lower layer for $\hat{\theta}(\underline{s}) \geq 0$

upper layer for $\hat{\theta}(\underline{s}) \leq 0$.

Denoting by $m_y^+(\underline{s})$ and $m_y^-(\underline{s})$ respectively the **algebraic values** of these two maximum resisting bending moments, we obtain the maximum resisting work for the element $\mathrm{d}L = \mathrm{d}L_x$ in the considered relevant virtual motion:

$$\begin{cases} \hat{\theta}(\underline{s})\, m_y^+(\underline{s})\, \mathrm{d}L_x & \text{if } \hat{\theta}(\underline{s}) \geq 0 \\ \hat{\theta}(\underline{s})\, m_y^-(\underline{s})\, \mathrm{d}L_x & \text{if } \hat{\theta}(\underline{s}) \leq 0. \end{cases} \tag{23}$$

In the same way, for $\underline{t}(\underline{s})$ along the (y) reinforcement direction, the **algebraic values** $m_x^+(\underline{s})$ and $m_x^-(\underline{s})$ are defined and determined from the reinforcement layers in the (x) reinforcement direction and the maximum resisting work for the element $\mathrm{d}L = \mathrm{d}L_y$ is written:

$$\begin{cases} \hat{\theta}(\underline{s})\, m_x^+(\underline{s})\, \mathrm{d}L_y & \text{if } \hat{\theta}(\underline{s}) \geq 0 \\ \hat{\theta}(\underline{s})\, m_x^-(\underline{s})\, \mathrm{d}L_y & \text{if } \hat{\theta}(\underline{s}) \leq 0. \end{cases} \tag{24}$$

We now consider the general case when $\underline{t}(\underline{s})$ is no longer along one of the reinforcement directions (Figure 8).

With $(\underline{t}(\underline{s}), \underline{n}(\underline{s}), \underline{e}_3)$ a right-handed triad, we introduce the unit vectors $\underline{e}_x$ and $\underline{e}_y$ along the (x) and (y) directions such that $\underline{n}(\underline{s})$ has positive components and may be written

$$\underline{n}(\underline{s}) = \underline{e}_x \cos\alpha(\underline{s}) + \underline{e}_y \sin\alpha(\underline{s}),\ 0 \le \alpha(\underline{s}) \le \pi/2 \tag{25}$$

while $\mathrm{d}L_x$ and $\mathrm{d}L_y$ are the projections of $\mathrm{d}L$ onto the (x) and (y) directions

$$\mathrm{d}L_x = \mathrm{d}L \sin\alpha(\underline{s}),\ \mathrm{d}L_y = \mathrm{d}L \cos\alpha(\underline{s}). \tag{26}$$

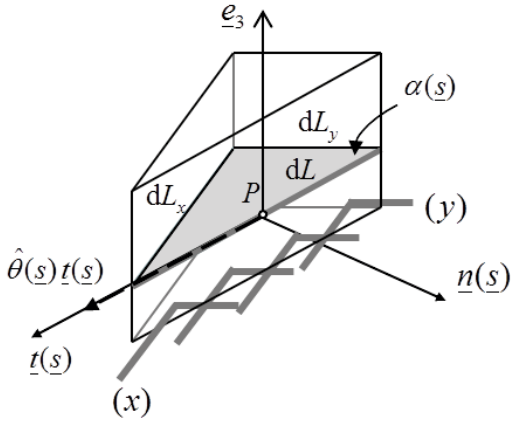

Figure 8. Rotation rate jump in the general case

The maximum resisting bending moment that can be developed in this relevant virtual motion is now governed and determined by the maximum resistance to traction in the direction $\underline{n}(\underline{s})$ which can be provided by both reinforcement directions, in the lower layers if $\hat{\theta}(\underline{s}) \ge 0$ or in the upper layer if $\hat{\theta}(\underline{s}) \le 0$. This amounts to summing the projections onto $\underline{n}(\underline{s})$ of the resistances developed in the (x) and (y) directions, taking into account the corresponding effective sections, $\mathrm{d}L_y$ and $\mathrm{d}L_x$ respectively.

Thus, the maximum resisting work for the element $\mathrm{d}L$ in the general case is[2]

$$\begin{cases} \hat{\theta}(\underline{s})\left(m_x^{+}(\underline{s})\cos^2\alpha(\underline{s}) + m_y^{+}(\underline{s})\sin^2\alpha(\underline{s})\right)\mathrm{d}L & \text{if } \hat{\theta}(\underline{s}) \ge 0 \\ \hat{\theta}(\underline{s})\left(m_x^{-}(\underline{s})\cos^2\alpha(\underline{s}) + m_y^{-}(\underline{s})\sin^2\alpha(\underline{s})\right)\mathrm{d}L & \text{if } \hat{\theta}(\underline{s}) \le 0. \end{cases} \tag{27}$$

Combining Eqs (16) and (27) we have, with simplified notations

$$\pi(\underline{n}, \hat{\theta}) = \mathrm{Sup}\left\{ \hat{\theta}\,\underline{\underline{M}}' : (\underline{n} \otimes \underline{n}) \,\middle|\, \underline{\underline{M}}' \in G \right\} = \begin{cases} \hat{\theta}\left(m_x^{+}\cos^2\alpha + m_y^{+}\sin^2\alpha\right) & \text{if } \hat{\theta} \ge 0 \\ \hat{\theta}\left(m_x^{-}\cos^2\alpha + m_y^{-}\sin^2\alpha\right) & \text{if } \hat{\theta} \le 0 \end{cases} \tag{28}$$

where G denotes the strength criterion to be determined for the composite constituent material.

[2] Note that the reasoning performed here is identical to the calculation of the normal stress on a facet with normal $\underline{n}$ when the principal stresses are given, within the framework of two-dimensional continuum mechanics.

Formally, it is possible to introduce the symmetric second rank tensors $\underline{\underline{m}}^+$ and $\underline{\underline{m}}^-$ defined by

$$\begin{cases} \underline{\underline{m}}^+ = m_x^+ \underline{e}_x \otimes \underline{e}_x + m_y^+ \underline{e}_y \otimes \underline{e}_y \\ \underline{\underline{m}}^- = m_x^- \underline{e}_x \otimes \underline{e}_x + m_y^- \underline{e}_y \otimes \underline{e}_y \end{cases} \tag{29}$$

so that Eq. (28) takes the reduced form

$$\pi(\underline{n}, \hat{\theta}) = \mathrm{Sup}\left\{ \hat{\theta}\, \underline{\underline{M}}' : (\underline{n} \otimes \underline{n}) \,\middle|\, \underline{\underline{M}}' \in G \right\} = \begin{cases} \hat{\theta}\, \underline{\underline{m}}^+ : (\underline{n} \otimes \underline{n}) \ \text{ if } \ \hat{\theta} \geq 0 \\ \hat{\theta}\, \underline{\underline{m}}^- : (\underline{n} \otimes \underline{n}) \ \text{ if } \ \hat{\theta} \leq 0. \end{cases} \tag{30}$$

Strength criterion

Eq. (30) is equivalent to

$$\begin{cases} \mathrm{Sup}\left\{ \underline{\underline{M}}' : (\underline{n} \otimes \underline{n}) \,\middle|\, \underline{\underline{M}}' \in G \right\} = \underline{\underline{m}}^+ : (\underline{n} \otimes \underline{n}) \\ \mathrm{Inf}\left\{ \underline{\underline{M}}' : (\underline{n} \otimes \underline{n}) \,\middle|\, \underline{\underline{M}}' \in G \right\} = \underline{\underline{m}}^- : (\underline{n} \otimes \underline{n}) \end{cases} \tag{31}$$

or, in other words, with $\underline{n}$ satisfying Eq. (25),

$$\left\{ \underline{\underline{M}}' \in G \right\} \subset \left\{ \forall \underline{n},\ \underline{\underline{m}}^- : (\underline{n} \otimes \underline{n}) \leq \underline{\underline{M}}' : (\underline{n} \otimes \underline{n}) \leq \underline{\underline{m}}^+ : (\underline{n} \otimes \underline{n}) \right\}. \tag{32}$$

Owing to the symmetry of the internal moment tensor $\underline{\underline{M}}$, Eq. (32) can be represented in the three-dimensional space with coordinates $M_{xx}, M_{yy}, \sqrt{2} M_{xy}$ where it describes the intersection of two circular cones with rectangular vertices at the points $\underline{\underline{m}}^+$ and $\underline{\underline{m}}^-$ respectively and with axes parallel to the bisector of the M_{xx} and M_{yy} axes in the (M_{xx}, M_{yy}) plane (Figure 9).

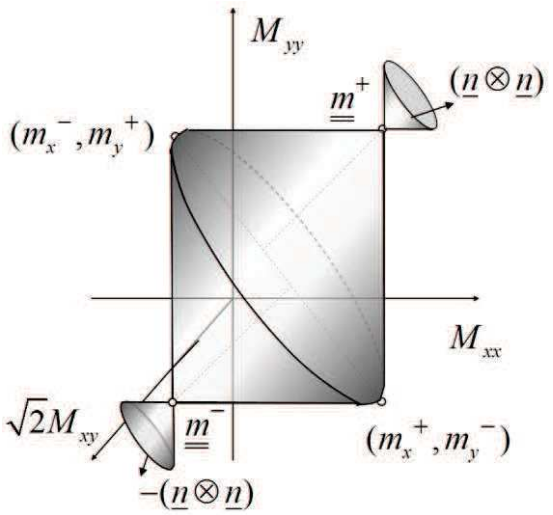

Figure 9. Johansen strength criterion

The **Johansen strength criterion** for such reinforced concrete slabs takes Eq. (32) as the definition of the strength criterion:

$$(33)\qquad \underline{\underline{M}}(\underline{s}) \in G(\underline{s}) \;\Leftrightarrow\; \left\{ \forall \underline{n} \text{ s. t. (25)},\ \underline{\underline{m}}^{-}(\underline{s}):(\underline{n}\otimes\underline{n}) \le \underline{\underline{M}}(\underline{s}):(\underline{n}\otimes\underline{n}) \le \underline{\underline{m}}^{+}(\underline{s}):(\underline{n}\otimes\underline{n}) \right\}$$

which means that the limit of resistance at a point P is reached when, at least for one particular direction $\underline{t}(\underline{s})$ and the associated normal $\underline{n}(\underline{s})$ (*cf.* Figure 8), the bending moment $M_{nn}(\underline{s})$ reaches its maximum positive value or its minimum negative value.

This criterion is **orthotropic** with the (x) and (y) directions as principal axes of orthotropy. Explicitly,

$$(34)\qquad \underline{\underline{M}} \in G \;\Leftrightarrow\; \begin{cases} (m_x^{+} - M_{xx})^{1/2}(m_y^{+} - M_{yy})^{1/2} \ge \left| M_{xy} \right| \\ (M_{xx} - m_x^{-})^{1/2}(M_{yy} - m_y^{-})^{1/2} \ge \left| M_{xy} \right|. \end{cases}$$

It is **isotropic** if $\underline{\underline{m}}^{+}(\underline{s})$ and $\underline{\underline{m}}^{-}(\underline{s})$ are isotropic tensors *i.e.* if $m_x{}^{+}(\underline{s}) = m_y{}^{+}(\underline{s}) = m^{+}(\underline{s})$ and $m_x{}^{-}(\underline{s}) = m_y{}^{-}(\underline{s}) = m^{-}(\underline{s})$. We get then for the strength criterion

$$(35)\qquad \underline{\underline{M}}(\underline{s}) \in G(\underline{s}) \;\Leftrightarrow\; \left\{ \forall \underline{n},\ m^{-}(\underline{s}) \le \underline{\underline{M}}(\underline{s}):(\underline{n}\otimes\underline{n}) \le m^{+}(\underline{s}) \right\}$$

and

$$(36)\qquad \underline{\underline{M}} \in G \;\Leftrightarrow\; \begin{cases} (m^{+} - M_{xx})^{1/2}(m^{+} - M_{yy})^{1/2} \ge \left| M_{xy} \right| \\ (M_{xx} - m^{-})^{1/2}(M_{yy} - m^{-})^{1/2} \ge \left| M_{xy} \right|. \end{cases}$$

An extensive analysis with full description of the corresponding π functions appears in [9].

π functions for the orthotropic Johansen criterion

Let us consider the case when the virtual principal rates of curvature $\hat{\chi}_1$ and $\hat{\chi}_2$ are of the same sign, either positive or negative.

- $\hat{\chi}_1 > 0, \hat{\chi}_2 > 0$ which implies $\hat{\chi}_{xx} > 0, \hat{\chi}_{yy} > 0$

We first note that the outward normal cone to the strength domain at the vertex $\underline{\underline{m}}^{+}$ is defined by the condition

$$(37)\qquad \sqrt{\underline{\underline{\hat{\chi}}}:\underline{\underline{\hat{\chi}}}} \le \operatorname{tr} \underline{\underline{\hat{\chi}}} \le \sqrt{2\,\underline{\underline{\hat{\chi}}}:\underline{\underline{\hat{\chi}}}}$$

which is satisfied (only) when $\hat{\chi}_1 > 0, \hat{\chi}_2 > 0$. It follows that the π function for any virtual rate of curvature tensor such that $\hat{\chi}_1 > 0, \hat{\chi}_2 > 0$ is written

$$(38)\qquad \pi(\underline{\underline{\hat{\chi}}}) = m_x{}^{+}\hat{\chi}_{xx} + m_y{}^{+}\hat{\chi}_{yy}$$

- $\hat{\chi}_1 < 0, \hat{\chi}_2 < 0$

In the same way we have, from the $\underline{\underline{m}}^-$ vertex,

$$\pi(\underline{\underline{\hat{\chi}}}) = m_x^- \hat{\chi}_{xx} + m_y^- \hat{\chi}_{yy}. \tag{39}$$

Regarding **anticlastic** virtual rate of curvature tensors (*i.e.* principal curvatures of opposite signs), we may mention the case when the twist component $\hat{\chi}_{xy}$ is equal to zero; $\hat{\chi}_{xx}$ and $\hat{\chi}_{yy}$ are the principal virtual rates of curvature and the π function is written

$$\begin{cases} \pi(\underline{\underline{\hat{\chi}}}) = m_x^+ \hat{\chi}_{xx} + m_y^- \hat{\chi}_{yy} \ \text{ if } \ \hat{\chi}_{xx} \geq 0,\ \hat{\chi}_{yy} \leq 0,\ \hat{\chi}_{xy} = 0 \\ \pi(\underline{\underline{\hat{\chi}}}) = m_x^- \hat{\chi}_{xx} + m_y^+ \hat{\chi}_{yy} \ \text{ if } \ \hat{\chi}_{xx} \leq 0,\ \hat{\chi}_{yy} \geq 0,\ \hat{\chi}_{xy} = 0. \end{cases} \tag{40}$$

For the virtual rotation jumps the π functions proceed from Eq. (30):

$$\pi(\underline{s}, \underline{n}, \hat{\theta}) = \begin{cases} \hat{\theta}\, \underline{\underline{m}}^+(\underline{s}) : (\underline{n} \otimes \underline{n}) \ \text{ if } \ \hat{\theta} \geq 0 \\ \hat{\theta}\, \underline{\underline{m}}^-(\underline{s}) : (\underline{n} \otimes \underline{n}) \ \text{ if } \ \hat{\theta} \leq 0. \end{cases} \tag{41}$$

π functions for the isotropic Johansen criterion

With the isotropic Johansen criterion (35) the π functions simplify

$$\begin{cases} \pi(\underline{s}, \underline{\underline{\hat{\chi}}}) = m^+(\underline{s}) \operatorname{tr} \underline{\underline{\hat{\chi}}} \ \text{ if } \ \hat{\chi}_1 \geq 0,\ \hat{\chi}_2 \geq 0 \\ \pi(\underline{s}, \underline{\underline{\hat{\chi}}}) = m^-(\underline{s}) \operatorname{tr} \underline{\underline{\hat{\chi}}} \ \text{ if } \ \hat{\chi}_1 \leq 0,\ \hat{\chi}_2 \leq 0 \\ \pi(\underline{s}, \underline{\underline{\hat{\chi}}}) = m^+(\underline{s}) \hat{\chi}_1 + m^-(\underline{s}) \hat{\chi}_2 \ \text{ if } \ \hat{\chi}_1 \hat{\chi}_2 \leq 0,\ \hat{\chi}_1 \geq \hat{\chi}_2 \end{cases} \tag{42}$$

and

$$\pi(\underline{s}, \underline{n}, \hat{\theta}) = \begin{cases} \hat{\theta}\, m^+(\underline{s}) \ \text{ if } \ \hat{\theta} \geq 0 \\ \hat{\theta}\, m^-(\underline{s}) \ \text{ if } \ \hat{\theta} \leq 0 \end{cases} \tag{43}$$

independent of $\underline{n}$, which is similar to Eqs. (20) and (22).

As a matter of fact, Eq. (43) is the general expression of the π function for a virtual rotation rate jump for **any isotropic** strength criterion.

Eqs (41) and (43) are the essential tools of the Johansen "Yield-line theory", an application of the kinematic exterior approach. In the English translation of original Johansen's original works the rotation rate jump lines of the piecewise continuous and continuously differentiable motions are known as "Yield-lines"; they are now most currently called **hinge lines** [9], (*cf.* § 4.1).

As a final comment, we may add that a different but quasi-equivalent presentation of the Johansen criterion is given in [9], together with a report of experiments performed for its direct validation [21]. Indirect validation comes from various tests (*e.g.* [6, 22]) on transversally loaded plates (*Cf.* Chapter I, Figure 8). From the theoretical viewpoint, justifications of the Johansen criterion as part of a constitutive law, based upon the behaviour of concrete and steel have been proposed [11, 23-25].

3.3 Some typical support strength conditions

Built-in support

This support (Figure 1) is the counterpart of the rigid support in the case of the one-dimensional curvilinear continuum (Chapter IX): no limitation is imposed on $V(\underline{s},\underline{n})$ and $\underline{\Gamma}(\underline{s},\underline{n})$ by the strength condition. It follows that

(44) $$\pi_s([\![\hat{w}]\!],[\![\underline{\hat{\omega}}]\!]) = +\infty \text{ if } [\![\hat{w}]\!] \neq 0 \text{ or } [\![\underline{\hat{\omega}}]\!] \neq 0 \ .$$

Recalling that along ∂S we have $[\![\hat{w}(\underline{s})]\!] = -\hat{w}(\underline{s})$ and $[\![\underline{\hat{v}}(\underline{s})]\!] = \underline{e}_3 \wedge [\![\underline{\hat{\omega}}(\underline{s})]\!] = -\underline{e}_3 \wedge \underline{\hat{\omega}}(\underline{s})$ with the Kirchhoff-Love condition being identically satisfied in S, it comes out that, along the concerned boundary, the relevant virtual motions must satisfy:

(45) $$\begin{cases} \hat{w}(\underline{s}) = 0 \\ \underline{\hat{v}}(\underline{s}) = \underline{\partial}\hat{w}(\underline{s}) = 0. \end{cases}$$

Simply supported bilateral support

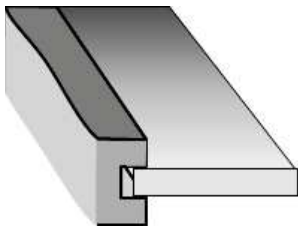

Figure 10. Simply supported bilateral support

It is the counterpart of the pinned support or axial support (Figure 10). The strength condition relates only to $\underline{\Gamma}(\underline{s},\underline{n})$

(46) $$\left[\mathbb{X}(\underline{s})\right].\underline{n}(\underline{s}) \in \mathcal{G}_s(\underline{s}) \ \Leftrightarrow \ \underline{\Gamma}(\underline{s},\underline{n}) = 0$$

from which

(47) $$\begin{cases} \pi_s([\![\hat{w}]\!],[\![\underline{\hat{\omega}}]\!]) = +\infty \text{ if } \hat{w} \neq 0 \\ \pi_s([\![\hat{w}]\!],[\![\underline{\hat{\omega}}]\!]) = 0 \text{ if } \hat{w} = 0. \end{cases}$$

Relevant virtual motions accept arbitrary rotation $\underline{\hat{\omega}}(\underline{s})$ with **no** vertical movement.

Simply supported unilateral support

The strength domain is defined by

(48) $$\left[\mathbb{X}(\underline{s})\right].\underline{n}(\underline{s}) \in \mathcal{G}_s(\underline{s}) \Leftrightarrow \begin{cases} V(\underline{s},\underline{n}) \geq 0 \\ \underline{\Gamma}(\underline{s},\underline{n}) = 0. \end{cases}$$

Hence, recalling that $[\![\hat{w}(\underline{s})]\!] = -\hat{w}(\underline{s})$,

(49) $$\begin{cases} \pi_s([\![\hat{w}]\!],[\![\underline{\hat{\omega}}]\!]) = +\infty \text{ if } \hat{w} < 0 \\ \pi_s([\![\hat{w}]\!],[\![\underline{\hat{\omega}}]\!]) = 0 \text{ if } \hat{w} \geq 0. \end{cases}$$

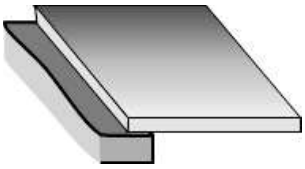

Figure 11. Simply supported unilateral support

Relevant virtual motions accept arbitrary rotation $\hat{\underline{\omega}}(\underline{s})$ and **uplift** $\hat{w}(\underline{s}) \geq 0$ from the support (Figure 11).

4 Final comments

Considering of the abundant literature which has been devoted to the topic, this Section will just point out some specificities of the Yield Design analysis of plates and thin slabs. The reader will refer to [9] for a deep survey of such subjects as

- the assessment of the physical and practical validity of the extreme loads determined on the two-dimensional model with respect to the original three-dimensional solid for metal plates and for reinforced concrete slabs;
- the various criteria proposed for orthotropic metal plates;
- as already mentioned, the various experiments performed for the validation of the Johansen criterion.

Reference [8], often referred to in [9], is the most valuable collection of the solutions that are available either for metal plates or for reinforced concrete slabs: "static" solutions for the interior approach, "kinematic" solutions for the exterior approach and even "complete" solutions.

4.1 Hinge line virtual motions

A notorious specificity of the Yield Design analysis of reinforced concrete slabs is the way the exterior approach is currently performed making use of piecewise continuously differentiable relevant virtual motions with **hinge lines** (the "yield lines" of the original Johansen terminology) connecting adjacent parts of the plates where the virtual motion is continuously differentiable. When two adjacent parts experience only rigid body motions, the corresponding hinge line is a straight line which bears the relative rotation between these two parts. The reader may refer to [26] and [9] for full details about the method.

To a certain extent these virtual motions recall the rigid block virtual mechanisms which are used in the Yield Design analysis of the three-dimensional continuum, especially in the case of plane problems. A token of this similarity is given by the rotation (rate) diagram introduced by Save with the "French" terminology "cinème", in English "rotation rate diagram" (*cf.* [9]), which is the counterpart of the hodograph for rigid block virtual mechanisms.

A simple illustrative example is given in Figure 12 in the case of a triangular slab with built-in supports along its boundary ABC. The considered virtual motion is defined by three positive hinge lines PA, PB, PC and three negative hinge lines AB, BC, CA. The three parts of the slab delimited by the hinge lines, namely

$\boxed{1}, \boxed{2}, \boxed{3}$ have rigid body rotations with the rotation rates $\underline{\hat{\theta}}_1, \underline{\hat{\theta}}_2, \underline{\hat{\theta}}_3$ about the negative hinge lines, while the relative rotation rates of each part with respect to the others, in the form $\underline{\hat{\theta}}_{ij} = \underline{\hat{\theta}}_i - \underline{\hat{\theta}}_j$, are collinear with the corresponding positive hinge lines (Figure 12a).

The rotation rate diagram (Figure 12b) is the geometric representation of Eq. (50) in the form of a Cremona-Maxwell diagram:

(50) $$\hat{\theta}_{13} + \hat{\theta}_{32} + \hat{\theta}_{21} = 0 .$$

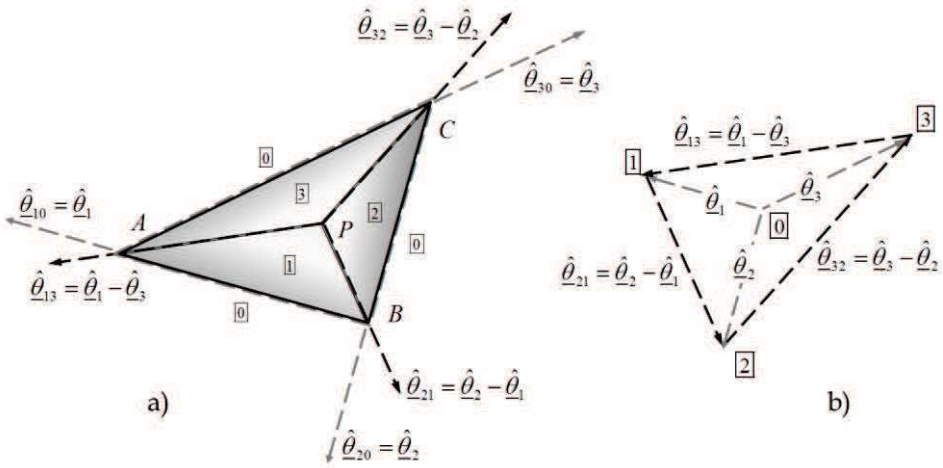

Figure 12. Simple example of a rotation rate diagram

In order for the considered virtual velocity field to be kinematically admissible the diagram must be closed for non-zero values of the rotation rates, as it is presently the case in Figure 12b. It is then possible to determine the algebraic magnitudes of the rotation rates from the knowledge of one of them and to express the maximum resisting rate of work in the considered virtual motion.

Hinge line virtual motions are thus relatively simple to operate, all the more so since hinge line patterns to be used in the method are often inspired by the observation of actual collapse mechanisms either in full scale or in reduced scale experiments (Chapter I, Figure 8).

As noted in § 3.2, Eq. (43) for the π function in a virtual rotation rate jump is valid whatever the **isotropic** strength criterion. Thence, any hinge line analysis performed with the Johansen isotropic criterion can be transposed to Tresca or von Mises plates simply by substituting $m_0(\underline{s})$ and $-m_0(\underline{s})$ for $m^+(\underline{s})$ and $m^-(\underline{s})$; when the constituent material is homogeneous the substitution turns out to be only necessary on the final result.

More sophisticated virtual motions are also implemented which combine concentrated deformation along hinge lines with distributed deformation ($\underline{\underline{\hat{\chi}}}(\underline{s}) \neq 0$) in S. In such cases, the rotation rate diagram comes out in a more elaborate form than in Figure 12b.

Similar to the hodograph in plane strain Yield Design analysis of the three-dimensional continuum, the rotation rate diagram is both a most efficient tool to check the kinematic admissibility of the considered relevant virtual motion and to determine the virtual rotation rate jumps.

4.2 Circular plate subjected to a uniformly distributed load

Kinematic exterior approach

An important illustrative example is the case of a circular plate S with centre O and radius R, supported along ∂S and subjected to a uniformly distributed vertical load $-p\,\underline{e}_3$, $(p>0)$. The constituent material of the plate is assumed to be homogeneous and to obey Johansen isotropic strength criterion and the support along ∂S is rigid (built-in support).

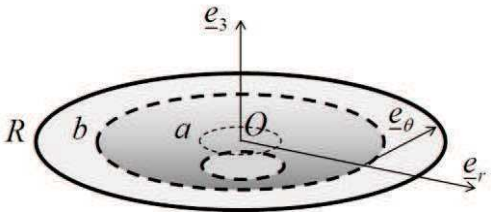

Figure 13. Circular plate subjected to uniformly distributed load

Using polar coordinates (r,θ) with centre O, we consider the Kirchhoff-Love virtual motions defined in the following way (Figure 13):

$$(51)\qquad \begin{cases} 0<a<b<R,\ \hat{f}>0 \\ \hat{w}(\underline{s})=-\hat{f}\ \text{ for } 0\le r\le a \\ \hat{w}(\underline{s})=-\hat{f}\left(\dfrac{b-r}{b-a}\right)\ \text{ for } a\le r\le b \\ \hat{w}(\underline{s})=0\ \text{ for } b\le r\le R, \end{cases}$$

where $\hat{f}$ stands for the virtual deflection rate in the centre of the plate and which depends on two geometrical parameters a,b.The corresponding velocity distributor field is continuous and piecewise continuously differentiable, exhibiting the positive rotation rate jump $\hat{\theta}_a=\dfrac{\hat{f}}{b-a}$ when crossing the circle $(r=a)$ [3] as a consequence of

$$(52)\qquad [\![\underline{\hat{\omega}}]\!]=-\underline{e}_3\wedge[\![\underline{\partial\hat{w}}]\!]=-\frac{\hat{f}}{b-a}\underline{e}_\theta$$

and, similarly, the negative rotation rate jump $\hat{\theta}_b=-\dfrac{\hat{f}}{b-a}$ when crossing the circle $(r=b)$. Those two circles are the hinge lines in the virtual motion.

[3] It is recalled that, according to Figure 7, the triad $(\underline{t},\underline{n},\underline{e}_3)$ is right handed which implies here that $\underline{t}$ is opposite to $\underline{e}_\theta$.

From the general expression of $\hat{\underline{\underline{\chi}}}$

$$\hat{\underline{\underline{\chi}}} = \frac{\partial^2 \hat{w}}{\partial r^2} \underline{e}_r \otimes \underline{e}_r + \left(\frac{1}{r}\frac{\partial^2 \hat{w}}{\partial r \partial \theta} - \frac{1}{r^2}\frac{\partial \hat{w}}{\partial \theta}\right)(\underline{e}_r \otimes \underline{e}_\theta + \underline{e}_\theta \otimes \underline{e}_r) + \left(\frac{1}{r}\frac{\partial \hat{w}}{\partial r} + \frac{1}{r^2}\frac{\partial^2 \hat{w}}{\partial \theta^2}\right)\underline{e}_\theta \otimes \underline{e}_\theta \tag{53}$$

we get here

$$\begin{cases} \hat{\underline{\underline{\chi}}} = 0 \ \text{ for } \ 0 < r < a \ \text{ and } \ b < r < R \\ \hat{\underline{\underline{\chi}}} = \dfrac{\hat{f}}{r(b-a)} \underline{e}_\theta \otimes \underline{e}_\theta \ \text{ for } \ a < r < b. \end{cases} \tag{54}$$

The virtual rate of work by the external forces (the uniformly distributed load p) is written

$$\mathcal{P}_{\mathrm{e}}(\hat{w}) = \frac{\pi}{3} p \hat{f}(a^2 + ab + b^2) \tag{55}$$

and the maximum resisting work comes from the contributions of both hinge lines, $(r = a)$ and $(r = b)$, and the distributed virtual deformation in the region $a < r < b$. The contribution of the built-in support along ∂S is equal to zero since the considered virtual motion is relevant for this support $\left(\hat{w}(R) = 0, \ \underline{\partial \hat{w}}(R) = 0\right)$. Referring to Eqs (42) and (43) we get

$$\mathcal{P}_{\mathrm{mr}}(\hat{w}) = 2\pi \frac{\hat{f}}{b-a}(m^+ a - m^- b) + 2\pi \hat{f} m^+ . \tag{56}$$

The kinematic exterior approach inequality results in

$$p \le 6(m^+ - m^-)\frac{b}{b^3 - a^3}. \tag{57}$$

The minimum of this equation with respect to a is obtained when $a \to 0$, which means that the virtual collapse mechanism tends to be conical. It is important to note that in this limit virtual collapse mechanism the contribution of the apex, namely $2\pi \dfrac{\hat{f}}{b-a} m^+ a$, **tends to zero**.

Minimizing with respect to b yields $b = R$, which means that the negative hinge line is situated **within the plate** at the boundary ∂S. The upper bound for the external load becomes

$$p\pi R^2 \le 6\pi(m^+ - m^-). \tag{58}$$

This upper bound is also valid for a Tresca or von Mises plate in the form

$$p\pi R^2 \le 12\pi m_0 \ . \tag{59}$$

It could be anticipated from dimensional analysis that the load carrying capacity of the circular plate, $p\pi R^2$, would be independent of the radius of the plate. This appears here on the upper bounds. Taking advantage of this result makes it possible, in the kinematic exterior approach, to take "concentrated" exterior forces into account, although they do not appear in the two-dimensional continuum plate

model. Such a load, topped by the limitation imposed by Eq. (58), is considered as the limit of an increasing uniformly distributed load on a decreasing circular area[4].

Static approach

In the case of isotropic Johansen or Tresca plates, a static interior approach can also be performed with the internal force fields $\underline{V}(r,\theta)$ and $\underline{\underline{M}}(r,\theta)$

$$(60)\qquad \begin{cases} \underline{\underline{M}}(r,\theta) = m^+(\underline{e}_r \otimes \underline{e}_r + \underline{e}_\theta \otimes \underline{e}_\theta) - (m^+ - m^-)\dfrac{r^2}{R^2}\underline{e}_r \otimes \underline{e}_r \\ \underline{V}(r,\theta) = -3(m^+ - m^-)\dfrac{r}{R^2}\underline{e}_r . \end{cases}$$

which are statically admissible with the load $p = \dfrac{6(m^+ - m^-)}{R^2}$ and comply with the strength criteria in the plate and in the support. It follows that the upper bound in Eq. (58), appears now also as a lower bound.

Complete solution

Referring to Chapter VI (Section 3), here is an example of a **complete solution** to the Yield Design problem where, both a kinematic exterior approach and a static interior one have been performed and yield the same value as an upper and a lower bound in this one positive parameter loading mode.

As stated in Chapter VI (Section 3), a straightforward conclusion is that the exact value of the extreme load has thus been obtained: $p\pi R^2 = 6\pi(m^+ - m^-)$ **is the load carrying capacity** of the plate.

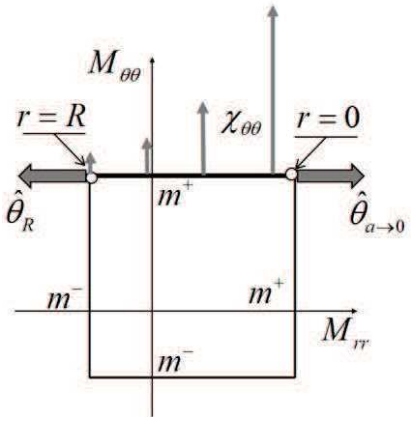

Figure 14. Verification of the "association theorem"

Moreover, comparing the components of $\underline{\underline{M}}(r,\theta)$ in Eq. (60) with the components of $\underline{\underline{\hat{\chi}}}(r,\theta)$ in Eq. (54) for $b = R$ and $a \to 0$, confirms that the "association theorem" (VI, § 3.2) is verified.

[4] A classical interpretation of a Dirac function!

As shown in Figure 14, $\hat{\underline{\underline{\chi}}}(r,\theta)$ is collinear with the outward normal to the boundary of the Johansen strength criterion along the segment

$$\begin{cases} M_{\theta\theta}(r,\theta) = m^+, \ 0 \le r \le R \\ M_{rr}(R,\theta) = m^- \le M_{rr}(r,\theta) \le M_{rr}(0,\theta) = m^+ \end{cases} \tag{61}$$

and the association theorem also holds for the negative rotation rate jump $\hat{\theta}_R$ along the hinge line $r = R$ in the plate, and the positive rotation rate jump $\hat{\theta}_{a\to 0}$ at the apex when $a \to 0$.

4.3 "Conical" virtual collapse mechanism

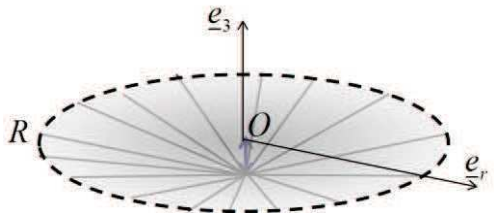

Figure 15. "Conical" virtual collapse mechanism

The "conical" virtual collapse mechanism (Figure 15) is the limit of the virtual motion described by Eq. (51) when $a \to 0$. It is quite frequently used, completely or partially, as a component of more sophisticated relevant kinematically admissible virtual motions, typical examples of which appear in Figure 16. It is important to note, as stated already earlier, that the apex of the cone is a singular point which does not contribute to the maximum resisting work in the mechanism. The only contributions come from the hinge line at the boundary of the cone $2\pi \hat{f}\, m^-$ and the distributed deformation in the cone $2\pi \hat{f}\, m^+$.

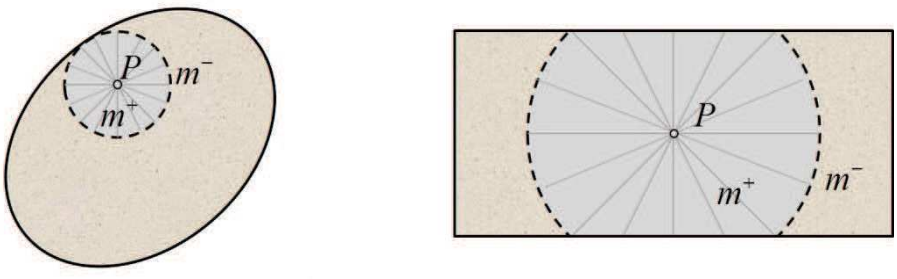

Figure 16. Johansen plates subjected to "concentrated loads"

REFERENCES

[1] MASSONNET, C. E. & SAVE, M. (1963) – *Calcul plastique des constructions, II, Structures spatiales*. CBLIA, Brussels.

[2] SAVE, M. & MASSONNET, C. E. (1973) – *Calcul plastique des constructions,* 2nd ed. CBLIA, Brussels.

[3] SAVE, M. & PRAGER, W. (1985) – *Structural Optimization*. Vol. 1, *Optimality Criteria*. Plenum Press, New York, London.

[4] LUBLINER, J. – (1990) – *Plasticity Theory*. MacMillan Publ. Company, New York.

[5] JOHANSEN, K. W. (1931) – Beregning af krydsarmerede jernbetonpladers brudmoment, *Bygningsstatiske Meddelelser*, **3**, 1, 1931, pp 1-18 (German version: "Bruchmomente der Kreuzweise bewehrten Platten", *Memoirs of the International Association for. Bridge and Structural Enineering*, **1**, 1932, pp 277-296.)

[6] JOHANSEN, K. W. (1952) – *Brudlinieteorier*, Gjellerup, Copenhagen, 1943, 189 pp. (English translation: *Yield-Line Theory*, Cement and Concrete Association, London, 1962).

[7] BRAESTRUP, M. W. (2007) – Yield line theory and concrete plasticity. Proc. *Morley Symposium on Concrete Plasticity and its Application*, University of Cambridge 23rd July, 2007, pp. 43-48.

[8] SAVE, M. (1995) – *Atlas of Limit Loads of Metal Plates, Shells and Disks*. Elsevier, Amsterdam.

[9] SAVE, M. A., MASSONNET, C. E. & DE SAXCE, G. (1998) – *Plastic limit analysis of plates, shells and disks*. Elsevier, Amsterdam.

[10] SAWCZUK, A. & JAEGER, T. (1963) – *Grenztragfähigkeits-Theorie der Platten*. Springer.

[11] NIELSEN, M. P. (1964) – *Limit Analysis of Reinforced Concrete Slabs*. Acta Polytechnica Scandinavia Ci 26, Copenhagen.

[12] HOPKINS, H. G. & PRAGER, W. (1953) – The Load-carrying Capacity of Circular Plates. *Journal of the Mechanics and Physics of Solids,* **2**, 1, 1-13.

[13] HOPKINS, H. G. & WANG, A. J. (1954) –Load-carrying Capacities for Circular Plates of Perfectly-plastic Material with Arbitrary Yield Conditions. *Journal of the Mechanics and Physics of Solids,* **3**, 117-129.

[14] DRUCKER, D. C. & HOPKINS, H. G. (1954) – Combined Concentrated and Distributed Load on Ideally Plastic Circular Plates. *Proceedings of the 2nd U.S. National Congress in Applied Mechanics,* A.S.M.E., Ann Arbor, Mich.

[15] MARKOWITZ, J. & HU, L. W. (1965) – Plastic Analysis of Orthotropic Circular Plates. *Proceedings A.S.C.E., Journal of the Engineering Mechanics Division,* **90**, EM5, 251.

[16] SHULL, H. E. & HU, L. W. (1963) – Load-carrying Capacities of Simply Supported Rectangular Plates. *Transactions A.S.M.E., Journal of Applied Mechanics*, **30**, 617-620.

[17] MASSONNET, C. E. (1967) – Complete Solutions Describing the Limit State of Reinforced Concrete Slabs. *Magazine of Concrete Research*, **19**, 18.

[18] SALENÇON, J. (1990): *Calcul à la rupture. Poutres, plaque et dalles minces en flexion.* Lecture Notes. École Nationale des Ponts et Chaussées, Paris, 46 p.

[19] SALENÇON, J. (2001) – *Handbook of Continuum Mechanics*. Springer-Verlag, Berlin, Heidelberg, New York.

[20] ŻYCZKOWSKI, M. (1981) – *Combined Loadings in the Theory of Plasticity*. PWN – Polish Scientific Publishers, Warsaw.

[21] BAUS, R. & TOLACCIA, S. (1963) – Calcul à la rupture des dalles en béton armé et étude expérimentale du critère de rupture en flexion pure,(Yield-line Theory and Experimental Investigation of the Yield Criterion of Reinforced Concrete Slabs in Pure Bending). *Annales de l'institut technique du bâtiment et des travaux publics*, 871-894, Paris, June 1963.

[22] LAMBLIN, D. O., GUERLEMENT, G. & SAVE M. A., (1981) – Model experiments for limit design of slabs. *Matériaux et Construction*, **14**, 5, 331-339.

[23] WOLFENSBERGER, R. (1964) – Traglast und optimale Bemessung von Platten. *Technische Forschungs- und beratungsstelle der Schweizerischen Zement Industrie*, Wildegg.

[24] KEMP, K. O. (1965) – The Yield Criterion for Orthotropically Reinforced Concrete Slabs. *International Journal of Mechanical Sciences*, **7**, 11, 737-746.

[25] MORLEY, C. T. (1966) – On the Yield Criterion of an Orthogonally Reinforced Concrete Slab Element. *Journal of the Mechanics and Physics of Solids,* **14**, 1, 33-47.

[26] COURBON, J. (1965) – *Résistance des matériaux*. Vol. 2. Dunod, Paris.

Alphabetical index

(Only the first and other significant occurences are mentioned)

A
Anisotropic materials — IV.3.2.
Arches — I.1.2; IX.4.
Association theorem — VI.3.3; XI.4.2.

B
Ball and socket joint — IX.3.2.
Beam — IX.4.
Bending moment — IX.1.3.
Bending — IX.3.1; XI.
Boundary data — III.4.1; IV.1.2.
Brittle material — II.3.
Built-in support — IX.3.3; XI.3.3.

C
Cauchy stress tensor — III.2.3.
Cinème — XI.4.
Circular plates — XI.4.2.
Cohesion — IV.4.3.
Compatibility equilibrium-resistance — I.1.3.
Complete solution — VI.3.3; XI.4.2.
Conical virtual mechanism — XI.4.3
Constitutive law — II.1.4; 3; IV.3.4.
Convex hull — IV.2.3; VIII.2.3.
Convex programming — VIII.3.2.
Convexity — IV.1.3; 2.2; VI.3.3; VIII.2.2.
COULOMB — I.1.2.
Coulomb's criterion — IV.4.3.
Curvature (rate of) — XI.2.2.
Curvilinear one-dimensional model — IX.1.

D
Design load effect — I.2.2; VII.3.2.
Design resistance effect — I.2.2; VII.3.2.
Dimensioning — VIII.1.
Director curve — IX.1.1.
Director sheet — X.1.
Discontinuous stress field — III.2.5.
Divergence theorem — III.3.2; X.3.2.
Domain of potential stability — VIII.2.
Drucker-Prager criterion — IV.4.3.
Dual definition — V.3.4; VI.3.1.
Ductility — IV.3.4.

E
Economic function — VIII.3.2.
Equations of motion — III.2.4.
Equilibrium equations (wrenches) — IX.1.3; X.3.2.
External forces — III.2.2; IX.1.3; X.2.1.
Exterior approach — VI; VIII.2.4; IX.2.3; XI.2.2.
Extreme load — II.2.2; IV.2.2.
Extreme value probability law — VIII.4.4.

F
Frame — IX.2.1.
Friction angle — IV.4.3.

G
GALILLEO — I.1.1.
Geometry changes — II.3.

H
Hadamard ('s compatibility condition) — XI.2.2.
Hinge curves — X.2.3.
Hinge lines — XI.3.2; 4.
Hinged support — I.1.3; XI.3.2.

I
Initial state of internal forces — II.2.2; IV.3.4.
Interaction formula — IX.2.1; 3.1.
Interfaces — IV.3.3; 4.2; V.3.5; V.4.2.
Interior approach — IV.2.3; VIII.2.3; IX.2.2; XI.2.1.
Internal forces — III.2.3; IX.1.3; X.2.2.
Internal moments tensor — X.2.3.
Isotropy — XI.3.1; XI.3.2.

J
Johansen strength criterion — XI.3.2.
Joints — IX.2.1; 3.2.

K
Kinematically admissible fields — III.4.3; V.2.
Kinematically admissible virtual motions — IX.2.3; XI.2.2.
Kinematical necessary condition — V.2.
Kirchhoff-Love condition — X.1.2; XI.2.2.

L
Limit loads— IV3.4.
Linear programming — VIII.3.2.
Load — IV.1.2.
Loading mode — IV.1.2.
Loading parameters — IV.1.2.
Loading path — II.1.4; 3; IV.3.4.
Lower bound estimate — IV.2.3; VIII.4.3.

M
Maximum plastic work — VI.2.1
Maximum resisting bending moment — IX.3.1; XI.3.2.
Maximum resisting work — V.3.2; IX.2.3;XI.2.2.
Membrane forces — X.2.3.
Metal plates — XI.3.1.
Micro-macro modelling — X.4; XI.1.2; 3.2.
Microstructure — IX.1; X.1.
Model uncertainties — VII.3.3.

N
Navier-Bernoulli condition — IX.1.2.
Normal force — IX.1.3.

O
Objective function — VIII.3.2.
One-dimensional continuum — IX.1.
Optimal dimensioning — VIII.3.
Orthotropy — XI.3.2.

P
Partial factors — I.2.2; VII.2.1.
Perfectly plastic material — II.3; IV.3.4.
Permanent loads — IV.3.1.
Pi-function — V.3; IX.3; XI.2.2; 3.
Pinned joint — IX.3.2.
Plane stress — XI.1.2.
Plates —X.1.
Positive homogeneity — VI.3.3.
Potentially safe dimensionings — VIII.2.2.
Potential stability — II.2.2;
Potentially safe loads — IV.2; IX.2.2.
Pre-stressing — II.3.
Principal stresses — III.2.6.
Probabilistic Yield Design problem — VIII.4.2.
Probability density function —VIII.4.3.
Probability of collapse — VIII.4.3
Probability of stability — VIII.4.3.

R
Rate of stretch — IX.1.2
Rate of extension — III.1.2.
Rate of volume dilatation — III.1.2.
Regular point — VI.3.2.
Reinforced concrete slabs — XI.3.2.
Relevant virtual velocity field — VI.2.
Relevant virtual motions — IX.2.3; XI.2.2.
Resistance parameters — VII.2.2; VIII.2.1.
Rigid joint — IX.3.2.
Rigid support — XI.3.3.
Rotation (rate) diagram — XI.4.
Rotation rate jump — XI.3.2.

S
Section — IX.3.1.
Shear force vector — X.2.3; XI.1.2; 3.3.
Shearing force — IX.1.3.
Simply supported support — XI.3.3.
Singular point — VI.3.2.
Slabs — X.1; XI.3.2.
Star-shaped domain — IV.3.2.
Static exterior approach — V.1.
Statically admissible fields — III.4.2; IX.2.2; XI.2.1.
Stochastic resistance parameters — VIII.4.2.
Stochastic loading parameters — VIII.4.2.
Strain rate (distributor) — IX.1.2.
Strain rate tensor — III.1.2; XI.1.2.
Strength criterion — IX.3; XI.3.
Strength domain — IV.1.3.
Stress vector continuity — III.2.5.
Structural supports — IX.2.1; 3.3.
Structures — IX.2.1.
Supports — IX.2.1; IX.3.3; XI.1.2; XI.3.3.
Support function — V.3.1.
Symmetry (Cauchy stress tensor) - III.2.3
Symmetry (internal moment tensor) - X.2.3;4.2; XI.1.2.
Symmetry (membrane force tensor) - X.2.3.

T
Tension cut-off — IV.4.1.
Tensorial distributor — X.1.2.

Tensorial wrench — X.3.3.
Theorem of virtual work — III.3.2; IX.1.4; X.3.
Transverse microstructure — IX.1.1; XI.1.1.
Tresca's criterion — IV.4.3.
Tresca plates — XI.3.1.
Truss— IX.2.1.
Twisting moment — IX.1.3.
Two-dimensional continuum — X.1.1.

U

ULSD — I.2.2; VII.
Upper bound estimate — VI.1; VIII.4.3.

V

Vaults— I.1.2; IX.4.
Velocity distributor — IX.1.2; X1.2.
Velocity field — III.1.2.
Virtual velocity jump — III.3.1.
Virtual (rate of) work — III.3.2.
Virtual velocity fields — III.3.1.
Virtual work equation — III.4.4.
Von Mises' criterion — IV.4.3.
Von Mises plates — XI.3.1.

W

Wrench of forces — IX.1.3.
Wrench of external forces — IX.1.3; X.3.3.
Wrench of internal forces — IX.1.3; X.3.3.

Y

Yield hinges — I.2.1.
Yield lines — XI.1.1; XI.3.2; 4.